

Die approbierte Originalversion dieser Dissertation ist an der Hauptbibliothek der Technischen Universität Wien aufgestellt (<http://www.ub.tuwien.ac.at>).

The approved original version of this thesis is available at the main library of the Vienna University of Technology (<http://www.ub.tuwien.ac.at/englweb/>).



TECHNISCHE
UNIVERSITÄT
WIEN

VIENNA
UNIVERSITY OF
TECHNOLOGY

DISSERTATION

Adaptive Resource Allocation for Multi-User Digital Subscriber Lines

ausgeführt zum Zwecke der Erlangung des akademischen Grades
eines Doktors der technischen Wissenschaften

eingereicht an der
Technischen Universität Wien
Fakultät für Elektrotechnik und Informationstechnik

durch

Dipl.-Ing. Driton Statovci
Favoritenstrasse 33/2/12, 1040 Wien
Matr. Nr. 9725264

Wien, im Juli 2005

Date of examination:

July 11th, 2005

Supervisor:

Prof. Dr. Hans Weinrichter
Institute of Communications and Radio-Frequency Engineering
Vienna University of Technology
Austria

Examiner:

Prof. Dr. Werner Henkel
School of Engineering and Science
International University Bremen
Germany

Abstract

The need for high-speed communications in access networks is continuously growing. Digital subscriber line (DSL) technology offers an attractive solution for providing high-speed communications over existing telephone wires. Crosstalk between the twisted-pairs is the main impairment in DSL communications. Current deployed DSL systems are designed as single-user systems with the assumption that they operate in a worst-case noise environment. As a result, they show poor performance when deployed in an actual network with multiple users. To significantly improve the performance of existing DSL systems the cable resources need to be assigned to the users more intelligently. The art of assigning cable resources to mitigate the crosstalk noise among the users is known as dynamic spectrum management (DSM). The main idea of DSM is that each user make a trade-off between maximizing his own bitrate and minimizing the crosstalk noise to the others.

This thesis studies DSM for DSL systems that are frequency division duplexing (FDD) based. We analyze DSL systems that use Zipper discrete multi-tone (DMT) modulation, which is part of the standards for very high speed DSL (VDSL) and VDSL2. In the first part, we describe the DSL environment and give an overview of DMT and Zipper. Previously proposed DSM algorithms for FDD systems optimize the user power allocation but assume a fixed band plan. However, to offer specific DSL services in a particular twisted-pair network, a search for an optimal band plan is needed in order to share the cable resources efficiently among users.

We address the problem of optimizing the band plan and power allocations in multi-user DSL systems. This optimization problem is unsolvable with existing algorithms. To solve it, we propose the normalized-rate iterative algorithm (NRIA). The NRIA *jointly* optimizes the FDD band plan and power allocations for a multi-user DSL system. The key is a practical and novel problem formulation: the user bitrates are coupled through relations that describe corresponding services in a network. Hence, the NRIA is designed to efficiently solve the DSM optimization problem with the operators' business models in mind. The main advantage of the NRIA compared to the other DSM proposals is its low computational complexity. Therefore, it is suitable for deployment in networks with many users. The NRIA can also be deployed in situations with a fixed band plan, as in asymmetric DSL (ADSL), to mitigate the crosstalk noise.

It is common that service providers want to ensure some of the users in the cable bundle predefined fixed bitrates while offering services to the remaining users on a best-effort basis. This reflects many business scenarios where a number of users in a network must be guaranteed a specific service. To solve this type of optimization problem we have developed the constrained normalized-rate iterative algorithm (C-NRIA), which is based on the NRIA. We will see that the C-NRIA needs only a *single* parameter to split the cable capacity among the two user groups.

Kurzfassung

Der Bedarf an Übertragungsverfahren für hohe Datenraten in Zugangsnetzen wächst kontinuierlich. Digital Subscriber Line (DSL) Technologie bietet eine attraktive Lösung, um hohe Datenraten über existierende Telefonleitungen übertragen zu können. Die wichtigste Beeinträchtigung bei DSL ist das Übersprechen zwischen verdrehten Leitungspaaren. Derzeit eingesetzte DSL-Systeme sind als Einbenutzersystem konzipiert um in einem Umfeld mit hohen Geräuschpegeln zu operieren. In realen Zugangsnetzen mit mehreren Benutzern erweisen sie sich jedoch als wenig leistungsfähig. Eine intelligentere Aufteilung von Kabelressourcen zwischen den Benutzern würde eine wesentliche Verbesserung bewirken. Ein Ansatz, die Kabelressourcen so aufzuteilen, dass das Übersprechen gemildert wird, nennt sich Dynamic Spectrum Management (DSM). Die zugrundeliegende Idee von DSM ist, dass jeder Benutzer einen Kompromiss zwischen der Maximierung seiner eigenen Datenrate und der Minimierung des Übersprechens zu anderen Benutzern anstrebt.

Diese Dissertation befasst sich mit DSM für DSL-Systeme, die Frequenzduplexverfahren (englisch: Frequency Division Duplexing, FDD) verwenden. In dieser Arbeit werden DSL-Systeme analysiert, die Zipper Discrete Multi-Tone (DMT) Modulation einsetzen, welche für Very High Speed DSL (VDSL) und VDSL2 standardisiert wurde. Im ersten Teil dieser Dissertation beschreiben wir das DSL-Umfeld und werfen einen Blick auf DMT und Zipper. Früher vorgeschlagene DSM-Algorithmen für FDD-Systeme optimierten die Leistungsverteilung bei festgelegtem Bandplan. Ein solcher Bandplan sollte jedoch ebenfalls optimiert werden, um die Leitungsressourcen bestmöglich unter den Benutzern aufzuteilen.

In dieser Dissertation befassen wir uns mit dem Problem, den Bandplan und die Leistungsverteilung in Mehrbenutzer-DSL-Systemen zu optimieren. Dieses Optimierungsproblem ist mit den existierenden Algorithmen nicht lösbar. Wir schlagen einen Algorithmus vor, den sogenannten Normalized-Rate Iterative Algorithm (NRIA). NRIA optimiert den FDD-Bandplan und die Leistungsverteilung *gemeinsam* in Mehrbenutzer-DSL-Systemen. Dem liegt eine neue Formulierung des Problems zugrunde, welche die Benutzerdatenraten durch Beziehungen verkoppelt, die ihrerseits durch die zugehörigen Dienste parametrisiert sind. NRIA wurde entworfen, um das DSM-Optimierungsproblem effizient im Hinblick auf die Geschäftsmodelle der Betreiber zu lösen. Der Hauptvorteil von NRIA, verglichen mit anderen DSM Vorschlägen, besteht in seiner geringen numerischen Komplexität. Aus diesem Grund ist NRIA für Zugangsnetze mit grosser Benutzerzahl geeignet. NRIA kann auch in Systemen mit festem Bandplan eingesetzt werden, um das Übersprechen zu mildern, beispielsweise in asymmetrischen DSL (ADSL).

Häufig tritt der Fall auf, dass Betreiber einem Teil Ihrer Kunden festgelegte Datenraten anbieten wollen, während den übrigen Kunden ein Service auf Best-Effort Basis angeboten wird. Dies ist interessant für Geschäftsmodelle, bei denen einer Anzahl von

Netzteilnehmern ein bestimmter Dienst garantiert werden soll. Um diese Variante des Optimierungsproblems zu lösen, haben wir den Constrained Normalized-Rate Iterative Algorithm (C-NRIA) entwickelt, der auf NRIA basiert. In dieser Arbeit wird gezeigt, dass C-NRIA lediglich *einen* Parameter benötigt, um die Kabelkapazität unter den beiden Benutzergruppen aufzuteilen.

Acknowledgments

There is a long list of people I wish to thank for supporting me in different ways during my time as a Ph.D. student and helping me finishing this thesis. First of all, I would like to express my deepest gratitude to my supervisor Professor Hans Weinrichter for his guidance, useful suggestions, and continuous support since I started my Ph.D. studies. He has not only encouraged me continuously to achieve this goal, but also assisted me financially by helping me to find interesting jobs first at Ahead Communications Systems and then at the Telecommunications Research Center Vienna (ftw.). I also wish to thank Professor Werner Henkel for being my second advisor and carefully reading my thesis. His comments have improved the content of this thesis.

Most of the work in this thesis was carried out within collaborative projects within ftw. These projects were supported by Alcatel, Infineon, and Telekom Austria and in addition received public funding within the framework of the Austrian *Kplus* Program. The above-mentioned projects were led by Tomas Nordström. I want to especially thank him for his guidance, continuous support, and useful suggestions. Tomas has always given me enthusiastic encouragement on my small achievements and motivated me to keep the work going.

I am grateful to all my colleagues at ftw. Particularly, I would like to thank Rickard Nilsson for co-authoring papers with me, Christoph Mecklenbräuer, Gottfried Lechner, Joachim Wehinger, Jossy Sayir, and Thomas Zemen for continuous support, and Edward Schofield for proofreading. I would also like to thank Markus Kommenda and Horst Rode for setting up a nice working environment, which has made my work much more flexible and enjoyable.

I would like to thank Professor Per Ödling from Lund University in Sweden for inviting me to his department to present my thesis work at an early stage. The discussions with him and the other participants have inspired me with new ideas for my work.

I wish to thank all my friends that have made my time in Vienna enjoyable. Particularly I would like to mention Astrit Ademaj, Idriz Smaili, Nysret Musliu, and Professor Salem Lepaja.

Many thanks go to my family and my relatives. Special thanks go to my father Raif; mother Hajrije; brothers Skender, Kamer, and Naser; and sisters Rahime and Florije. Thank you for never stopping believing in me all the time, as this encouraged me to believe in myself to reach my dreams.

Finally, but most importantly, I would like to thank my wife Valbona for her continuous support. Without her patience, love, and help it would have been impossible for me to finish this thesis. She has taken great responsibility to care for our two wonderful sons Ardit and Art. Ardit and Art, you are the stars of my life; therefore, I would like to thank you especially, and hope that I can now spend more time with you.

Contents

1	Introduction	1
1.1	Digital Subscriber Line Technologies	1
1.2	Research Motivation	3
1.3	Research Contributions	4
1.4	Outline of the Thesis	5
2	DSL Environment	7
2.1	DSL Access Network Structure	7
2.2	Discrete Multi-Tone Modulation	11
2.2.1	DMT Transmission System	11
2.2.2	Digital Duplexing Technique for DMT systems	21
2.3	Comparison of DMT and Single-Carrier Modulation	24
2.4	Noise	27
2.4.1	Background Noise	27
2.4.2	Crosstalk Noise	27
2.4.3	Radio Noise	33
2.4.4	Impulse Noise	34
3	Spectrum Management for DSL Systems	35
3.1	Static Spectrum Management	36
3.1.1	T1.417 DSL Static Spectrum Management Standard	37
3.1.2	An Example of Spectral Compatibility Evaluation	43
3.1.3	Upstream Power Back-Off in VDSL	44
3.2	Dynamic Spectrum Management	47
3.2.1	Spectral Balancing	49
3.2.2	Vectoring	52
4	The Normalized-Rate Iterative Algorithm	55
4.1	System Model	56
4.2	Bitrate Relations Used by the NRIA	60
4.3	Problem Formulation	61
4.4	The Normalized-Rate Iterative Algorithm	64
4.4.1	Algorithmic Details	65
4.5	Complexity of the NRIA	73
4.6	Initialization of the Input Parameters in the NRIA	75
4.7	Overview of the NRIA Compared to the IWFA	79

5	Performance and Properties of the NRIA	83
5.1	Common Simulation Parameters	84
5.2	Rate Regions of the IWFA, the OSBA, and the NRIA	84
5.3	Comparison of the NRIA with the IWFA	86
5.3.1	Two-User Case: Fixed Length	87
5.3.2	Two-User Case: Variable Length	94
5.3.3	Multi-User Case	96
5.4	Comparison of the NRIA with the OSBA	98
5.4.1	Comparison for the Symmetric Bitrates	98
5.4.2	Comparison for the Asymmetric Bitrates	99
5.4.3	Performance Loss in the NRIA over the OSBA	100
5.5	Flexibility of the NRIA in the Bitrate Assignment	103
5.6	Comparison of the NRIA with the bi-IWFA	105
5.6.1	Convergence of the IWFA and the bi-IWFA	106
5.6.2	Simulations	108
5.7	Comparison of the NRIA with the UPBO in VDSL	111
5.7.1	Simulation Environment	111
5.7.2	Simulation Results	112
5.8	Comparison of the NRIA with an Exhaustive Search	117
6	The Constrained Normalized-Rate Iterative Algorithm	119
6.1	Mathematical Framework	120
6.1.1	Single Transmission Direction	120
6.1.2	Downstream and Upstream Transmission Directions	122
6.2	Problem Formulation	125
6.3	The Constrained Normalized-Rate Iterative Algorithm	127
6.4	Simulation Results	129
7	Conclusions	133
A	Derivations of Some Proprieties of the NRIA and the C-NRIA	135
A.1	Relation Between the Downstream and Upstream Bitrates of Each User in the NRIA	135
A.2	Discussion of Postulate 1, Section 4.4.1.5	136
A.3	Complexity of the Modified Fixed-Margin Water-Filling Algorithm	138
A.4	Proof of Theorem 1, Section 6.1.1	142
B	Abbreviations	145
C	Notation	147
	Bibliography	151

List of Figures

2.1	The loop length distribution in different countries	8
2.2	Structure of a typical loop plant	8
2.3	Twisted-pair cable topologies	9
2.4	A basic DMT transmission scheme	12
2.5	Illustration of subcarriers and subchannels	13
2.6	Adding of cyclic prefix	15
2.7	Equivalent discrete-time channel model	17
2.8	Alignment of the DFT window within the received DMT symbols	21
2.9	Adding of cyclic prefix and cyclic suffix	22
2.10	Illustration of timing advance in Zipper-DMT systems	23
2.11	Selection of cyclic suffix length in Zipper-DMT systems	24
2.12	Schematic of single-carrier modulation transmission system	25
2.13	NEXT and FEXT crosstalk signals	28
2.14	Measured NEXT couplings and ETSI NEXT model	29
2.15	Measured EL-FEXT couplings and ETSI EL-FEXT model	30
2.16	Illustration of NEXT and FEXT in distributed networks	31
3.1	Transmit PSD templates of spectrum management classes.	38
3.2	The network topology used to evaluate the system performance	39
3.3	The reach of ADSL system	44
3.4	Two standardized VDSL band plans	44
3.5	Near-far problem in VDSL	45
3.6	DSM network structure in an unbundled access network	48
3.7	Topology of DSL access network for spectral balancing	50
3.8	Upstream vectoring transmission	53
3.9	Downstream vectoring transmission	53
4.1	An example of a distributed multi-user DSL environment	57
4.2	Illustration of the Gaussian interference channel	58
4.3	An example of a network scenario with two users	67
4.4	An example of initial subcarrier allocation	68
4.5	An example of initial subcarrier allocation with $N = 4096$	68
4.6	An illustration of the search for a subcarrier allocation	69
4.7	Another illustration of the search for a subcarrier allocation	70
4.8	Illustration of the ping-pong effect	71
4.9	Example of the number of target bitrate corrections	73
4.10	The simulation scenario used by the NRIA	76

4.11	Users' downstream and upstream bitrates for various K	76
4.12	Users' downstream and upstream bitrates depending on M	77
4.13	The downstream and upstream convergence behaviors of the NRIA	78
4.14	An example of the convergence behavior in the NRIA	79
5.1	Illustration of rate regions of the IWFA and the OSBA	85
5.2	An example of two-dimensional rate region of the NRIA	86
5.3	PSDs of ETSI VDSL "Noise Model A"	87
5.4	A two-user case network scenario	88
5.5	Insertion losses and FEXT couplings for scenario in Figure 5.4	88
5.6	Rate regions of the IWFA and the NRIA for $a = 1$	89
5.7	Rate regions of the IWFA and the NRIA for $a = 1.25$	91
5.8	Downstream PSDs of the NRIA and the IWFA for $a = 1.25$	92
5.9	Upstream PSDs of the NRIA and the IWFA for $a = 1.25$	93
5.10	Network scenario used for variable length simulations	94
5.11	IWFA rate region for the network scenario in Figure 5.10	94
5.12	Equal and symmetric bitrates of the NRIA and the IWFA	95
5.13	The Multi-user scenario used to compare the NRIA with the IWFA	96
5.14	Rate regions of the OSBA and the NRIA for $a = 1$	98
5.15	Rate regions of the OSBA and the NRIA for $a = 1.25$	99
5.16	Downstream PSDs of the NRIA and the OSBA for $a = 1.25$	101
5.17	Upstream PSDs of the NRIA and the OSBA for $a = 1.25$	102
5.18	Rate regions of the IWFA, the OSBA, and the NRIA for $a = 1.25$	103
5.19	Rate regions of the NRIA for different values of a	104
5.20	Rate regions of the NRIA for $a = 2$	105
5.21	Virtual FEXT used to model the NEXT by the bi-IWFA	107
5.22	Network scenario used to compare the NRIA and the bi-IWFA	108
5.23	Supported bitrates for the NRIA and the bi-IWFA	108
5.24	Downstream and upstream PSDs of the bi-IWFA	109
5.25	Downstream and upstream PSDs of the NRIA	110
5.26	Simulation scenario used to compare the NRIA with the UPBO	111
5.27	Measured EL-FEXT for a 0.4 mm cable	112
5.28	Measured insertion losses for a 0.4 mm cable	112
5.29	Supported bitrates for UPBO with 99% worst-case and measured FEXT	113
5.30	Comparison of the ETSI UPBO with the NRIA for $a = 1$ and $a = 1.5$	114
5.31	Downstream and upstream PSDs for the UPBO	115
5.32	Downstream and upstream PSDs for the NRIA	116
5.33	Comparison of the NRIA with the exhaustive search	117
6.1	Illustration of the search space for the balancing parameter s	122
6.2	A network scenario with four users	130
6.3	Bitrates of the fixed-rate and variable-rate users for different s	132

List of Tables

2.1	Wire diameters and loop resistances of typical cables	10
2.2	Amateur radio (HAM) frequency bands	34
3.1	The required SNR for PAM and QAM to achieve a BER of 10^7	41
4.1	Relations between different bitrates and users' priority at 18 Mbit/s	61
4.2	Relations between different bitrates and users' priority at 31.5 Mbit/s . . .	61
4.3	Computational complexity of the modified FM-WF algorithm	74
5.1	Comparison of the NRIA with the IWFA, symmetric bitrates	89
5.2	Comparison of the NRIA with the IWFA, asymmetric bitrates	90
5.3	User priority values used for simulation	96
5.4	Supported bitrates in the IWFA	97
5.5	Supported bitrates in the NRIA	97
5.6	Comparison of the NRIA with the OSBA, symmetric bitrates	98
5.7	Comparison of the NRIA with the OSBA, asymmetric bitrates	99
5.8	Some bitrate combinations supported by the NRIA	104
6.1	Calculated user priority values for selected target bitrates	129
6.2	Supported bitrates and the priority values for $T_{1,DS}^F = 33$ Mbit/s	130
6.3	Supported bitrates and the priority values for $T_{1,DS}^F = 36$ Mbit/s	131
6.4	The values of shifting parameter θ versus the balancing parameter s	132
A.1	Maximum number of operations in the modified FM-WF algorithm	141

Chapter 1

Introduction

Broadband access is one of the fastest growing technologies. This growth is expected to continue with the emergence of several new applications and services that require high bitrates, such as music and movie sharing, video-conferencing, teleworking, video-on-demand, and high-definition television. One of the most popular technologies to offer broadband access is the digital subscriber line (DSL). DSL provides high-speed digital communication over twisted-pair telephone networks. Based on data provided by the DSL Forum [36] the number of the DSL subscribers in February 2005 passed the 100 million mark, with a global growth in 2004 close to 60%.

At the end of 2004, there were five countries with over 20% of their telephone lines used to deliver DSL services and in another nine countries the penetration was over 15%. The penetration of DSL systems will continue to grow in the future and with that also the crosstalk (interference) impairment will increase. As a result, the performance and reliability of DSL systems will mainly be determined by techniques deployed to mitigate this crosstalk. This thesis deals with techniques for adaptive resource allocation, which perform crosstalk mitigation in DSL systems that use discrete multi-tone (DMT) modulation. DMT modulation is used in asymmetric DSL (ADSL), ADSL2, ADSL2+, very high speed DSL (VDSL), and VDSL2.

This chapter proceeds as follows. Section 1.1 gives a short overview of DSL technologies. Section 1.2 describes the motivation for research and development of new techniques for crosstalk mitigation. Section 1.3 describes the major contributions of the thesis, and Section 1.4 gives an outline of the thesis.

1.1 Digital Subscriber Line Technologies

Digital subscriber line (DSL) technologies use twisted-pair cables as a physical medium to carry their signals to and from customers to some sort of central office (CO). Multiple twisted pairs are grouped in bundles, where each bundle typically contains from 10 to 50 twisted pairs. Multiple bundles are grouped together in a cable; a cable can contain up to 4200 twisted pairs [87].

The use of telephone lines for transmitting digital data was introduced in the late 1950s by means of voice-band modems. Voice-band modems utilize the same bandwidth as used for transmission of speech signals (0.3–3.4 kHz). The first generation of voice-band modems transmitted at 300 bit/s full-duplex. The latest generation of voice-band modems standardized by the International Telecommunication Union (ITU) as V.90 modems enable downstream (towards customers) bitrates up to 56 kbit/s and upstream (from cus-

tomers) bitrates up to 33 kbit/s.

Using frequencies above 4 kHz for transmitting digital data over telephone lines started with T1 and E1 carriers, which were originally intended for use as trunks between COs. T1 carriers were first deployed by AT&T in 1962 [100]. T1 and E1 carriers were used later in access telephone networks to offer services to business customers. The first systems designed for transmitting digital data over telephone access networks have been the basic rate integrated services digital network (BRI) systems. In 1986, the first BRI systems were deployed and this can also be seen as the beginning of the era of DSL communications. A BRI system sends data simultaneously in both directions and in the same frequencies by using an echo-cancellation (EC) transmission scheme. BRI supports 160 kbit/s symmetric bitrates and targets private customers.

High-bitrate DSL (HDSL) was developed to replace the expensive T1/E1 carriers. HDSL provides symmetric bitrates of 1.544 Mbit/s (T1) or 2.048 Mbit/s (E1) over two or three twisted pairs. HDSL systems, like BRI systems, operate in EC transmission mode. To achieve the same bitrate and the same reach as HDSL, but over a single twisted pair, symmetric high-bitrate DSL (SHDSL) was later developed.

The most widely deployed DSL technology is asymmetric DSL (ADSL), which is designed to offer asymmetric services usually to private customers. ADSL uses discrete multi-tone (DMT) modulation with 256 subcarriers and frequencies up to 1.104 MHz. ADSL systems may use either EC (partly overlapped transmission bands) or frequency division duplexing (FDD) transmission scheme. In the FDD scheme different frequencies are used for transmission in the downstream and upstream directions. ADSL supports downstream bitrates up to 9 Mbit/s and upstream bitrates up to 1 Mbit/s. To offer even higher downstream bitrates in ADSL, ITU is just completing the ADSL2+ standard, which uses 512 subcarriers and frequencies up to 2.208 MHz.

The most advanced DSL technology is very high speed DSL (VDSL), which uses FDD transmission and is designed to offer either asymmetric or symmetric services. VDSL utilizes frequencies up to 12 MHz and can use either quadrature amplitude modulation (QAM) or DMT modulation. VDSL DMT-based systems operate in the so-called digital-FDD (D-FDD) mode also known as Zipper-DMT. With the Zipper-DMT the downstream and upstream transmission directions are synchronized in time and rely on signal orthogonality to avoid the near echo without deploying filters to separate the downstream bands from the upstream bands. The near echo is an undesired signal that leaks into the received path from the transmit path. VDSL supports asymmetric services with downstream bitrates up to 52 Mbit/s and upstream bitrates up to 6.5 Mbit/s, and symmetric services with up to 26 Mbit/s in both directions. Currently, the ITU standardization body is working in specifying the VDSL2 standard, which uses only Zipper-DMT. In VDSL2 there are proposals to use frequencies up to 30 MHz.

The topology of DSL access networks is the same as that of local telephone access networks. This is because DSLs use the same infrastructure as used to offer analog telephone services. DSL access networks have special distributed topologies, which mainly depend on the distribution of customers. Currently, DSL systems are usually deployed from a central office, but in the near future DSL systems (especially VDSL and VDSL2) will also be deployed from cabinets. This is either to shorten the length of the subcarrier lines to offer high bitrates or to extend the coverage area with DSL services. To connect the cabinet to the central office optical fiber communication systems will be used in general.

Access networks used by DSL systems were designed and optimized to carry voice-band signals in frequencies up to 4 kHz. The signals travelling in different twisted pairs interfere with each other due to the crosstalk coupling (capacitive and inductive couplings) between the twisted pairs. This interference signal in DSL is called crosstalk. Crosstalk is the major impairment in DSL communication systems.

1.2 Research Motivation

The crosstalk coupling increases with frequency. Today's DSL systems utilize frequencies up to 12 MHz with an extension in the near future up to 30 MHz. Furthermore, in the future the penetration of deployed DSL systems will increase. As a result, the performance and reliability of DSL systems will be mainly determined by the methods used for *spectrum management* in DSL access networks. Spectrum management [5] in DSL refers to processes that are intended to minimize the potential interference between systems deployed in the same metallic loop cable and maximize the utility of the frequency spectrum of the cables.

Current DSL systems are designed as single-user systems and their spectra are fixed and optimized under the assumption that they operate in a worst-case noise environment. This conservative strategy was motivated by the goal of maximizing the reliability of DSL systems. One such form of spectrum management in DSL is usually called static spectrum management (SSM). Following this design strategy and method of spectra optimization results in overly pessimistic reach/bitrates figures and sometimes fails to deliver the specified DSL services that might have been possible.

Although each DSL system uses a single twisted pair¹ the crosstalk couplings turn the cable bundle into a common channel for all users. As a result, the DSL channel is a multi-user channel and should be considered as such, and DSL systems should be designed as multi-user communication systems. To better utilize the capacity of the multi-user DSL channel, the spectra of DSL systems should be designed jointly and optimized to adapt to the actual network environment with the aim to mitigate crosstalk. This approach of assigning cable resources to customers adaptively is called dynamic spectrum management (DSM)².

In wireless systems an immense amount of work has been done to characterize the multi-user communication techniques that can be deployed to mitigate interference (crosstalk). The basic ideas from wireless techniques can also be applied in DSL systems. However, there are some fundamental differences in DSL, especially concerning the channel transmission characteristics. The DSL channel is quasi-static and changes very slowly over time in contrast to the time-variant wireless channel. Therefore, we can assume that the channel in DSL is perfectly known at the transmitter and the receiver in advance. In wireless communications, a flat-fading channel can often be assumed for practical implementation; thus, the total power control for each user is sufficient to mitigate the interference. In DSL, in contrast, the twisted-pair channels are severely frequency-selective.

Due to the transmission characteristics of the multi-user DSL communication channel,

¹Some DSL systems may use multiple twisted pairs, but they can be seen as independent DSL systems, each of them using a single twisted pair.

²Note that the term DSM is also used to describe techniques that aim to cancel crosstalk.

we should consider for each user the allocation of power versus frequency and a total power control to minimize the performance loss due to crosstalk. This should be performed in both transmission directions, because DSL systems offer bi-directional transmission. In this work, we assume that DSL systems use an FDD transmission scheme, which reduces the complexity of the DSL system, because it eliminates the need for an echo canceler. In general, the performance loss by using FDD is negligible, especially when we see the complexity of an FDD system compared to the complexity of an EC system. If not otherwise stated we further assume that we use synchronous Zipper-DMT systems. This is because both residual near-echo and self-NEXT can be cancelled completely in the digital domain without increasing the complexity of the DSL systems. Furthermore, in Zipper-DMT systems (and also in any DMT based system) any power level can be loaded in each subcarrier.

Currently deployed DSL systems assume a fixed frequency band plan. A fixed band plan in DMT systems results in a fixed subcarrier allocation assigned to the downstream and upstream transmission directions. Using a fixed band plan often prevents service providers from offering desired symmetric and asymmetric services to customers. To use the capacity of the multi-user DSL channel in an optimal way, we should also search for an optimal band plan in addition to the optimal power allocation and the total power control for each transmission direction and each user. In this thesis, the term *user* is generic, comprising a twisted-pair line and two modems located at both ends of the line. To simplify the optimization problem we assume that the band plan is common to all users. With Zipper-DMT each subcarrier can be assigned either to the downstream or to the upstream direction. Unfortunately, the Zipper concept does not tell us which is the best band plan to achieve the desired services.

1.3 Research Contributions

In general the optimization problems for finding the optimal band plan and optimal power allocations for all users are very challenging from a computational point of view. This is because such optimization problems are high-dimensional and involve both discrete and continuous variables. For a multi-user DSL channel, where the aim is to mitigate the crosstalk, the optimization problem is unfortunately unsolvable with existing algorithms. This is due to its non-convexity. The optimization problem is non-convex even for a fixed band plan if only optimal power allocations are considered.

The main contributions of this thesis are two new algorithms to solve the problem of determining an optimal band plan and optimal power allocations in a multi-user DSL channel in a sub-optimal way: the normalized-rate iterative algorithm (NRIA) and the constrained normalized-rate iterative algorithm (C-NRIA). The difference between the two algorithms is that they optimize the utilization of the cable capacity under different constraints. Both algorithms are simple to implement and have low computational complexity. As a result they can be deployed in any network scenario with any number of users.

The NRIA and the C-NRIA can be deployed in all DMT based systems, particularly in VDSL (DMT based) and VDSL2, to find an optimized band plan and optimized power allocations for all users in both transmission directions simultaneously. Even if ADSL,

ADSL2, and ADSL2+ are designed to have fixed band plans, the NRA and C-NRA algorithms can still be deployed to find optimized power allocations.

This thesis is based mainly on the following papers:

- I. D. Statovci, T. Nordström, and R. Nilsson, “The normalized-rate iterative algorithm: A practical dynamic spectrum management method for DSL,” *Accepted for publication in EURASIP Applied Signal Processing Advanced Signal Processing Techniques for Digital Subscriber Lines*, 2005.
- II. D. Statovci and T. Nordström, “Adaptive subcarrier allocation, power control, and power allocation for multiuser FDD-DMT systems,” in *Proc. of the IEEE International Conference on Communications, ICC*, Paris, France, Jun. 2004, pp. 11–15.
- III. D. Statovci and T. Nordström, “Adaptive resource allocation in multiuser FDD-DMT systems,” in *Proc. of the European Signal Processing Conference, EUSIPCO*, Vienna, Austria, Sep. 2004, pp. 1213-1216.
- IV. D. Statovci, T. Nordström, and R. Nilsson, “The constrained normalized-rate iterative algorithm,” *submitted to the IEEE Global Telecommunications Conference, GLOBECOM*, 2005.
- V. T. Nordström, D. Bengtsson, and D. Statovci, “Simulating xDSL,” *to be submitted for publication*, 2005.
- VI. D. Statovci, R. Nilsson, and T. Nordström, “Generic detection model for DMT based modems,” *ETSI/STC TM6 contribution 034t23r2*, Nov. 2003.

1.4 Outline of the Thesis

This thesis contains seven chapters, whose content we briefly describe here.

Chapter 1 briefly gives an overview of DSL technologies, the motivation for the research, summarizes research contributions, and gives a short outline of this thesis.

Chapter 2 describes the DSL environment and reviews the fundamental principles of DSL transmission systems. First, we start by giving a short overview of the DSL access network structure. Then we describe in detail discrete multi-tone (DMT) modulation including the DMT transmission system and Zipper-DMT. We show how to select the Zipper-DMT parameters in multi-line environments. Afterwards we briefly compare DMT modulation with single-carrier modulation (SCM) and highlight the advantages of DMT over SCM in practical DSL transmission systems. At the end of this chapter we describe the typical noise sources encountered in DSL and how different noise sources are modeled and their power spectral densities (PSDs) are calculated analytically. Parts of this chapter have been published in paper V.

Chapter 3 gives a survey of spectrum management for DSL. We will describe two forms of spectrum management for DSL systems: static spectrum management (SSM) and dynamic spectrum management (DSM). We briefly describe the American National Standards Institute, ANSI, T1.417 standard for SSM and mention the drawbacks of SSM in real network environments. We describe upstream power back-off (UPBO) for DSL in more detail as one of the most advanced techniques for SSM. Then, we give the description of state-of-the-art of DSM where we describe conceptually the most promising techniques and the main algorithms proposed. Parts of this chapter have been published in papers V and VI.

Chapter 4 presents a novel practical solution for dynamic spectrum management in digital subscriber line systems: the normalized-rate iterative algorithm (NRIA). Supported by a novel formulation of the optimization problem, the NRIA is the only DSM algorithm that jointly addresses spectrum balancing for D-FDD systems and power allocations for all users sharing a common cable bundle. With a focus on being easily implementable and having a low computational complexity rather than obtaining the highest possible theoretical performance, the NRIA is designed to solve the DSM optimization problem efficiently with the operators' business models in mind. This is achieved by using two types of parameters: the desired network asymmetry and the desired user priorities. The NRIA is a centralized DSM algorithm for finding efficient power allocations for all users and an optimized band plan common to all users. In this chapter we also analyze the complexity of the NRIA and show how to initialize the input parameters in the NRIA to achieve good performance and fast convergence. Parts of this chapter have been published in papers I, II, and III.

Chapter 5 describes the properties of the NRIA and compares the performance of the NRIA with the other algorithms proposed for spectrum management in DSL. We compare the NRIA with three other DSM algorithms: the iterative water-filling algorithm (IWFA), the optimal spectrum balancing algorithm (OSBA), and the bi-directional IWFA (bi-IWFA). We show that the NRIA achieves better bitrate performance than the IWFA and the bi-IWFA and that its performance is almost as good as the OSBA, but with dramatically lower computational complexity. Additionally, we show that the NRIA can achieve bitrate combinations that cannot be supported by any other DSM algorithm. We also compare the NRIA with the standardized upstream power back-off (UPBO) in VDSL and with an exhaustive search for an "optimal" subcarrier allocation. Parts of this chapter have been published in papers I, II, and III.

Chapter 6 extends the NRIA by ensuring predefined fixed bitrates to some of the users in the cable bundle while offering bitrates to the remaining users on a best-effort basis. We call this new DSM algorithm the constrained normalized-rate iterative algorithm (C-NRIA). We show that it is sufficient to introduce only *one* parameter, which we term the balancing parameter, to split the cable capacity among the two user groups. The C-NRIA searches for the appropriate value of this balancing parameter to split the cable capacity among these two user groups in both transmission directions. This form of cable resource allocation reflects many business scenarios where a number of users must be guaranteed specific services. Parts of this chapter have been published in paper IV.

Chapter 7 concludes this thesis with a summary of its most important results.

Chapter 2

DSL Environment

Various digital subscriber line (DSL) technologies enable transmission of high bitrates over ordinary telephone subscriber lines. The telephone subscriber line infrastructure, also named the loop plant, was designed and optimized to provide plain old telephone service (POTS) to customers in frequencies between approximately 0.3 kHz and 3.4 kHz. The same existing loop plant is used today to carry DSL signals in frequencies up to approximately 12 MHz. For future DSL systems, like VDSL2, it is proposed to utilize the frequencies up to 30 MHz; this is feasible by using sophisticated digital signal processing schemes that have become practically reasonable due to advances in microelectronics. A loop plant intended and optimized for both POTS and DSL would have been designed quite differently compared to the current infrastructure designed only for POTS. This would particularly concern the design of cables [51].

This chapter presents the fundamental principles of DSL transmission systems and the DSL environment in order to give a better understanding of the problems to be analyzed in subsequent chapters. This chapter proceeds as follows. Section 2.1 gives a short overview of the DSL access network structure. Section 2.2 describes in detail discrete multi-tone (DMT) modulation, including the DMT transmission system and digital duplexing technique. Section 2.3 briefly compares DMT modulation with single-carrier modulation (SCM). Section 2.4 describes the typical noise sources encountered in the DSL loop plant and how the different noise sources are modeled and their power spectral densities (PSDs) are calculated analytically.

2.1 DSL Access Network Structure

DSL access networks usually have the same structure as local telephone access networks. This is because DSL technologies use the same telephone subscriber line infrastructure to offer different services to customers. The telephone subscriber line infrastructure is also named the loop plant [100, 101]. The term loop refers to a single twisted-pair telephone line used to connect a customer to a central office (CO). Loop plants have different structures from country to country, and moreover, they very often have different structures within the same country.

The structure of a loop plant depends mainly on the number and distribution of customers that a single CO serves and the constraints under which the loop plant is designed. For illustration purposes, Figure 2.1 shows the loop length distribution in different countries. It can be seen that each country has a different loop length distribution. For instance, the average length of loops in Italy is approximately 1.2 km, whereas in the United States

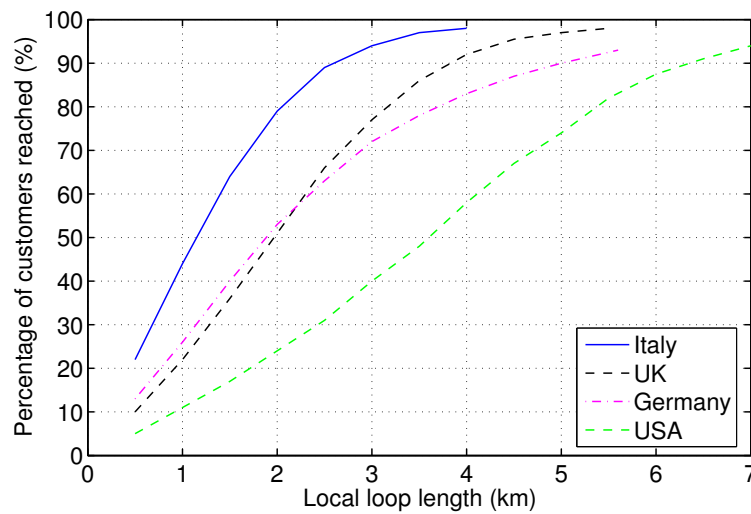


FIGURE 2.1: The loop length distribution in different countries (source: [89]).

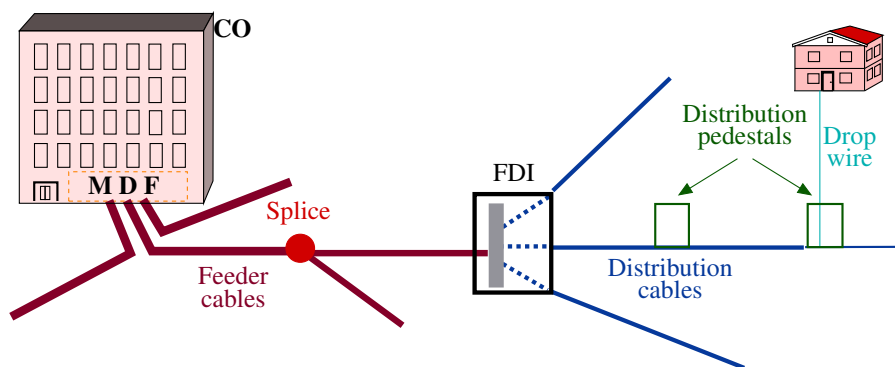


FIGURE 2.2: Structure of a typical loop plant. CO is the central office, MDF is the main distribution frame, FDI is the feeder distribution interface.

it is approximately 3.6 km. Nevertheless, a typical loop plant has a structure as shown in Figure 2.2.

The first cable section in the loop plant is the feeder plant. The feeder plant connects the main distribution frame (MDF), which is located inside the CO, with many feeder distribution interfaces (FDIs). The MDF is a large wire cross-connect frame that permits any incoming line to be connected to any port of any CO equipment. Depending on the number of customers that a CO serves, in a single MDF many feeder plant cables can be terminated. One CO can serve over 100,000 telephone lines. The task of feeder plant cables is to link the CO to the customer areas with large numbers of customers. One feeder plant cable typically contains from 1,500 to 3,000 lines. The length of feeder plant cables is usually smaller than 3 km. A single feeder plant cable can be spread out in two or more feeder plant cables as shown in Figure 2.2 in the node labelled splice.

The FDI typically serves from 1,500 to 3,000 lines and has only a cross-connect field and no active electronics. FDI's are usually located no more than 1 km from the customer

premise equipment (CPE). The loops emanating from an FDI are called the distribution plant. The cables used in the distribution plant are called distribution cables and contain 25 to 1,000 twisted pairs. At the distribution terminal or wiring pedestal the distribution cables are split into drop wires, each of which typically contains 4 to 6 twisted pairs. The number of wiring pedestals in a distribution cable depends very much on the distribution of customers that use the same distribution cable connected to the FDI. The twisted pairs in drop wire are mostly shorter than 300 m and are terminated at the customer premises interfaces.

There are also COs that serve only several hundred telephone lines and in these cases there are no feeder plant cables and distribution cables are connected directly to MDF. Hereafter, we will usually not distinguish between the FDIs and the pedestals, but rather refer to them both as the cabinet.

Sometimes other services like POTS and ISDN¹ must coexist together with some particular DSL services on the same twisted pair. The easiest way to fulfill this constraint is to divide the frequencies between the two services by using frequency division multiplexing. However, the signal levels outside the frequencies used for transmission in those particular DSL systems as well as POTS or ISDN systems are still above the allowed levels. To reduce the signals to acceptable levels a splitter filter, which consists of a low-pass filter and a high-pass filter, is installed at the point where those particular DSL services enter into the loop plant at the CO side and at customer side. The splitter filter separates the high-frequency signals used for those particular DSL services from the low-frequency signals used for POTS and ISDN services.

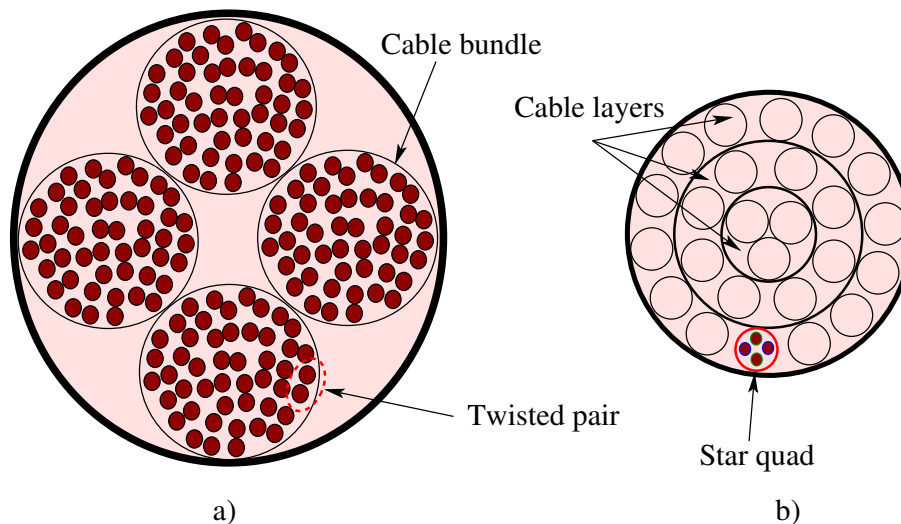


FIGURE 2.3: Twisted-pair cable topologies: a) with four bundles of 25 pairs each, b) of a layered cable with 25 star quads.

Twisted pairs within a cable are grouped into bundles (sometimes called basic bundles) of 10, 25, or 50 twisted pairs. The logical internal layout of a cable with four bundles of 25 twisted pairs each is shown in Figure 2.3a. The twisted pairs within a bundle have no specific topology, but they are all twisted together arbitrarily. However, in some countries,

¹We consider ISDN as a DSL service, as do many other authors.

TABLE 2.1: Wire diameters and loop resistances of non-loaded loops at DC of typical cables at 21°C (source: [100]).

Wires diameter		Loop resistance
in AWG	~ in mm	in Ω/km
28	0.32	426
26	0.4	274
24	0.5	172
22	0.63	108

e.g., Austria, layered cables are used. In these layered cables the twisted pairs are grouped into star quads and star quads within a bundle are organized in layers, for example as shown in Figure 2.3b for a cable (it can also be a bundle) with 25 quads. For a detailed description of different cable layout structures see [88] and the references therein.

To keep the loop attenuation as low as possible, with the goal of better transmission quality, it is required to have low loop resistance values. Low loop attenuation can be achieved by using wires with larger diameters. But, using wires with larger diameters becomes impractical when we get close to the CO due to the huge number of lines feeding in. Usually, the feeder plant cables have wires with a diameter of 0.32 mm or 0.4 mm. In other parts of the loop plant, cables with thicker wires are used. Table 2.1 shows the typical wire diameters of cables used in the loop plant as well as their typical loop resistance values at DC at a temperature of 21°C. In some standardization bodies and countries the wire diameters are given in American wire gauges (AWG) and not in metric values.

In cases where the loop length is longer than 5.5 km, the attenuation and the transmission characteristics of the twisted pair inside the voice band become so bad that the speech quality is not acceptable. To reduce attenuation of the voice, series inductance (load coils) are placed at fixed length intervals along the loop. The loops that include load coils are called loaded loops. The drawback of loaded loops is that they have unacceptable attenuation above the voice band and cannot be used for DSL transmission at all. Therefore, to use such loops for DSL transmission first all loading coils must be removed.

In some countries, so-called bridged taps are used. A bridged tap is an additional unused twisted pair connected to a subscriber loop at one end and is unterminated at the other end. The main reason for using bridged taps was to permit more users to reuse the same twisted pair along the cable route. The reflection of signals from the open end of a bridged tap causes signal loss and distortion. In the United States approximately 80% of loops include bridged taps [100]. In Europe bridged taps are uncommon. To model the twisted-pair channel different empirical models have been developed. For a description of different empirical models the interested reader is referred to [114] and the references therein.

With the aim of shortening the subscriber loop length, digital loop carrier (DLC) systems are deployed in many countries. A DLC system replaces a large number of lines in the feeder plant cable between the CO and FDI with a particular multiplexing system. Recent DLC systems use optical fibers as a physical medium for data transmission. Fur-

thermore, in the near future it is foreseen to shorten the subscriber loop length further by deploying optical fibers down to the distribution pedestals (cabinets) with so-called fiber-to-the-cabinet (FTTCab) systems. Due to the shortening of the subscriber loop length and deploying new systems such as VDSL and VDSL2 bitrates up to 100 Mbit/s can be delivered to each user.

2.2 Discrete Multi-Tone Modulation

Multi-carrier modulation (MCM) is a special form of frequency division multiplexing (FDM) [9], where a given transmission bandwidth is partitioned into many narrowband channels. These narrowband channels are usually called subchannels. In MCM a data stream to be transmitted is divided into several data streams that are sent over the transmission channel in parallel. These data streams are used to modulate several subcarriers. The term “subcarrier” in DSL is called a tone by some authors, but we will use the term subcarrier throughout this work. In wireline transmission systems the type of MCM that uses the discrete Fourier transform (DFT) to perform channel partitioning is termed discrete multi-tone (DMT) modulation. As an aside, a similar MCM scheme used in wireless transmission systems is termed orthogonal frequency division multiplexing (OFDM).

The transmission characteristics of a twisted-pair channel are strongly frequency selective, because the attenuation of the twisted pair increases with the frequency. However, when we select the subchannels “sufficiently” narrow, the subchannel’s transmission characteristics can be considered as frequency non-selective. Therefore, DMT transmission systems allow very simple equalization; this is one of the main reasons why they have recently received much attention for deployment in practical systems compared to single-carrier modulation (SCM) transmission systems, which usually require very complex equalization schemes.

In this section, we first describe basic principles of DMT transmission systems. Then we show how the so-called digital duplexing is implemented, which allows bi-directional transmission without a guard band between the downstream and upstream transmission bands. We will also analyze the deployment of the digital duplexing technique in multi-line DSL transmission environments.

2.2.1 DMT Transmission System

In early MCM transmission schemes [16, 91] it was proposed to use a bank of sinusoidal generators as subcarrier frequencies and that these MCM systems should operate in continuous time. To keep the interference between the subchannels low, a precise phase offset and sampling time are required in receiver for each subcarrier. Therefore, the practical implementation was very complex and the whole approach was even questioned. However, Weinstein and Ebert [119] have shown that the modulation and demodulation processes in the MCM scheme can be performed by means of inverse DFT (IDFT) and DFT respectively. Furthermore, Weinstein and Ebert have also shown that when the output of IDFT symbols are applied serially to a digital-to-analog (D/A) converter and a low-pass filter, a signal is obtained at the output that closely approximates the signal obtained by an ideal system that uses a bank of sinusoidal generators. Therefore, a bank of sinusoidal

generators is not required and the complete modulation and demodulation can be implemented digitally. Due to the digital implementation of modulation and demodulation the implementation complexity of such a transmission system is tremendously reduced.

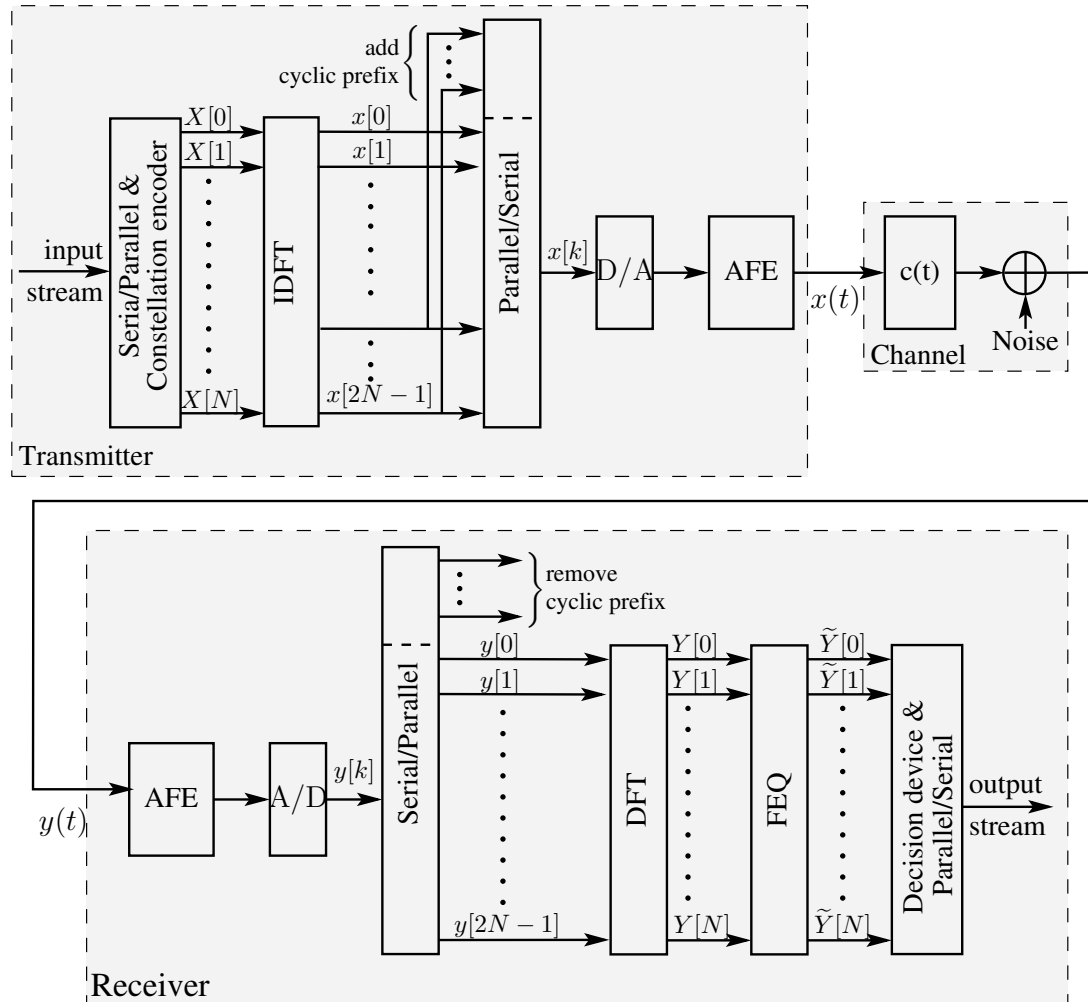


FIGURE 2.4: A basic DMT transmission scheme where a cyclic prefix is used as a guard interval. DFT denotes discrete Fourier Transform; IDFT denotes inverse DFT; D/A and A/D are digital-to-analog and analog-to-digital converters, respectively; AFE is analog front-end; FEQ is frequency-domain equalizer, N denotes the number of subcarriers at positive frequencies and of the “subcarrier” at DC.

Figure 2.4 shows a simplified scheme of a DMT transmission system for the case where a cyclic prefix is used as a guard interval between two successive DMT symbols. DMT is a baseband MCM scheme, therefore, the output of the IDFT in principle is converted to a serial stream and the resulting low-pass filtered analog signal is transmitted over the channel. The overall impulse response of all transmission components between D/A and analog-to-digital (A/D) converters has a non-ideal impulse response. Thus, successive transmission of DMT symbols causes inter-symbol-interference (ISI) and inter-channel-interference (ICI) in the receiver. The ISI is defined as the interference between signals within the same subchannels of successive DMT symbols and the ICI is defined as the

interference between adjacent subchannels within the same DMT symbol. To avoid ISI and ICI a guard interval is inserted between two successive DMT symbols, as will be explained in Section 2.2.1.2.

2.2.1.1 DMT Transmitter

DMT modulation is a block transmission technique, so the input data stream in the “Serial/Parallel & Constellation encoder” in Figure 2.4 is blocked successively. The values of the time-domain coefficients $x[k]$, for $k = 0, \dots, 2N - 1$, in the output of IDFT must be real due to the fact that the twisted-pair channels have baseband transmission characteristics. To assure this constraint the frequency-domain components $X[n]$ with indices greater than N (we assume throughout this work that N is always an even number) must be selected as complex conjugates of the frequency-domain components with indices smaller than N ; namely

$$X[n] = X^*[2N - n], \quad \text{for } n = N + 1, N + 2, \dots, 2N - 1. \quad (2.1)$$

Furthermore, the frequency-domain components $X[0]$ and $X[N]$ must be real, because the subchannels assigned to the subcarrier at DC ($n = 0$) and at the Nyquist frequency ($n = N$) have half of the bandwidth of the other subchannels [30]. With this selection of parameters the number of signal dimensions within a DMT symbol is twice the number of subcarriers. This DMT transmission system is usually called a transmission system with N subcarriers (not counting the “special subcarrier” at DC) and with $N + 1$ subchannels, as illustrated in Figure 2.5. Note that the spectrum in Figure 2.5 is shown for positive frequencies and therefore we have not shown the “subcarriers” in the negative frequencies. Due to the complex conjugate symmetry in (2.1) the spectra of subcarriers in the negative frequencies mirror the spectra of the subcarriers in the positive frequencies.

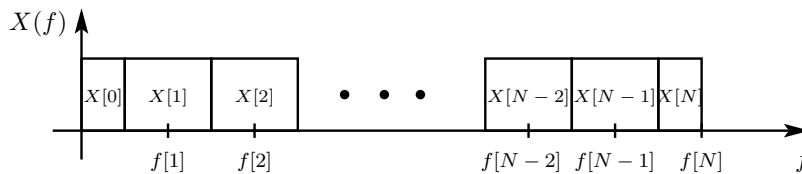


FIGURE 2.5: Illustration of subcarriers and subchannels, and allocation of frequency-domain components over the subchannels in a DSL DMT-based system.

Each data block of the input data stream is divided into $N + 1$ sub-blocks and each sub-block includes $R[n]$ bits. The bits $R[n]$ are transmitted over the n -th subchannel. Thus, the total number of bits R that are transmitted in a DMT symbol is

$$R = \sum_{n=0}^N R[n].$$

The number of bits $R[n]$ that can be transmitted in a subchannel n depends on the transmit signal power, the channel transfer function, and the noise on that particular subchannel.

Theoretically, this number $R[n]$ can take any nonnegative real value (also zero). However, in the current DMT systems it takes only nonnegative integer values, usually in the range 0 to 15. The ‘‘Constellation encoder’’ in Figure 2.4 maps these $R[n]$ bits to one of $2^{R[n]}$ points in an appropriate signal constellation. For the reasons explained above the signal constellations for subchannels with indices 1 to $N - 1$ are quadrature amplitude modulation (QAM) constellations, whereas for subchannels 0 and N they are pulse amplitude modulation (PAM) constellations.

The time-domain coefficients of the m -th data block in the output of the IDFT, $x_m[k]$, are calculated as

$$x_m[k] = \frac{1}{\sqrt{2N}} \sum_{n=0}^{2N-1} X_m[n] e^{j\frac{2\pi}{2N}nk}, \quad \text{for } k = 0, 1, \dots, 2N - 1, \quad (2.2)$$

where $X_m[n]$ is the frequency-domain component of subchannel n associated with the m -th data block. The frequency-domain components are the values of the signal constellation points that are selected depending on the input data values. In practical systems the subchannels indexed with 0 and N are usually not used, in which case $X_m[0] = X_m[N] = 0$ for all m . Therefore, throughout this work we will use the terms subcarrier and subchannel interchangeably. Under the assumption that $X_m[0] = X_m[N] = 0$ for all m , (2.2) can be written as

$$\begin{aligned} x_m[k] &= \frac{1}{\sqrt{2N}} \sum_{n=1}^{N-1} \left(X_m[n] e^{j\frac{2\pi}{2N}nk} + X_m^*[n] e^{-j\frac{2\pi}{2N}nk} \right) \\ &= \sqrt{\frac{2}{N}} \cdot \Re \left\{ \sum_{n=1}^{N-1} X_m[n] e^{j\frac{2\pi}{2N}nk} \right\}, \quad \text{for } k = 0, 1, \dots, 2N - 1, \end{aligned}$$

When we represent the frequency-domain components $X_m[n]$ and time-domain coefficients $x_m[k]$ in vector form,

$$\begin{aligned} \mathbf{X}_m &= [X_m[0], X_m[1], \dots, X_m[2N - 1]]^T, \\ \mathbf{x}_m &= [x_m[0], x_m[1], \dots, x_m[2N - 1]]^T, \end{aligned} \quad (2.3)$$

(2.3) can be represented as

$$\mathbf{x}_m = \text{IDFT}(\mathbf{X}_m).$$

The IDFT can be efficiently calculated with the inverse fast Fourier transform (IFFT) [80, Chapter 9]. Hereafter, we will not distinguish between \mathbf{x}_m and \mathbf{X}_m , but we call them the m -th DMT symbol.

The twisted-pair channels do not fulfill the Nyquist criterion [85] for a distortion-free transmission, because the twisted-pair channels are dispersive. Therefore, successive transmission of DMT symbols over the channel in the receiver causes ISI and the subcarriers will also lose the orthogonality resulting in ICI. Thus, for successive symbol transmission and a non-ideal impulse response the DMT channel partitioning does not satisfy the generalized Nyquist criterion [30] necessary for an ISI- and ICI-free transmission. Techniques for avoiding ISI and ICI are presented in the following subsection.

2.2.1.2 Guard Interval Insertion

As we mentioned, successive transmission of DMT symbols over a non-ideal channel causes ISI and ICI, which appear at the output of the DFT in the receiver. To avoid ISI and ICI a guard interval is inserted between two successive DMT symbols before they are transmitted over the channel. The serial concatenation of the data included in the DMT symbol and the redundant data included in the guard interval will be called a transmitted DMT symbol. Depending on the redundant data that are added in the guard interval, there are two main strategies: addition of a cyclic prefix (CP) and zero padding (ZP). We analyze here in more detail the adding of CP, first proposed in [81], at the transmitter as shown in Figure 2.4, because it is used in all current and perhaps future DMT transmission systems.

The CP is simply a repetition of the last L_p time-domain coefficients from the DMT symbol being transmitted at the beginning of the DMT symbol as shown in Figure 2.6. The length of CP is selected such that: $L_p \geq L - 1$, where L is the overall impulse response between the D/A and A/D blocks in Figure 2.4 counted in sample periods. The CP causes the transmitted sequence (the transmitted DMT symbol) to appear periodic to the channel with memory of length L_p , and therefore provides the required condition for the discrete convolution theorem to hold [81]. Thus, due to the adding of the CP to the DMT symbol before transmission over the channel, the linear convolutive channel is converted to a circular one. For this reason addition of a CP provides an ISI- and ICI-free transmission over dispersive communication channels, such as twisted-pair channels.

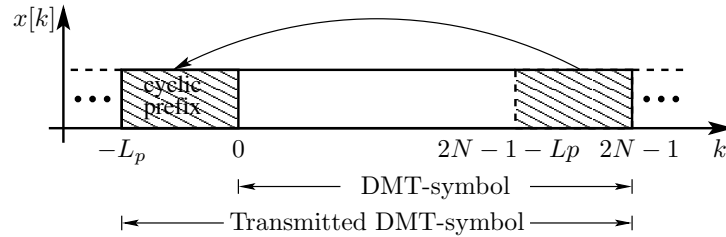


FIGURE 2.6: Illustration of adding a cyclic prefix (CP) with length L_p to a DMT symbol.

The m -th transmitted DMT symbol $x_m^{\text{CP}}[k]$ is given by

$$x_m^{\text{CP}}[k] = \begin{cases} x_m[k + 2N], & \text{for } k = -L_p, -L_p + 1, \dots, -1, \\ x_m[k], & \text{for } k = 0, 1, \dots, 2N - 1. \end{cases} \quad (2.4)$$

Substituting (2.2) into (2.4) and using the $2N$ -periodicity of the complex functions $e^{j\frac{2\pi}{2N}nk}$, the m -th transmitted DMT symbol $x_m^{\text{CP}}[k]$ can also be written as

$$x_m^{\text{CP}}[k] = \frac{1}{\sqrt{2N}} \sum_{n=0}^{2N-1} X_m[n] e^{j\frac{2\pi}{2N}nk}, \quad \text{for } k = -L_p, \dots, -1, 0, 1, \dots, 2N - 1, \quad (2.5)$$

The discrete signal $x[k]$ in the output of serial-to-parallel block is given as a concate-

nation of all transmitted DMT symbols $x_m^{\text{CP}}[k]$:

$$x[k] = \sum_{m=-\infty}^{\infty} x_m^{\text{CP}}[k - m(2N + L_p)], \quad \forall k.$$

We can transmit only continuous time-domain signals over a twisted-pair channel. Therefore, the discrete-time sequence $x[k]$ must be converted into a continuous-time signal. This transformation is done by means of a D/A converter and a low-pass filter. The low-pass filter in Figure 2.4 is included in the AFE block. In a practical realization of a DMT transmission system, the AFE comprises a low-pass analog filter, line drivers, and a hybrid. For a detailed analysis and the requirements of AFE at the transmitter and at the receiver in different DMT systems the interested reader is referred to [10, 101] and the references therein. Hereafter, we assume that D/A and A/D converters are ideal.

Let us denote the common impulse response of both D/A and AFE at the transmitter by $s(t)$. The continuous-time signal $x(t)$ of the corresponding discrete-time signal $x[k]$ transmitted over the channel is given by

$$x(t) = \sum_{k=-\infty}^{\infty} x[k]s(t - kT),$$

where T is the time duration between two successive samples at the D/A converter.

The second method that can be used to avoid ISI and ICI is to add zeros after each DMT symbol, known as zero-padding (ZP) [7, 70]. In this case, instead of removing the CP at the receiver side as in Figure 2.4, we should perform the DFT on a vector of length $2N + L_p$ instead of $2N$ as explained in [94, 68]. To use the FFT algorithm to calculate the DFT we would actually need to extend the length of the input vector to $4N$. However, it is shown in [7, 70] that it is possible with some simple additional operations to reduce the size of the vector at the input of the DFT block to $2N$. Thus, the CP-based and ZP-based DMT systems have the same complexity concerning the DFT size in the receiver. Concerning transmission power ZP has advantages over CP, because in the ZP case no power is transmitted in the guard interval. However, we will show in Sections 2.2.1.4 and 2.2.2 why for DMT transmission systems (wireline systems) is recommended the CP extension over the ZP extension. Therefore, in this work we will only analyze DMT transmission systems that are CP-based. Hereafter, we will always assume that the guard interval is always longer than the duration of the channel impulse response.

Due to extending the DMT symbols by CP before transmitting them over the transmission channel, we suffer from a bandwidth-efficiency loss (a loss in bitrate) and also a loss in the transmit power compared to an ideal virtual system without a CP extension. The parameter that quantifies this loss is defined as efficiency and is given by

$$\varepsilon = \frac{2N}{2N + L_p}. \quad (2.6)$$

With respect to the bandwidth-efficiency, the efficiency parameter shows how well the available bandwidth is used for transmitting useful data. With respect to the transmit power, due to the use of signal constellations with many points and random selection of

signal points for transmission, it shows how well in the average the transmit power is used for transmitting useful data. Thus, this decrease in efficiency in the transmission system due to the CP extension is the price that we have to pay for a simplified receiver structure, as we will show in the following section.

2.2.1.3 DMT Receiver

Let us denote the impulse response of the channel by $c(t)$. The signal at the input of the receiver $y(t)$, is given by

$$y(t) = x(t) * c(t) + u(t),$$

where the sign $*$ denotes convolution and $u(t)$ is continuous-time noise on the channel.

To simplify the mathematical analysis we use from now on the equivalent discrete-time channel [85] model. For the level of detail given in Figure 2.4, the equivalent discrete-time channel comprises: D/A and A/D converters, AFE components at transmitter, AFE components at the receiver, and the channel, as shown in Figure 2.7.

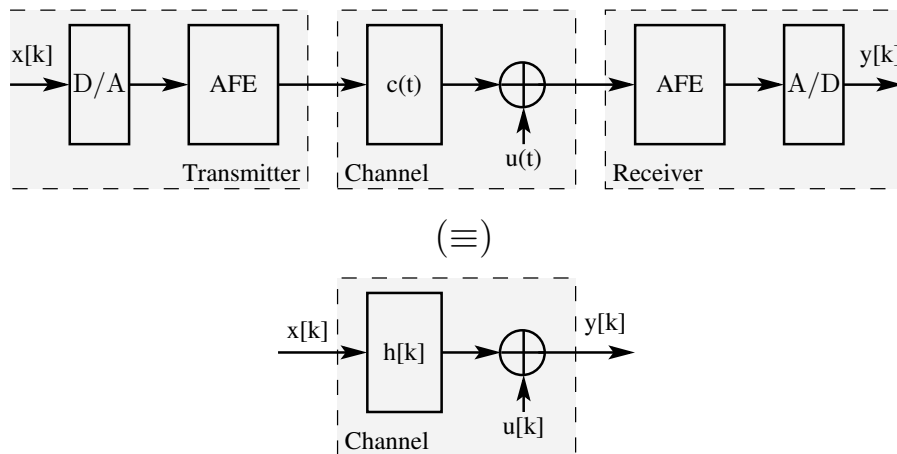


FIGURE 2.7: Equivalent discrete-time channel model.

Let us denote by $g(t)$ the common impulse responses of both AFE and A/D converter at the receiver. The impulse response of the equivalent discrete-time channel $h[k]$ is given by

$$h[k] = h(kT),$$

with

$$h(t) = s(t) * c(t) * g(t),$$

where T is again the time duration between two successive samples in the D/A and A/D converters. The received discrete signal $y[k]$ at the input of the serial-to-parallel converter

at the receiver is given by

$$y[k] = x[k] * h[k] + u[k] = \sum_{l=0}^{L-1} x[l]h[k-l] + u[k],$$

where L is the length of the impulse response of the equivalent discrete-time channel, and where $u[k]$ is discrete-time noise, which is the sampled version of the continuous-time noise $u(t)$ after it has been passed through the AFE of the receiver.

We assume that the length of the impulse response of the equivalent discrete channel is shorter than or equal to the length of the CP plus one; thus, $L \leq L_p + 1$, where L_p is the length of the cyclic prefix. For the cases when this criterion is not satisfied a time-domain equalizer can be used to reduce the impulse response of the discrete channel to $L \leq L_p + 1$. For the analysis of design methods for time-domain equalizers for DMT transmission systems and the performance of different time-domain equalizers the interested reader is referred to [44].

The received sequence $y[k]$ is blocked prior to decoding into blocks of length $2N + L_p$. Under the assumption that $L \leq L_p + 1$, there is no ISI and no ICI. After discarding the first L_p samples, the m -th received DMT symbol $\mathbf{y}_m = [y_m[0], y_m[1], \dots, y_m[2N-1]]^T$ depends only on the m -th transmitted DMT symbol \mathbf{x}_m . Both the transmitted DMT symbol \mathbf{x}_m and the impulse response of the equivalent discrete channel have a finite length. On the other hand, we want the frequency-domain components for any transmitted symbol to fulfill the criterion $Y[n] = H[n]X[n]$ as in the case of an ideal transmission channel, where $H[n]$ is the discrete Fourier transform (DFT) of $h[k]$. This is achieved by the circular convolution operation as explained in [80, pp 524]. Now, the received time-domain coefficients of the m -th block are calculated as

$$\begin{aligned} y_m[k] &= x_m[k] \circledast h[k] \\ &= \sum_{l=0}^{2N-1} x_m[l]h[((k-l))_{2N}], \quad \text{for } k = 0, 1, \dots, 2N-1, \end{aligned}$$

where \circledast denotes the circular convolution operation and $((k-l))_{2N}$ denotes $(k-l)$ modulo $2N$. The $h[k]$ values for $k > L$ are zero. The m -th received DMT symbol is usually written as

$$\mathbf{y}_m = \mathbf{H}\mathbf{x}_m,$$

where \mathbf{x}_m is the same vector as defined in (2.3) and \mathbf{H} is a $2N \times 2N$ circulant matrix [30] given as

$$\mathbf{H} = \begin{bmatrix} h[0] & 0 & \dots & 0 & h[L_p] & h[L_p-1] & \dots & h[1] \\ h[1] & h[0] & \dots & 0 & 0 & h[L_p] & \dots & h[2] \\ \vdots & \vdots & \vdots & \vdots & \vdots & \vdots & \vdots & \vdots \\ 0 & 0 & \dots & h[L_p] & h[L_p-1] & h[L_p-2] & \dots & h[0] \end{bmatrix}.$$

The $2N$ time-domain coefficients of \mathbf{y}_m are provided to the input of the DFT block in

Figure 2.4. The output of the DFT block contains the received frequency-domain components $Y_m[n]$, which are calculated as

$$Y_m[n] = \frac{1}{\sqrt{2N}} \sum_{k=0}^{2N-1} y_m[k] e^{-j\frac{2\pi}{2N}kn}, \quad \text{for } n = 0, 1, \dots, 2N-1,$$

or more compactly as

$$\mathbf{Y}_m = \text{DFT}(\mathbf{y}_m).$$

Like the IDFT, the DFT can be efficiently calculated with the fast Fourier transform (FFT) [80, Chapter 9].

The received frequency-domain components $Y_m[n]$ are then normalized independently for each subcarrier (see Figure 2.4) to compensate for the channel frequency response by

$$\tilde{Y}_m[n] = \frac{Y_m[n]}{H[n]}, \quad \text{for } n = 0, 1, \dots, N,$$

where $H[n]$ is the transfer function (a complex value) of the equivalent discrete-time channel of the n -th subcarrier that is calculated at the subcarrier frequency. This normalization process in MCM is usually called a frequency-domain equalizer (FEQ). The FEQ performs gain and phase adjustments before the data are sent to the decision device². Since the transfer function of the channel on a particular subcarrier can be time-variant, the gain and phase adjustments in DMT systems are usually performed adaptively. To estimate the gain and phase adjustments zero-forcing (ZF) algorithm is usually used. After the decision process in Figure 2.4 the data are converted to a serial data stream and sent to the output of the DMT receiver. DSL systems are designed to achieve a bit-error rate (BER) of 10^{-7} . However, in practice DMT systems works with a lower BER due to the assumption of a 6 dB noise margin (see Chapter 3). Therefore, we can assume with high probability that $\tilde{Y}_m[n] = X_m[n]$.

2.2.1.4 DMT Receiver Synchronization

Up to now, we have assumed that the synchronization between the transmitter and the receiver is perfect. In this section, we describe the methods that can be used to achieve synchronization at the DMT receiver (the DMT receiver is synchronized with the DMT transmitter). During the analysis we will always assume that the length of the CP is greater or equal than the impulse response duration of the equivalent discrete channel minus one; thus, $L_p \geq L - 1$. Otherwise, no matter how well synchronization is performed, as we have explained, there will be ISI and ICI and therefore, the receiver suffers some performance degradation. Since there is no frequency shift in the twisted-pair channel [10], the recovery of the sampling clock is equivalent to the recovery of the subcarrier frequencies.

²All “modern” DSL transmission systems use some form of channel coding. For the sake of simplicity we have not shown this in Figure 2.4, because we will include the gain achieved by channel coding schemes in our analysis by using the signal-to-noise ratio gap (SNR gap) concept as explained in Chapter 4.

In DMT transmission systems two types of synchronization can be distinguished: sample synchronization and symbol synchronization [82]. Sample synchronization guarantees frequency alignment of the D/A sampling clock at the transmitter with the A/D sampling clock at the receiver. Symbol synchronization guarantees detection of the correct DMT symbol boundaries from the received signal and determines which $2N$ samples should be forwarded to the DFT block.

The initial synchronization between transmitter and receiver is performed during the initialization phase, which is called acquisition [93]. Usually the sampling clocks in the DSL system are generated locally by a crystal oscillator, so any DMT system uses a mechanism to correct continuously for a possible sampling clock offset. The process by which the receiver maintains the correct sampling frequency is called tracking [93].

Conceptually, based on the data used to perform synchronization at the receiver, synchronizers can be divided into two groups. In the first group redundant data are transmitted over the channel for the aim of synchronization in the form of a pilot signal at a known subcarrier. This form of synchronization is used in ADSL [5, 58] transmission systems and is an optional choice for VDSL [3, 40]. The second form of synchronization operates on the redundant data in the received bearing signal that are included in the cyclic prefix [112]. However, it is worth mentioning that a method has also been proposed for synchronization [93], in which known DMT symbols are transmitted repeatedly during the modem initialization phase for synchronization purposes. During the modem operation phase the synchronization is maintained based on the decoded bearing data.

The performance of DMT transmission systems is very sensitive to the sampling clock offset. The sampling clock offset is compensated only at the remote side (customer premises modem) since the same recovered clock is used for both detection of downstream data and modulation of the upstream data, thereby not requiring any pilots in the upstream direction. This process is known as loop timing [100]. The effects of a sampling clock frequency offset are twofold [82, 84]: the useful signal symbol is rotated and attenuated; and it gives rise to ICI. To correct the sampling frequency offset in the continuous time domain it is possible to use a voltage-controlled crystal oscillator (VCXO) [30] as part of a phase locked loop (PLL) [30]. However, in DMT systems it is more common to perform the correction digitally for simplicity of implementation. Pollet *et al.* [82] have shown that the correction can be performed in the discrete-time domain, in the frequency domain, or in the hybrid time/frequency domain. The hybrid time/frequency domain method is considered by Pollet *et al.* [82] as the most suitable for DMT systems. The same authors study the performance of the hybrid time domain/frequency domain method in [83]. Hereafter, we will no longer consider the sampling clock offset, but we will assume that it is recovered perfectly by one of the methods mentioned in this paragraph.

Even if the sampling clock is recovered accurately, because DMT systems process data in blocks, the right samples (DMT symbol) should be selected to be forwarded to the DFT block. A correct alignment of the received DMT symbols with the DFT window is crucial for the performance of a DMT transmission system. As Figure 2.8 shows, we can distinguish four cases. In the first case, there is a perfect alignment of the DFT window with the received DMT symbol. In this case, we only remove the CP and the remaining $2N$ samples are forwarded to the DFT block. In the second case, we assume that the DFT window is misaligned by a time shift in sample periods to the left but with no more than $T_{\Delta} = L_p - L + 1$ samples, where L_p is the length of the CP and L is the length of the

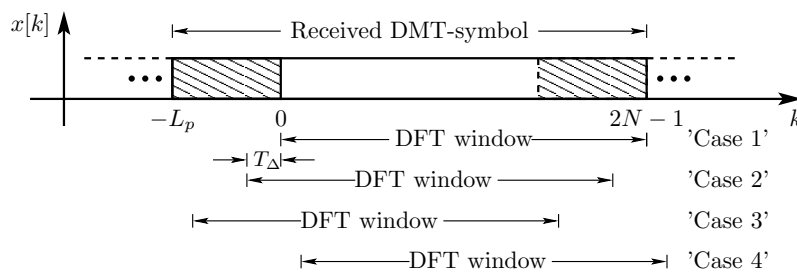


FIGURE 2.8: Illustration of possible alignments of the DFT window within the received DMT symbols.

impulse response of the equivalent discrete-time channel. Note that we have assumed in the introduction of this section that $L_p \geq L - 1$. In this case, due to the CP extension it is still possible to decode the DMT symbol correctly, because the last $2N$ samples forwarded to the DFT block are valid samples, but are merely shifted cyclicly by T_Δ samples. This shifting can be corrected by cyclicly shifting in the time domain or equivalently by phase rotation in the frequency domain. In practice this correction is usually performed in the frequency domain while performing equalization. This is one of the advantages of the CP extension over the ZP extension. In the third and fourth cases, the DMT symbols are unrecoverable, because after removing the initial CP samples, the $2N$ samples forwarded to DFT comprise samples from two DMT symbols.

To achieve DMT symbol alignment different symbol synchronization algorithms have been proposed. The most straightforward way to find the boundary of a DMT symbol is to exploit the redundant data in the cyclic prefix [56, 112, 113]. In this method the starting position of the DMT symbol is found by performing a continuous cross-correlation at the output of the A/D converter between the conjugate sampled signal and the sampled signal delayed by $2N$ samples. The maximum of the cross-correlation indicates the symbol boundaries.

2.2.2 Digital Duplexing Technique for DMT systems

DSL transmission systems usually use the same twisted pair for transmitting data simultaneously in the downstream and upstream transmission directions, which is usually called bi-directional transmission. To separate the downstream and upstream signals, both the European Telecommunication Standards Institute, ETSI, and the American National Standards Institute, ANSI, very high speed DSL (VDSL) standards use frequency division duplexing (FDD). Practically, we can use an echo canceler to cancel the so-called near echo signal, which is an undesired signal that leaks through the hybrid circuit in the received path from the transmit path. However, in general the performance loss by using FDD is negligible³, especially when we see the complexity of an FDD system compared to the complexity of an EC system. The definition of self-NEXT is given in Section 2.4.2

We have shown in Section 2.2.1.2 that in DMT transmission systems the orthogonality between the subcarriers used in the same transmission direction is maintained by inserting

³Strictly speaking, some performance improvement of the echo cancelled transmission scheme over the FDD transmission scheme can be obtained if in DMT-based systems the subcarriers with a moderate self-NEXT noise are used for both transmission directions simultaneously.

a guard interval, usually a CP, between two successive DMT symbols. However, if the orthogonality between the downstream and upstream subcarriers in the FDD transmission schemes is not maintained, the near echo is not orthogonal to the desired received signal. The near echo is especially high in the subcarriers that are located near the edges that separate downstream and upstream transmission bands. Furthermore, concerning the multi-user case there is also self-NEXT noise. To remove (or at least to reduce to a negligible level) the near echo signal and self-NEXT noise we can deploy a band-pass filter for each subband and insert a frequency guard band between the downstream and upstream bands as in ADSL [58]. However, this would increase the implementation complexity in multi-band systems like VDSL [3,40] or in transmission systems in which the subcarriers are assigned adaptively to the downstream or the upstream to better serve the needs of all users.

Sjöberg *et al.* [98] have introduced a method to perform FDD for DMT systems entirely in the digital domain, which allows downstream and upstream transmission without a guard band between the downstream and upstream transmission bands. The authors called this digital duplexing technique “Zipper”. In Zipper, the orthogonality between the subcarriers assigned in the downstream and upstream directions is maintained by adding a cyclic suffix (CS) in addition to the CP before the DMT symbol is transmitted over the channel as shown in Figure 2.9. The sum of CP and CS is called the cyclic extension (CE). With Zipper-DMT any subcarrier can be allocated arbitrarily to either the downstream or the upstream direction. However, Zipper-DMT does not tell us how they should be allocated. The subcarrier allocation that optimizes the performance of all DMT systems is a very complex optimization problem, which we will analyze in detail in Chapters 4 and 6. Here, we will only graphically justify how the orthogonality between the downstream and upstream subcarriers is maintained on a single line. An analysis of Zipper-DMT when deployed in a multi-line environment is given in Section 2.2.2.1.

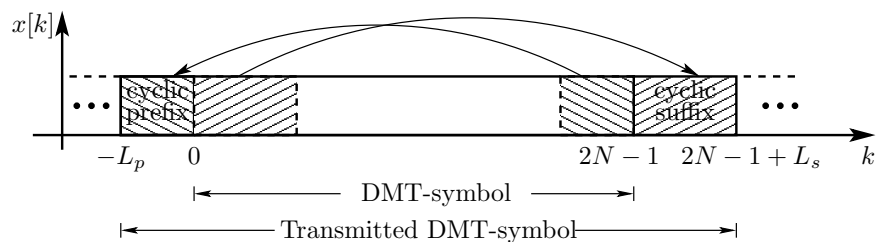


FIGURE 2.9: Illustration of adding a cyclic prefix and cyclic suffix of lengths L_p and L_s , respectively.

The DMT signal at the receiver consists of the desired received signal (the one in which we are interested in) and the signal that is transmitted in the opposite direction (as near echo signal). Therefore, in the Zipper-DMT duplexing scheme, the transmission of DMT symbols must be coordinated at both sides and both sides must work synchronously (to maintain the orthogonality between the subcarriers assigned to downstream and upstream). This is achieved by the so-called timing advance [30] technique, which ensures that the signal contribution of downstream and upstream is kept within a single DMT symbol. To achieve this goal, the length of the CS should be greater than or equal to the delay T_D (counted in sample periods) the equivalent discrete-time channel induces

in the transmitted signal. When this criterion is fulfilled the near echo signal is orthogonal to the desired received signal. Figure 2.10 illustrates the case when $T_D = L_s$ and when the length of the CS is greater than the length of the CP. It shows that the transmitters at both sides simultaneously start transmitting a new DMT symbol.

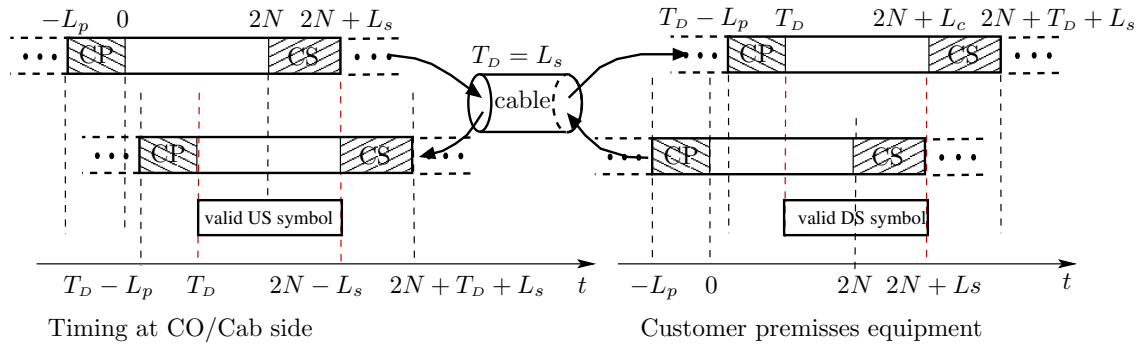


FIGURE 2.10: Illustration of how timing advance in Zipper-DMT systems achieves orthogonality between the subcarriers used in the downstream and upstream transmission directions.

The efficiency of Zipper-DMT systems is calculated similarly to the efficiency of DMT systems given by (2.6), except that the L_p is replaced with L_e , where L_p and L_e denote the length of the CP and the CE, respectively.

2.2.2.1 Digital Duplexing in Multi-Line Environments

We have shown that to maintain orthogonality between the subcarriers used in the downstream and upstream transmission directions, the transmitters at both sides must work synchronously. In a multi-line environment a receiver is not only receiving its intended signal and the near echo signal, but also the crosstalk signals from the other systems deployed in the neighboring lines. The near echo signal, self-NEXT, and self-FEXT are orthogonal to the desired received signal in the FDD transmission systems that use Zipper-DMT if the following two criteria are fulfilled:

1. The subcarrier allocations assigned in the downstream and upstream transmission directions for all users deployed in the same cable (cable bundle) are the same.
2. Orthogonality is maintained not only among the subcarriers on one line but also among the subcarriers on all lines by means of the timing advance technique.

To achieve these two conditions, all DMT systems deployed in a cable bundle have to be synchronized in both time and frequency [98]. Thus, all transmission systems must use the same sampling clock. Furthermore, the $2N$ samples forwarded to the DFT block of each user needs to comprise samples not only from a single DMT symbol of its own signals (both near echo signal and desired received signal), but also from a single DMT symbol of all crosstalk signals. An algorithm that synchronizes DMT systems autonomously when they are deployed only from the CO is proposed in [74].

One question that arises about Zipper-DMT, when it is deployed in a multi-line environment, is how to select the length of the CE (the length of CP and CS). The answer to this question is that the length of the CP should be selected as $L_p \geq L - 1$, where now L is the longest impulse response of the equivalent discrete-time channel of any line in the

cable bundle. On the other hand, the length of CS should be selected as $L_s \geq T_D$, where T_D is the longest delay in sample periods of any signal (either desired or crosstalk) in the cable bundle.

The selection of the length of the CP is obvious for any network scenario as we estimate (calculate) the impulse response of all lines independently. Therefore, we select the length of the CP to fulfill the above-mentioned criterion $L_p \geq L - 1$. In the systems that use a time-domain equalizer the length of the CP can be selected to be shorter.

The selection of the length of the CS is more tricky. Therefore, we illustrate the selection of the length of the CS for two network scenarios, each with two users, as shown in Figure 2.11. For the network scenario in Figure 2.11a, the length of the CS is determined either by the delay of the desired signal on line 2 denoted by T_{D2} , or the delay of the crosstalk signal denoted by T_{DXT} , as it is the largest delay of all possible signal paths. The highest value of either T_{D2} or T_{DXT} determines the length of the CS. For the network scenario in Figure 2.11b, the length of the CS is determined by the delay of the crosstalk signal denoted by T_{DXT} , because this is the largest delay of all possible signal paths.

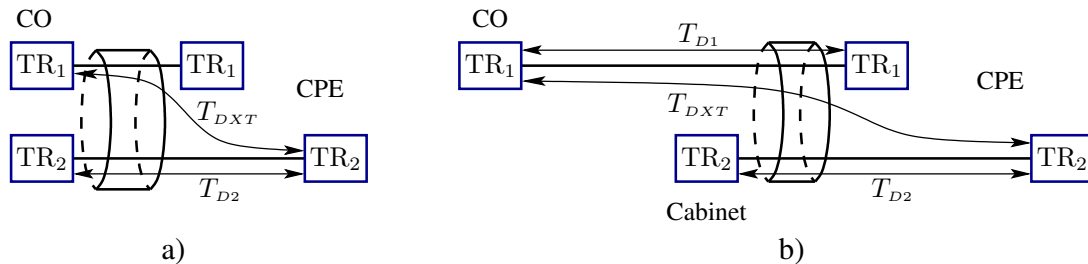


FIGURE 2.11: Illustration of the selection of the cyclic suffix length in Zipper-DMT systems; CO is the central office, CPE is the customer premises equipment, and TR denotes transceivers. a) for a network scenario with only one CO, b) for a network scenario with a CO and a Cabinet.

2.3 Comparison of DMT and Single-Carrier Modulation

We described DMT modulation in detail in the previous section. Two proposed single-carrier modulation (SCM) schemes for VDSL transmission are quadrature amplitude modulation (QAM) and carrierless amplitude/phase (CAP) modulation. Both QAM and CAP theoretically show the same performance, but for a given complexity of implementation, CAP usually performs slightly better than QAM [18]. However, since our aim here is not to analyze the performance of CAP and QAM we will assume that they show the same performance, and henceforth we will refer to them both as SCM. Note that SCM in this section does not mean that there is only one carrier frequency for a transmission direction, but merely as a generic name to distinguish it from MCM. This is because, for example, in standardized VDSL SCM-based systems up to two carriers can be used for each transmission direction. A simplified scheme of QAM-based SCM transmitter and receiver structures for a single frequency band is shown in Figure 2.12.

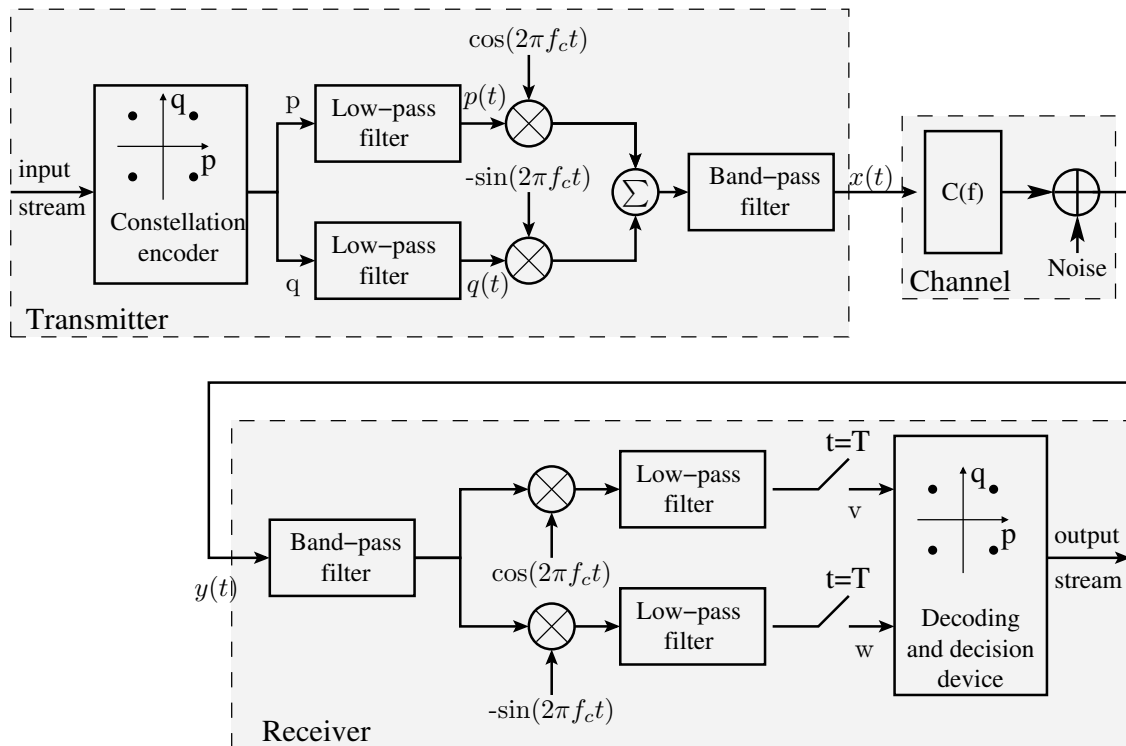


FIGURE 2.12: Simplified schematic of transmitter and receiver of QAM-based SCM transmission systems. The schematic shows only the circuit blocks for one transmission band. For the transmission systems that use more bands as for instance VDSL SCM-based systems the input of each transmission band is modulated separately. The signal to transmit over the twisted-pair channel is then generated by adding the output signals of band-pass filters.

From a theoretical point of view it is shown in [25, 26] that SCM and DMT systems have the same performance when the following two conditions are fulfilled [101]:

1. Each continuous set of adjacent used bands in the DMT system can be replaced by a single band in the SCM system whose symbol rate is equal to the width of the set of used adjacent DMT bands and whose carrier/center frequency is exactly in the middle.
2. The average number of bits/Hz must be the same in the two systems in each used band.

Thus, the relative advantages and disadvantages of SCM and DMT transmission systems depend only on practical realization aspects.

We have shown in Section 2.2.2 that in the case of DMT it is possible to perform the duplexing process entirely in the digital domain. The price that we have to pay for this, as we showed in Section 2.2.1.2 and Section 2.2.2, is the loss in transmit power and bandwidth-efficiency due to the addition of CP and CS. In the case of a standardized VDSL DMT-based modem this loss is 7.8 %. However, it can be smaller or larger when the length of the CE is selected to match a particular network scenario. The increase or decrease of CE length does not increase the complexity of the DMT system. This is a very nice property of DMT systems. In the case of SCM systems, we see in Figure 2.12 that we

need an analog band-pass filter for each transmission band. To reduce the complexity in the analog filter design the transmission bands must be placed sufficiently apart from each other. In the case of VDSL SCM-based systems we have a bandwidth loss on average of approximately 25% [29], depending on how many bands are used for transmission. Thus, DMT modulation has benefits over SCM concerning spectrum utilization.

DMT modulation is very immune to noise and has the ability to be adapted perfectly to the channel conditions. In the case of impulse noise, DMT will spread the energy of the impulse over many subcarriers due to the DFT operation in the receiver, thereby reducing the loss in performance, whereas in SCM it may cause errors at impulse amplitudes. Adding transmitter and receiver windowing in DMT modulation makes DMT systems very robust against narrowband interference like radio frequency interference (RFI). Thus, the narrowband interference will only affect some subcarriers, which can be ignored and not used for data transmission. It is known that SCM systems are inherently less susceptible to narrowband interference [92]. However, the performance of transmission systems depends on the average SNR and, due to narrowband interference, there is performance loss in SCM systems compared to DMT systems. DMT modulation is very robust in adapting to the channel transmission characteristics. For instance, in lines that have bridged taps, DMT modulation will ignore the subcarriers that are severely attenuated by the notches in the channel transfer function produced by the bridged taps. The notches in the SCM case affect the entire band and to compensate for them a very complex decision feed-back equalizer (DFE) [100] scheme is required.

Concerning deployment of DMT and SCM in multi-line environments, DMT has also a tremendous advantage over SCM. First, DMT allows a flexible shaping of transmit PSD⁴ and independent PSD levels on each subcarrier. Therefore, any optimized spectrum allocation can be implemented in practice without increasing the implementation complexity. Furthermore, as we mentioned in Section 2.2.2, any band plan can be selected without any increase in complexity. The band plan shows the allocation of the bandwidth in the downstream and upstream transmission directions. Thus, the band plan can be optimized per cable bundle, resulting in an adaptation of downstream and upstream subcarrier allocations to better fulfill the requirements of all users in any network scenario. In the case of SCM the band plan must be held fixed, because changing band plans requires changes in the hardware, such as changes in the band-pass filters shown in Figure 2.12.

DMT systems have some disadvantages compared to SCM systems. First, DMT systems (also all MCM systems) have a high peak-to-average ratio (PAR) [10]. A high PAR requires a wide dynamic range of all components, both digital and analog. However, different methods have been proposed to reduce the PAR of MCM systems; see for example [52] and the references therein. Second, DMT systems have a longer transmission latency compared to SCM systems due to the block processing. A long transmission latency can be very annoying for instance in voice applications or online gaming. The long transmission latency can be reduced by decreasing the number of subcarriers, but this will also reduce the efficiency and the performance of DMT transmission systems.

⁴The PSD specifies the signal power allocation versus frequency.

2.4 Noise

Noise in a subscriber line DSL transmission system arises from internal and external noise sources. The internal noise sources are the thermal noise of the twisted pair and the noise generated inside the modem itself. The internal noise in DSL systems is usually called background noise. The external noise arises due to imperfect balancing, or more accurately, due to the imperfect and insufficient twisting of the twisted-pair wires within the cable. The balance in the twisted-pair channel is best in the POTS band and it worsens at higher frequencies. Noise due to imperfect balancing can be crosstalk noise, radio interference, and impulse noise.

2.4.1 Background Noise

The PSD of background noise due to the thermal noise on copper, which is generated by Brownian motion of the electrons in the copper, is approximately -174 dBm/Hz [17] at room temperature. The level of noise generated in the modem itself depends mainly on the noise generated in the AFE of the modem. A well designed AFE can achieve a PSD noise floor level between -155 and -160 dBm/Hz [101]. The background noise, which includes not only thermal noise on copper and AFE noise but also the noise from all other unknown sources has been shown to be frequency dependent [120]. Measurements performed in a central office and presented in [120] show that the background noise increases with frequency. However, the measurements made by Bellcore⁵ in a residential area show that this is not always the case: the background noise can also decrease with frequency.

The probability density of the background noise is very close to, but not exactly, Gaussian [17]. However, for DSL system design purposes it is widely accepted to use a frequency flat background noise level of -140 dBm/Hz with a Gaussian probability density.

2.4.2 Crosstalk Noise

The major impairment in all DSL systems is the crosstalk noise, otherwise known simply as crosstalk. Crosstalk is the signal that is induced into a twisted pair from the signals that are travelling in other twisted pairs of the same cable or cable bundle. Crosstalk is caused by the inductive and capacitive couplings between the twisted pairs. Twisted pairs are not shielded and in most cables neither are the binders within the cables; thus, it is only twisting that prevents twisted pairs from disturbing each other as first introduced by Alexander G. Bell [8] in 1881.

The two common forms of crosstalk are near-end crosstalk (NEXT) and far-end crosstalk (FEXT). To illustrate NEXT and FEXT signals conceptually, we use a generic cable with only two twisted pairs of the same length, as shown in Figure 2.13. Furthermore, we assume that victim (disturbed) modems are deployed in the first twisted pair denoted as Loop 1 and disturber modems are deployed in the second twisted pair denoted as Loop 2. NEXT is the signal coupled from Loop 2 into Loop 1 and travelling in the opposite direction to the desired signal. FEXT is the signal coupled from Loop 2 into

⁵These measurements are also presented in [17].

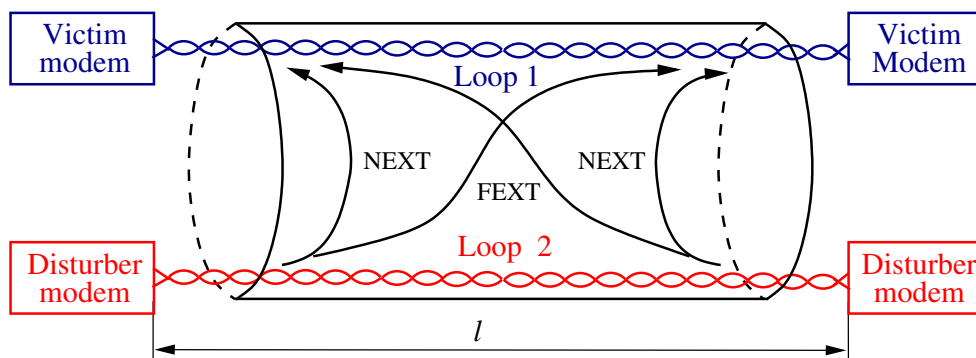


FIGURE 2.13: Illustration of NEXT and FEXT crosstalk signals.

Loop 1 and travelling in the same direction as the desired signal. Both NEXT and FEXT signals are illustrated graphically in Figure 2.13. Depending on the signals that cause the crosstalk, it can be self-crosstalk or alien-crosstalk. In the case of self-crosstalk the victim modem and disturber modems are of the same type and use the same line codes. In the case of alien-crosstalk the victim modem and disturber modems are of different type and use different line-codes.

The crosstalk signal from one twisted pair to another twisted pair is characterized by a transfer function that depends on frequency. Let us denote the squared magnitude of the channel transfer function from Loop v to u by

$$\mathcal{H}_{uv}(f) = |H_{uv}(f)|^2. \quad (2.7)$$

$H_{uv}(f)$ represents the direct channel when $v = u$ and either FEXT or NEXT when $v \neq u$. If the disturber signal in Loop v has a PSD $\mathcal{P}_{v,\text{Dist}}(f)$, then the PSD of the crosstalk signal in Loop u , $\mathcal{P}_{u,\text{XT}}(f)$, is calculated as

$$\mathcal{P}_{u,\text{XT}}(f) = \mathcal{H}_{uv}(f)\mathcal{P}_{v,\text{Dist}}(f). \quad (2.8)$$

Equation (2.8) can be used to calculate the PSD of the crosstalk signal when the victim and disturber modems are deployed in loops with the same lengths. In Section 2.4.2.3 we describe how to calculate the PSD of the crosstalk signal when the loops have different lengths.

The crosstalk coupling between twisted pairs in a cable is random in nature. It depends on the structure of the cable and is also different between different twisted pairs within a cable. To model crosstalk coupling the statistical coupling characteristics of several cables are investigated. Currently, the 99% worst-case crosstalk coupling levels are used by the standardization bodies to define the performance requirements for DSL systems and by service providers to predict the coverage and achievable bitrates. Note that some authors call the 99% worst-case crosstalk coupling as the 1% worst-case crosstalk coupling. The 99% worst-case crosstalk coupling means that on average only 1% of all tested cables should have worse crosstalk coupling than the 99% worst-case coupling level at any frequency.

Within the standardization bodies, various models have been developed to represent the 99% worst-case crosstalk models and these models are always adopted according to recent

studies. However, there have also been complementary studies showing that the models are either too conservative [111] or too liberal. In this section we describe the crosstalk coupling models that are currently used by the ETSI⁶, because we will apply these models in simulations in the following chapters. In addition to the crosstalk coupling models we show how to combine the noise from the disturbers of the same type and different types.

2.4.2.1 ETSI NEXT Model

The 99% worst-case NEXT coupling is defined [40] as

$$\mathcal{H}_{uv,\text{NEXT}}(f) = 10^{\frac{K_{\text{NEXT}}}{10}} \cdot \left(\frac{f}{1 \text{ MHz}} \right)^{1.5} \cdot \left(1 - (\mathcal{H}_{uu}(f, l))^2 \right), \quad (2.9)$$

where f denotes the frequency in Hz; l denotes the NEXT coupling length in km; \mathcal{H}_{uu} denotes the squared magnitude of the channel transfer function of length l (in the model it is assumed that all twisted pairs within the cable have identical transfer functions), K_{NEXT} is the empirically-determined value of NEXT coupling in dB at 1 MHz, and is typically -50 dB [39, 40].

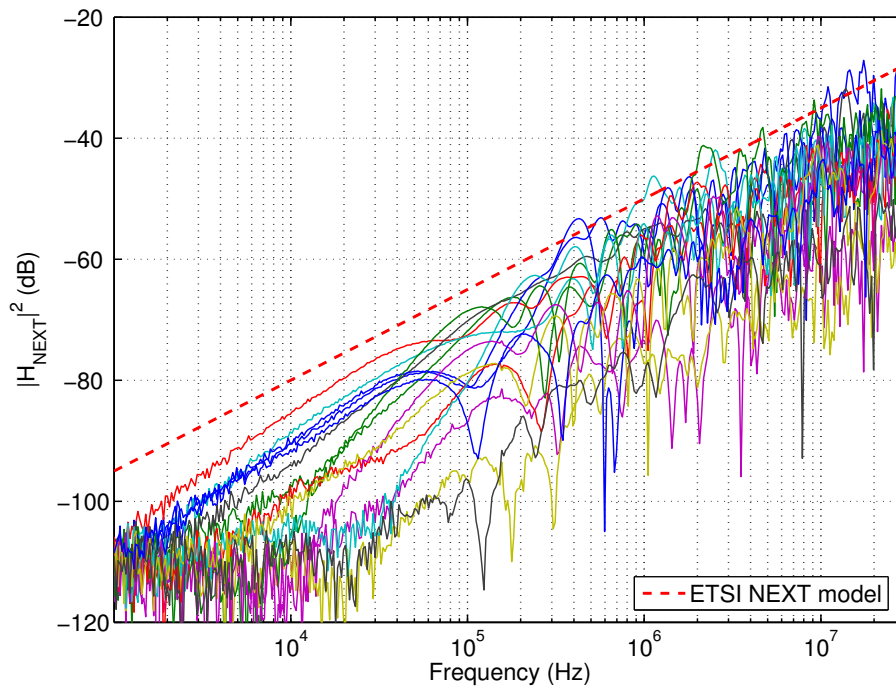


FIGURE 2.14: Some measured NEXT pair-to-pair couplings of a 50-pair cable with 0.4 mm conductors of length 762 m (vendor identification F02YHJA2Y 50x2x0.4). In addition we also show the 99% worst-case ETSI model.

In (2.9), it is shown that NEXT couplings depend on the coupling length, which is included explicitly in the channel transfer function of the victim loop. To be exact, we

⁶The major difference between the ANSI and ETSI crosstalk models is that in ANSI the crosstalk models depend on the number of twisted pairs within the cable, whereas for ETSI they do not.

should represent the equal-level NEXT coupling values as in the case of FEXT, as we will describe it in Section 2.4.2.2. It is shown in [111] that we can assume the measurements to be accurate when we neglect the loop length coupling dependence for the case when the cable length is longer than approximately 300 m. Without loss of generality, we also use the same assumption here in presenting the NEXT coupling measurements of a cable of length 762 m. Figure 2.14 shows some measured NEXT pair-to-pair couplings of a 50-pair cable that has 0.4 mm conductors of length 762 m (vendor identification F02YHJA2Y 50x2x0.4) as well as the 99% worst-case ETSI model.

2.4.2.2 ETSI FEXT Model

The 99% worst-case FEXT coupling is defined [40] as

$$\mathcal{H}_{uv,\text{FEXT}}(f) = 10^{\frac{K_{\text{FEXT}}}{10}} \cdot \left(\frac{f}{1 \text{ MHz}} \right)^2 \cdot l \cdot \mathcal{H}_{uv}(f, l), \quad (2.10)$$

where f denotes the frequency in Hz; l denotes the FEXT coupling length in kilometers; $\mathcal{H}_{uv}(f, l)$ denotes the squared magnitude of the channel transfer function of length l (in the model it is assumed that all twisted pairs within the cable have identical transfer functions); K_{FEXT} is the empirical value of the FEXT coupling in dB at 1 MHz, and is typically -45 dB [39, 40].

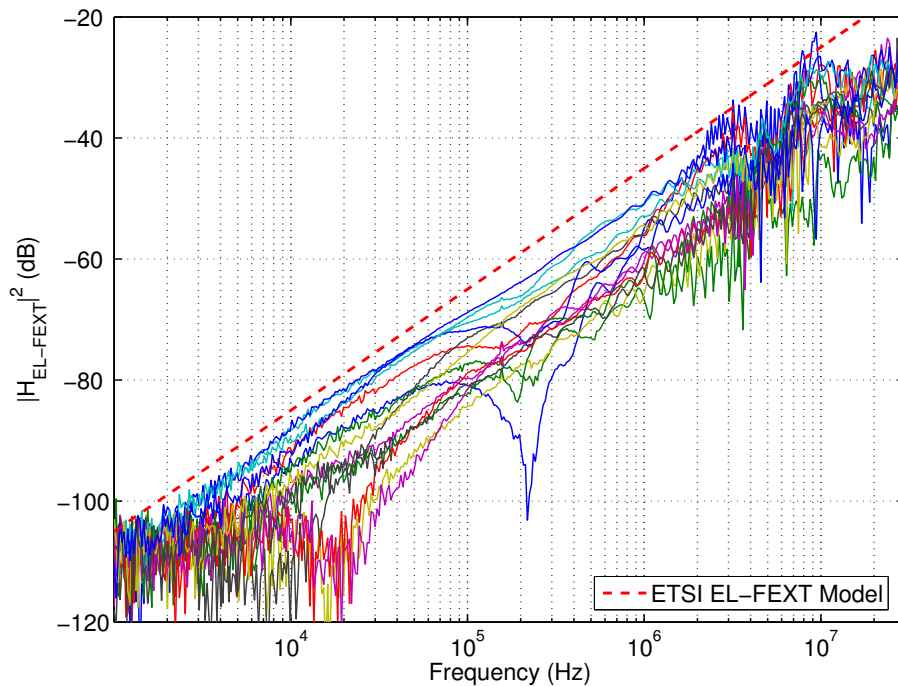


FIGURE 2.15: Some measured equal-level FEXT (EL-FEXT) couplings of a 50-pair cable with 0.4 mm conductors. In addition, the 99% worst-case ETSI EL-FEXT model is also shown. The measured values and the ETSI model are normalized to 1 km.

In practice, FEXT measurements are rarely reported, because they depend on coupling lengths and the channel transfer function of the loop. Usually, the loop properties of

the cable are removed from measurements, leading to the so-called equal-level FEXT (EL-FEXT). EL-FEXT is defined as:

$$\mathcal{H}_{\text{EL-FEXT}}(f) = \underbrace{\mathcal{H}_{uv,\text{FEXT}}}_{\text{measured}} \cdot \frac{1 \text{ km}}{l} \cdot \frac{1}{\mathcal{H}_{uu}(f, l)}.$$

Figure 2.15 shows some calculated EL-FEXT pair-to-pair couplings from the measured values of 50-pair cable with 0.4 mm conductors of length 762 m (vendor identification F02YHJA2Y 50x2x0.4) as well as 99% worst-case ETSI and ANSI EL-FEXT models.

2.4.2.3 Crosstalk Calculation in Distributed Networks

We can use (2.8) to calculate the crosstalk noise when the disturber and the victim modems are deployed in the loops with the same length. However, the loops usually have different lengths as customers are at different distances from the CO. In addition, there are situations where DSL systems are deployed simultaneously from the CO and the cabinet as illustrated in Figure 2.16. In these cases, we have to take into account pre-attenuation of the signal and post-attenuation of the crosstalk. To simplify explanation, we analyze only the case with two loops, as shown in Figure 2.16, and when the loops have equal attenuation per unit length.

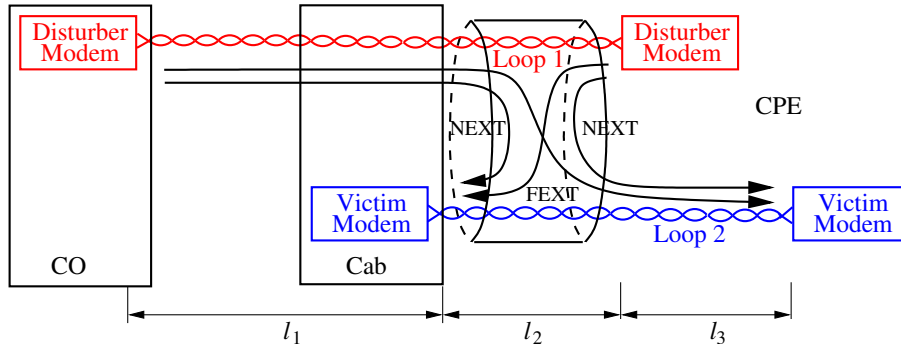


FIGURE 2.16: Illustration of NEXT and FEXT in distributed networks.

The NEXT noise induced into the victim modem located at the cabinet is calculated as the pre-attenuation of the signal, as

$$\mathcal{P}_{2,\text{NEXT}}(f) = \mathcal{P}_{1,\text{Dist}}(f) \cdot \mathcal{H}_{11}(f, l_1) \cdot \mathcal{H}_{21,\text{NEXT}}(f),$$

where $\mathcal{H}_{11}(f, l_1)$ denotes the squared magnitude of the channel transfer function of Loop 1 for the segment l_1 .

The FEXT noise into the victim system located at the customer premises equipment is calculated first as the pre-attenuation of the signal and then as the post-attenuation of the FEXT noise, as

$$\mathcal{P}_{2,\text{FEXT}}(f) = \mathcal{P}_{1,\text{Dist}}(f) \cdot \mathcal{H}_{11}(f, l_1) \cdot \mathcal{H}_{21,\text{FEXT}}(f, l_2) \cdot \mathcal{H}_{22}(f, l_3),$$

where $\mathcal{H}_{11}(f, l_1)$ denotes the squared magnitude of the channel transfer function of Loop 1 for the segment l_1 , $\mathcal{H}_{21,\text{FEXT}}(f, l_2)$ denotes the squared magnitude of the FEXT coupling

in the segment l_2 , and $\mathcal{H}_{22}(f, l_3)$ denotes the squared magnitude of the channel transfer function of Loop 2 for the segment l_3 . For more detailed analysis and crosstalk noise calculation in distributed networks the interested reader may consult [76].

2.4.2.4 Crosstalk Noise Combination

We show in this section how to calculate the crosstalk noise from multiple disturbers of the same type and of different types. For the sake of simplicity, we only describe the case when all loops have the same length. The extension to distributed networks is straightforward by using the models described in Section 2.4.2.3. Using (2.8) and the above models for NEXT and FEXT couplings we can calculate the crosstalk noise of a single disturber. The calculated noise is likely to be exceeded by 1% or less. When there are many disturbers, we can further calculate the crosstalk noise on a loop by measuring the crosstalk couplings and summing the crosstalk noise powers of the disturbers one by one. However, for the purpose of predicting the performance (either the reach or supported bitrates), the above described crosstalk models are currently used. In this case, by summing the crosstalk noise of the disturbers one by one we get a very pessimistic performance, because we assume that all disturbers are deployed to the twisted pair that has a 99% worst-case coupling.

To model the crosstalk noise, either NEXT or FEXT, from η disturbers of the same type, $\mathcal{P}_{\text{XT},\eta}(f)$, it has been found empirically [47] that it can be calculated as the crosstalk noise of a single user multiplied by $\eta^{0.6}$ as

$$\mathcal{P}_{\text{XT},\eta}(f) = \eta^{0.6} \cdot \mathcal{H}_{\text{XT}}(f) \cdot \mathcal{P}_{\text{Dist}}(f), \quad (2.11)$$

where $\mathcal{H}_{\text{XT}}(f)$ is one of the models in (2.9) or (2.10). As we are dealing with worst-case scenarios, the assumption here is that the first disturber is deployed in the loop with the strongest crosstalk coupling, then the second disturber in the loop with the second strongest coupling, and so on. Thus, the crosstalk noise strength does not increase linearly with the number of disturbers, but with the number of disturbers to the power of 0.6. With this model, the NEXT and FEXT noise are calculated independently and the crosstalk noise is then simply calculated by summing them.

When modelling more complex DSL network scenarios, we also need to be able to combine noise contributions from many different signal types. It has been found that simply adding the crosstalk noise for different types of disturbers becomes too pessimistic as it assumes that all η_t different disturbers of type t simultaneously use the first t worst disturbing pairs. The operators within the Full Service Access Network (FSAN) group have proposed a crosstalk combination method [47] that is now widely accepted as a better way to combine crosstalk noise from different sources and is given by

$$\mathcal{P}_{\text{XT}}(f) = \left(\sum_t \left(\mathcal{P}_{\text{XT},\eta_t}(f) \right)^{\frac{1}{0.6}} \right)^{0.6}, \quad (2.12)$$

where $\mathcal{P}_{\text{XT},\eta_t}(f)$ is crosstalk (NEXT or FEXT) noise of type t of η_t disturbers and is calculated as in (2.11). This formula has a nice property that it reduces to (2.11) when we calculate the crosstalk noise from only one type of disturbers. We clarify this with an

example. We suppose that η_1 disturbers have PSD, $\mathcal{P}_{\text{Dist},1}(f)$, and η_2 disturbers have PSD, $\mathcal{P}_{\text{Dist},2}(f)$. With (2.12) and (2.11) we have,

$$\mathcal{P}_{\text{XT}}(f) = \left\{ [\eta_1^{0.6} \cdot \mathcal{H}_{\text{XT}}(f) \cdot \mathcal{P}_{\text{Dist},1}(f)]^{\frac{1}{0.6}} + [\eta_2^{0.6} \cdot \mathcal{H}_{\text{XT}}(f) \cdot \mathcal{P}_{\text{Dist},2}(f)]^{\frac{1}{0.6}} \right\}^{0.6}. \quad (2.13)$$

Let us suppose that $\mathcal{P}_{\text{Dist},1}(f) = \mathcal{P}_{\text{Dist},2}(f) = \mathcal{P}_{\text{Dist}}(f)$. From this assumption and some simple algebra, (2.13) simplifies to

$$\mathcal{P}_{\text{XT}}(f) = (\eta_1 + \eta_2)^{0.6} \mathcal{H}_{\text{XT}}(f) \cdot \mathcal{P}_{\text{Dist}}(f),$$

which is just (2.11) with $\eta_1 + \eta_2$ disturbers.

2.4.3 Radio Noise

DSL signals are transmitted and received in differential mode (DM) (the voltage between the two wires in a twisted-pair loop), but due to the imperfect balancing there is a conversion of the DM signal to the common-mode (CM) signal (voltages with respect to ground earth) and vice versa. Due to this DM-to-CM and CM-to-DM conversation, the unshielded twisted pair works as an antenna; thus, it radiates and picks up radio-frequency (RF) signals. The radiated RF signal from the twisted pair is known as RF egress and the received RF signal is known as RF ingress. Well-balanced twisted-pair loops reduce the RF egress and RF ingress [101]. We now briefly describe RF ingress, which we refer to as RF interference (RFI) noise.

There are two main sources of RFI noise that DSL receivers have to cope with: AM radio and amateur (known as HAM) radio interference noise. Practically all DSL systems have to cope with AM radio interference noise as AM radio transmitters transmit at frequencies from 148.5 kHz up to 1606.5 kHz (long wave (LW) and medium wave (MW) bands). Although AM radio transmitters can transmit with high power up to 2000 kW in the LW band and up to 600 kW in the MW band in Europe and up to 50 kW in the MW band in the USA, they are not as harmful as HAM transmitters. This is because AM radio transmitters are usually located far away from DSL receivers. Furthermore, the twisted-pair lines are better balanced in the frequency range of AM signals than at high frequencies where HAM transmitters operate. The level of signals coupled in a subscriber line depends on the distance to the AM radio transmitter, but typical values of the power coupled in the DM into the input of the receiver are from -90 dBm/Hz to -120 dBm/Hz [34].

There is no unique worldwide HAM frequency band plan, but three HAM frequency band plans are defined for three regions. In Region 2, which includes all European countries, in the frequency range from 1.81 MHz to 29.7 MHz nine HAM bands are allocated, which occupy the frequencies listed in Table 2.2. Thus, HAM radio noise will only affect ADSL2+ [60], VDSL [3, 40], and VDSL2 systems. Although, HAM radios only transmit with power up to 400 W in Europe and up to 1 kW in the USA, they are more harmful than AM radio. This is because HAM transmitters can be located just a few meters from in-house wiring where the balance can be very poor and where untwisted-pair cables are also sometimes used. A HAM transmitter operating at a distance of 10 m from the subscriber

TABLE 2.2: Amateur radio (HAM) frequency bands for Region 2, which includes all European countries.

Start Frequency (MHz)	Stop Frequency (MHz)
1.810	2.000
3.500	3.800
7.000	7.100
10.100	10.150
14.000	14.350
18.068	18.168
21.000	21.450
24.890	24.990
28.000	29.790

loop can induce a power of -34 dBm/Hz in DM into the input of the receiver [100]. Furthermore, HAM radio transmits with single sideband suppressed carrier, which means that the RF signal is only radiated when transmitting voice and for all other periods the HAM transmitter is quiet with little or no RF power radiated. Therefore, the HAM RFI noise is not predictable in advance, and thus developing an RFI cancellation scheme is rather challenging. Within this work, we will not analyze RFI ingress and RFI egress any further. For a detailed analysis and description of techniques for cancelling RFI noise the interested reader can refer to [73].

2.4.4 Impulse Noise

Impulse noise is nonstationary noise from temporary electromagnetic events that is coupled into a twisted-pair loop. For example, sources of impulse noise include the ringing of phones on lines sharing the same cable binder, switching devices in the CO, various electrical devices at the customer premises, and atmospheric electrical surges. Due to the nonstationary and sporadic nature of impulse noise its statistical properties are of central interest for designers of DSL systems. The statistical properties of impulse noise vary between countries. The measurements of France Telecom [101] have shown that about 90% of impulses have a duration of less than $250 \mu\text{s}$ and an amplitude of less than 10 mV.

Currently, the mostly used analytical model for the aim of simulating impulse noise is the Cook pulse [31]. However, a very interesting approach to modelling the impulse noise is also given in [69]. As with RFI noise, a well-balanced twisted-pair loop reduces the amplitude of impulse noise induced in the DM. Impulse noise is typically combated in DSL systems with forward-error correction. We will not further analyze the effect of impulse noise on the performance of DSL systems, but we will assume that errors due to impulse noise are corrected perfectly by forward-error correction schemes.

Chapter 3

Spectrum Management for DSL Systems

The major impairment in digital subscriber line (DSL) transmission systems is the crosstalk noise [17, 100], otherwise known simply as crosstalk. Crosstalk is the interference signal that is coupled into a twisted pair from signals transmitted in other twisted pairs in the same cable bundle or neighboring cable bundles. Section 2.4.2 showed that the crosstalk is caused by capacitive and inductive couplings between the twisted pairs due to improper balancing. The level of crosstalk depends on the level of the transmitted signals, the level of the crosstalk coupling functions between the twisted pairs, and the penetration and types of deployed DSL systems. The crosstalk between the twisted pairs of different cable bundles is much lower than between the twisted pairs within a cable bundle. As a result, the crosstalk from the neighboring cable bundles is usually ignored for the purpose of spectrum management and is considered as background noise.

During recent years the number of standardized DSL technologies has rapidly increased. The number of deployed DSL systems is also increasing continuously (see Chapter 1). Thus, *spectral compatibility* and *spectrum management* have become crucial to ensure DSL's continuing success. Spectral compatibility [5] is defined as the capability of DSL systems to coexist in the same bundle and operate satisfactorily in the presence of crosstalk noise from each other. Spectrum management [5] in DSL refers to processes that are intended to minimize the potential interference between systems deployed in the same metallic loop cable, and maximize the utility of the frequency spectrum of the cables. Thus, spectrum management can also be defined as the process of optimizing the utilization of the loop plant capacity while ensuring spectral compatibility.

Currently, spectral compatibility among different deployed DSL systems is ensured by assuming a worst-case crosstalk environment. This way of ensuring spectral compatibility in DSL is called static spectrum management (SSM)¹. In practice, the crosstalk depends on the level of the transmit signal of the disturbers and the actual crosstalk couplings. The latter depends strongly on the location of the victim (disturbed) and disturber twisted pairs. Thus, current deployed DSL systems ignore the actual structure of DSL access networks, which is distributed as was described in Chapter 2. As a result, very often the reach/bitrate figures are very pessimistic and far below what can actually be achieved. Furthermore, the crosstalk varies over time due, for example, to DSL modems being switched on and off.

¹In literature, this is usually called spectrum management, but recently it is usually termed static spectrum management to distinguish from dynamic spectrum management.

Dynamic spectrum management (DSM) aims to increase the utilization of loop plant capacity and to improve the reliability of DSL transmission systems by adapting the spectra of DSL systems to the actual network environment. Thus, the actual crosstalk couplings and optionally the time-dependent nature of the crosstalk are incorporated into the optimization process to improve the performance of DSL systems. The term DSM has also been used to describe techniques that aim to cancel the crosstalk. Thus, DSM considers the DSL access network as a multi-user system. DSM can also be defined as a set of techniques that aim to optimally exploit the capacity of the loop plant.

This chapter proceeds as follows. Section 3.1 describes SSM, with its main focus on upstream power back-off in very high speed DSL (VDSL), which is the most sophisticated SSM technique; Section 3.2 can be seen as a tutorial on DSM, where we will also describe the two most promising techniques for DSM: spectral balancing and vectoring.

3.1 Static Spectrum Management

To open up telecom markets to new competition, regulators have demanded ‘unbundling’ in many countries [77]. The unbundling refers to the process by which competitive local exchange carriers (CLECs) must be allowed to lease some telephone lines or bandwidth from the incumbent local exchange carrier (ILEC). In an unbundled network the ILEC is both a loop provider and service provider, because it owns the cable infrastructure and provides services to customers. On the other hand CLECs are only service providers. Unbundling creates a new situation compared to the past, when the ILEC could select to offer only those DSL technologies and services that were spectrally compatible with their existing networks and ignore all others. In an unbundled network the CLECs may lease any telephone line and deploy on it any allowed DSL technology.

The number and type of deployed DSL systems is continuously increasing. This increases the crosstalk and might also cause service outages if the loop plant is not managed properly. Therefore, there is a need to provide rules and guidelines to define exactly which signals can be placed on twisted-pair cables. These rules and guidelines should ensure spectral compatibility between deployed DSL systems. Note that both the ILEC and the CLECs must follow the same rules and guidelines when deploying their DSL systems in an unbundled network.

Different countries have different structures of DSL access networks and also use different cable types, as Section 2.1 described. Hence, rules and guidelines optimized to ensure spectral compatibility in one country might not be optimal for another country. Thus, standards that provide rules and guidelines should be national based, and it is the obligation of national regulatory authorities to develop rules and guidelines appropriate for their own national DSL access networks. In the United States, the Committee T1E1.4, which is sponsored by the Alliance for Telecommunications Industry Solutions, ATIS, and accredited by the American National Standards Institute, ANSI, has written two standards for spectrum management: T1.417 Issue-1 [2] and T1.417 Issue-2 [5]². The first issue analyzes the spectral compatibility of DSL systems deployed between the central office (CO) and customer sides. The second issue extends the first one by also analyzing DSL systems deployed from cabinets (remote terminals), VDSL systems, and lines

²Unfortunately, I do not have access to the newest versions due to changing the policy in the ANSI.

that include repeaters. In Europe, the European Telecommunication Standards Institute, ETSI, transmission and multiplexing (TM) technical committee is working on spectrum management for metallic access networks. ETSI's work includes the Technical Reports TR 101 830 series [38, 42, 43], which are in early draft stages. We will briefly describe only T1.417 static spectrum management [5] when systems are deployed only from the CO.

3.1.1 T1.417 DSL Static Spectrum Management Standard

The aim of a spectrum management standard is to establish rules and guidelines to ensure spectral compatibility among all existing "basis systems". In Section 3.1.2 we give an example of how to determine spectral compatibility between different DSL systems. The basis systems are the DSL systems, which are standardized and unstandardized systems currently deployed in the loop plant. T1.417 Issue-2 considers the following systems to be basis systems:

- Voice grade services (including speech, data, and call processing signals that use the frequency spectrum below 4 kHz)
- Enhanced business services (P-Phone)
- Digital data services (DDS)
- Basic rate integrated services digital network (BRI)
- High-bitrate DSL (HDSL)
- HDSL2
- Asynchronous DSL (ADSL), non-overlapping upstream/downstream mode
- Rate-adaptive ADSL (RADSL)
- Splitterless ADSL
- Symmetric high-bitrate DSL (SHDSL)
- Very high speed DSL (VDSL).

This list is not fixed, and moreover, new DSL technologies can be added or removed from the basis systems list. Being a basis system in no way ensures conformance with the standard, and basis systems themselves may not be spectrally compatible on many loops [64].

The T1.417 standard defines two methods determining spectral compatibility: signal power limitations (Method A) and an analytical method (Method B).

3.1.1.1 Spectral Compatibility by Signal Power Limitations (Method A)

The level of crosstalk noise depends on the level of the disturber signals. A strong signal transfers more power to other twisted pairs than a weaker signal. Furthermore, as shown in Section 2.4.2, crosstalk couplings increase with frequency. As a result, the power allocated to higher frequencies couples more crosstalk into the neighboring twisted pairs than the power allocated to lower frequencies. Thus, one method to control the crosstalk noise and also to ensure the spectral compatibility among different DSL systems is to constrain the transmit power and power spectral densities (PSD) at the points where the signals enter the subscriber loop. The PSD specifies the signal power allocation versus frequency.

In the early days of standard development it was proposed to define a single PSD mask on the frequency range from zero to infinity for the aim of spectral compatibility calculation. But, it was recognized that such a PSD mask could be very restrictive, so it was agreed to define different DSL spectrum management classes classified in terms of PSDs. The spectrum management classes are technology independent, as one class can comprise more than one DSL technology.

T1.417 specifies nine spectrum management classes. Each spectrum management class is specified with one PSD mask or with two PSD masks (one PSD mask for each transmission direction). As with basis systems, new spectrum management classes can be added as new DSL technologies become standardized. *PSD masks* are defined for any DSL technology and provide some limits on the transmitted PSD. However, for the aim of crosstalk noise calculation we need to model transmit signal PSDs more accurately, as the PSDs depend on deployed DSL technologies and the type of modulation used. This has led to the definition of *PSD templates*. *PSD templates* are used to calculate the crosstalk noise that specific spectrum management classes cause in a particular system [115].

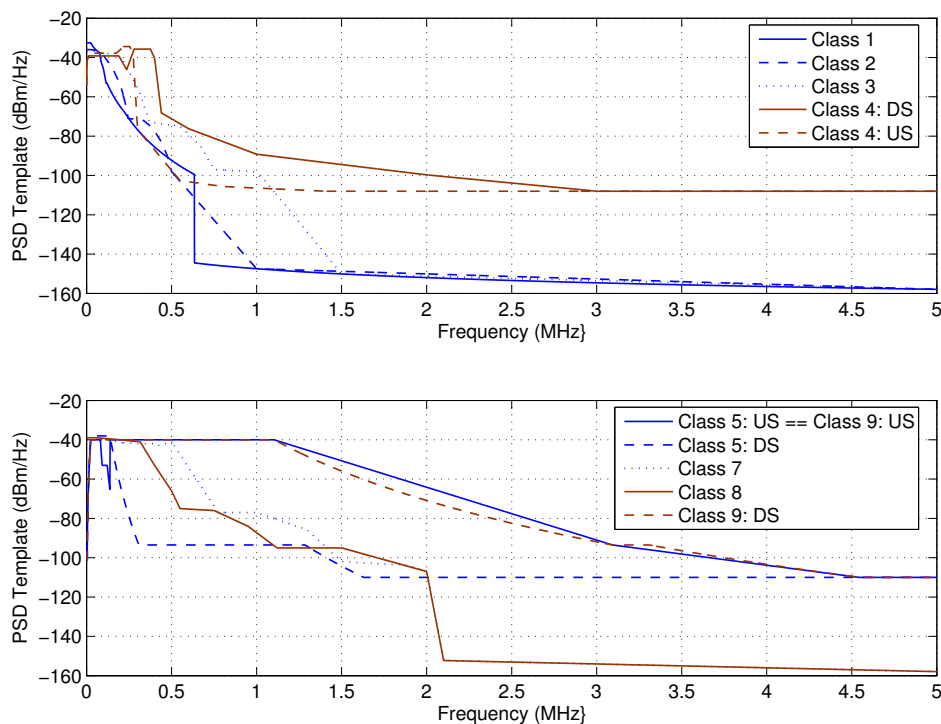


FIGURE 3.1: Transmit PSD templates of spectrum management classes.

The transmit PSD templates of spectrum management classes are shown in Figure 3.1. The transmit PSD templates of spectrum management class 6, which specifies VDSL systems, are not shown. We analyze transmit PSDs of VDSL systems in Section 3.1.3. The PSD mask of a particular spectrum management class is usually defined to be +3.5 dB higher than the corresponding PSD template [90].

For each spectrum management class the total average transmit power is also limited,

which is usually more than 1 dB below the transmit power of the corresponding PSD template. Any system that transmits with a PSD mask no greater than the PSD mask of a specific class and fulfills the total average transmit power is considered to belong to that spectrum management class.

3.1.1.2 Analytical Method of Determining Spectral Compatibility (Method B)

The main goal in developing the analytical method of determining spectral compatibility was to establish a framework to facilitate calculation of the system performance degradation resulting from crosstalk by means of simulation. In addition, this method allows flexibility in innovation of new DSL technologies that further improve the resource utilization of the cooper loop plant. To ensure widespread deployment, the 99% worst-case crosstalk coupling models and the crosstalk noise combination methods described in Section 2.4.2 are used to calculate the crosstalk noise.

Figure 3.2 shows the network topology used to calculate the crosstalk in the basis system (denoted as the victim). To calculate the crosstalk from only existing DSL technologies the reference disturbers are usually selected to represent the worst-case noise environment. When calculating the impact of a new DSL technology on the basis system, the appropriate number of reference disturbers are replaced with new DSL systems, as described in Annex A of the T1.417 standard.

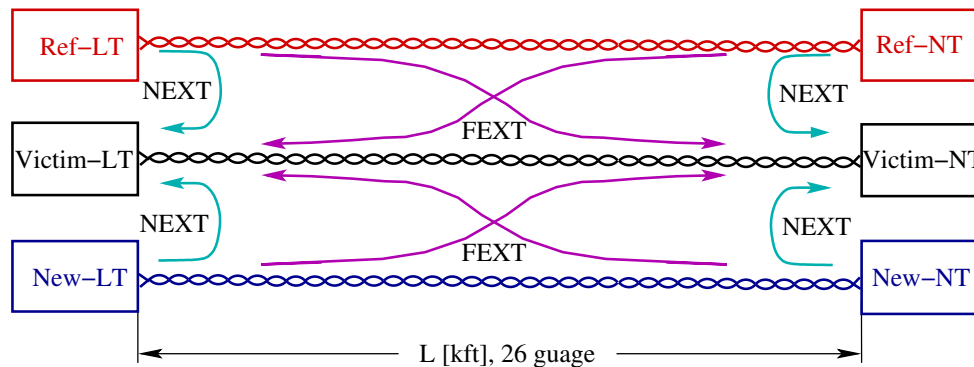


FIGURE 3.2: The network topology used to evaluate the performance of the system under study. Victim-LT and Victim-NT denote transceiver units of the victim modems at the line termination (LT) and network termination (NT) sides, respectively. Ref-LT and Ref-NT, and New-LT and New-NT denote reference and new system disturbers at the LT and NT sides, respectively.

The main task for the analytical method of determining spectral compatibility is to determine if the noise margin of the victim systems (the victim-LT and victim-NT modems in Figure 3.2) is higher or lower than the target noise margin. The noise margin is defined as the amount by which the signal-to-noise ratio (SNR) can be reduced and still not exceed a specified bit-error rate (BER) at a predefined bitrate. In the remainder of this chapter ‘margin’ refers to noise margin. The system under study can be any basis system. The target loop length L is given in equivalent working length (EWL) and is defined as

$$EWL = L_{26} + 0.75L_{24} + 0.6L_{22} + 0.4L_{19}, \quad (\text{kft})$$

where L_{26} , L_{24} , L_{22} , and L_{19} are the actual working lengths of 26, 24, 22, and 19 AWG loop lengths in kilofeet (kft) ³.

The EWL and target bitrates of the DSL systems that support different bitrates are selected *a priori*. The margin calculation is performed independently in the upstream and downstream directions, because the system under study and disturbers may have different transmit PSD masks in both transmission directions. If the calculated margin of the system under study is above the target margin the new system is declared spectrally compatible with the selected basis system for the given loop length. If this is not the case, the target loop length is decreased by some value, usually in resolution of 500 feet (152 m), and the test is repeated until the margin of the system under study is greater than or equal to the target margin.

The calculation of the margin depends on the modulation technique that is used in the system under study. For the DSL systems that use single-carrier modulation (SCM) the margin in dB is computed by

$$\gamma_{\text{Noise,dB}} = \text{SNR}_{\text{Out,dB}} - \text{SNR}_{\text{Req,dB}},$$

where $\text{SNR}_{\text{Out,dB}}$ denotes the SNR in dB at the output of the equalizer at receiver and $\text{SNR}_{\text{Req,dB}}$ denotes the required SNR in dB of a SCM system to achieve a given BER. Current DSL systems work with $\gamma_{\text{Noise,dB}} = 6$ dB. Note that VDSL SCM-based systems may use two carrier frequencies (one per each band) per transmission direction, but they are considered single-carrier systems.

$\text{SNR}_{\text{Req,dB}}$ is calculated based on the Shannon capacity formula and the Gap approximation as:

$$\text{SNR}_{\text{Req,dB}} = 10 \log_{10} \left[\Gamma \cdot \left(2^{\frac{2R}{D}} - 1 \right) \right], \quad (3.1)$$

where D denotes the dimension of the signal constellation, thus $D = 1$ and $D = 2$ for pulse amplitude modulation (PAM) and quadrature amplitude modulation (QAM) signal constellations, respectively. R denotes the number of bits transmitted per symbol. Γ is the SNR gap, given by [76] (see also [75]) as

$$\Gamma = \frac{\gamma_{\text{Mod}} \cdot \gamma_{\text{Loss}}}{\gamma_{\text{Code}}}, \quad (3.2)$$

where γ_{Mod} is modulation gap⁴, which represents the SNR that is required to transmit symbols at a certain BER for a given modulation scheme; γ_{Code} is coding gain; and γ_{Loss} is used to model the loss in SNR, due to imperfect receiver design, from the point where the signal enters the receiver until it reaches the decision device (see Figure 2.4). The exact value of the SNR gap depends on the practical system realization. Usually the SNR gap is given in dB, which from (3.2) is calculated as

$$\Gamma_{\text{dB}} = \gamma_{\text{Mod,dB}} + \gamma_{\text{Loss,dB}} - \gamma_{\text{Code,dB}}. \quad (3.3)$$

Table 3.1 shows some values of $\text{SNR}_{\text{Req,dB}}$ for PAM and QAM signal constellations

³ 1 kft=304.8 m

⁴ Some authors call this the Shannon gap

TABLE 3.1: The required SNR in dB for PAM and QAM signal constellations to achieve a BER of 10^{-7} for different R , and for $\gamma_{\text{Mod,dB}} = 9.75$ dB, $\gamma_{\text{Code,dB}} = 0$ dB, and $\gamma_{\text{Loss,dB}} = 0$ dB.

Bits (R)	SNR _{Req,dB}	
	PAM	QAM
2	21.26	14.27
3	27.49	17.95
4	33.56	21.26
6	45.52	27.49
8	57.66	33.56
10	69.70	39.59

calculated based on (3.1) for different numbers of bits, R , and for $\gamma_{\text{Mod,dB}} = 9.75$ dB, $\gamma_{\text{Code,dB}} = 0$ dB, and $\gamma_{\text{Loss,dB}} = 0$ dB.

The $\text{SNR}_{\text{Out,dB}}$ value depends on the used line code. Most single-carrier DSL systems use a receiver with a decision-feedback equalizer (DFE). For SCM systems that use trellis coded modulation the feedback part of DFE is implemented in the transmitter as a Tomlinson-Harashima precoder. The SNR at the output of the DFE for PAM and QAM is calculated by the modified Wiener-Hopf equations, derived by Saltz for an ideal DFE [5, 25] as

$$\text{SNR}_{\text{Out,dB}} = \frac{1}{F_S} \int_0^{F_S} 10 \log_{10}(1 + \text{SNR}_F(f)) df,$$

where $\text{SNR}_F(f)$ denotes the folded received SNR and F_S denotes the symbol rate. The folded received SNR is computed by

$$\text{SNR}_F(f) = \sum_{k=-\infty}^{\infty} \frac{\mathcal{P}(f + k \cdot F_S) \cdot \mathcal{H}(f + k \cdot F_S)}{\mathcal{N}(f + k \cdot F_S)},$$

where $\mathcal{P}(f)$ denotes the transmit PSD of the signal, $\mathcal{H}(f)$ denotes the squared magnitude of the channel transfer function, and $\mathcal{N}(f)$ denotes the PSD of the total noise at the receiver. In practice, a folded SNR calculated out to four times the Nyquist rate is sufficient for all current DSL signals [5].

We show now how to calculate the margin in DSL systems that use discrete multi-tone (DMT) modulation. We assume that only two-dimensional signal constellations are used, because all current DMT systems use only QAM signal constellations. The number of bits loaded on subcarrier n based on the Shannon capacity formula and Gap approximation [30] is calculated by

$$R[n] = \log_2 \left(1 + \frac{\text{SNR}[n]}{\Gamma} \right),$$

where Γ is the SNR gap and $\text{SNR}[n]$ is the SNR at the receiver on subcarrier n , which is computed by

$$\text{SNR}[n] = \frac{\mathcal{P}[n]\mathcal{H}[n]}{\mathcal{N}[n]},$$

where $\mathcal{P}[n]$, $\mathcal{H}[n]$, and $\mathcal{N}[n]$ denote the transmit PSD of the signal, the squared magnitude of the channel transfer function, and the noise PSD at the receiver on subcarrier n , respectively .

The number of bits transmitted in a DMT symbol is calculated as the sum of bits transmitted over all used subcarriers. The average number of bits \tilde{R} over all N subcarriers is computed by

$$\begin{aligned} \tilde{R} &= \frac{1}{N} \sum_{n=1}^N R[n] = \frac{1}{N} \sum_{n=1}^N \log_2 \left(1 + \frac{\text{SNR}[n]}{\Gamma} \right) \\ &= \frac{1}{N} \log_2 \left(\prod_{n=1}^N \left[1 + \frac{\text{SNR}[n]}{\Gamma} \right] \right) \end{aligned} \quad (3.4)$$

$$\triangleq \log_2 \left(1 + \frac{\text{SNR}_{\text{Avg}}}{\Gamma} \right), \quad (3.5)$$

where SNR_{Avg} denotes the average SNR over all used subcarriers N . From (3.4) and (3.5) the SNR_{Avg} is calculated as:

$$\text{SNR}_{\text{Avg}} = \Gamma \cdot \left\{ \left[\prod_{n=1}^N \left(1 + \frac{\text{SNR}[n]}{\Gamma} \right) \right]^{\frac{1}{N}} - 1 \right\}.$$

We are interested to calculate the margin (the noise margin). Therefore, after including the margin in (3.5), it can be written as

$$\tilde{R} = \log_2 \left(1 + \frac{\text{SNR}_{\text{Avg}}}{\Gamma \cdot \gamma_{\text{Noise}}} \right), \quad (3.6)$$

where γ_{Noise} denotes the margin. Equation (3.6) can also be written as

$$\Gamma \cdot \gamma_{\text{Noise}} = \frac{\text{SNR}_{\text{Avg}}}{2^{\tilde{R}} - 1},$$

Base on (3.2) and after some mathematical operation, the margin in dB from (3.6) is computed by

$$\gamma_{\text{Noise_dB}} = 10 \log_{10} \left(\frac{\text{SNR}_{\text{Avg}}}{2^{\tilde{R}} - 1} \right) + \gamma_{\text{Code_dB}} - \gamma_{\text{Mod_dB}} - \gamma_{\text{Loss_dB}},$$

where $\gamma_{\text{Code_dB}}$, $\gamma_{\text{Mod_dB}}$, and $\gamma_{\text{Loss_dB}}$ are the same parameters as defined in (3.3). For a detailed analysis of how the margin and the performance of different DMT systems are calculated the interested reader is referred to [42, 102].

3.1.1.3 Additional Requirements

For spectral compatibility, a DSL system or a spectrum management class must either satisfy the PSD mask constraints or have a positive margin for a predefined target bitrate and loop length. However, to be declared standards-compliant it must also meet the limits on transverse balance and longitudinal output voltage as well as the deployment guidelines as specified in the T1.417 standard.

It is worth mentioning that standard compliance only ensures that the system is spectrally compatible, but this does not ensure that the system can legally be deployed. The rules for the allowable deployment are defined by the regulatory authority of the relevant country.

3.1.2 An Example of Spectral Compatibility Evaluation

ADSL is the most widely deployed DSL technology. Therefore, in this section we evaluate the spectral compatibility of an ADSL over POTS [58] system that operates in the frequency division duplexing (FDD) mode with some other DSL systems. It is well known that ADSL is a rate adaptive system. Thus, in addition to fixing the loop length, we also need to fix the downstream and upstream bitrates in order to evaluate spectral compatibility. We perform the spectral compatibility evaluation for an upstream bitrate of 256 kbit/s and downstream bitrate of 1 Mbit/s. We further assume that the evaluation loop length is selected to be 3.5 km for a 0.4 mm cable (26-AWG) and only the following DSL technologies can be deployed in the network: ADSL with 1 Mbit/s and 256 kbit/s bitrates in the downstream and upstream directions, respectively; SHDSL [61] with bitrates from 192 kbit/s to 2304 kbit/s in steps of 64 kbit/s, 2B1Q ISDN, and HDSL [57] transmitting at 1160 kbaud. The transmit PSD templates of 2B1Q ISDN and HDSL used to calculate the crosstalk noise are specified in [79].

To calculate the line reach of the ADSL system we assume that there are 49 other disturbing lines populated with the above mentioned DSL technologies. For all simulations we use the ETSI NEXT and FEXT models as specified in Section 2.4.2. Figure 3.3 shows the ADSL downstream and upstream reach for the selected downstream and upstream bitrates. The chart shows that in the downstream the ADSL achieves the longest reach under self-noise disturbance. The reason is that the ADSL modems operate only under self-FEXT, which is less harmful, because the self-FEXT is attenuated in the same way as the victim signal.

ADSL shows the worst performance under crosstalk from SHDSL disturbers. The reason for this is that the PSD mask of SHDSL⁵ disturbers at 2304 kbit/s overlap with the downstream PSD mask of ADSL and the PSD mask of SHDSL at 896 kbit/s also overlap with the upstream PSD mask of ADSL. From the charts, we conclude that with the exception of SHDSL at specific bitrates all other DSL systems are spectrally compatible with ADSL (for the selected ADSL bitrates and target reach). In the upstream direction, SHDSL at all bitrates is spectrally compatible with ADSL, whereas in the downstream direction is spectrally compatible only at bitrates below 1984 kbit/s.

For instance, SHDSL transmitting at 2304 kbit/s is allowed to be deployed only on lines shorter than approximately 3.27 km. In a similar way to this example, we can evaluate the

⁵Note that in SHDSL the downstream and upstream transmit PSDs overlap.

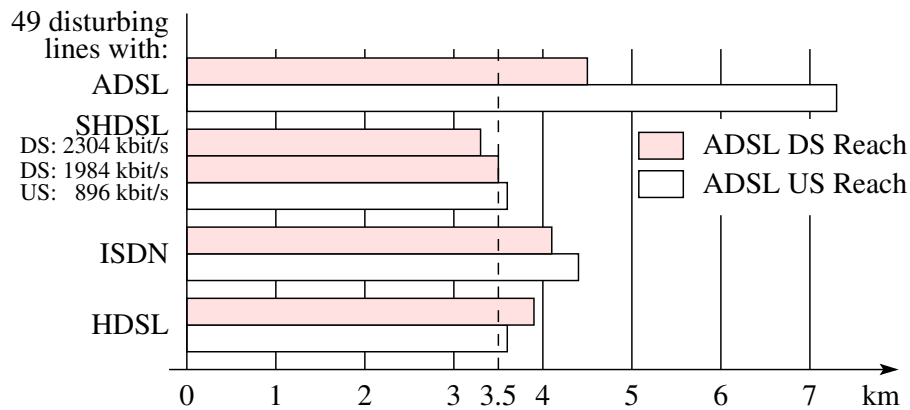


FIGURE 3.3: The reach of ADSL systems for different types of DSL disturbers. The bitrates for the ADSL are selected at 1 Mbit/s and 256 kbit/s for the downstream and upstream, respectively.

spectral compatibility among many DSL technologies or spectrum management classes. From the reaches calculated for different services and DSL technologies, we can then establish the deployment guidelines.

3.1.3 Upstream Power Back-Off in VDSL

We show in Section 3.1.1 that the collocation of modems at both sides is assumed for the aim of spectral compatibility evaluation. Note that in the T1.417 Issue-2 standard [5] collocation of the modems at the customer side is assumed to evaluate spectral compatibility between the systems that are deployed from CO and those deployed from the cabinet. However, we will not analyze such network scenarios and we assume that the modems are deployed either from CO or cabinet.

The assumption for the collocation of modems at CO or cabinet is realistic, but not for the modems at the customer side due to their distribution. Thus, in DSL access networks the so-called *near-far problem* arises in the upstream transmission direction when DSL systems use FDD. The near-far problem occurs when the crosstalk generated by the shorter lines in the cable binder reduces the capacity of the longer lines if all modems transmit with the same PSD.

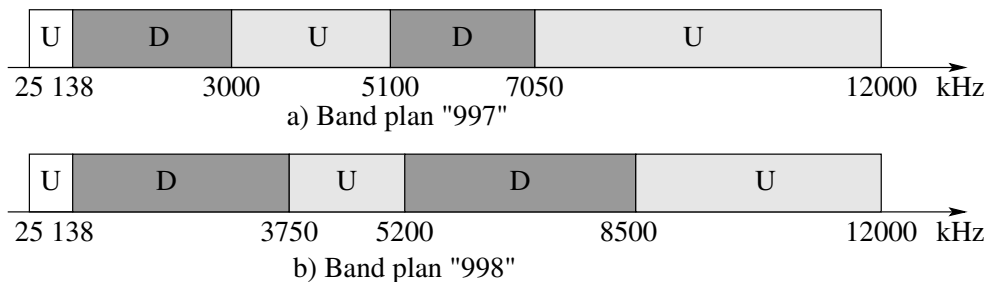


FIGURE 3.4: Two standardized VDSL band plans.

VDSL is the most advanced DSL technology that utilizes the frequencies from 25 kHz

to 12 MHz⁶. Two standardized frequency band plans for VDSL are shown in Figure 3.4. VDSL uses FDD to mitigate the self-NEXT, so VDSL systems operate under self-FEXT noise and alien crosstalk (both NEXT and FEXT). Furthermore, due to the high FEXT couplings at high frequencies, the near-far problem becomes crucial for the upstream performance of VDSL systems. The near-far problem also arises in the other DSL systems that use FDD, like ADSL, but it is not so crucial as in VDSL due to low FEXT couplings at low frequencies. Deploying a single PSD mask constraint to all modems for the aim of spectrum management in VDSL results in pessimistic reach/bitrate figures. For illustration purposes, Figure 3.5 shows the bitrates supported by VDSL systems in the upstream direction for 20 collocated modems depending on the loop length and 20 equally spaced distributed modems with a maximum loop length of 1500 m. For all simulations we have used the standardized frequency band plan “997”. From the plots it can be seen that there is a significant performance loss in VDSL systems when they are distributed due to the near-far problem.

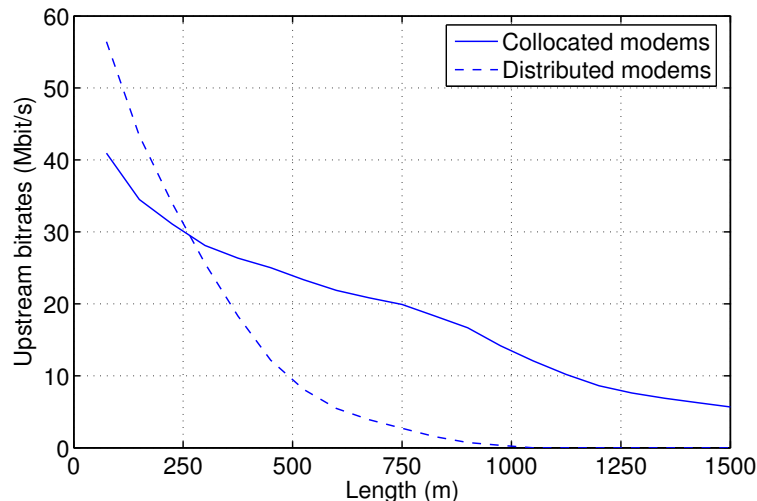


FIGURE 3.5: Bitrates supported by VDSL systems for band plan “997” in the upstream direction for 20 collocated modems depending on the loop length and 20 equally spaced distributed modems.

An obvious way to solve the near-far problem is to reduce the crosstalk coming from a particular subscriber loop by decreasing the transmit PSD on that loop. Such a reduction of the transmit power in DSL is called *power back-off* (PBO). When the transmit power is reduced only in the upstream, as in VDSL, it is called upstream PBO (UPBO). Different UPBO methods have been proposed for VDSL. For an overview of the proposed methods see [63, 96] and the references therein. Finding the optimal UPBO is still an unsolved optimization problem, although it appears a simple problem. For example, in [19] an optimal solution for the UPBO was formulated based on simulated annealing. However, simulated annealing cannot guarantee the convergence to the global optimum.

⁶In VDSL2 it is foreseen to use frequencies up to 30 MHz [110].

3.1.3.1 Standardized Upstream Power Back-Off in VDSL

To keep the UBPO in VDSL simple, different standardization bodies have agreed to define the UPBO in terms of the reference PSD. This UPBO method is called the reference PSD method. It was agreed that the level of PBO should not depend explicitly on the length of the loop, but on the channel transfer function (insertion loss). Therefore, the transmit signal PSD, $\mathcal{P}_u(f)$, for a particular user u is given by [5]

$$\mathcal{P}_u(f) = \mathcal{P}_{\text{REF}}(f) + 10\log_{10}(\mathcal{H}_{uu}(f)), \quad (\text{dBm/Hz})$$

where $\mathcal{P}_{\text{REF}}(f)$ denotes the reference PSD and $\mathcal{H}_{uu}(f)$ denotes the squared magnitude of the channel transfer function of user u . However, the transmit PSD should never exceed the maximum transmit PSD mask, $\mathcal{P}_u^{\text{max}}(f)$; thus,

$$\mathcal{P}_u(f) = \min\left(\mathcal{P}_{\text{REF}}(f) + 10\log_{10}(\mathcal{H}_{uu}(f)), \mathcal{P}_u^{\text{max}}(f)\right). \quad (\text{dBm/Hz})$$

The reference PSD, $\mathcal{P}_{\text{REF}}(f)$, determines the maximum received PSD on any loop. By constraining the received PSD it is much simpler to predict the worst-case self-FEXT noise from the other lines. The reference PSD is just a parameterized function of frequency that should be designed to optimize certain objectives. Because service providers are usually interested in offering fixed-bitrate services, maximizing the reach for a predefined set of bitrates is usually selected as a design objective.

Now the question arises of how to select the reference PSD, $\mathcal{P}_{\text{REF}}(f)$, that maximizes the reach. One solution is to search exhaustively for the maximum reach among all possible reference PSD realizations. Unfortunately, this is not feasible in practice. Therefore, to make the search feasible, the standardization bodies have agreed to restrict the search to a reference PSD of the form:

$$\mathcal{P}_{\text{REF}}(f) = \psi + \phi\sqrt{f}, \quad (\text{dBm/Hz})$$

where f is given in MHz, and ψ and ϕ are the parameters that should be found to maximize the reach.

To better utilize the cable resources in VDSL standards it was specified that the reference PSD should be different for each upstream band. The major parameters that determine the optimal reference PSDs are: alien noise, maximum transmit PSD mask, cable types, and network topology. A detailed analysis of the influence of these parameters on the optimal reference PSDs can be found in [96].

Operators can estimate an average alien noise environment and determine to which predefined noise model it belongs. For instance, ETSI defines six alien noise models for VDSL, from A through F [40]. Operators must decide in advance which VDSL band plan should they use in their networks. It is bad practice to mix different band plans in the same cable bundle—otherwise VDSL systems will operate in a self-NEXT limited environment although they are designed to be self-FEXT limited. Schelstraete shows in [95] that a single common reference PSD can be used for normal and boosted transmit PSD masks; whereas in [96] he shows that reference PSD that optimizes the reach for protected services on a 0.4 mm cable also performs very well on a 0.5 mm cable and vice

versa. To make the reference PSDs independent of any particular network scenario the standardization bodies have proposed to use the worst-case model for self-FEXT noise.

Different methods have been proposed to calculate the worst-case self-FEXT in distributed networks [78, 96, 107]. We describe in [107] why the proposed method in [96] is not appropriate to calculate the worst-case self-FEXT in distributed networks especially when VDSL DMT-based systems are deployed. Therefore, this paper proposed a new method to calculate the worst-case self-FEXT in distributed networks.

When we use the worst-case self-FEXT to find the optimized reference PSDs, we can use the following cost function:

$$\text{Cost} = \min_i \{L_{\text{NoUPBO}}(S_i) - L_{\text{UPBO}}(S_i, \psi_{1U}, \phi_{1U}, \psi_{2U}, \phi_{2U})\},$$

where S_i denotes a set of bitrates for which the reference PSDs are optimized; $L_{\text{UPBO}}(S_i, \psi_{1U}, \phi_{1U}, \psi_{2U}, \phi_{2U})$ denotes the reach with UPBO and worst-case self-FEXT; $L_{\text{NoUPBO}}(S_i)$ denotes the reach without UPBO and collocated disturbers; superscripts 1U and 2U denote the first and second upstream bands. A similar approach was used in [78, 96] to find the optimal reference PSDs. We developed an algorithm in [107] based on the Nelder-Mead simplex method [72, 67] to search for reference PSDs.

Different reference PSDs are used in different standardization bodies. For instance for alien crosstalk noise models A and B, ETSI defines the following reference PSDs [40]: $\mathcal{P}_{\text{REF}, 1U}(f) = -47.3 - 28.01\sqrt{f}$ and $\mathcal{P}_{\text{REF}, 2U}(f) = -54 - 19.22\sqrt{f}$, where the frequency f is given in MHz. We will use these values for simulations in Section 5.7 when we will describe in detail the drawbacks of UPBO with fixed reference PSDs when it is deployed in an actual network scenario. Furthermore, as shown in Section 2.1 each country has a different loop length distribution and uses different types of cables. VDSL performance can therefore be improved when the reference PSDs are optimized for each cable bundle.

3.2 Dynamic Spectrum Management

The major drawback of all static spectrum management (SSM) techniques described in Section 3.1 is that they are developed based on statistical cable parameters and worst-case noise scenarios. This strategy was motivated by the goal of improving the reliability of DSL systems with no need for a central agent that controls their spectra. In practice, however, it results in overly pessimistic bitrates due to a poorly optimized resource allocation among different loops. Furthermore, if the system environment changes in a practical scenario due to unmodeled noise sources the initial reliability of DSL systems easily vanishes.

To improve the reliability and increase the bitrates of DSL systems, Cioffi *et al.* have proposed to use dynamic spectrum management (DSM) [6, 86, 101]. Dynamic spectrum management (DSM) increases the utilization of the loop plant capacity by adapting the spectra of DSL systems to the actual network environment. Thus, the actual crosstalk couplings and optionally the time-dependent nature of the crosstalk are incorporated in the optimization process to increase the bitrates and to improve the reliability of the DSL systems. The term DSM has also been used to describe the techniques that aim to cancel crosstalk. Thus, DSM considers the DSL access network as a multi-user system. DSM

can also be defined as a set of techniques that aim to utilize the capacity of the loop plant optimally.

A reference network model for DSM is shown in Figure 3.6. It shows that the spectrum management center (SMC) can be located anywhere. Furthermore, in an unbundled network the SMC should be managed by an independent entity. Depending on the deployed systems and the algorithm used for optimization, the SMC performs different tasks. For instance, it can calculate channel transfer coupling functions on behalf of ILEC and CLECs from the data that the ILEC and CLECs have gathered and have sent to the SMC; it can help in exchanging different parameters among the ILEC and CLECs, like bitrates, transmit PSDs, and noise margins for all DSL systems; it can also dynamically calculate downstream and upstream spectra for modems that may alter their transmit PSD masks, aiming to improve the reliability and bitrates of all DSL systems. Although not shown in Figure 3.6 each ILEC and CLECs might have their SMCs to simplify communication between the “main” SMC and the modems under its control.

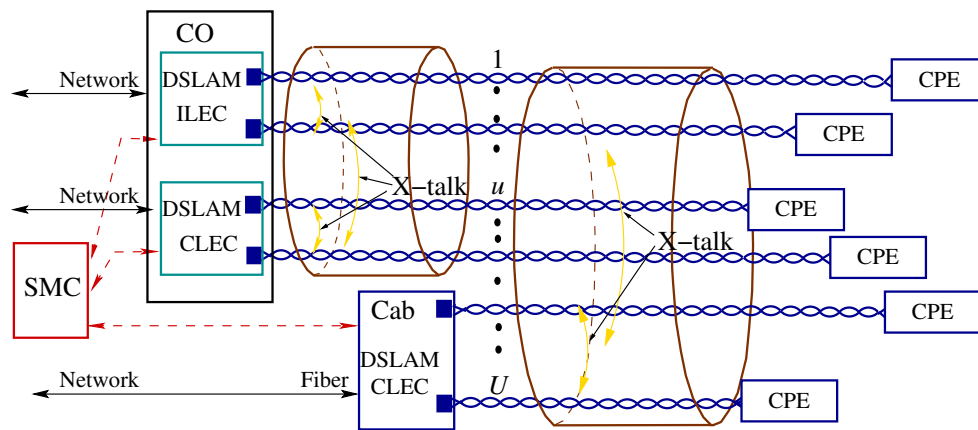


FIGURE 3.6: An example of DSM network structure in an unbundled access network. SMC is the spectrum management center, ILEC is the incumbent local exchange carrier, CLEC is the competitive local exchange carrier, and DSLAM is the digital subscriber line access multiplexer.

Methods that can be used to optimize the utilization of cable resources depend on the deployed DSL systems and the level of coordination among them. Four DSM levels of coordination are usually defined:

- *Level 0:* There is no coordination of signals and spectra between different lines, as is the case for currently deployed DSL systems based on SSM.
- *Level 1:* Bitrates are controlled by the SMC and spectra (usually power allocations) are optimized in each line autonomously aiming to minimize bitrate loss due to crosstalk in all lines.
- *Level 2:* Bitrates and spectra (power allocations and optionally band plan) are controlled and optimized by the SMC aiming to minimize bitrate loss due to crosstalk in all lines.
- *Level 3:* Signals in multiple lines are allowed to be processed jointly aiming to cancel the crosstalk.

Depending on the coordination level different techniques can be applied to perform DSM. At Level 0 different multi-user detection (MUD) techniques can be used [20, 35,

124]. Actually, the MUD can be used with all levels of coordination, but they provide only modest gains with only one or two significant disturbers and have high complexity [101]. Therefore, when coordination is possible other techniques should be used for DSM. The two most promising are:

1. Spectral balancing, which can be used with Level 1 or Level 2.
2. Vectoring (discussed in Section 3.2.2), which can be used with Level 3.

All DSM techniques need to know the multiple-input multiple-output (MIMO) channel matrix. Depending on the coordination level different methods can be used to identify (estimate) the channel matrix. For Level 0 the DSL systems on each line must estimate the channel matrix blindly. The expectation maximization (EM) algorithm was considered for this purpose in [1].

When coordination among lines is possible, simple methods can be used to perform channel identification. Zeng *et al.* in [123], by reasoning that it is simple to identify (estimate) the crosstalk couplings if the transmitted and received signals are both known, propose a method in which all modems gather the received signals that have been transmitted by all modems in turn during a predefined time period. The transmitted and received signals are then sent to the SMC, which estimates all required channel coupling functions by using a least-squares estimator. In the method proposed in [123] it is not required that the transmitters and receivers work synchronously while they send the data to estimate the channel, but instead it estimates the timing differences of the transmitted and received signals. Simplifications are possible with Level 3 coordination, as the time arrivals of received signals are exactly known. In this thesis, we will not further consider the identification of the channel matrix, but instead assume that it is perfectly known.

3.2.1 Spectral Balancing

Spectral balancing can be deployed in all DSL systems that can alter their transmit spectra. DMT systems allow this, because they can transmit any power level in each subcarrier. For DSL systems that are designed based on single-carrier modulation, there are difficulties applying spectral balancing due to the implications that arise in the design of the filters (see Figure 2.12).

An example of a DSL access network topology for spectral balancing when DSL systems are deployed only from the CO is shown in Figure 3.7. For the case when the systems are deployed simultaneously from the CO and the cabinet, the DSL access network for spectral balancing has the structure that was shown in Figure 3.6. Spectral balancing requires Level 1 or Level 2 coordination. Depending on the level of coordination the SMC performs the following tasks by spectral balancing. At Level 1, the SMC controls the bitrates that can be used by all users. At Level 2, the SMC, depending on the deployed algorithm, controls bitrates, calculates the PSD masks, and calculates an optimized band plan.

For spectral balancing, the channel is modeled as an interference channel with no signal coordination between transmitters or receivers. Thus, neither joint encoding at the transmitter side nor joint decoding at the receiver side are possible. For the general case, the capacity (bitrate) region of the interference channel is still an unsolved problem in information theory [32]. The capacity of the interference channel is known only in a few special cases. For instance, Carleial showed in [13] that the capacity region of the

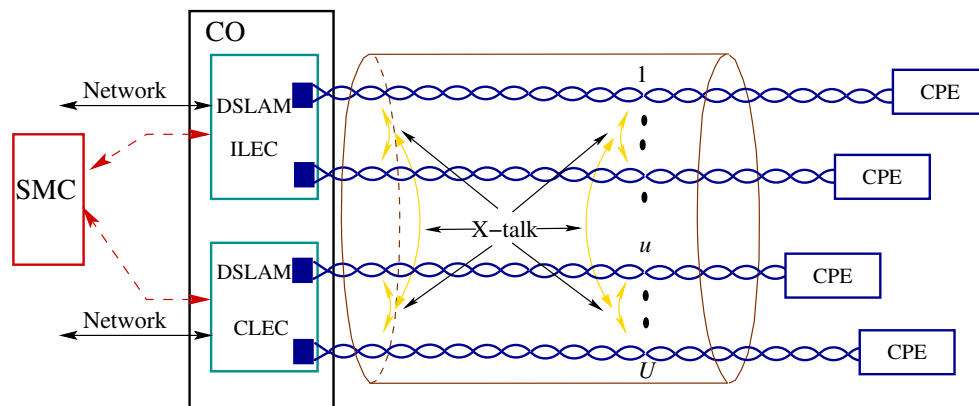


FIGURE 3.7: An example of a DSL access network topology for spectral balancing when DSL systems are deployed only from the CO.

interference channel is known in the case of strong interference. He showed that under strong interference each receiver can decode the interference signals from the other users perfectly by treating his own signal of interest as noise. After that the interference signals can be subtracted from the received signal. This strategy allows the receiver to decode its own signal as if there were no interference at all.

From a practical point of view Carleial's scheme is too complex to implement. Furthermore, in general in DSL the interference channels are weaker than the direct channel. Therefore, for the sake of the simple receiver design, all current DSL systems treat the crosstalk noise as background noise. The problem that is addressed in current DSL systems for spectral balancing is how to coordinate the spectra of DSL systems such that the bitrates of all users are "jointly" maximized. Thus, all proposed PBO methods, especially those for VDSL as described in Section 3.1.3.1, can be considered as techniques for spectral balancing.

A technique proposed by Sendonaris *et al.* to optimize the spectra (power and subcarrier allocation) of all users for both directions is presented in [97]. Here, the optimization is performed under the following assumptions: equal and symmetric bitrates for all users, equal channel transfer functions on all lines with only NEXT noise present, and collocation of modems at both sides. The idea is to divide the bandwidth into N equal independent subchannels and to make a threshold test that for all subchannels smaller than n to use equal PSD for both transmission directions, whereas for all other subchannels to use frequency division duplexing. An extension of work in [97] to account for the presence of FEXT noise, in addition to NEXT noise, is presented in [37]. In [37] the problem is solved with generalized Benders decomposition [46]. However, the assumption in both [97] and [37] that the victim modem and disturbers are collocated is unrealistic. DSL network networks have special distributed structures, as we described in Section 2.1.

It is well known that for a single-user case the optimal power allocation for a given total power constraint is found by the water filling algorithm [30, 100]. For a known band plan and total power constraint for each user in a multi-user DSL interference channel, Yu *et al.* [122] have proposed to use the so-called iterative water-filling algorithm (IWFA) to find the transmit PSDs of all users. The IWFA, as the name indicates, iterates successively through all users, and in each iteration water-filling is performed as in the single-user case

by considering the interference signal from the other users as noise. When the IWFA converges, the power allocations found for all users are the so-called “competitively” optimal power allocations. Yu *et al.* showed in [122] that the competitively optimal power allocations for DSL channels of interest always exists. They called the convergence point of the competitively optimal power allocations a “Nash equilibrium” point. We analyze the criteria for the existence of a Nash equilibrium point in interference DSL channels in Section 5.6.1.

A Nash equilibrium point [66, 71] for the competitively optimal power allocations can be defined as a point such that each user’s power allocation is optimal against the power allocations of the other users. Competitively optimal power allocations are in general not optimal, but as was shown in [65, 122] they give significant improvements compared to different power back-off algorithms and SSM. In the IWFA, the total power constraints of all users are changed iteratively until the target bitrates of all users are achieved. It is important that the target bitrates of all users have to be within the achievable rate region⁷, since otherwise some or all of the users would operate with negative margin [122]. Since in the IWFA the users do not need to know the bitrates of the other users and the total noise can be measured (estimated) locally, it can be deployed in a distributed manner; thus, it requires Level 1 coordination.

Calculation of the optimal power allocations for the interference channel is in general a difficult optimization problem, because the total bitrate expression (the sum of the bitrates of all users) is neither concave nor convex with respect to the power allocations of all users. It is shown in [14, 15, 22] that the optimal power allocations for the interference channel can be found by using the dual decomposition. In [14, 15] the resulting algorithm has been named optimal spectrum balancing algorithm (OSBA). The complexity of the OSBA grows exponentially with the number of loops and it performs an exhaustive search to find the pairs of bitrates that can be supported. Therefore the OSBA effectively fails to deliver any result in a reasonable time if the number of loops is larger than a few. Furthermore, as the OSBA in each iteration needs to know the power allocations of all users, it can be deployed only in a centralized manner; thus, it requires Level 2 coordination.

As recognized by many authors [27, 110, 104, 105], using a fixed band plan prevents achieving the desired downstream and upstream bitrate combinations among users. Cioffi *et al.* [24, 27] have recognized that sometimes improvement can be achieved if the so-called bi-directional IWFA (bi-IWFA) is used. The bi-IWFA does not fix the band plan, but assumes an echo-cancelled transmission scheme and lets the IWFA decide for each loop which subcarriers should be used for the downstream or the upstream transmission direction exclusively and which should be used simultaneously for both transmission directions. We will analyze the performance of the bi-IWFA in Section 5.6. The bi-IWFA, like IWFA, can be deployed in a distributed manner; therefore, it needs to know the target bitrates of all users in advance and they must be achievable.

Deploying the bi-IWFA increases the complexity of DSL systems because it requires an echo canceler in each modem. We have analyzed in Section 2.2.2 that with Zipper-DMT each subcarrier can be assigned in each direction without increasing the implementation complexity of the transmission system. Therefore, to keep the simplicity of Zipper-DMT transmission systems and to achieve the highest bitrates, we should search for an optimal

⁷Each proposed algorithm for the spectral balancing has its one rate region.

band plan and optimal power allocations for all user. These types of optimization problems belong to the class of mixed-integer nonlinear optimization problems [46], which in general are very challenging from a computational point of view. Unfortunately for DSL they are still unsolved problems. We will show in Section 4.3 why this is the case.

Both the IWFA and the bi-IWFA are simple to implement and have low complexity. They have a drawback that they need to know the target bitrates of all users in advance and they should be achievable which is difficult to determine. As mentioned, the bi-IWFA requires an echo canceler, which increases the complexity of the DSL systems. With these problems in mind, we have developed a DSM algorithm that we call the normalized-rate iterative algorithm (NRIA) [103, 104, 105]. The NRIA is based on the iterative water-filling algorithm (IWFA) [122] for finding good power allocations, but extends the IWFA by automatically deriving achievable bitrates of all users and searching for an optimized band plan. Since the NRIA needs to know the bitrates of all users and the band plan in each iteration, it requires Level 2 coordination. The NRIA is the only DSM algorithm that jointly addresses the problem of subcarrier allocation for frequency division duplexing systems and power allocations for all users sharing a common cable bundle. We will not describe the NRIA further in this section, because the NRIA and its derivative, the constrained NRIA (C-NRIA) [106], will be described in detail in the following chapters.

3.2.2 Vectoring

The highest bitrates over a multiple-input multiple-output (MIMO) channel with crosstalk noise impairment can be achieved by coordination of signals. When the signals are coordinated, we can transmit over a MIMO channel such that the crosstalk is cancelled or precompensated (the crosstalk is eliminated at the transmitter side). Depending on the assumption about the collocation of modems different techniques can be used to coordinate the signals.

Honig *et al.* in [53, 54] have proposed, under the assumption that the twisted-pair cable have a collocated termination on both sides, a signal processing scheme to cancel both the NEXT and the FEXT. Taubök and Henkel in [109] have proposed, for the DMT systems and assuming an FDD transmission scheme, to use singular value decomposition to cancel the FEXT.

For most practical applications of interest the modems are not collocated on both sides. When DSL systems are only deployed from the CO or the cabinet, the modems are collocated at the CO or at the cabinet, but not at the customer side. Therefore, the coordination of signals at both sides of the cable is very difficult, if not infeasible with reasonable complexity, due to the distribution of modems at the customer side. Coordination at the CO or the cabinet is simple, since we have access to transmitted and received signals of all users. Simplification in signal processing is possible if DMT with FDD transmission is assumed, as recognized by Ginis and Cioffi in [48], because the crosstalk cancellation or precompensation can be performed per subcarrier.

The aim of using vectoring in DSL is to enable self-FEXT free transmission over cable bundles. This is performed by considering the cable bundle as a MIMO system and using joint signal processing at the receiver side for the upstream transmission and at the transmitter side for the downstream transmission. Thus, vectoring requires Level 3 coordination. To deploy vectoring, the transceivers corresponding to a single cable bundle

must be collocated at the CO or the cabinet and controlled by a single network service provider. Such network scenarios will become common when network service providers install optical network units (ONUs) at cabinets to shorten the loop length to customers, when they are interested in offering higher bitrates. We will briefly describe the multiple access channel and broadcast channel, which are used to model the channel for vectoring in the upstream and downstream transmission directions, respectively.

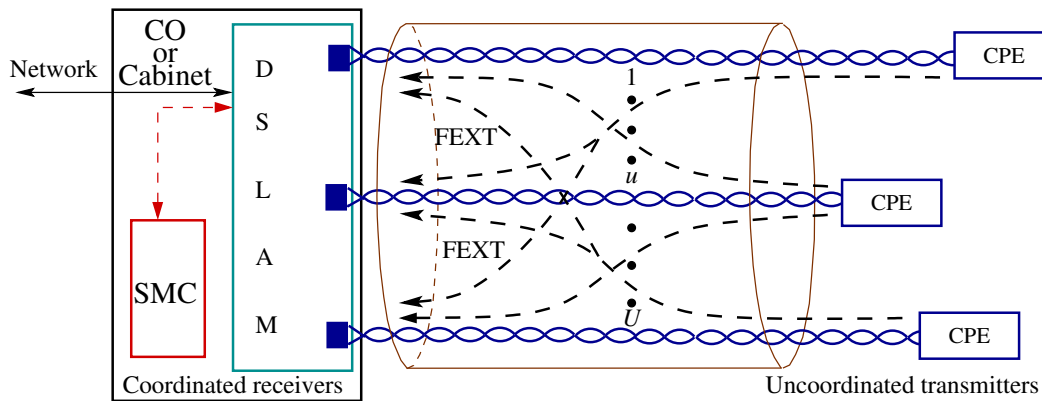


FIGURE 3.8: A multiple access channel model for the case when vectoring is used for the upstream transmission direction. For this case, all modems at the receiver sides are coordinated, whereas the modems at transmitter sides are uncoordinated.

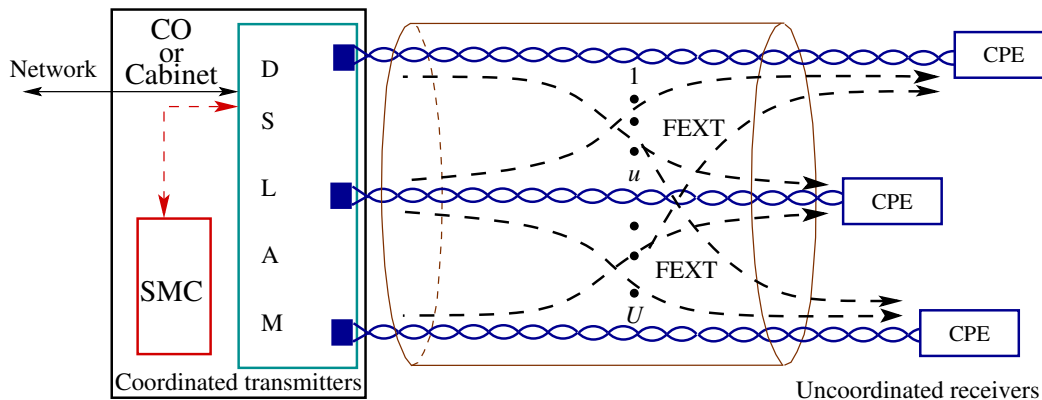


FIGURE 3.9: A broadcast channel model for the case when vectoring is used for the downstream transmission direction. For this case all modems at transmitter side are coordinated, whereas the modems at receiver sides are uncoordinated.

A multiple access channels (or multipoint-to-point communications) and a broadcast channel (or point-to-multipoint communication) are well known in information theory and wireless communications [33, 117]. In the wireless multiple access channel, multiple mobile stations transmit to one base station over a common channel, whereas in the wireless broadcast channel one base station transmits to multiple mobile stations. In DSL, analogously, in the multiple access channel multiple modems transmit to a single DSLAM as shown in Figure 3.8, whereas in the broadcast channel a single DSLAM transmits to

multiple modems as illustrated in Figure 3.9. These channel models are characterized as a vector multiple access channel and a vector broadcast channel, since the inputs and outputs in vectoring systems are vectors. Other network scenarios are also possible, where some users use multiple lines to communicate with the CO or the cabinet.

For vectoring, two main methods proposed to perform crosstalk cancellation for the upstream and crosstalk precompensation for the downstream are: the first method uses crosstalk cancellation via QR decomposition [48, 49]; the second method uses zero-forcing (ZF) criteria [15]. Both crosstalk cancellation via QR decomposition and the ZF are near-optimal. However, ZF is simple to implement and has low latency in signal processing [15], so it is the preferred scheme for practical implementation.

Although in vectoring the received signals at both the CO and customer sides are crosstalk-free, to achieve the highest bitrates the calculation of the optimal power allocation for each user is required. For the upstream, if an optimal decision feed-back canceler is used, the problem of finding the optimal power allocations for all users is a convex programming problem [15]. However, although the optimization problem is convex, no closed form solution is known and numerical convex optimization algorithms must be used [118]. For the downstream, if an optimal precoder is used, the problem of finding optimal power allocations also becomes a convex programming problem [15]. However, as in the upstream case, no closed form solution is known and numerical convex optimization algorithms must be used there too. It was shown in [48] that there is a negligible loss in bitrate compared to the single-user bound if power allocation for each user is performed as in the single-user case (single-user water-filling).

As mentioned in the section on spectral balancing, to achieve the desired downstream and upstream bitrates for each user, sometimes we should not only determine the optimal power allocation for each user, but also an optimized band plan. Fortunately, for vectoring systems, this optimization problem can be solved (as for the fixed subcarrier allocation the optimization problem is convex), but it still has a high computational complexity. An example of finding an optimized band plan for symmetric services is given in [48].

Finally, it is worth mentioning that from a practical point of view vectoring should be deployed in loops with moderate length (say up to 1 km). For longer loop lengths the FEXT becomes negligible due to the loop attenuation and therefore improvements in performance will be small.

Chapter 4

The Normalized-Rate Iterative Algorithm

Currently, each digital subscriber line (DSL) system runs independently from all other systems deployed in the same cable bundle. As described in Chapter 3, in the development of currently deployed DSL systems, a single-user¹ scenario was assumed with worst case crosstalk models. This conservative strategy was motivated by the goal of maximizing the robustness of DSL systems. In practice, however, it often leads to overly conservative performance figures and sometimes even to failures to deliver a specific DSL service. This is often due to a poorly optimized resource allocation among different loops in a cable bundle, combined with unnecessarily high noise margins, which result in too pessimistic bitrates. Furthermore, if the system environment changes in a practical scenario, *e.g.*, where unmodeled noise sources appear, the initial robustness of a static deployed DSL system easily breaks down. In Section 3.2 we explained that spectral balancing and vectoring are two of the most promising techniques for DSM. Hereafter in this work the term DSM refers to spectral balancing if not otherwise specified.

With an active approach to copper bundle resource management, the spectra in the individual loops can be balanced much more efficiently against each other. Combined with more accurate crosstalk figures obtained from accurate on-line cable measurements, higher and more balanced bitrates can be achieved on most loops. In the literature, this is often referred to as dynamic spectrum management (DSM), although currently only active power control and power allocations over a predefined static spectrum band plan between the downstream and upstream is considered.

In this chapter, we present a novel practically applicable DSM method for DSL called the normalized-rate iterative algorithm (NRIA). The NRIA is a centralized DSM algorithm (commonly referred to as DSM ‘Level 2’) based on the iterative water-filling algorithm (IWFA) [122] for finding good power allocations, extending the IWFA by automatically deriving achievable bitrates and searching for an optimized band plan.

The NRIA jointly balances the spectrum between the downstream and upstream directions, *i.e.*, it finds an effective common band plan for frequency division duplexing (FDD) DSLs, and performs power allocations for all users in a cable bundle. The NRIA is sub-optimal in the sense that the power allocations are based on the IWFA, and the frequency allocation is based on an *ad hoc* solution.

Compared to other DSM methods, the NRIA has essentially two major advantages:

¹As mentioned also in Chapter 1, the term *user* is generic, comprising a twisted-pair line and two modems located at both ends of the line.

high performance and low computational complexity. Since the NRIA optimizes the band plan, better performance can be achieved than with the IWFA, which uses a static (fixed) band plan. Compared to the optimal spectrum balancing algorithm (OSBA) [14, 15, 22], which in theory can deliver the highest bitrates for a given band plan, the NRIA can in practice achieve almost as good performance but with a dramatically lower computational complexity. This is crucial especially for the more realistic cases where the number of loops in a bundle is more than a few. In this case, since the complexity of the OSBA grows exponentially with the number of loops, it effectively fails to deliver any result in a reasonable time. Furthermore, due to the extended capability of searching for an optimized band plan, the NRIA supports several downstream and upstream bitrate combinations that cannot be supported by any other proposed DSM algorithm.

Another practically important advantage of the NRIA over the IWFA is that it needs no prior knowledge about the achievable bitrates, which are difficult to specify in advance (before running the algorithm). Since the NRIA finds these bitrates automatically, no prior knowledge about them is required. Furthermore, tractable operating points for desirable business models can easily be achieved, because the NRIA has a parameter for selecting the desired downstream and upstream asymmetry and parameters for selecting the user priorities.

As with the OSBA, a potential drawback of the NRIA, however, is that it is a centralized algorithm operated by a common DSM agent. Nevertheless, a DSM agent may be necessary in practice since the pairs of user bitrates that can be supported by a distributed DSM algorithm like the IWFA must be calculated by a central agent. In Section 4.7 we conceptually describe how the NRIA can be extended to be deployed in a semi-distributed manner.

This chapter is organized as follows. Section 4.1 describes the system model that the NRIA is designed to handle. Section 4.2 shows some fundamental bitrate relations used by the NRIA. Section 4.3 formulates the multi-user optimization problem for an optimal subcarrier allocation (common to all users), power control, and power allocation. In the same section we describe why such an optimization problem cannot be solved with existing algorithms. Section 4.4 describes the NRIA as a suboptimal but practical solution to the optimization problem formulated in Section 4.3. Section 4.5 analyzes the complexity of the NRIA. Section 4.6 shows how to initialize the input parameters in the NRIA to achieve good performance and fast convergence. Finally, Section 4.7 briefly overviews the NRIA compared to the IWFA.

4.1 System Model

Figure 4.1 shows a typical network scenario that the NRIA is designed to handle. Specifically, it is assumed that both ends of the cable can be distributed; at the line termination (LT) side, the loops can be connected to a central office (CO) as well as a cabinet; at the network termination (NT) side, the loops are connected to customer premises equipments (CPEs), which are usually distributed in space. We assume that some of the DSL systems deployed from the CO and cabinet use the same cable bundle in the loops' segments between the cabinet and the CPEs as illustrated in Figure 4.1. We use the terms *downstream* when transmitting from an LT to an NT modem and *upstream* for transmission in the

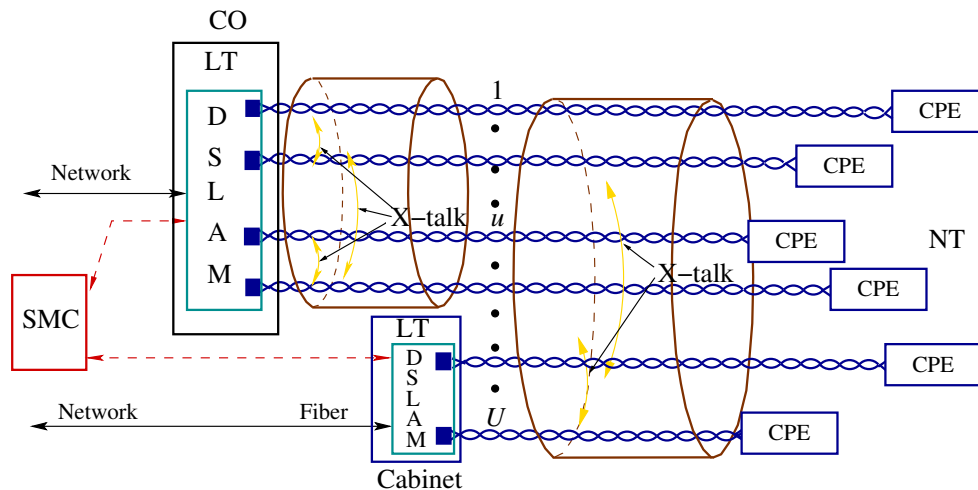


FIGURE 4.1: A distributed multi-user DSL environment with customer premises equipment (CPE) connected to a central office (CO) as well as to a cabinet. SMC denotes the spectrum management center. DSLAM denotes DSL access multiplexer. LT and NT denote line termination and network termination sides, respectively.

opposite direction from an NT to an LT modem.

The crucial assumption with this network model is that *all* loops have *unique* crosstalk couplings between each other. This assumption is valid in practice. Even if some cables are collocated at one end, or even at both ends, they will still have different crosstalk couplings due to other differences, such as in the twists, the locations of the loops within a bundle, and the loop termination at the NT and LT sides. For example, it is not always the case that the longest loop in a network has the poorest DSL channel conditions.

The NRIA relies on a spectrum management center (SMC), which can be located anywhere, as shown in Figure 4.1. First, the SMC collects all channel characteristics in the network from individual modems, including the crosstalk channels, during an off-line period. Different methods have been proposed to collect and calculate/estimate the channel characteristics as described in Section 3.2. We will not analyze here how these data can be collected—we will only assume that they are available at the SMC. Secondly, the SMC runs the NRIA in order to find a common band plan and individual transmit PSD for each modem. Finally, these parameters are returned by the SMC to all modems before they start to operate.

For the network scenario shown in Figure 4.1 we assume that neither the transmitters nor the receivers at both the NT and LT sides coordinate their signals. Thus, the transmission system can be considered as consisting of $2U$ transmitter-receiver pairs (twice the number of the users U , because we assume bi-directional transmission) sharing the same channel. The background noise² in DSL systems can be considered Gaussian as described in Section 2.4.1 and is typically smaller than the interference signal. This channel model is known as a Gaussian interference channel [33]. A simple example of a Gaussian interference channel with two users, when DSL systems are transmitting only in one transmission direction, is shown in Figure 4.2. For this case the received signals in

²The typical values of background noise encountered in DSL systems are presented in Section 2.4.1.

the input of both receivers $y_1(t)$ and $y_2(t)$ are given by

$$\begin{aligned} y_1(t) &= h_{11}(t) * x_1(t) + h_{12}(t) * x_2(t) + n(t), \\ y_2(t) &= h_{22}(t) * x_2(t) + h_{21}(t) * x_1(t) + n(t), \end{aligned}$$

where the $*$ sign denotes convolution; $x_1(t)$ and $x_2(t)$ denote the transmitted signals of the first and second user, respectively; $h_{11}(t)$ and $h_{22}(t)$ denote the channel impulse response of the first and second loop, respectively; $h_{21}(t)$ denotes the impulse response from the first loop to the second loop; $h_{12}(t)$ denotes the impulse response from the second loop to the first loop; and $n(t)$ is the background noise. The receiver model that we will assume throughout this chapter considers the interference signals received from all other transmitters as noise and treats them as background noise. This strategy simplifies the design of DSL receivers tremendously.

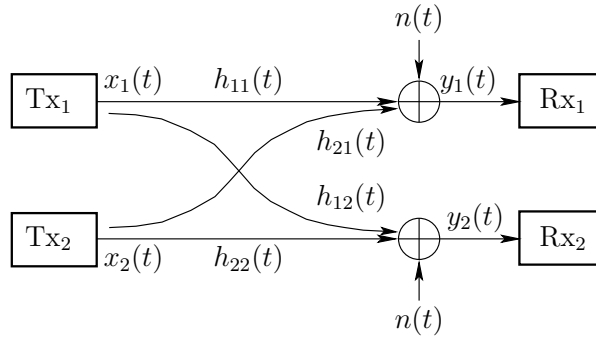


FIGURE 4.2: Illustration of the Gaussian interference channel for the two-user case.

To make efficient dynamic spectral balancing possible, high flexibility in selecting the transmission spectra is needed by the DSL system. Multicarrier modulation combined with digital frequency division duplexing (D-FDD), like the Zipper [98] duplexing method based on discrete multitone modulation (DMT), offers this flexibility as described in Section 2.2.2. Since Zipper-DMT is also part of current VDSL and VDSL2 standards, we assume that it is used. Furthermore, full network synchronization is also assumed [74] in order to avoid any efficiency loss due to silent guard bands between the downstream and upstream bands, to avoid flexibility loss in frequency planning [99], and to make crosstalk noise on different subcarriers independent. Without network synchronization, the signal energy assigned by one user on one subcarrier will also leak over to neighboring subcarriers for the other users, due to the asynchrony, and thus appear as non-orthogonal NEXT and FEXT.

With network synchronization of a Zipper-DMT system, a received frequency-domain component after the DFT demodulator as shown in Figure 2.4 on subcarrier n for user u , Y_u^n , can be expressed as

$$Y_u^n = H_{uu}^n X_u^n + \sum_{\substack{v=1 \\ v \neq u}}^U H_{uv}^n X_v^n + V_u^n,$$

where X_u^n and X_v^n are the transmitted frequency-domain components of user u and user v on subcarrier n , respectively. V_u^n is the background noise of user u on subcarrier n . H_{uv}^n is the channel transfer function from user v to user u , *i.e.*, it represents either the direct channel (with $v = u$), or far end crosstalk (FEXT). To simplify the notation we have not shown and also we will not show in the following the subscript FEXT to denote the FEXT coupling channel transfer function, but we will assume this.

Note that with synchronization and D-FDD, *i.e.*, synchronous Zipper, self-NEXT is completely eliminated through orthogonality, regardless of the selected band plan (the downstream and upstream subcarriers). Therefore, the desired frequency-domain component X_u^n is disturbed by self-FEXT that originates from all other users from the corresponding subcarrier n .

The number of bits in a DMT symbol for user u in the upstream transmission direction is

$$R_{u,US} = \sum_{n \in I_{US}} R_u^n, \quad (4.1)$$

where R_u^n is the number of bits for user u on subcarrier n and I_{US} represents the set of upstream subcarrier indices, which are used for the upstream transmission direction. The number of downstream bits, $R_{u,DS}$, is derived correspondingly. To calculate the number of bits that are transmitted per second the $R_{u,US}$ is multiplied with the number of DMT symbols that are transmitted in one second. The NRFA calculates an optimized D-FDD band plan as one part of the DSM process. That is, it finds $R_{u,DS}$ and $R_{u,US}$ for $u = 1, 2, \dots, U$ by iteratively redirecting subcarriers to the downstream or the upstream direction.

Let us denote the squared magnitude of the channel transfer function from user v to u on subcarrier n by

$$\mathcal{H}_{uv}^n = |H_{uv}^n|^2.$$

Based on the Shannon capacity formula and the assumption made above that the receivers treat the crosstalk signal as a noise, the number of bits loaded on subcarrier n by user u , for two-dimensional symbols, is

$$R_u^n = \log_2 \left(1 + \frac{\mathcal{H}_{uu}^n \mathcal{P}_u^n}{\Gamma \mathcal{N}_u^n} \right), \quad (4.2)$$

where \mathcal{P}_u^n denotes the PSD of the signal, \mathcal{N}_u^n denotes the PSD of the noise on subcarrier n , and Γ is the signal-to-noise ratio (SNR) gap, which for a given bit error rate and signal constellation represents the loss compared to the Shannon channel capacity. The noise is calculated by

$$\mathcal{N}_u^n = \sum_{\substack{v=1 \\ v \neq u}}^U \mathcal{H}_{uv}^n \mathcal{P}_v^n + \mathcal{P}_V^n, \quad (4.3)$$

where \mathcal{P}_V^n denotes the PSD of the background noise on subcarrier n .

4.2 Bitrate Relations Used by the NRIA

In this section, we define some simple but usable bitrate relations in order to describe the optimization problem that we aim to solve with the NRIA in Section 4.4. The definition of such bitrate relations is unique and they are defined with business models in mind.

The NRIA uses an predefined asymmetry parameter, a , that specifies the ratio between the total desired downstream and upstream bitrates

$$a = \frac{\sum_{u=1}^U R_{u,DS}}{\sum_{u=1}^U R_{u,US}}. \quad (4.4)$$

Two “special cases” arise when $a = 0$ and $a = \infty$. For $a = 0$, the total cable capacity is assigned to the upstream transmission direction; thus, we transmit only in the upstream. For $a = \infty$, the total cable capacity is assigned to the downstream transmission direction; thus, we transmit only in the downstream.

For a given transmission direction dir with $dir \in \{DS, US\}$, we do not know *a priori* which bitrates can be supported by each user. Therefore, we assign to each user u a priority value $\alpha_{u,dir}$, which specifies how much of the total cable capacity for a certain transmission direction shall be assigned to user u . Hence, we specify the relation between the user priorities and bitrates as

$$\frac{R_{1,dir}}{\alpha_{1,dir}} = \frac{R_{2,dir}}{\alpha_{2,dir}} = \dots = \frac{R_{U,dir}}{\alpha_{U,dir}}, \quad (4.5)$$

with

$$\sum_{u=1}^U \alpha_{u,dir} = 1. \quad (4.6)$$

A “special case” arises when $\alpha_{u,dir} = 0$. In this case, the user u is not transmitting in the particular direction dir ; thus, it is removed from (4.5).

When we define the bitrate relations as in (4.4), (4.5), and (4.6) the downstream and upstream bitrates for each user are related, as shown in Appendix C.1, by

$$R_{u,DS} = a \cdot \frac{\alpha_{u,DS}}{\alpha_{u,US}} \cdot R_{u,US}, \quad \text{for } u = 1, 2, \dots, U. \quad (4.7)$$

Note that the bitrate relations in (4.7) hold when a , $\alpha_{u,DS}$, $\alpha_{u,US}$ are not zero.

Let us illustrate the defined bitrate relations with a simple hypothetical two-user example, consisting of one private user and one business user. First, let us assume that the two-twisted-pair cable has a total capacity of 18 Mbit/s (which is in reality unknown), and let us assume that we have a business model that specifies the asymmetry $a = 2$ between the downstream and upstream directions. From the formulas above, we now have $R_{1,DS} + R_{2,DS} = 12$ and $R_{1,US} + R_{2,US} = 6$. Next, let us assign in the downstream $\alpha_{1,DS} = 1/3$ to the private user and $\alpha_{2,DS} = 2/3$ to the business user, which gives

downstream bitrates of 4 Mbit/s and 8 Mbit/s to the private user and to the business user, respectively.

Similarly, in the upstream let us assign $\alpha_{1,US} = 1/6$ to the private user and $\alpha_{2,US} = 5/6$ to the business user, which gives upstream bitrates of 1 Mbit/s and 5 Mbit/s to the private and to the business user, respectively. It can easily be verified that the users' bitrates and priority values fulfill (4.5) and (4.6), respectively. Table 4.1 summarizes the different parameter values given in this example. Note that in a similar way we could have derived the user priority values and the asymmetry parameter a based on the downstream and upstream bitrates we aim to offer the users. Let us select the bitrates that we aim to offer the users as $R_{1,DS} = 4$ Mbit/s, $R_{2,DS} = 8$ Mbit/s, $R_{1,US} = 1$ Mbit/s, and $R_{2,US} = 5$ Mbit/s. By using (4.4), (4.5), and (4.6) we find that $a = 2$ and the user priority values are shown in Table 4.1.

TABLE 4.1: Relations between different bitrates and users' priority values when the two-twisted-pair cable has a capacity of 18 Mbit/s.

User u	User priorities		User bitrates (Mbit/s)		Norm. bitrates (Mbit/s)	
	$\alpha_{u,DS}$	$\alpha_{u,US}$	$R_{u,DS}$	$R_{u,US}$	$\frac{R_{u,DS}}{\alpha_{u,DS}}$	$\frac{R_{u,US}}{\alpha_{u,US}}$
1	1/3	1/6	4	1	12	6
2	2/3	5/6	8	5	12	6
Σ	1	1	12	6		

In an actual scenario, we do not know before hand which bitrates can be supported. However, the NRIA uses the given asymmetry parameter a and the user priority values $\alpha_{u,dir}$ to find the desired operating point (*i.e.*, the bitrates of all users), since the quantities represented by these parameters are always related through (4.4), (4.5) and (4.6). For example, let us assume that we have selected the a and $\alpha_{u,dir}$ values as in Table 4.1. If the two-twisted-pair cable actually had a capacity of 31.5 Mbit/s then the bitrates shown in Table 4.2 would be supported.

TABLE 4.2: Relations between different bitrates and users' priority values when the two-twisted-pair cable has a capacity of 31.5 Mbit/s.

User u	User priorities		User bitrates (Mbit/s)		Norm. bitrates (Mbit/s)	
	$\alpha_{u,DS}$	$\alpha_{u,US}$	$R_{u,DS}$	$R_{u,US}$	$\frac{R_{u,DS}}{\alpha_{u,DS}}$	$\frac{R_{u,US}}{\alpha_{u,US}}$
1	1/3	1/6	7	1.75	21	10.5
2	2/3	5/6	14	8.75	21	10.5
Σ	1	1	21	10.5		

4.3 Problem Formulation

The IWFA and the OSBA assume a fixed D-FDD band plan. This makes it difficult to balance the bitrates between the downstream and upstream transmission directions. As a result often in one transmission direction we achieve much higher bitrates than we wish

to offer, but in the other direction we cannot offer the desired bitrates. Furthermore, in a particular direction, the IWFA assumes that the target bitrates of all users are known *a priori* and that they are achievable. On the other hand the OSBA uses some form of exhaustive search, which is time consuming, to find the desired operation point. Therefore, with these problems in mind we take a different approach with the NRIA.

As mentioned earlier, the NRIA aims to jointly optimize the plan and the power allocations of all users. That is, the NRIA selects the downstream and upstream subcarriers common to all users represented by the sets I_{DS} and I_{US} , with $I_{DS} \cap I_{US} = \emptyset$. Hence, the users' downstream and upstream bitrates will depend on each other, a property that is often desirable for practical business models. The dependency of the downstream and upstream bitrates guides the NRIA to desirable operating points, as in the two examples given in Section 4.2. Furthermore, to jointly optimize the power allocations among all users, two vectors are to be found for each user, specifying the power allocation in downstream, $\mathcal{P}_{u,DS} = [\mathcal{P}_{u,DS}^0, \mathcal{P}_{u,DS}^1, \dots, \mathcal{P}_{u,DS}^{N-1}]$, and upstream, $\mathcal{P}_{u,US} = [\mathcal{P}_{u,US}^0, \mathcal{P}_{u,US}^1, \dots, \mathcal{P}_{u,US}^{N-1}]$. In addition, each user should satisfy a total power constraint: $0 \leq \sum_n \mathcal{P}_{u,DS}^n \leq \mathcal{P}_{u,DS}^{\max}$, and $0 \leq \sum_n \mathcal{P}_{u,US}^n \leq \mathcal{P}_{u,US}^{\max}$, where $\mathcal{P}_{u,DS}^{\max}$ and $\mathcal{P}_{u,US}^{\max}$ denote the maximum total power allowed for user u in the downstream and upstream, respectively. Usually the maximum total power constraint is selected the same for all users.

We aim to jointly maximize the bitrates in the downstream and upstream directions for all users under the constraints that the bitrates satisfy the predefined relations (4.4), (4.5) and (4.6). Hence, it is of no practical interest to impose a maximized total bitrate without further constraints, since this leads the situation were the users close to the CO (or cabinet) being given very high bitrates at the price of the distant users, who will get very low bitrates or no DSL service at all.

When formulating the optimization problem, it is convenient to use two indicators for each subcarrier, β_{DS}^n and β_{US}^n , which specify the transmission direction. Due to the D-FDD Zipper type transmission scheme³, the subcarrier indicators fulfill $\beta_{DS}^n = 1 - \beta_{US}^n$ for $n = 0, 1, \dots, N - 1$. For the upstream transmission direction, the relation between β_{US} and I_{US} is given by:

$$\beta_{US}^n = \begin{cases} 1, & \text{if } n \in I_{US}, \\ 0, & \text{otherwise.} \end{cases} \quad (4.8)$$

A corresponding relation holds for the downstream direction. Using these indicators, (4.1) can be written as

$$R_{u,US} = \sum_{n \in I_{US}} R_u^n = \sum_{n=0}^{N-1} \beta_{US}^n R_u^n. \quad (4.9)$$

³Without loss of generality, we do not consider the silent (unused) subcarriers.

The optimization problem can now be formulated as:

$$\text{maximize } \sum_{u=1}^U (R_{u,DS} + R_{u,US}), \quad (4.10a)$$

subject to:

$$\sum_{u=1}^U R_{u,DS} = a \sum_{u=1}^U R_{u,US}, \quad (4.10b)$$

$$\frac{R_{1,DS}}{\alpha_{1,DS}} = \frac{R_{2,DS}}{\alpha_{2,DS}} = \dots = \frac{R_{U,DS}}{\alpha_{U,DS}}, \quad (4.10c)$$

$$\frac{R_{1,US}}{\alpha_{1,US}} = \frac{R_{2,US}}{\alpha_{2,US}} = \dots = \frac{R_{U,US}}{\alpha_{U,US}}, \quad (4.10d)$$

$$\sum_{u=1}^U \alpha_{u,DS} = 1, \quad \sum_{u=1}^U \alpha_{u,US} = 1, \quad (4.10e)$$

$$\sum_{n=0}^{N-1} \beta_{DS}^n \mathcal{P}_{u,DS}^n \leq \mathcal{P}_{u,DS}^{\max}, \quad u = 1, 2, \dots, U, \quad (4.10f)$$

$$\sum_{n=0}^{N-1} \beta_{US}^n \mathcal{P}_{u,US}^n \leq \mathcal{P}_{u,US}^{\max}, \quad u = 1, 2, \dots, U, \quad (4.10g)$$

$$\beta_{DS}^n = 1 - \beta_{US}^n, \quad n = 0, 1, \dots, N-1, \quad (4.10h)$$

$$\beta_{DS}^n, \beta_{US}^n \in \{0, 1\}, \quad (4.10i)$$

$$\mathcal{P}_{u,DS}^n, \mathcal{P}_{u,US}^n \in [0, \mathbb{R}^+]. \quad (4.10j)$$

The asymmetry parameter a and the user priority values $\alpha_{u,dir}$, are all constants and a designer's choice for the NRIA, as explained in Section 4.2. Equations (4.10b) to (4.10d) show the relation among different bitrates according to the definitions in Section 4.2. Equations (4.10f) and (4.10g) ensure the downstream and upstream maximum total power constraints for each user. Note that the subcarrier usage indicators, β_n^{DS} and β_n^{US} , are not really needed neither in (4.10f) nor in (4.10g), because no power will be allocated anyway to those subcarriers where β_n^{DS} and β_n^{US} are zero, due to (4.9). However, we hope that this helps the reader to recognize that no power will be allocated when β_n^{DS} and β_n^{US} are zero. Equation (4.10h) ensures D-FDD transmission per cable bundle, when the subcarrier usage indicators are constrained to take values only from the binary field as defined in (4.10i)

A PSD constraint can often be given for practical implementations of DSL modems. A PSD constraint is given either to simplify the design of analog front-end of a DSL system or to protect the deployed systems in the network that cannot change the transmit PSD mask to adapt to the noise environment, as for instance in the first generation of the ADSL modems. In these cases the allowed power range $[0, \mathbb{R}^+]$ in (4.10j) should be exchanged with $[0, \dots, \mathcal{P}_{u,dir}^{n,\max}]$, where $\mathcal{P}_{u,dir}^{n,\max}$ denotes the maximum PSD level allowed for user u on subcarrier n for a given transmission direction. In practice, the PSD mask constraint is usually the same for all DSL systems of the same type.

The optimization problem (4.10) involves binary variables from (4.10i) and continuous

variables for the PSDs. Furthermore, we have nonlinear relations between binary and continuous variables in the objective function (4.10a) as well as in the constraints (4.10b), (4.10c), and (4.10d), which are related also through (4.9). Therefore, (4.10) is a mixed-integer nonlinear optimization problem [46], which in general is very challenging from a computational point of view. For fixed downstream and upstream subcarrier allocations, the objective function (4.10a) as well as the constraints (4.10b), (4.10c), and (4.10d) are neither convex nor concave with respect to the users' power allocations. Thus, this type of optimization problem is not solvable with existing algorithms [46, 50].

In theory, it is possible to exhaustively try all possible combinations of subcarrier allocations and for each allocation to try all possible combinations of PSD mask realizations for all users. However, the number of combinations is tremendously high and practically infeasible. For instance, in VDSL Zipper-DMT [4, 40, 41] with 4096 subcarriers this results in 2^{4096} possible combinations of subcarrier allocations. The number of possible combinations of PSD mask realizations of all users, when bit-loading is used, for a particular transmission direction is $(R^{n,\max} + 1)^{N_{dir} \cdot U}$, where $R^{n,\max}$ denotes the maximum number of bits that can be loaded on subcarriers, and N_{dir} is the number of subcarriers used in a particular transmission direction. Thus, a rather typical case with $R^{n,\max} = 15$ bits, $U = 10$ users, and $N_{dir} = 2048$ upstream subcarriers has 16^{20480} possible PSD mask realizations.

For a similar optimization problem but with a fixed band plan (subcarrier allocation), a dual decomposition method has been suggested [14, 15, 22]. In particular, the OSBA has reduced the search space for possible PSD mask realizations and has linear complexity in the number of subcarriers N_{dir} . However, the OSBA still has a complexity that increases exponentially with the number of users U making it too complex for most of the DSL access network scenarios that are found in practice.

In the following section, we propose the normalized-rate iterative algorithm that solves the formulated optimization problem in a suboptimal way. We will show in Section 4.5 that our proposed algorithm has low computational complexity. Therefore the NRIA can be deployed in any network scenario with any number of users included in the optimization process.

4.4 The Normalized-Rate Iterative Algorithm

The normalized-rate iterative algorithm (NRIA) will solve the optimization problem formulated in Section 4.3 in a suboptimal way, because:

- To make the algorithm tractable we have constrained it to search in a reduced space for optimized downstream and upstream subcarrier allocations (band plan), and
- It is based on Yu's iterative water-filling algorithm [122], which finds the competitively optimal power allocations, which are, for the (Gaussian) interference channel, not globally optimal [122].

The NRIA consists of two levels of nested iterations: an *outer stage* that searches for an optimized band plan; and an *inner stage*, which calculates the downstream and upstream bitrates that can be supported by each user. The inner stage is performed independently for each transmission direction, since D-FDD is considered.

In the outer stage to make the band plan optimization tractable, the NRIA divides the total number of subcarriers into a small number of subbands with equal number of subcarriers per subband. The subbands are assigned to the downstream and upstream directions in alternating order, cf. Section 4.4.1.2 “Initial Band Plan”. Then, depending on the downstream and upstream supported bitrates in the inner stage, the subband edges (and with that also the downstream and upstream subcarrier allocations) are adapted so that the desired asymmetry a is achieved. This is described in more detail in Section 4.4.1.3 “Change Band Plan”.

In the inner stage, a modified version of the fixed-margin water-filling (FM-WF) algorithm is deployed, which implicitly performs power control and power allocation, cf. Section 4.4.1.4 “Modified Fixed-Margin Water-Filling (FM-WF) Algorithm”. The power control is achieved by constraining the users to only utilize the power needed to support the bitrates that satisfy the relations defined in (4.5) and to jointly maximize the bitrates of all users.

In the inner stage, the algorithm iterates over all users, which are ordered as described in Section 4.4.1.1 “User Ordering”, and derives a new target bitrate for each iteration. To achieve this, the NRIA uses the normalized supported bitrates $\bar{R}_{u,dir}[i] = R_{u,dir}[i]/\alpha_{u,dir}$, obtained in the last iterations. The target bitrate $T_{u,dir}[i + 1]$ is the bitrate that the NRIA aims to achieve for user u in the next iteration. Because it is difficult to make any probabilistic assumptions about any truly achievable bitrates with the given constraints and degrees of freedom, the NRIA makes a simple *ad hoc* estimate, which is the average of some past normalized achieved bitrates

$$T_{u,dir}[i + 1] = \frac{\alpha_{u,dir}}{M} \sum_{m=0}^{M-1} \bar{R}_{dir}[i - m]. \quad (4.11)$$

The appropriate memory M is somewhat related to the number of users. We will show by simulation in Section 4.6 that the NRIA works well when the memory M is selected equal to the number of users in the network scenario, thus, $M = U$.

The pseudo-code of the NRIA is listed as Algorithm 1. The outer stage of the NRIA is the *Main Function* and the inner stage the *CalcRatesPSDs Function*. The NRIA does not need any PSD mask constraint as the maximum total power constraint is sufficient to ensure spectral compatibility among the DSL systems included in the optimization process. Sometimes, however, to ensure spectral compatibility among all DSL systems deployed in the same cable bundle a PSD mask constraint is required. A PSD mask constraint can simply be incorporated into the algorithm in the function *ModifiedFM-WF* as it is an inherent property of any type of water-filling (bit-loading) algorithm.

4.4.1 Algorithmic Details

This section describes the NRIA in detail. We start describing the task of each function in Algorithm 1. After that, we describe the technique to check if the NRIA has converged to a “wrong” point.

Algorithm 1 The Normalized-Rate Iterative Algorithm**Preset Values**

$a_{\text{Target}}, \alpha_{1,\text{DS}}, \dots, \alpha_{U,\text{DS}}, \alpha_{1,\text{US}}, \dots, \alpha_{U,\text{US}},$
 $K, M_{\text{DS}}, M_{\text{US}}$

Initialize

$U_{\text{DS}} = \text{UserOrdering}(\text{DS})$
 $U_{\text{US}} = \text{UserOrdering}(\text{US})$
 $I_{\text{DS}}, I_{\text{US}} = \text{InitialBandPlan}(K)$

Main Function**repeat**

$\forall u : \mathcal{P}_{u,\text{DS}} = 0, \mathcal{P}_{u,\text{US}} = 0$ {Set PSD masks to zero}
 $T_{\text{DS}} = \infty, T_{\text{US}} = \infty$ {Set targets to infinity}
 $R_{\text{DS}}, \mathcal{P}_{\text{DS}} = \text{CalcRatesPSDs}(\text{DS}, \mathcal{P}_{\text{DS}}, T_{\text{DS}}, M_{\text{DS}})$
 $R_{\text{US}}, \mathcal{P}_{\text{US}} = \text{CalcRatesPSDs}(\text{US}, \mathcal{P}_{\text{US}}, T_{\text{US}}, M_{\text{US}})$
 $a = \frac{\sum_{u=1}^U R_{u,\text{DS}}}{\sum_{u=1}^U R_{u,\text{US}}}$
 $I_{\text{DS}}, I_{\text{US}} = \text{ChangeBandPlan}(a, a_{\text{Target}}, I_{\text{DS}}, I_{\text{US}})$

until a has reached the desired accuracy a_{Target} or the maximal number of iterations in the outer stage O_{max} has been examined.

CalcRatesPSDs Function

$R_{\text{dir}}, \mathcal{P}_{\text{dir}} = \text{CalcRatesPSDs}(\text{dir}, \mathcal{P}_{\text{dir}}, T_{\text{dir}}, M_{\text{dir}})$
 $i = 1$

repeat

for $u \in U_{\text{dir}}$ **do**

for $n \in I_{\text{dir}}$ **do**

$$\mathcal{N}_{u,\text{dir}}^n = \sum_{\substack{v=1 \\ v \neq u}}^U \mathcal{H}_{uv}^n \mathcal{P}_{v,\text{dir}}^n + \mathcal{P}_V^n$$

end for

$R_{u,\text{dir}}, \mathcal{P}_{u,\text{dir}} = \text{ModifiedFM-WF}(\mathcal{N}_{u,\text{dir}}, T_{\text{dir}}, \mathcal{P}_{u,\text{dir}}^{\text{max}})$

$$\bar{R}_{\text{dir}}[i] = \frac{R_{u,\text{dir}}}{\alpha_{u,\text{dir}}}$$

if $i < M_{\text{dir}}$ **then** $r = i$ **else** $r = M_{\text{dir}}$

$$T_{\text{dir}} = \frac{\alpha_{u,\text{dir}}}{r} \sum_{k=i-r+1}^i \bar{R}_{\text{dir}}[k]$$

$i = i + 1$

end for

until $R_{u,\text{dir}}$ and power allocations of all users have reached the desired accuracy, and at least one user utilizes a power that is close to the maximum total power with a predefined accuracy.

4.4.1.1 User Ordering

Due to the estimation of the target bitrates in each iteration of the inner stage, the user ordering over which the NRIA iterates becomes important for the convergence speed of the algorithm. To speed up convergence, the users should first be arranged in decreasing priority order and the users within the same priority group should be arranged in order of decreasing line-attenuation. The NRIA performs this ordering independently for both transmission directions.

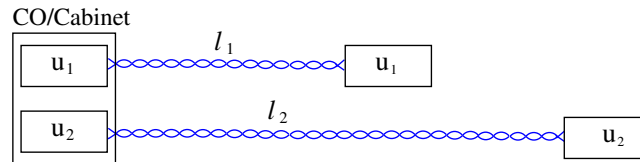


FIGURE 4.3: An example of a network scenario with two users.

We elaborate on these statements with an example for a network scenario with two users shown in Figure 4.3. We analyze only the upstream transmission direction.

1. We first elaborate on the second goal as it is simple to describe and to understand: Users with the same priority should be arranged in order of decreasing line-attenuation. Due to our assumption that both users have equal priorities, they should support equal bitrates. The longest loop (the second user) determines the maximum bitrate that can be supported by both users. We start the iteration with the second user and do water-filling, with the target bitrate initialized to a very high value (theoretically infinity). The second user will use the maximum total power. In the next iteration we do water-filling in the first user. The first user will only use the power needed to achieve the bitrate that has been achieved by the second user (due to the assumption that both users have equal priorities). Thus, with such an ordering we start to perform power control from the second iteration.
2. We elaborate now on the first goal: The users should first be arranged in decreasing priority order. These two cases might arise:

Case 1: The second user has higher priority than the first user. Thus, we start the iterations with the second user. This case is trivial and is the same as that explained above.

Case 2: The first user has higher priority than the second user. With our proposed strategy we start the iterations with the first user. Without loss of generality, let us assume that we have assigned to the first user much higher priority than to the second user; thus $\alpha_{1,US} \gg \alpha_{2,US}$. Furthermore, let us assume that loop attenuation of the second user is only marginally higher than that of the first user over all frequencies. We start the iterations with the first user and do water-filling. Thus, the first user will use the maximum total power. In the next iteration we do water-filling for the second user. The second user will not use the maximum total power. This is true, because by assumption the second user is deployed in the loop that has marginally higher attenuation than the first user and it should support much lower bitrate than the first user. For the cases when $\alpha_{1,US}$ is only marginally higher than $\alpha_{2,US}$ and the loop attenuation of the second user is much higher than that of the first user at all frequencies, it would be better to start the iterations with the second user.

The reason for this is that the second user will use the maximum total power and not the first user, because the second user is disturbed more by the first user than vice versa. However, this will only increase the number of iterations and will have not strong impact on the algorithm's performance.

4.4.1.2 Initial Band Plan

The NRIA partitions the available spectrum into K subbands, with N/K subcarriers in each. In order to simplify the description but without loss of generality, we assume that both N and K are powers of two. This is satisfied when the number of subcarriers is selected as $N = 2^l$, where l is a natural number. An example with four subbands is shown in Figure 4.4. It is also possible to start with an upstream subband at low frequencies. However, in practice, we usually start with a downstream subband to be spectrally compatible with ADSL [58], ADSL2 [59], and ADSL2+ [60] downstream transmission. In a straightforward way we can extend the NRIA to use some predefined subcarriers only in one particular transmission direction. We can also run the NRIA with a fixed band plan to find only the power allocations of users as for instance in ADSL, ADSL2, and ADSL2+ systems, which are designed to have a fixed band plan. In this case, there is no **repeat** loop in *Main Function* in Algorithm 1.

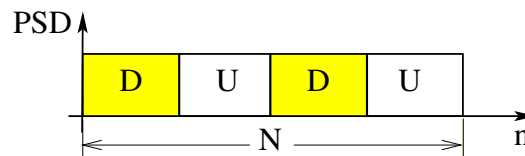


FIGURE 4.4: An example of initial subcarrier allocation, where the total number of available subcarriers N are divided into $K = 4$ subbands.

When there are some unused or silent subcarriers, they are simply zeroed in the algorithm in both transmission directions and kept outside the optimization process. For example if we design a system that uses the subcarriers from $n = 32$ to $n = 2782$ (128 kHz to 12 MHz) as one of the specified bandwidth in the VDSL standard [4, 40, 41], then the initial subcarrier allocation for this case is shown in Figure 4.5. It shows that, although we have selected four subbands, two for each transmission direction, the number of subbands has been reduced to three (two for downstream and one for upstream), since only subcarriers in the range $n = \{32, \dots, 2782\}$ are used out of $N = 4096$ subcarriers.

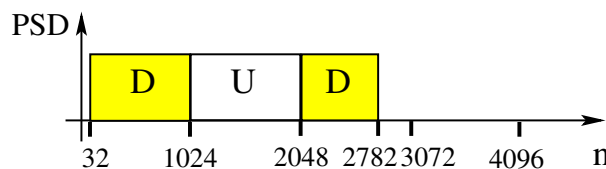


FIGURE 4.5: An example of initial subcarrier allocation with $N = 4096$, where only subcarriers $n = \{32, \dots, 2782\}$ are used out of $N = 4096$ subcarriers.

4.4.1.3 Change Band Plan

For a given subcarrier allocation, the inner stage of the NRA calculates the bitrates for all users in the downstream and upstream directions. Then, depending on the achieved bitrates of all users and the predefined asymmetry a , the NRA performs a binary search within the subbands for a new subcarrier allocation. This is performed with the constraint given in (4.10b). There are three cases:

- c1. $\sum_{u=1}^U R_{u,DS} > a \sum_{u=1}^U R_{u,US}$, which indicates that more subcarriers should be assigned in the upstream direction.
- c2. $\sum_{u=1}^U R_{u,DS} < a \sum_{u=1}^U R_{u,US}$, which indicates that more subcarriers should be assigned in the downstream direction.
- c3. $\sum_{u=1}^U R_{u,DS} = a \sum_{u=1}^U R_{u,US}$, which indicates that an optimized subcarrier allocation has been found and that the outer stage, and also the whole NRA, is complete.

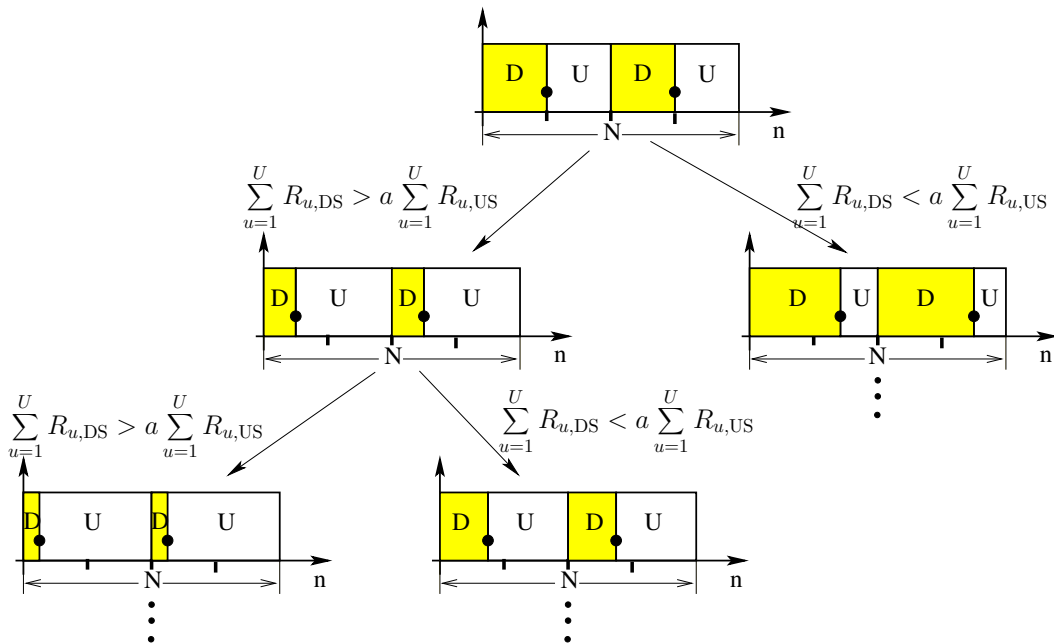


FIGURE 4.6: Illustration of the search for a subcarrier allocation, when right-hand downstream subband edges are moved to the right or to the left.

A binary search within the subbands for the new downstream and upstream subcarrier allocations is performed, depending on the criteria c1 and c2, by simultaneously moving all right-hand downstream subband edges dotted with bullets to the right or to the left as shown in Figure 4.6. We can also move the left-hand downstream subband edges dotted with bullets as shown in Figure 4.7, but in practice, for the reasons given in Section 4.4.1.2 “Initial Band Plan”, we should usually move right-hand downstream subband edges. Note that when we move the left-hand downstream subband edges the number of subbands can be increased by one compared to the initial number of subbands, as is shown in Figure 4.7. The subcarrier allocation is the same for all users, since D-FDD is considered.

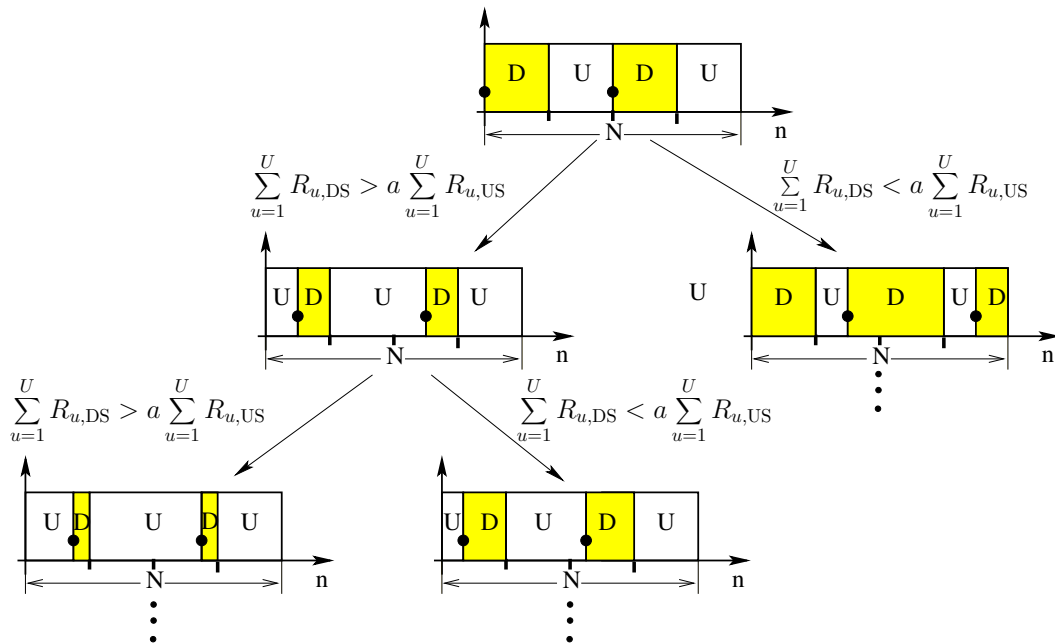


FIGURE 4.7: Illustration of the search for a subcarrier allocation, when left-hand downstream subband edges are moved to the right or to the left.

A complexity analysis of the maximum number of iterations to find an optimized subcarrier allocation is given in Section 4.5.

4.4.1.4 Modified Fixed-Margin Water-Filling (FM-WF) Algorithm

The water-filling (bit-loading) algorithm used in the inner stage is a modified version of the FM-WF algorithm [101]. The FM-WF algorithm uses only the power needed to achieve a predefined target bitrate. As described, we do not know *a priori* if a specific target bitrate can be supported for a given maximum total power. Therefore, we have modified the fixed-margin water-filling algorithm as follows: if the target bitrate can be supported, then only the power needed to support that bitrate is used; otherwise, the maximum total power is used and the supported bitrate is calculated.

The pseudo-code of the modified FM-WF algorithm, when continuous bit-loading is used as a water-filling algorithm, is listed as Algorithm 3 in Appendix A.3.

4.4.1.5 Check the Convergence Point

One solution to find the downstream and upstream bitrates that maximize (4.10a) while satisfying the defined bitrate relations is to exhaustively test all possible maximum total power constraints among the users and to select the appropriate bitrates. Due to the number of combinations that we have to test this is in practice infeasible. However, since the NRA estimates target bitrates for each user, it can converge to a point where the sum of the users' bitrates is lower than can actually be achieved compared to an exhaustive search. Fortunately, by using Postulate 1 below, such cases can always be detected and an improved estimate of the corresponding target bitrates can be derived.

Postulate 1 Consider a multi-user D-FDD transmission system operating in an interference channel where each receiver considers the crosstalk signal as noise. For such a multi-user system the sum of the user bitrates increases when the power of each user increases.

In Appendix A.2, we discuss the validity of this Postulate 1 and prove it for a special case.

Postulate 1 ensures that the NRIA has converged to a “wrong” point if none of the modems has utilized the maximum total power after finishing the inner stage. For these cases, a performance improvement is achieved if the last M values of normalized supported bitrates \bar{R} are increased by some amount $\Delta\bar{R}$, and we continue iterating in the inner stage. When the sum of the user bitrates is increased and the user bitrate relations defined in (4.5) are preserved, the bitrates of all users are increased jointly.

Now the question arises how to select the value of $\Delta\bar{R}$ that maximizes the convergence speed of the NRIA and still ensure its stability. If we select high $\Delta\bar{R}$, it will increase the convergence speed of the algorithm, but it can cause the so-called “ping-pong” effect as illustrated in Figure 4.8 for a two-user case. In the “ping-pong” effect we always iterate between the points above and below the boundary of the rate region. The rate region characterizes all possible pairs of bitrates that can be supported by all users subject to the total power constraints⁴. For illustration purposes, let us assume that we have found the rate region by exhaustive search throughout all possible total power constraints. When the ping-pong effect arises we cannot approach the rate region boundary, because we cannot force any user to use a maximum power that is close to the maximum total power with a predefined accuracy.

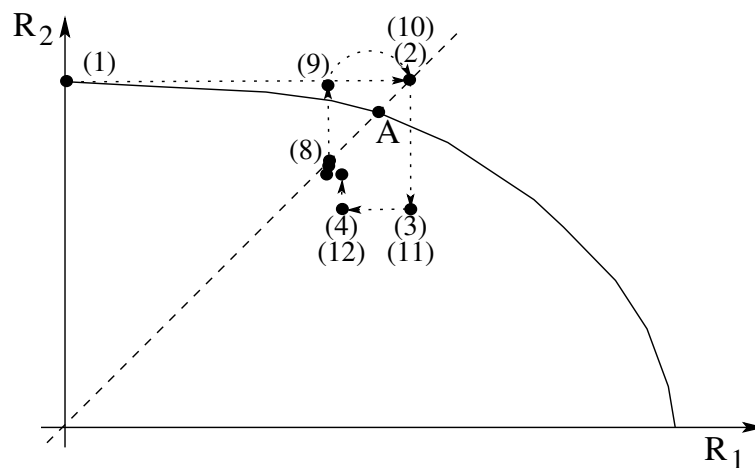


FIGURE 4.8: Illustration of the ping-pong effect.

Let us now describe how the ping-pong effect can arise for a network scenario with two users. Suppose that both users have equal priorities; thus, we are searching for equal bitrates for two users. The dashed line in Figure 4.8 shows the region where the bitrates

⁴A detailed analysis of the NRIA rate regions is given in Section 5.2.

of both users are equal. We denote with $P_{1,A}^{\text{used}}$ the power used by the first and with $P_{2,A}^{\text{used}}$ the power used by the second user, where the dashed line intersects the boundary of the rate region, cf. Figure 4.8. Due to Postulate 1 at least one user will utilize the maximum total power. In our case this is the second user, because it is deployed on the loop with the highest attenuation; thus, $P_{2,A}^{\text{used}} = P^{\text{max}}$. By our definition in Section 4.4.1.1 “User Ordering” we start iterations with the second user. The iterations proceed as denoted with the arrows in Figure 4.8. Note that each point in Figure 4.8 shows the supported bitrate of one user in a particular iteration and the other user in the previous iteration. Let us assume that after the eighth iteration the inner stage has achieved the desired accuracy on the predefined bitrate relations and on the power allocations. Furthermore, we assume that none of the users has used the maximum total power. Thus, as Figure 4.8 shows, the NRIA has converged to a wrong point.

Due to our assumption that none of the users has used the maximum total power we need to improve the estimates of the target bitrates of all users. Assume that we have selected a large $\Delta\bar{R}$. In the ninth iteration the second user is supporting a bitrate that is marginally smaller than in the first iteration. Assume also that in the tenth iteration the pair of user bitrates that is supported is practically the same as that supported in the second iteration as shown in Figure 4.8. In the eleventh iteration the pair of supported bitrates is the same as in the third iteration. This process is repeated and we can never approach the boundary of the rate region. However, when we select the $\Delta\bar{R}$ value small enough the ping-pong effect never arises. Furthermore, we will be tight to the boundary of the rate region as we will force one of the user to utilize a power that is close to the maximum total power with a predefined accuracy.

We propose to change $\Delta\bar{R}$ adaptively, depending on the maximum total power P^{max} , and the maximum power used by any user P^{used} . Due to our definition in (4.5), at the convergence point, all the last M normalized bitrates are approximately equal. Thus, we propose to increase the $\Delta\bar{R}$ by

$$\Delta\bar{R} = \lambda \cdot \frac{P^{\text{max}} - P^{\text{used}}}{P^{\text{max}}} \cdot \bar{R},$$

where \bar{R} is any one of the last M normalized supported bitrates and λ is a scaling factor.

Figure 4.9 shows the number of corrections in the estimate of the target bitrate T_{US} , for different values of the scaling factor λ . The values of T_{US} and λ are shown for the case when P^{max} and P^{used} are given in dBm. The simulations were performed with the target bitrate T_{US} initialized to 400 kbit/s and for the network scenario shown in Figure 4.3, where the lengths of the first and second loops are 600 m and 1200 m, respectively. During the simulation we assumed that both users have equal priorities; thus $\alpha_{1,\text{US}} = \alpha_{2,\text{US}} = 0.5$.

The number of corrections in the estimate of the target bitrate in Figure 4.9 is high for low values of λ . However, when the NRIA converges to a wrong point, it will already be in the upper part of the curves shown in Figure 4.9. For P^{max} and P^{used} given in dBm, the NRIA is found to work well with any value of the scaling factor in the interval $0 < \lambda \leq 0.05$. Also for values of the scaling factor $\lambda > 0.05$ the NRIA still works, but to ensure convergence we recommend to select it smaller than or equal to 0.5.

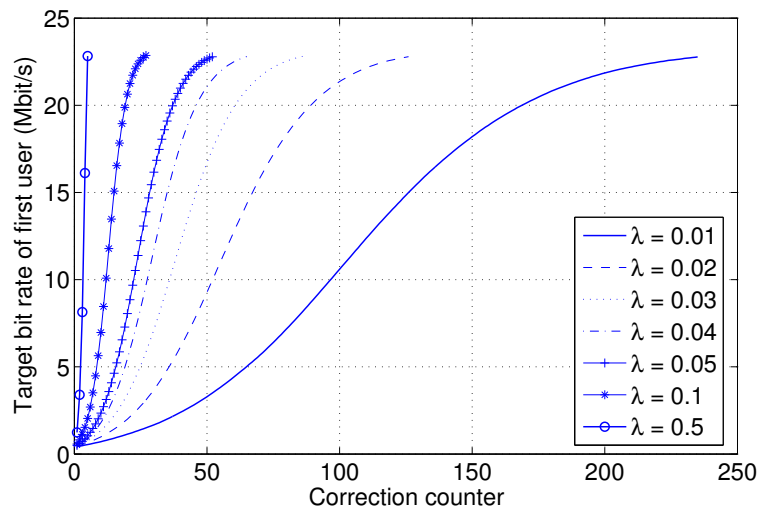


FIGURE 4.9: Example of the number of target bitrate corrections for a user that is initialized at 400 kbit/s.

4.5 Complexity of the NRIA

This section analyzes the computational complexity of the NRIA. We will show that the NRIA has low complexity, which makes it attractive for deployment in network scenarios with many users included in the optimization process. In the analysis done below we will ignore the complexity of performing user ordering, changing the band plan, calculating the asymmetry parameter a , and calculating the target bitrate T , since they have smaller complexity than the water-filling (bit-loading) algorithm and calculating the noise. Thus, the complexity of the NRIA is determined by: the number of the iteration in the outer stage, the *Main Function*; the number of iterations in the inner stage, the *CalcRate-SPSDs Function*; the number of users included in the optimization process; and the type of water-filling (bit-loading) algorithm used in the function *ModifiedFM-WF*, all shown in Algorithm 1.

The number of iterations in the outer stage depends on the number of subcarriers per subband and on the predefined accuracy with which the inequalities in criteria c1 and c2 in Section 4.4.1.3 “Change Band Plan” should be satisfied. However, the *maximum* number of iterations O_{\max} in the outer stage can always be determined in advance, and this depends only on the number of subcarriers per subband, which as shown in 4.4.1, “Initial Band Plan”, is equal to N/K . Therefore, due to the binary search within the subbands for an optimized subcarrier allocation the maximum number of iterations in the outer stage is: $O_{\max} = \log_2(N/K) + 1$. For example, when the number of subcarriers is $N = 4096$, as in VDSL, and when we select $K = 8$ subbands, then $O_{\max} = \log_2(512) + 1 = 10$.

The number of iterations in the inner stage depends on: the number of users included in the optimization process, the topology of the network scenario, the asymmetry parameter a , the user priorities values $\alpha_{u,dir}$, and the type of water-filling algorithm used. Unfortunately, the maximum number of iterations in the inner stage cannot be determined in advance. Thus, the only way to calculate the exact number of operations in the NRIA is to calculate it for a particular network scenario.

The pseudo-code of the NRIA in Algorithm 1 shows that the actual number of opera-

tions to calculate the noise for a particular transmission direction requires N_{dir} additions and $(U - 1) \cdot N_{dir}$ multiplications, where N_{dir} denotes the number of subcarriers used in a particular transmission direction. Therefore, the calculation of the noise over all outer stage iterations has a complexity of order $\mathcal{O}_{dir}^N(U \cdot \tilde{N}_{dir})$, where \tilde{N}_{dir} denotes the average number of subcarriers assigned in a particular direction over all outer stage iterations.

The number of operations required to calculate the bitrates and power allocations in function *ModifiedFM-WF* is unknown in advance, since it depends on the type of water-filling algorithm used to perform power/bit allocations, the topology of the network scenario, and the values of user priorities. In Appendix A.3 we compute the number of operations in the modified FM-WF algorithm when continuous bit-loading is used as the water-filling algorithm. We showed that on average it has a computational complexity of order $\mathcal{O}(N_{dir} \log_2 N_{dir})$, which is of the same order as that of any water-filling algorithm.

Table 4.3 lists the computational complexity of the modified FM-WF algorithm for the majority of the algorithms that have been proposed in the past to perform bit-loading. Appendix A.3 determines the computational complexity for the continuous bit-loading algorithm. The computational complexity values for Fischer and Huber [45], Chow et al. [21], Hughes–Hartogs [55], and Levin-Campello [11, 12] algorithms are taken from [12].

TABLE 4.3: Computational complexity of the modified FM-WF algorithm for different bit-loading algorithms. N_{dir} denotes the number of used subcarriers on a particular transmission direction.

Bit-loading algorithm	Complexity of the modified FM-WF algorithm	Optimality concerning the single user case
Continuous	$\mathcal{O}(N_{dir} \log_2 N_{dir})$	Optimal
Fischer and Huber	$\mathcal{O}(N_{dir} \log_2 N_{dir})$	Suboptimal
Chow <i>et al.</i>	$\mathcal{O}(N_{dir} \log_2 N_{dir})$	Suboptimal
Hughes–Hartogs	$\mathcal{O}(N_{dir} \log_2 N_{dir})$	Suboptimal
Levin-Campello	$\mathcal{O}(N_{dir})$	Optimal

Usually, the number of iterations in the downstream and upstream inner stages are different. Thus, the computational complexity of the NRIA is given by

$$C_{NRIA} = O \cdot \left(\sum_{t=1}^{i_{DS}} \left(\mathcal{O}_{DS}^{N,t} + \mathcal{O}_{DS}^{R,t} \right) + \sum_{t=1}^{i_{US}} \left(\mathcal{O}_{N,US}^{N,t} + \mathcal{O}_{US}^{R,t} \right) \right), \quad (4.12)$$

where O denotes the number of iterations in the outer stage; i_{DS} and i_{US} denote the number of iterations in the inner stage in the downstream and upstream transmission directions, respectively; $\mathcal{O}_{DS}^{N,t}$ and $\mathcal{O}_{US}^{N,t}$ are the number of operations at iteration t to calculate the noise in downstream and upstream directions, respectively; and $\mathcal{O}_{DS}^{R,t}$ and $\mathcal{O}_{US}^{R,t}$ are the number of operations in the modified FM-WF algorithm at iteration t in the downstream and upstream directions, respectively. From (4.12) we conclude that the NRIA has a computational complexity that depends on: the number of the users U ; the number of iterations in the outer stage O ; the number of iterations in the downstream inner stage i_{DS} ; the number of iterations in the upstream inner stage i_{US} ; the average complexity of the modified FM-WF algorithm W_{DS}^R in downstream direction over all downstream inner

stage iterations; and the average complexity of the modified FM-WF algorithm W_{DS}^R in upstream direction over all upstream inner stage iterations. Thus, based on (4.12)

$$C_{\text{NRIA}} = \mathcal{O}\left(\mathcal{O} \cdot i_{\text{DS}} \left(U \cdot \tilde{N}_{\text{DS}} + W_{\text{DS}}^R\right)\right) + \mathcal{O}\left(\mathcal{O} \cdot i_{\text{US}} \left(\cdot U \tilde{N}_{\text{US}} + \cdot W_{\text{US}}^R\right)\right),$$

where \tilde{N}_{DS} denotes the average number of subcarriers assigned in downstream over all downstream outer stage iterations and \tilde{N}_{US} denotes the average number of subcarriers assigned in upstream over all upstream outer stage iterations.

When the Levin-Campello bit-loading algorithm is used in the modified FM-WF algorithm, the NRIA has an average complexity

$$C_{\text{NRIA}} = \mathcal{O}\left(\mathcal{O} \cdot i_{\text{DS}} \cdot \tilde{N}_{\text{DS}} (U + 1)\right) + \mathcal{O}\left(\mathcal{O} \cdot i_{\text{US}} \cdot \tilde{N}_{\text{US}} (U + 1)\right).$$

For all other algorithms in Table 4.3, the NRIA has an average complexity

$$C_{\text{NRIA}} = \mathcal{O}\left(\mathcal{O} \cdot i_{\text{DS}} \cdot \tilde{N}_{\text{DS}} \left(U + \log_2 \tilde{N}_{\text{DS}}\right)\right) + \mathcal{O}\left(\mathcal{O} \cdot i_{\text{US}} \cdot \tilde{N}_{\text{US}} \left(U + \log_2 \tilde{N}_{\text{US}}\right)\right).$$

In Section 5.4 we will show that the NRIA has much lower complexity than the OSBA. In Section 4.7 we will show that the NRIA also has much lower complexity than the IWFA, when the target bitrates of all users in the IWFA are unknown in advance. For the case when the target bitrates of all users in the IWFA are known in advance, the NRIA might have moderately higher or moderately lower complexity than the IWFA, depending on the number of corrections in the total power constraints required in the IWFA.

4.6 Initialization of the Input Parameters in the NRIA

This section, by means of simulation, shows how to initialize the input parameters in the NRIA to achieve good performance and fast convergence. All simulations are based on a VDSL Zipper-DMT type system [4, 40, 41], because this is the only standardized DSL technology which supports D-FDD transmission. There is little or no flexibility to change the standardized VDSL band plans, but they can easily be changed to be much more flexible since D-FDD is an inherent property in Zipper duplexing.

For all simulations we use continuous bit-loading algorithm (also known as water-filling algorithm) without PSD-mask constraints. The maximum total power for each user and each transmission direction is set to 11.5 dBm. The center frequency separation between two successive subcarriers is 4.3125 kHz and the DMT symbol rate is 4 kHz, as specified in the VDSL DMT standards [4, 40, 41]. Furthermore, we assume a DMT system with 2048 subcarriers. To achieve a bit error rate of 10^{-7} we assumed an SNR gap, $\Gamma = 12.3$ dB. This SNR gap, based on (3.3) after adding the noise margin in SNR gap, is derived as: $\Gamma_{\text{dB}} = \gamma_{\text{Mod,dB}} + \gamma_{\text{Loss,dB}} - \gamma_{\text{Code,dB}} + \gamma_{\text{Noise,dB}} = 9.8 + 0 - 3.5 + 6 = 12.3$ dB, where $\gamma_{\text{Mod,dB}}$ denotes the modulation gap, which for QAM is 9.8 dB [101]; $\gamma_{\text{Noise,dB}}$ denotes the noise margin, which is assumed to be 6 dB; $\gamma_{\text{Loss,dB}}$ denotes the loss in the SNR, which is assumed to be 0 dB; and $\gamma_{\text{Code,dB}}$ denotes the coding gain, which is set to 3.5 dB.

First, we analyze the impact of the parameters K (number of subbands), M_{DS} and M_{US}

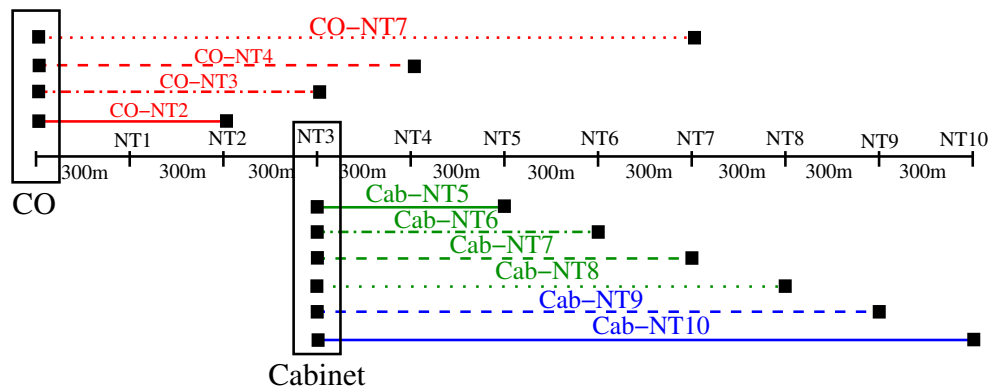


FIGURE 4.10: The simulation scenario used to analyze the initialization of input parameters in the NRIA.

(number of the last normalized bitrates used to calculate the target bitrates) on the performance of the NRIA. Then, based on the simulation results we conclude how to select the initial values of K , M_{DS} , and M_{US} to achieve good performance and fast convergence.

The simulations are performed for the network scenario shown in Figure 4.10. The reason for selecting such a network scenario is to account for a distributed structure of DSL access networks, to simulate an access network with multiple users, and to select a DSL access network in which DSL systems are deployed simultaneously from a CO and a cabinet. The cable model used is the so-called “BT_dwug” [114], which has 0.5 mm conductors. The FEXT model used is the same as specified in Section 2.4.2.2 with $K_{FEXT} = -45$ dB at 1 MHz. The background noise is set to a flat level of $\mathcal{P}_V = -140$ dBm/Hz. Due to assuming of 99% worst-case FEXT coupling between all lines to calculate the FEXT noise we have used the crosstalk noise combination method described in Section 2.4.2.4. Furthermore, we assume that all users have the same priority values on both transmission directions and the asymmetry parameter is set to $a = 1$. Thus, we are searching for symmetric bitrates and equal bitrates for all users. To search for the subcarrier allocation we use the search scheme shown in Figure 4.6.

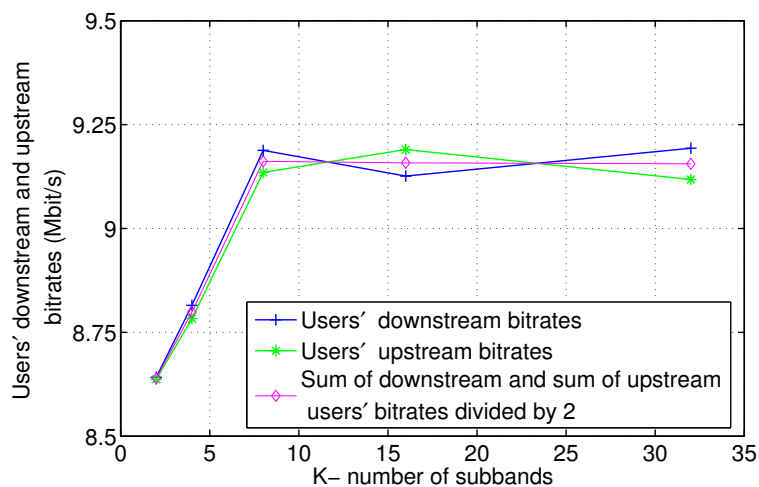


FIGURE 4.11: Users' downstream and upstream bitrates for various numbers of subbands K .

We start by considering the impact of the number of subbands on the performance of the NRIA. For all simulations the M_{DS} and M_{US} are set to 100, which is ten times the number of users in the simulation scenario. This increases the number of iterations in the inner stage i_{dir} , but for the network scenario in Figure 4.10 this assures that we achieve the maximum bitrates without the need to check the convergence point. We perform simulations for $K = 2, 4, 8, 16$, and 32 subbands.

In Figure 4.11 we see only a minor increase in the total downstream and upstream bitrates when K is increased above 8. Furthermore, a value of $K = 8$ or $K = 16$ subbands has typically been sufficient for all network scenarios we have simulated to achieve any desired bitrate relations defined by (4.4) and (4.5). We also see that, as a result of the simultaneous movement of “subband edges”, the accuracy in users’ supported bitrates in the downstream and upstream directions decreases when the number of subbands increases. It is possible to extend the NRIA to increase the accuracy of users’ downstream and upstream bitrates by fine-tuning of a single subband edge after the NRIA has converged. However, the required number of iterations then increases and improvements from a practical point of view are small. The subcarrier allocations for downstream and upstream for $K = 8$ subbands was found to be:

$$\begin{aligned} I_{DS} &= \{1 \dots 149, 513 \dots 661, 1025 \dots 1173, 1537 \dots 1685\} \\ I_{US} &= \{150 \dots 512, 662 \dots 1024, 1174 \dots 1536, 1686 \dots 2047\}. \end{aligned} \quad (4.13)$$

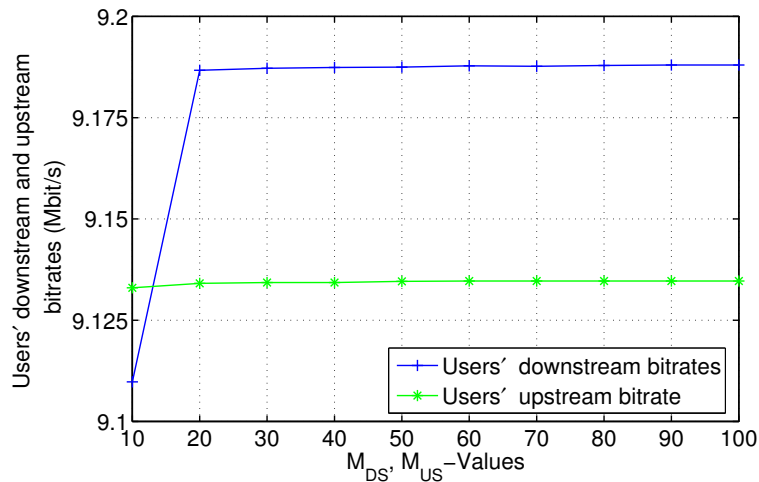


FIGURE 4.12: Users’ downstream and upstream bitrates depending on the number of the last M_{DS} and M_{US} normalized supported bitrates used to calculate the users’ target bitrates.

Now we consider the impact of M_{DS} and M_{US} on the algorithm’s performance and its convergence behavior. We fix the number of subbands to $K = 8$ and use the resulting subcarrier allocation for the downstream and upstream directions given in (4.13). Here we will not check the accuracy of the convergence point, but only analyze the users’ downstream and upstream supported bitrates depending on M_{DS} and M_{US} values.

We have performed simulations for $M_{DS} = M_{US} = 10, 20, \dots, 100$. Figure 4.12. presents the results, which show only a small improvement in the users’ supported bitrates

if M_{DS} and M_{US} are increased above U . This is due to user ordering as described in Section 4.4.1.1.

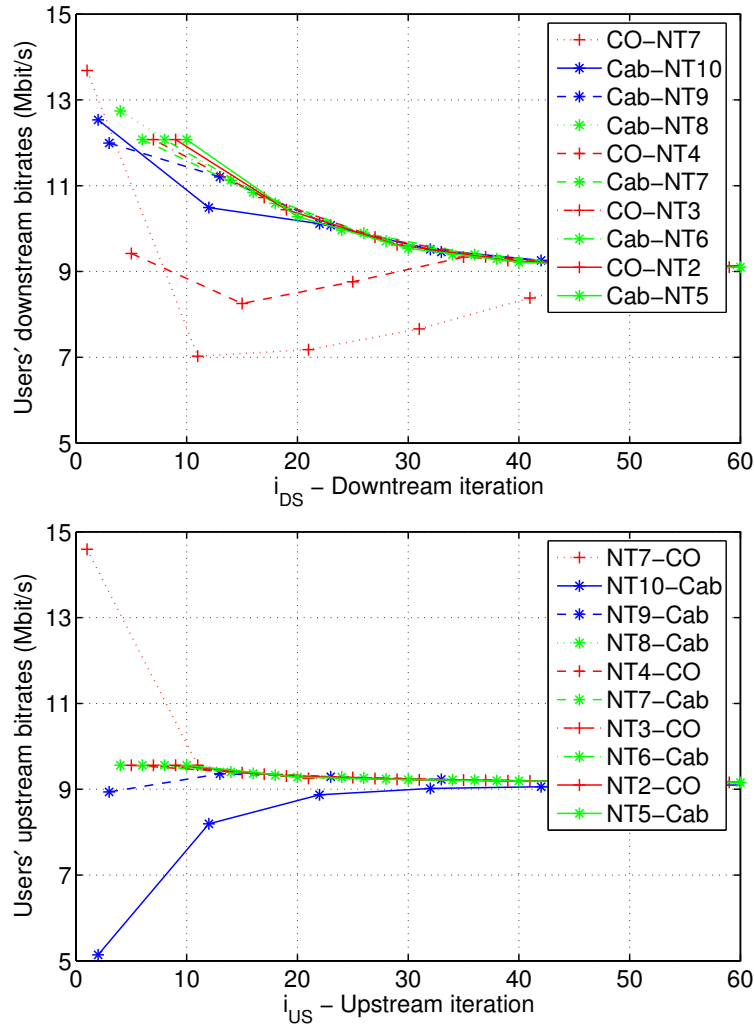


FIGURE 4.13: The downstream and upstream convergence behaviors of the NRIA for the network scenario in Figure 4.10.

The downstream and upstream convergence behaviors of the NRIA for $M_{US} = 10$ are shown in Figure 4.13. The plots show that in both directions the NRIA converges exponentially. In our experience the NRIA always converges exponentially when no correction in the estimate of the users' target bitrates, as described in Section 4.4.1.5, is performed. The convergence speed of the NRIA slows when a correction in the estimate of the user target bitrates is performed. An example of the convergence behavior of the NRIA for a network scenario with two users is shown in Figure 4.14, which shows that the NRIA corrects the estimates of the users' target bitrates after the twelfth iteration.

The simulations for the plots in Figure 4.14 were performed for $M_{DS} = M_{US} = 2$, which is equal to the number of users in the network scenario. Increasing the values of M_{DS} and M_{US} sometimes protects the NRIA from converging to a wrong point, but not always. Both strategies—either selecting large M values or performing corrections in the estimate of the users' target bitrates—increase the number of iterations in the inner stage.

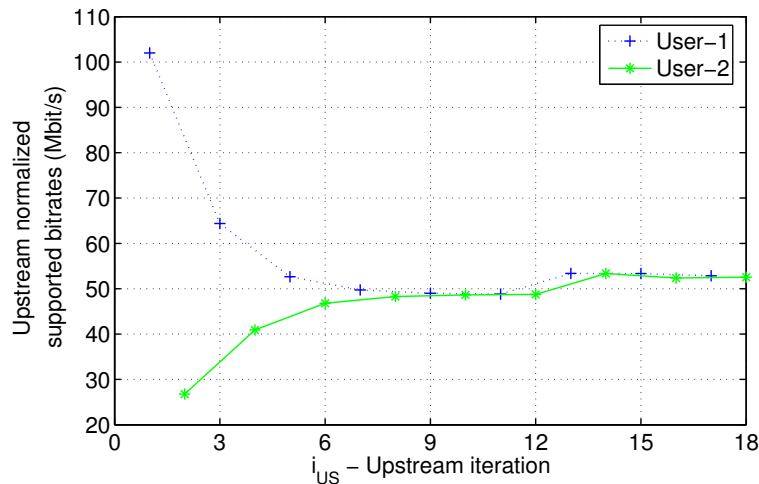


FIGURE 4.14: An example of the convergence behavior in the NRIA for a network scenario with two users.

Therefore, a trade-off should be made when selecting the M values. In our experience, in the general case, selecting M values equal to the number of users in the network scenario is a good trade-off.

Finally, it is worth mentioning that the NRIA might converge to a wrong point especially when the FEXT interference level between the users is large. The reason for this can be explained as follows. Assume that we have fixed the bitrates of all users and they are achievable. When a user changes his transmit PSD substantially this will also alter the noise for the other users substantially. Therefore, the other users will also change their transmit PSDs substantially to compensate for the change in the noise levels to achieve the specified bit-error rate (BER). This results in increasing non-convexity in the optimization problem in (4.10). Therefore, a linear estimation approach of the target bitrates of all users as in (4.11) is not appropriate. When the FEXT interference level between the users is very small only the background noise and the loop attenuation determine the performance of each user. If we instead assume that the FEXT interference is so small that each user in each iteration will perform power allocation as in the single-user case. It is well-known that for the single-user case the power allocation is a convex optimization problem [30]. Therefore, when the FEXT interference level between the users is very small, each user will only adjust its power to fulfill the defined bitrate relation and not to improve the performance of the other users.

4.7 Overview of the NRIA Compared to the IWFA

We mentioned in Section 4.4 that the NRIA is based in the IWFA. Compared to the IWFA, the NRIA has two major differences:

- The NRIA searches for an optimized band plan (downstream and upstream subcarrier allocations) common to all users.
- The NRIA estimates the target bitrates of all users, rather than assuming that they are known in advance or searching for them exhaustively.

As mentioned in Section 4.6 there is little or no flexibility to change the currently standardized VDSL band plans. In the VDSL standards [4,40,41], two fixed spectra band plans usually known as “997” and “998”, have been standardized (see Section 3.1.3). The ITU [62] has also standardized the so-called “flexible VDSL Spectrum Plan”⁵, where the frequency of the last subband edge between the downstream and upstream is selected freely. The flexible band plan appeared of interest only in Sweden, where it was first proposed, but now it has attracted interest in many other countries. Furthermore, there is a discussion in standardization to allow a variable band plan in VDSL2 [110]. The NRIA allows full flexibility in the subcarrier allocation between the downstream and upstream transmission directions. Due to using the D-FDD transmission scheme any subcarrier in VDSL or VDSL2 systems can be assigned in either the downstream or the upstream direction without increasing the implementation complexity of the transmission system.

Section 4.4 showed that the NRIA estimates the target bitrates of all users with a simple *ad hoc* method. The IWFA either assumes that the target bitrates of all users are known in advance or searches for them exhaustively. Yu *et al.* in [122] have proposed to calculate the sets of achievable bitrates of all users in the IWFA by running through all possible combinations of maximum total power constraints. Unfortunately in practice there is a large number of such combinations whenever the number of users included in the optimization process is moderately high. For example, assume that twenty users are included in the optimization process and we select for each user only ten different maximum total power constraints. The total number of combinations to examine is 10^{20} . Thus, we have to run the IWFA algorithm 10^{20} times to calculate the sets of target bitrates that can be supported by the IWFA, which is infeasible in practice.

The NRIA always outperforms the IWFA concerning the supported bitrate, because the NRIA uses the flexibility to search for an optimized subcarrier allocation to better satisfy the requirement of all users. For a fixed subcarrier allocation the NRIA cannot outperform the IWFA when the IWFA iterates with the same user order as the NRIA. The reason for this is that the inner stage of the NRIA is based on the IWFA. However, for this case, the NRIA can be used to calculate the sets of maximum achievable users’ bitrates that can be supported by the IWFA. Yu *et al.* in [122] have shown that IWFA converges to the same point independently of how we start the iterations when the convergence criteria are fulfilled. We will analyze in detail the convergence criteria of the IWFA in Section 5.6.1. However, when the convergence criteria are not fulfilled the performance of the IWFA in our experience might depend on the user order during the iterations as we will discuss in Section 5.6.1. In the NRIA the iterations are started as described in Section 4.4.1.1 “User Ordering”. Therefore, for a fixed band plan, the NRIA might outperform the IWFA if in the IWFA the iterations are not started in the same user order as in the NRIA.

For a fixed band plan the IWFA might outperform the NRIA in some specific situation, when the integer bit-loading algorithm is used within the modified FM-WF algorithm. We explain here how this can arise with an example for the network scenario shown in Figure 4.3. Assume that the integer bit-loading algorithm is used with a specified maximum number of bits per subcarriers. We assign the first user a much higher priority value than the second user. Let us assume that we have selected the loop length of the first user such that it loads (allocates) in each subcarrier the maximum number of bits and has

⁵The interested reader can also read an interesting description on the VDSL spectrum issues in [101], Chapter 7.

not used the maximum total power. We also assume that the second user supports the bitrate calculated from (4.5) and has not used the maximum total power. Since for this case none of the users has used the maximum total power in the NRIA, the IWFA shows better performance (for a fixed band plan), because it assumes no relation among the user bitrates.

We should clarify that the problem analyzed in the last paragraph is not related to the advantage of the IWFA compared to the NRIA. It relates instead to the new constraint we have imposed in (4.2), which was not taken into account during the problem formulation in Section 4.3. The NRIA can be extended in a straightforward way to consider those specific network scenarios. However, from a practical point of view this is not important, since we are always interested in offering users specific bitrates related by (4.5). Furthermore, if we do not allow any of the users included in the optimization process to use the maximum total power, the interference noise to the other users (not included in the optimization process) is reduced and their performance is improved.

In Sections 4.3 and 4.4 we have set no constraints on the maximum number of bits per subcarrier. Furthermore, we have assumed that any real number of bits per subcarrier can be loaded. When we use integer bit-loading the problem discussed in the last two paragraphs might arise. For this situation none of the users uses the maximum total power; this contradicts Postulate 1. Therefore, when integer bit-loading is used as a water-filling algorithm within the modified FM-WF algorithm, we should build a control within the NRIA to check when the described problem arises. Otherwise, the control convergence criteria will never be fulfilled. We will not describe here how the control is built, because it is implementation specific. But the idea is simple; if all users have loaded the maximum number of bits in all subcarriers, do not check the convergence point.

We mentioned in the introduction to this chapter that a potential drawback of the NRIA is that it is a centralized algorithm, while the IWFA is a distributed algorithm. Conceptually, the NRIA can be extended in a straightforward way to be deployed in a semi-distributed manner as follows. We start with a initial band plan. For this fixed band plan the supported bitrates of all users in the last M_{dir} iterations are sufficient for each user to calculate his one target bitrate. The supported bitrates among the users can be interchanged with the help of a DSM agent (SMC in Figure 4.1). After this, the users can perform power allocation in a distributed way for known target bitrates, since each user at either the LT or the NT side can locally estimate the noise. In a particular iteration only the target bitrate of a user who performs power allocation is calculated. This user performs power allocation in a distributed way with the modified FM-WF algorithm as described in Section 4.4.1.4. After the inner stage of the NRIA converges the SMC provides the new band plan to all users for the next outer stage iteration and the inner stage iterations are repeated again. This process is repeated until the NRIA converges.

Chapter 5

Performance and Properties of the NRIA

We have described how there are two strategies to perform spectrum management in DSL systems: static spectrum management (SSM) and dynamic spectrum management (DSM). We have also mentioned that power back-off (PBO) is the most advanced technique for SSM and that spectral balancing is the most promising technique for DSM. Note that as mentioned in Chapter 4 we use the term DSM to refer to spectral balancing if not otherwise specified.

We introduced in Chapter 4 a novel algorithm for DSM: the normalized-rate iterative algorithm (NRIA) [103, 104, 105]. The NRIA is the only DSM algorithm that finds an optimized band plan (downstream and upstream subcarrier allocations) and finds optimized power allocations for all users sharing a common cable bundle. The iterative water-filling algorithm (IWFA) [122] finds optimized power allocations for all users under the assumption that the band plan is fixed and known in advance. The optimal spectrum balancing algorithm (OSBA) [14, 15], as the name implies, finds the “optimal”¹ power allocations for all users and assumes, like the IWFA, that the band plan is fixed and known in advance. The bi-directional IWFA (bi-IWFA) [24] finds optimized power allocations for all users, but compared to the IWFA there is no restriction in the band plan. Furthermore, with the bi-IWFA each subcarrier can be used simultaneously in both transmission directions; so it requires an echo-cancelled transmission scheme.

In this chapter we compare the performance of the NRIA with the IWFA, the OSBA, the bi-IWFA, and the UPBO as well as analyze some other properties of the NRIA. This chapter is organized as follows. Section 5.1 gives the common parameters for all simulations. Section 5.2 describes the rate regions of the IWFA, the OSBA, and the NRIA. We will use the rate region concept to compare the performance of the NRIA with the IWFA and the OSBA for a two-user case scenario. Sections 5.3 and 5.4 compare the NRIA with the IWFA and with the OSBA, respectively. Section 5.5 analyzes the flexibility of the NRIA to assign a broad range of downstream and upstream bitrate combinations to the users. Sections 5.6 and 5.7 compare the NRIA with the bi-IWFA and the standardized UPBO, respectively. In Section 5.8 we compare the NRIA with an exhaustive search for an “optimal” subcarrier allocation.

¹The optimality is proved by the authors under some specific conditions.

5.1 Common Simulation Parameters

We mentioned in Section 4.6 that the Zipper-DMT type VDSL system [4, 40, 41] is the only standardized DSL technology that supports digital frequency division duplexing (D-FDD) transmission. Therefore, all simulations have been performed for this type of transmission systems. We described digital duplexing in detail in Section 2.2.2.

We will use the continuous bit-loading algorithm to compare the performance of the NRIA with the bi-IWFA for easier interpretation of the power allocations in the bi-IWFA. We also use the continuous bit-loading algorithm to compare the NRIA with an exhaustive search for an “optimal” subcarrier allocation. However, in order to perform a fair comparison between the NRIA and the IWFA, the OSBA, and the UPBO we use the Levin-Campello [11] algorithm to ensure integer bit-loading. If not otherwise specified the maximum number of bits per subcarrier is set to fifteen.

The center frequency separation between two successive subcarriers is 4.3125 kHz and the DMT symbol rate is 4 kHz, as specified in the VDSL DMT standards. The maximum total power P^{\max} for each user and each transmission direction is set to 11.5 dBm. To take into account for the power loss in the cyclic prefix and the cyclic suffix, the maximum total power used in the bit-loading algorithm \bar{P}^{\max} , is reduced according to (2.6) by:

$$\bar{P}^{\max} = P^{\max} \cdot \frac{2N}{2N + L_e},$$

where N denotes the number of subcarriers in the DMT system and L_e denotes the length of the cyclic extension in sample periods, which is calculated as the sum of samples included in the cyclic prefix and the cyclic suffix; thus, $L_e = L_p + L_s$. For all simulations we use either $N = 2048$ or $N = 4096$ subcarriers. The length of the cyclic extension is selected as specified in the VDSL standards [4, 40, 41], as $L_e = 320$ or $L_e = 640$ corresponding to $N = 2048$ and $N = 4096$ subcarriers, respectively.

To achieve a bit error rate of 10^{-7} we have assumed a signal-to-noise ratio (SNR) gap of $\Gamma = 12.3$ dB. This SNR gap, based on (3.3) after adding the noise margin in SNR gap, is derived as: $\Gamma_{\text{dB}} = \gamma_{\text{Mod,dB}} + \gamma_{\text{Loss,dB}} - \gamma_{\text{Code,dB}} + \gamma_{\text{Noise,dB}} = 9.8 + 0 - 3.5 + 6 = 12.3$ dB, where $\gamma_{\text{Mod,dB}}$ denotes the modulation gap, which for QAM is 9.8 dB [101]; $\gamma_{\text{Noise,dB}}$ denotes the noise margin, which is assumed to be 6 dB; $\gamma_{\text{Loss,dB}}$ denotes the loss in the SNR that occurs until the signal has reached the decision device, which is assumed to be 0 dB; and $\gamma_{\text{Code,dB}}$ denotes the coding gain which is set to 3.5 dB. All other parameters are selected for specific simulations, and will be introduced when the simulation environment is described.

5.2 Rate Regions of the IWFA, the OSBA, and the NRIA

To compare the performance of the NRIA with the IWFA and the OSBA the rate region concept is sometimes used. The rate region characterizes all possible bitrate combinations among the users subject to the power constraints. Due to the fixed subcarrier allocation, the downstream and upstream rate regions of the IWFA and the OSBA are independent

and U -dimensional. For example, in a two-user case the rate regions of the IWFA and the OSBA can be plotted in a two-dimensional space, as shown in Figure 5.1, and any pair of bitrates can be selected independently from the downstream and upstream rate regions. Furthermore, any pair of bitrates that lies inside the rate regions can be supported by the IWFA and the OSBA. However, the OSBA finds the optimal power allocations only for those pairs of bitrates that lies on the rate region boundaries, because only those pairs of bitrates maximize the weighted sum of the bitrates [15].

Since the NRIA searches for optimized downstream and upstream subcarrier allocations, the downstream and upstream rate regions becomes dependent. For a two-user case the NRIA finds two pairs of downstream and upstream bitrates $(R_{1,DS}, R_{1,US})$ and $(R_{2,US}, R_{2,US})$, which are related by three independent parameters; a , $\alpha_{1,DS}$, and $\alpha_{2,US}$ as described in Section 4.2. Thus, the NRIA rate regions for the two-user case are five-dimensional. This is difficult to visualize and to compare with the two-dimensional rate regions of the IWFA and the OSBA. Furthermore, the NRIA finds only those pairs of bitrates that lie on the rate regions boundaries, because only those pairs of bitrates maximize the sum of downstream and upstream bitrates and satisfy the relations defined in (4.5) and (4.7). Actually, in practice we can reduce the downstream and upstream bitrates of all users such that (4.5) and (4.7) are satisfied. However, the resulting pairs of bitrates do not maximize the sum of downstream and upstream bitrates. Therefore in this chapter we confine to the pairs of bitrates that maximize the sum of the downstream and upstream bitrates of all users.

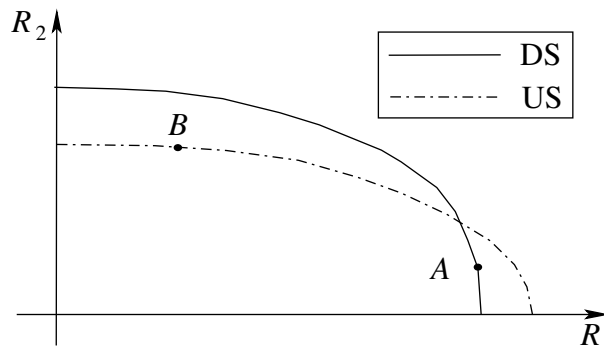


FIGURE 5.1: Illustration of rate regions of the IWFA and the OSBA.

One way to compare the NRIA with the IWFA and the OSBA is to calculate the parameters needed by the NRIA from the two-dimensional rate regions spanned by the IWFA and the OSBA. For example, let us select the pair of bitrates at point A for the downstream and the pair of bitrates at point B for the upstream as shown in Figure 5.1. For these two pairs of bitrates we can calculate the asymmetry parameter a and the users' priority values $\alpha_{u,DS}$ and $\alpha_{u,US}$ needed in NRIA by using (4.4) and (4.5). We can repeat this for any two pairs of downstream and upstream bitrates and draw the corresponding downstream and upstream rate regions of the NRIA. However, this strategy excludes a large portion of the bitrates that are supported by the NRIA but not by the IWFA and the OSBA. Hence, such a comparison would therefore become quite skewed.

Instead, we will use another way to compare the three algorithms. We will assume equal downstream and upstream user priorities for the NRIA, which for the two-user case

from (4.7) yields:

$$R_{u,DS} = aR_{u,US}, \text{ for } u = 1, 2.$$

Under this assumption for the two-user case, the rate region of the NRIA is reduced to a three-dimensional space. We will show some plots of the NRIA three-dimensional rate regions to better illustrate the space of the bitrate combinations that can be supported by the NRIA but not by the IWFA or the OSBA. For a fixed asymmetry parameter value a we can plot the rate regions of the NRIA in two-dimensional space. This strategy reduces the NRIA rate region space to the same order as that of the IWFA and the OSBA, which simplifies the comparison among the three algorithms. However, note that the NRIA will now only support those downstream and upstream bitrates for which $\alpha_{u,DS} = \alpha_{u,US}$. Thus, we calculate two pairs of downstream and upstream bitrates $(R_{1,US}, R_{2,US})$ and $(R_{1,DS}, R_{2,DS}) = (aR_{1,US}, aR_{2,US})$, respectively. As a result, depending on a , the downstream bitrates are either expanded or contracted compared to the upstream bitrates. That is, two pairs of downstream and upstream bitrates lie on a line that also crosses the origin of the bitrate axes. This line will be included in some plots to better illustrate the bitrate relations between different algorithms.

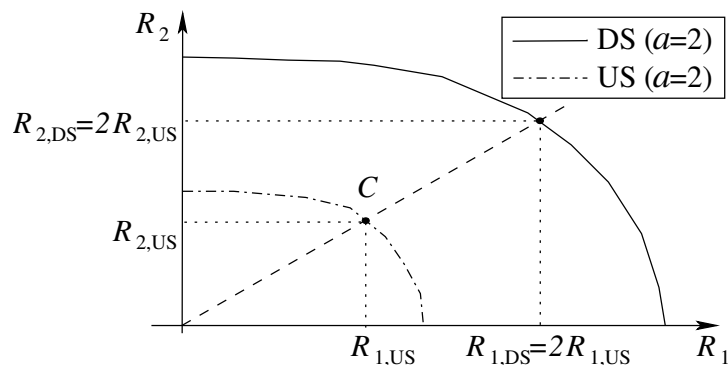


FIGURE 5.2: An example of rate region of the NRIA for two-user case when $\alpha_{1,DS} = \alpha_{1,US}$, and $\alpha_{2,DS} = \alpha_{2,US}$ and for asymmetry parameter value $a = 2$.

Figure 5.2 shows an example of the rate regions of the NRIA for the asymmetry parameter value set to $a = 2$. In the same plot are also shown a pair of downstream bitrates at point C and a pair of upstream bitrates at point D , which lie on a line (dashed line) that crosses the origin. Note that for the symmetric case, with $a = 1$, $C = D$ and the corresponding rate regions coincide.

5.3 Comparison of the NRIA with the IWFA

In this section we compare the performance of the NRIA with the iterative water-filling algorithm (IWFA) [122] for the two-user and multi-user cases. As mentioned the IWFA assumes a fixed frequency band plan, and therefore, for all simulations concerning the IWFA we will use one of the standardized frequency band plans: the band plan “997” (see Section 3.1.3), without guard bands, with the corresponding downstream and upstream

subcarriers:

$$\begin{aligned} I_{DS} &= \{32 \dots 695, 1183 \dots 1634\}, \text{ and} \\ I_{US} &= \{696 \dots 1182, 1635 \dots 2782\}. \end{aligned} \quad (5.1)$$

The cable type and the FEXT model used are the same as specified in Section 4.6, when analyzing the initialization of input parameters in the NRIA. We use a DMT system with 4096 subcarriers, but only the subcarriers in the range from 32 to 2782 are used, which corresponds to frequencies from 138 kHz to 12 MHz. Moreover, for all simulations we have also included alien noise according to ETSI VDSL “Noise model A” [40] in addition to the background noise. The PSDs of ETSI VDSL “Noise model A” at both LT and NT side are shown in Figure 5.3.

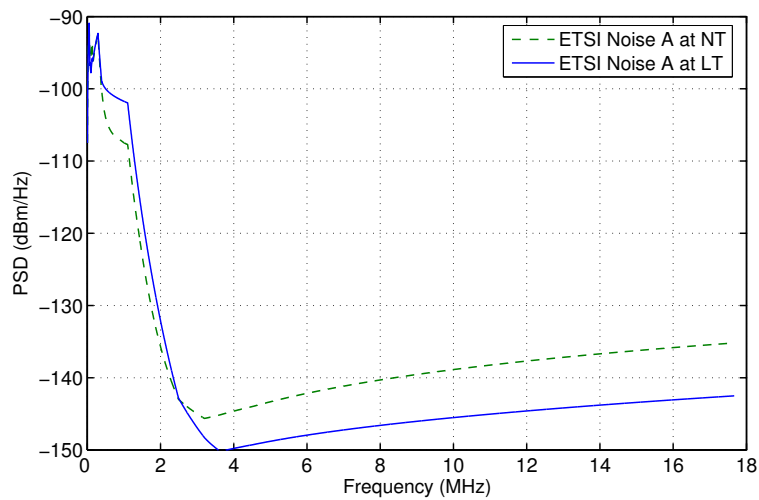


FIGURE 5.3: PSDs of ETSI VDSL “Noise Model A” at NT and LT sides.

As suggested in Section 4.6 selecting $K = 8$ subbands (four for each transmission direction) in the NRIA is typically sufficient to achieve the desired bitrates, which is also used for all simulations in this section. Furthermore, as explained in Section 4.6 we set $M_{DS} = M_{US} = U$ for all simulations where M_{DS} and M_{US} show the number of the last normalized bitrates used to calculate the target bitrates.

5.3.1 Two-User Case: Fixed Length

For all simulations we will use the network scenario shown in Figure 5.4. The insertion loss (the direct channel) and the FEXT couplings of this two-user scenario are shown in Figure 5.5. This is essentially the same network scenario as in [14], which was used to compare the OSBA with the IWFA. However, we have not collocated four modems at each node. This is because the IWFA, due to the iterative process, might generate different PSDs to support equal bitrates for the collocated modems although they have the same FEXT couplings. Furthermore, in practice even if the modems are collocated there are different FEXT coupling functions between different twisted pairs.

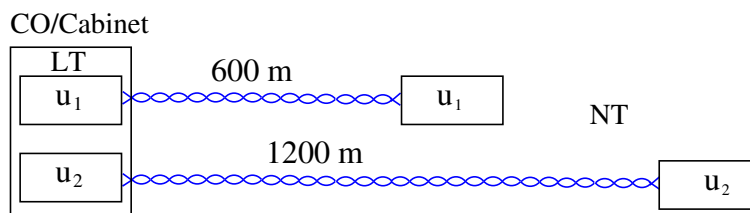


FIGURE 5.4: Network scenario used for most of the simulations. CO denotes the central office. LT and NT denote line termination and network terminations sides, respectively.

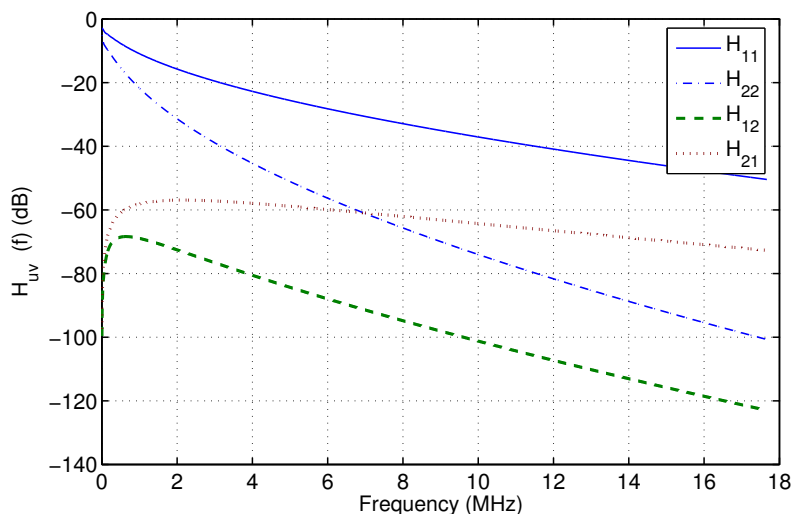


FIGURE 5.5: The insertion losses (the direct channel) and the FEXT couplings for the two-user case network scenario given in Figure 5.4.

5.3.1.1 Comparison for the Symmetric Bitrates

Figure 5.6 shows the downstream and upstream rate regions for the IWFA and for the NRIA with $a = 1$. The NRIA forces symmetric bitrates for each user when $a = 1$, because, as described in Section 5.2, we have assumed equal downstream and upstream user priorities for each user; thus, $\alpha_{u,US} = \alpha_{u,DS}$, for $u = 1, 2$. The NRIA has optimized the sharing of the cable resources for symmetric bitrates. Therefore, to compare the NRIA with the IWFA we also need to find the corresponding symmetric bitrates for the IWFA. They are located where the boundaries of the downstream and upstream IWFA rate regions intersect. This shows that the IWFA in this case supports symmetric bitrates only for two pairs (one for each transmission direction) of user bitrate combinations. In the other hand, the NRIA supports symmetric bitrates for all pairs of user bitrate combinations that lie in the boundary of the NRIA rate region in Figure 5.6. There are also network scenarios for which the IWFA cannot support symmetric bitrates (see for example Figure 5.11). The NRIA supports symmetric bitrates in any network scenario, due to using the flexibility to assign the subcarriers adaptively in downstream and upstream to match better the needs of all users.

The bitrate figures for the symmetric case are summarized in Table 5.1. We see that if we fix the bitrate of user u_1 to 53.35 Mbit/s, as achieved by the IWFA, the NRIA can

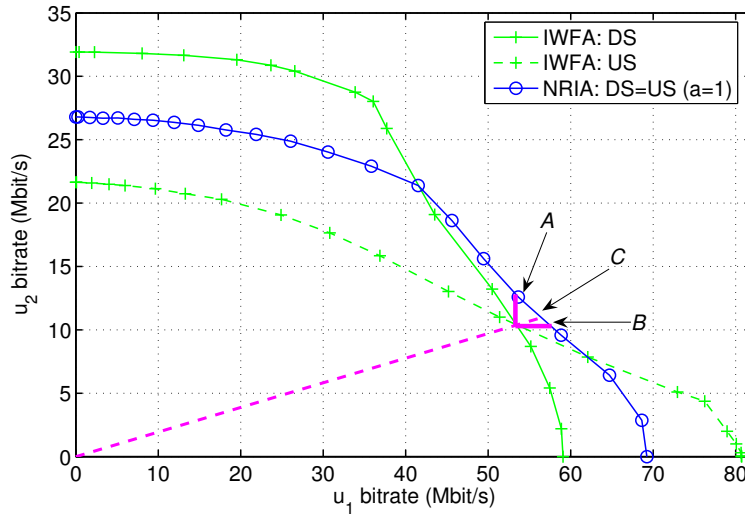


FIGURE 5.6: Downstream and upstream rate regions of the IWFA and the NRIA for $a = 1$, $\alpha_{1,DS} = \alpha_{1,US}$, and $\alpha_{2,DS} = \alpha_{2,US}$.

TABLE 5.1: Comparison of the NRIA with the IWFA, symmetric bitrates ($a = 1.00$).

Algorithm	Direction	User u_1 (Mbit/s)	User u_2 (Mbit/s)	Increase (%)
IWFA	DS/US	53.35	10.36	—
NRIA fix u_1 (A)	DS/US	53.35	12.80	23.5
NRIA fix u_2 (B)	DS/US	57.50	10.36	7.78
NRIA (C)	DS/US	56.46	10.96	5.82

increase the bitrate of user u_2 from 10.36 to 12.80 Mbit/s (point A, an increase of 23%). If we instead fix the bitrate of u_2 at 10.36 Mbit/s the NRIA can increase the bitrate of u_1 from 53.35 to 57.50 Mbit/s (point B, an increase of 8%). The gain is smaller for the latter case, since u_1 disturbs u_2 more than vice versa, due to the upstream near-far problem, which we described in Section 3.1.3.

For distributed DSL access networks in general, decreasing one user's bitrate does not necessarily increase another user's bitrate correspondingly. Therefore, in a third comparison the users' bitrate relations of the NRIA and the IWFA are equal

$$\left(\frac{R_1}{R_2}\right)_{\text{IWFA}} = \left(\frac{R_1}{R_2}\right)_{\text{NRIA}} = \frac{\alpha_1}{\alpha_2}. \quad (5.2)$$

This is depicted in Figure 5.6 at point C, where the dashed line (corresponding to (5.2)) intersects with the NRIA's rate region boundary. For this case, a total bitrate increase of about 6% is achieved with the NRIA compared to the IWFA.

As discussed in Section 4.7 for a fixed subcarrier allocation, when only the inner stage of the NRIA is used, the NRIA cannot outperform the IWFA since the inner stage of the NRIA is based on the IWFA. However, in this case the NRIA can be used to calculate the sets of maximum achievable user bitrates for the IWFA. The alternative, to calculate

the sets of achievable bitrates in the IWFA by exhaustively testing all possible maximum total power constraints [122] requires much higher computational complexity even for this simple two-user network scenario.

5.3.1.2 Comparison for the Asymmetric Bitrates

The NRIA supports any asymmetric bitrates for each user by setting the asymmetry parameter a to a desired value. Note, from (4.7) it can be recognized that the desired asymmetry for each user can be achieved also for $a = 1$ by selecting the downstream and upstream priority values appropriately for each user. However, for the reasons explained in Section 5.2 we have assumed equal downstream and upstream priorities for each user. Therefore, the asymmetry parameter a is sufficient to achieve the desired asymmetry for each user. At the other hand, the IWFA only supports those asymmetric users' bitrates that are spanned by all combinations of the pairs of bitrates that lie in the downstream and upstream boundary rate regions, where the boundary rate regions do not intersect. This shows that the space of the asymmetric bitrate combinations spanned by the IWFA is much smaller than that of the NRIA.

To compare the performance of the NRIA with the IWFA we have selected the asymmetry parameter $a = 1.25$ in the NRIA. Again, we should compare the NRIA with the IWFA for which $a = 1.25$. In Figure 5.7 the bitrates for this case are found at the intersections of the dashed line with the IWFA downstream and upstream rate region boundaries. These bitrates are summarized in Table 5.2; it can be verified that they satisfy the priority relations:

$$\begin{aligned} \left(\frac{R_{1,DS}}{R_{2,DS}} \right)_{IWFA} &= \left(\frac{R_{1,DS}}{R_{2,DS}} \right)_{NRIA} = \frac{\alpha_{1,DS}}{\alpha_{2,DS}}, \\ \left(\frac{R_{1,US}}{R_{2,US}} \right)_{IWFA} &= \left(\frac{R_{1,US}}{R_{2,US}} \right)_{NRIA} = \frac{\alpha_{1,US}}{\alpha_{2,US}}. \end{aligned} \quad (5.3)$$

We see that the NRIA achieves an increase of more than 12% in each transmission direction.

TABLE 5.2: Comparison of the NRIA with the IWFA, asymmetric bitrates ($a = 1.25$).

Algorithm	Direction	User u_1 (Mbit/s)	User u_2 (Mbit/s)	Increase (%)
IWFA	DS	41.25	21.42	—
IWFA	US	33.25	16.88	—
NRIA	DS	46.60	23.88	12.4
NRIA	US	37.24	19.19	12.5

The IWFA supports asymmetric bitrates for $a = 1.25$, as for the symmetric bitrates, only for two pairs of user bitrates. In contrast, the NRIA supports symmetric bitrates for all pairs of bitrates that lie on the boundary rate regions and intersect the line that crosses the origin of the bitrate axes.

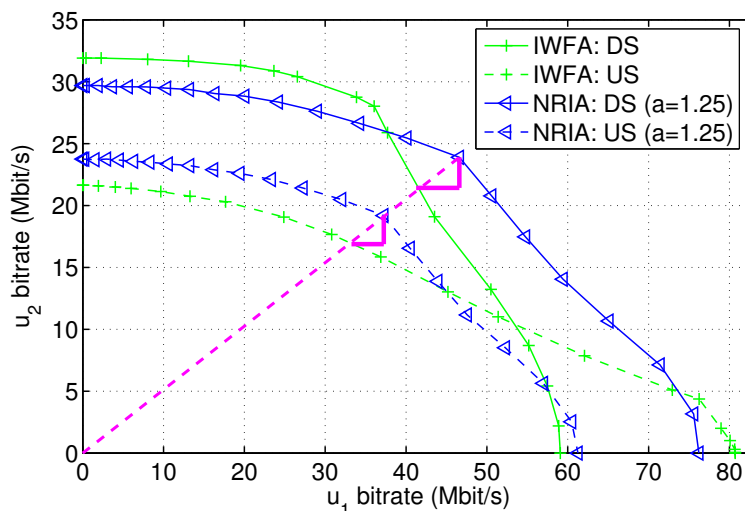


FIGURE 5.7: Downstream and upstream rate regions of the IWFA and the NRIA for $a = 1.25$, $\alpha_{1,DS} = \alpha_{1,US}$, and $\alpha_{2,DS} = \alpha_{2,US}$.

5.3.1.3 Performance Improvement of the NRIA over the IWFA

We have showed that the NRIA performs better than the IWFA for both symmetric and asymmetric bitrates. The increase in the bitrates is due to a better optimized band plan as well as power allocations found by the NRIA compared to the fixed band plan and power allocations found by the IWFA. We analyze this in detail for a particular case when the asymmetry parameter is $a = 1.25$.

The optimized downstream and upstream subcarriers found by the NRIA for this two-user network scenario with $K = 8$ subbands, $a = 1.25$ asymmetry, and the bitrates given in Table 5.2 are:

$$I_{DS} = \{32 \dots 477, 1025 \dots 1501, 2049 \dots 2525\}, \text{ and}$$

$$I_{US} = \{478 \dots 1024, 1502 \dots 2048, 2526 \dots 2782\}.$$

Note that although we have selected eight subbands (four for each transmission direction), they have been reduced to six subbands (three for each transmission direction) since only subcarriers in the range $\{32, \dots, 2782\}$ are used (out of 4096 total). The subcarrier allocations used in the IWFA are given in (5.1).

The corresponding downstream and upstream transmit PSDs of the IWFA and the NRIA when $a = 1.25$ are shown in Figures 5.8 and 5.9. The transmit PSDs of the NRIA and the IWFA are non-smooth due to the integer bit-loading algorithm. However, the PSDs of the NRIA and the IWFA are almost flat over all used subcarriers. The PSDs of the IWFA are almost flat as shown in [108, 116] when the integer bit-loading algorithm is used. Because the inner stage of the NRIA is based on the IWFA, the PSDs generated by the NRIA are likewise almost flat when the integer bit-loading algorithm is used.

Let us start analyzing the downstream transmission direction. With the IWFA both subbands are fully utilized by both users as shown in Figure 5.8. From the supported bitrates shown in Table 5.2 we have assigned a higher bitrate to the user u_1 than to u_2 . Although user u_1 has lower loop attenuation compared to u_2 (cf. Figure 5.5), u_1 has used

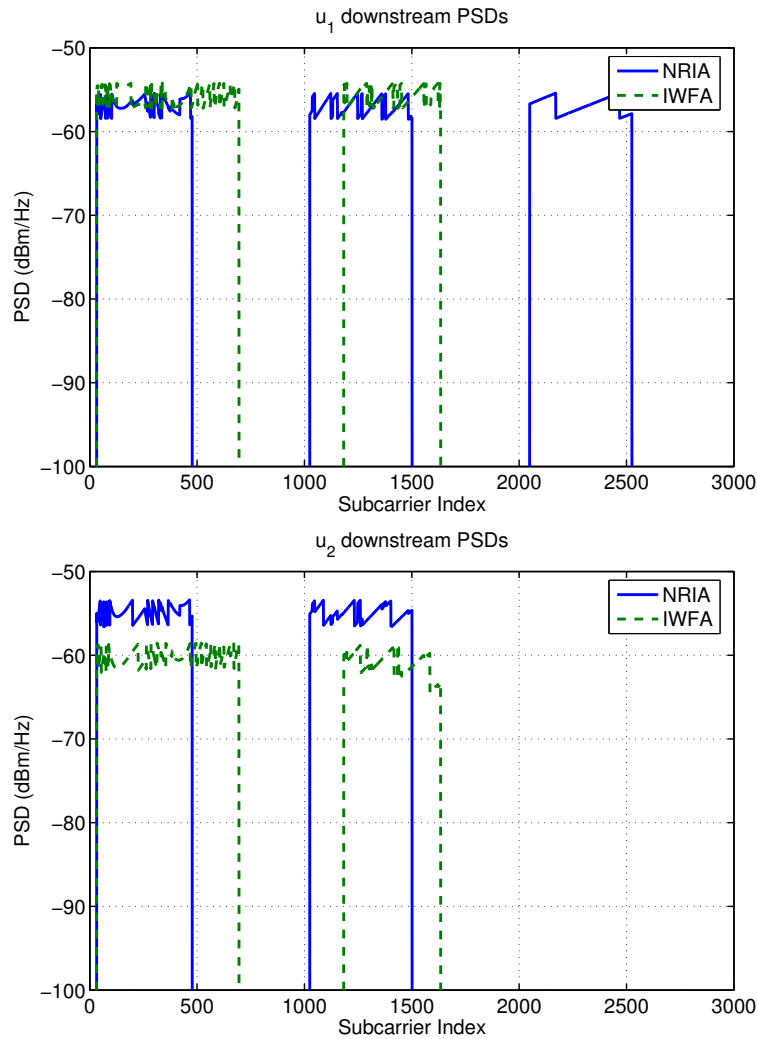


FIGURE 5.8: Downstream transmit PSDs of the NRIA and the IWFA for users' bitrates given in Table 5.2. With these transmit PSDs the NRIA achieves an increase of 12.4% in bitrates compared to the IWFA.

the maximum total power and is determining the maximum downstream bitrates of u_2 and himself. In the case of the NRIA, u_2 utilizes only the first two subbands, because the loop on which u_2 has been deployed has high noise-to-channel-gain ratio in the third downstream subband and hence it is not attractive for him. However, the third subband can be utilized by u_1 , because it has low loop attenuation (cf. Figure 5.5) and u_1 is not receiving noise from u_2 in the third subband. Both u_1 and u_2 use more or less the maximum total power. Therefore, the downstream bitrates supported by the NRIA are higher than those supported by the IWFA for both users.

From Figure 5.9, in the upstream transmission direction in the case of the IWFA, u_1 is utilizing both upstream assigned subbands. However, u_2 is only utilizing the frequencies of the second subbands up to approximately 8.7 MHz (subcarrier 2019), due to the high noise-to-channel-gain ratio at high frequencies. The same situation occurs with the NRIA, where u_1 is utilizing all three assigned upstream subbands, whereas u_2 utilizes only the first subband and the second subband up to approximately 7.9 MHz (subcarrier 1830). In

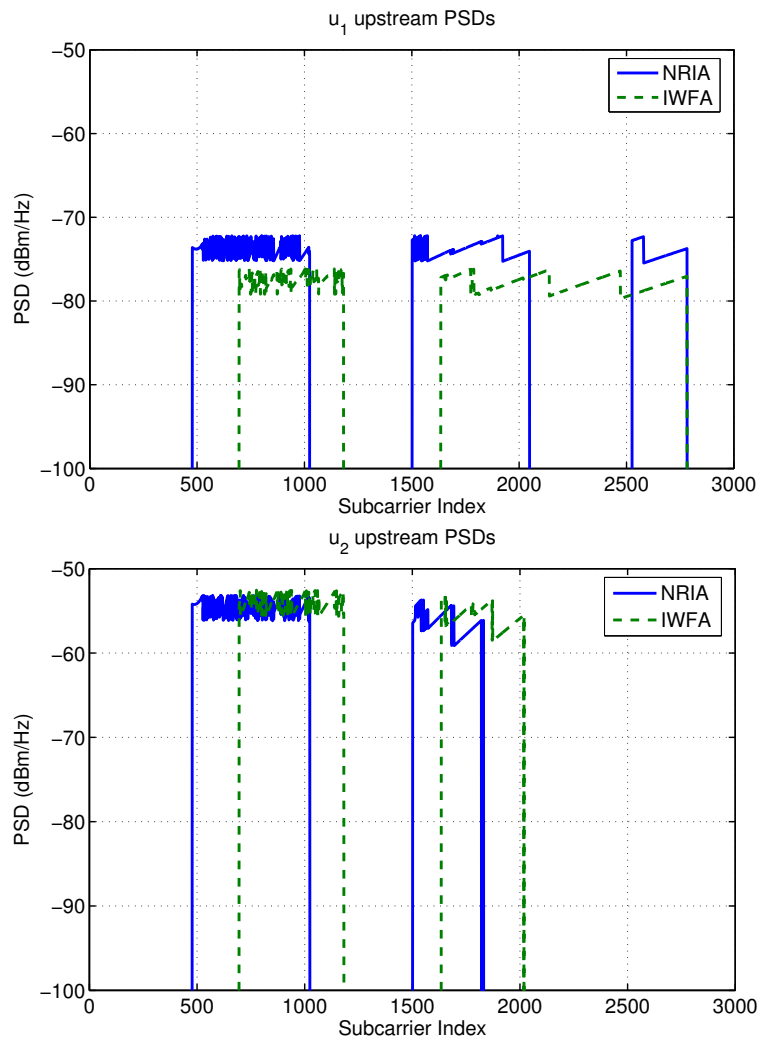


FIGURE 5.9: Upstream transmit PSDs of the NRIA and the IWFA for users' bitrates given in Table 5.2. With these transmit PSDs the NRIA achieves an increase of 12.5% in bitrates compared to the IWFA.

both algorithms u_2 uses the maximum total power, because it is disturbed more by u_1 than vice versa due to the upstream near-far problem.

In the upstream transmission direction both the NRIA and the IWFA perform power allocation for user u_2 with the same levels and use approximately the same number of subcarriers. However, in the case of the NRIA in the average the subcarriers used are allocated at low frequencies where the noise-to-channel-gain ratio is also low. Therefore user u_2 in the case of the NRIA can load in total more bits over all used subcarriers. With the IWFA user u_1 utilizes more subcarriers than with the NRIA, but in the case of the IWFA it allocates low power levels over all used subcarriers. Furthermore, on average the subcarriers assigned in the IWFA are allocated at high frequencies compared to the NRIA. Thus, user u_1 achieves a lower bitrate in the IWFA than in the NRIA.

5.3.2 Two-User Case: Variable Length

To compare the performance of the NRIA with the IWFA for the two-user case in a broad range of scenarios we varied the length of the second loop in Figure 5.4. We ran the simulations with the loop lengths for the second user from 100 m to 2000 m in 100 m increments as illustrated in Figure 5.10. We use the integer bit-loading algorithm in both the NRIA and the IWFA. Thus, the IWFA might outperform the NRIA if we fix the maximum number of bits to a specific value for reasons explained in Section 4.7. We can extend the NRIA in a straightforward way to recognize these cases. However, to perform a fair comparison we use another method: we allow the bit-loading algorithm to load any number of bits per subcarrier.

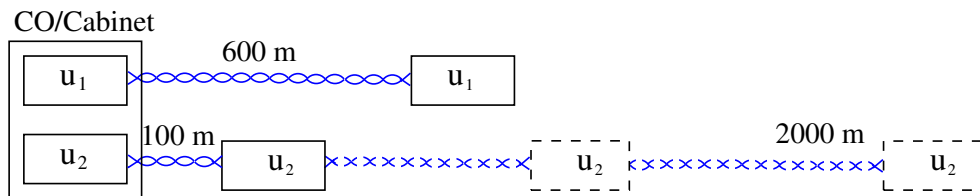


FIGURE 5.10: The two-user network scenario used for variable length simulations.

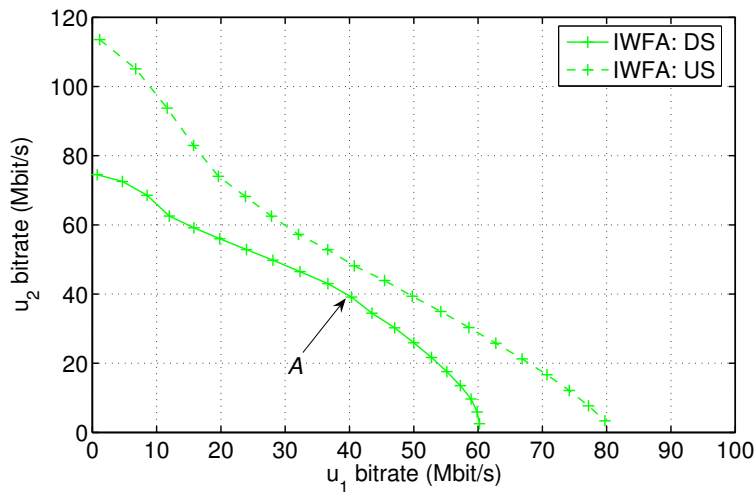


FIGURE 5.11: IWFA rate region for the network scenario in Figure 5.10 when the loop length of the second user is 300 m.

To simplify the comparison we assign to both users equal downstream and upstream priority values as explained in Section 5.2. We also set the asymmetry values equal to one, $a = 1$, in the NRIA. Thus, in the NRIA we search for equal and symmetric bitrates.

Under these constraints, the optimization problem that the NRIA will solve is defined as:

$$\begin{aligned} & \text{maximize} && \sum_{u=1}^2 (R_{u,DS} + R_{u,US}), \\ & \text{subject to:} && \\ & && R_{1,DS} = R_{1,US} = R_{2,DS} = R_{2,US}. \end{aligned}$$

Although the frequency band plan “997” used in the IWFA targets symmetric bitrates, the supported bitrates will not be symmetric (the downstream and upstream rate region curves do not intersect) for each loop length due to the use of a fixed band plan. For instance, Figure 5.11 shows the rate region of the IWFA when the length of the second loop is set to 300 m. We are searching for equal and symmetric bitrates. Therefore, for the IWFA we select the pair of bitrates from the rate region curve with lower bitrates for both transmission directions. One such pair of bitrates is showed in Figure 5.11 at point A.

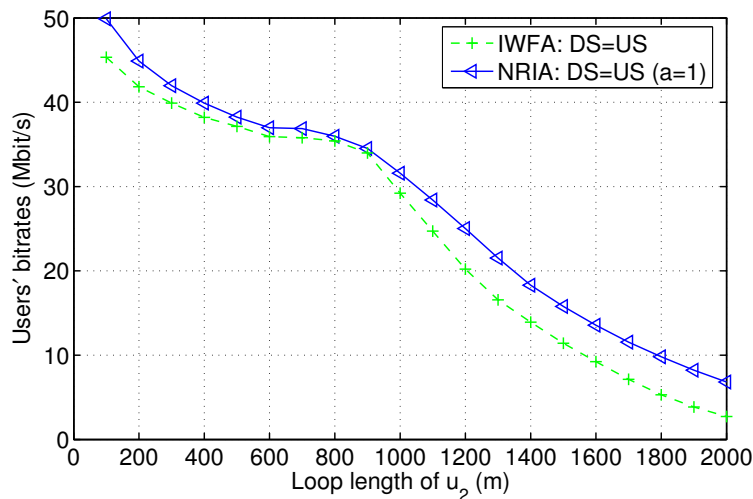


FIGURE 5.12: Symmetric bitrates of the NRIA and the IWFA with a variable loop length for the second user and with the loop length of the first user fixed at 600 m.

Figure 5.12 shows the equal and symmetric bitrates of the NRIA and the IWFA. The NRIA has the greatest improvement over the IWFA when the loops of the two users are of different lengths. From the plots it can be seen that the NRIA achieves an increase in bitrate from approximately 1.5 % (with the length of u_2 equal to 900 m) to over 143 % (with the length of u_2 equal to 2000 m) compared to the bitrates supported by the IWFA. Note that the performance improvements shown are for equal and symmetric bitrates and compared to the standardized band plan “997”, which also aims for symmetric bitrates. For other bitrate combinations the NRIA can achieve even higher performance improvement. Furthermore, the advantages of the NRIA over the IWFA are not only the increased bitrates, but also the flexibility of the NRIA to assign a broad range of the downstream and upstream bitrate combinations to the users, as will be shown in Section 5.5.

5.3.3 Multi-User Case

In Section 5.3.1 we analyzed in detail the performance of the NRIA compared to the performance of the IWFA for a network scenario with two users and fixed loop lengths. In Section 5.3.2 we extended the analysis to variable loop lengths. In this section we analyze the performance of the NRIA compared to the performance of the IWFA for a network scenario with multiple users and fixed loop lengths. The simulation scenario is shown in Figure 5.13 with ten users and a distance of 100 m between two successive users.

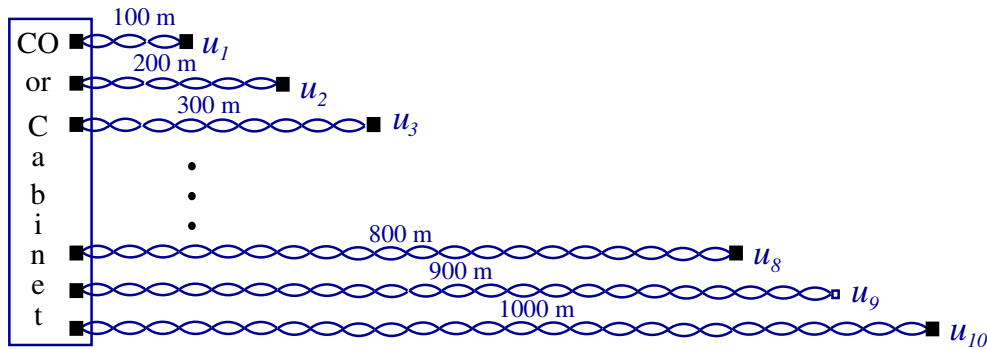


FIGURE 5.13: The Multi-user network simulation scenario used to compare the NRIA with the IWFA.

TABLE 5.3: User priority values used for simulation.

u	c1	c2	c3	c4	c5	c6	c7	c8	c9	c10
1	0.11	0.04	0.01	0.04	0.07	0.07	0.12	0.09	0.12	0.08
2	0.11	0.09	0.03	0.10	0.09	0.09	0.17	0.01	0.13	0.15
3	0.15	0.16	0.01	0.04	0.06	0.17	0.03	0.03	0.14	0.09
4	0.04	0.07	0.19	0.11	0.09	0.15	0.12	0.12	0.07	0.05
5	0.06	0.21	0.09	0.19	0.14	0.02	0.04	0.17	0.11	0.03
6	0.21	0.17	0.17	0.09	0.10	0.15	0.18	0.12	0.04	0.10
7	0.05	0.09	0.18	0.16	0.20	0.14	0.06	0.14	0.15	0.17
8	0.03	0.04	0.08	0.09	0.04	0.06	0.06	0.04	0.07	0.17
9	0.09	0.09	0.18	0.05	0.11	0.13	0.06	0.13	0.06	0.13
10	0.14	0.03	0.07	0.13	0.10	0.01	0.16	0.15	0.11	0.04
Σ	1	1	1	1	1	1	1	1	1	1

In the multi-user case we cannot plot the rate regions of the NRIA and the IWFA due to the high number of dimensions. To simplify the comparison we will perform the simulation under the following conditions. We assign equal downstream and upstream priority values as explained in Section 5.2. We perform the simulation for ten different cases. For each case the user priority values are generated randomly; these values are shown in Table 5.3. Furthermore, the asymmetry parameter a in the NRIA is set equal to one, so in the NRIA we search for symmetric bitrates. For all simulations we use the integer bit-loading algorithm and allow it to load any number of bits per subcarrier. Because we are searching

for symmetric bitrates, in the IWFA we select the bitrates from the direction with smaller bitrate values for the same reasons described in Section 5.3.2.

TABLE 5.4: Supported bitrates in the IWFA for the user priority values shown in Table 5.3.

u	User bitrates (Mbit/s)									
	c1	c2	c3	c4	c5	c6	c7	c8	c9	c10
1	17.14	6.92	1.43	6.23	11.46	12.40	18.34	12.98	21.86	13.33
2	17.14	15.56	4.28	15.57	14.74	15.95	25.98	1.44	23.68	25.00
3	23.37	27.64	1.43	6.23	9.82	30.12	4.59	4.33	25.50	15.00
4	6.23	12.09	27.08	17.13	14.74	26.58	18.34	17.31	12.76	8.34
5	9.35	36.26	12.83	29.58	22.92	3.54	6.12	24.52	20.04	5.00
6	32.72	29.35	24.23	14.02	16.38	26.58	27.51	17.31	7.29	16.67
7	7.79	15.54	25.66	24.92	32.75	24.81	9.17	20.20	27.33	28.33
8	4.68	6.90	11.41	14.02	6.55	10.63	9.17	5.77	12.76	28.34
9	14.02	15.54	25.66	7.79	18.01	23.04	9.17	18.76	10.93	21.67
10	21.82	5.18	9.98	20.24	16.38	1.77	24.46	21.64	20.04	6.67
Σ	154.2	171.0	144.0	155.7	163.7	175.4	152.5	144.3	182.2	168.3

TABLE 5.5: Supported bitrates in the NRIA for the user priority values shown in Table 5.3.

u	User bitrates (Mbit/s)									
	c1	c2	c3	c4	c5	c6	c7	c8	c9	c10
1	19.16	7.16	1.56	7.09	12.45	13.32	20.98	15.11	25.10	14.13
2	19.16	16.10	4.69	17.72	16.00	17.12	29.72	1.68	27.18	26.49
3	26.14	28.62	1.56	7.09	10.66	32.32	5.25	5.04	29.27	15.89
4	6.97	12.52	29.71	19.49	15.99	28.52	20.98	20.14	14.64	8.83
5	10.46	37.54	14.08	33.66	24.88	3.80	7.00	28.54	23.00	5.30
6	36.59	30.39	26.58	15.95	17.76	28.51	31.47	20.15	8.36	17.66
7	8.72	16.09	28.15	28.35	35.52	26.61	10.49	23.50	31.35	30.01
8	5.23	7.15	12.51	15.95	7.10	11.40	10.49	6.72	14.63	30.01
9	15.68	16.10	28.15	8.86	19.54	24.65	10.49	21.83	12.54	22.95
10	24.40	5.37	10.95	23.04	17.76	1.90	27.98	25.19	22.96	7.06
Σ	172.5	177.0	157.9	177.2	177.7	188.2	174.8	167.9	209.0	178.3

The bitrates supported by the IWFA and the NRIA for the user priority values in Table 5.3 are summarized in Tables 5.4 and 5.5, respectively. From the results in tables we conclude that the NRIA achieves an increase in bitrate from over 3% (case ‘c2’) to over 16% (case ‘c8’) compared to the bitrates supported by the IWFA. Note as mentioned in Section 5.3.2 the performance improvements are shown for symmetric bitrates and compared to the standardized band plan “997”, which also aims for symmetric bitrates.

5.4 Comparison of the NRIA with the OSBA

In this section we compare the NRIA with the optimal spectrum balancing algorithm (OSBA) [14, 15]. The OSBA assumes a fixed subcarrier allocation. Thus, all conclusions concerning the symmetric and asymmetric bitrate combinations supported by the IWFA also hold for the OSBA. Therefore we will not repeat them again in this section.

We compare the NRIA with the OSBA only for the two-user case, due to the high computational complexity of the OSBA when more than two users are included in the optimization process. For all simulations, we use the same two-user scenario as shown in Figure 5.4, which was used to compare the NRIA with the IWFA. Since the OSBA assumes a fixed band plan we use the same subcarrier allocations as used in Section 5.3 for the IWFA. All other simulation parameters are the same as those in Section 5.3.

5.4.1 Comparison for the Symmetric Bitrates

Figure 5.14 shows the downstream and upstream rate regions for the NRIA with symmetric bitrates $a = 1$ and for the OSBA with varying asymmetry. The corresponding symmetric bitrates for the OSBA are summarized in Table 5.6.

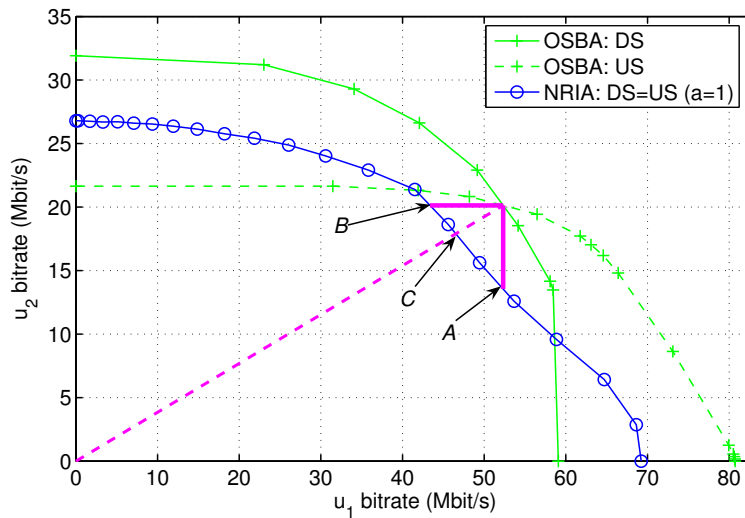


FIGURE 5.14: Downstream and upstream rate regions of the OSBA and the NRIA for $a = 1$, $\alpha_{1,DS} = \alpha_{1,US}$, and $\alpha_{2,DS} = \alpha_{2,US}$.

TABLE 5.6: Comparison of the NRIA with the OSBA, symmetric bitrates ($a = 1.00$).

Algorithm	Direction	User u_1 (Mbit/s)	User u_2 (Mbit/s)	Loss (%)
OSBA	DS/US	52.32	20.13	—
NRIA fix u_1 (A)	DS/US	52.32	13.55	33.3
NRIA fix u_2 (B)	DS/US	43.37	20.13	17.2
NRIA (C)	DS/US	46.52	17.90	11.1

To allow user u_1 to have 52.32 Mbit/s with the NRIA, as achieved by the OSBA, user u_2 can only have 13.55 Mbit/s (point A , a loss of 33%). Alternatively, to allow u_2 to have 20.13 Mbit/s with the NRIA, as achieved by the OSBA, u_1 can have only 43.37 Mbit/s (point B , a loss of 17%). Finally, when we want to have the same bitrate relations with the NRIA as with the OSBA, then the bitrates given in Table 5.6 can be supported, which corresponds to a loss of 11% (point C in Figure 5.14).

5.4.2 Comparison for the Asymmetric Bitrates

To compare the performance of the NRIA with the OSBA for asymmetric bitrates we select the same asymmetry parameter value as used to compare the NRIA with the IWFA for the asymmetric bitrates; thus, $a = 1.25$. The rate regions of the OSBA and the NRIA with $a = 1.25$ are shown in Figure 5.15. The supported downstream and upstream bitrates of both the NRIA and the OSBA that satisfy relations (5.3) are summarized in Table 5.7. For this case the NRIA suffers a loss of less than 5% in both transmission directions

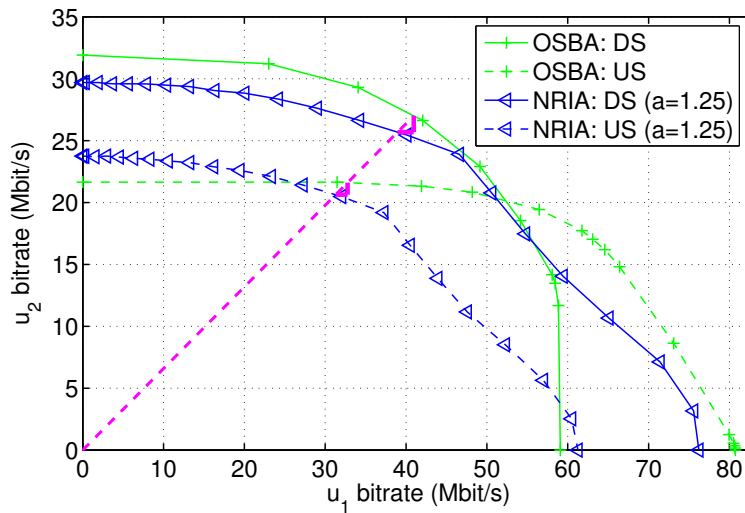


FIGURE 5.15: Downstream and upstream rate regions of the OSBA and the NRIA for $a = 1.25$, $\alpha_{1,DS} = \alpha_{1,US}$, and $\alpha_{2,DS} = \alpha_{2,US}$.

TABLE 5.7: Comparison of the NRIA with the OSBA, asymmetric bitrates ($a = 1.25$).

Algorithm	Direction	User u_1 (Mbit/s)	User u_2 (Mbit/s)	Loss (%)
OSBA	DS	40.95	27.00	—
OSBA	US	32.76	21.60	—
NRIA	DS	38.95	25.68	4.9
NRIA	US	31.29	20.63	4.5

5.4.3 Performance Loss in the NRIA over the OSBA

The bitrates shown in Tables 5.6 and 5.7 are not surprising, since the OSBA can in theory deliver the highest possible bitrates for a given band plan. The price is a much higher computational complexity compared to the NRIA, even for this two-user scenario. We showed in Section 4.5 that when the Levin-Campello bit-loading algorithm is used, the computational complexity of the NRIA is:

$$C_{\text{NRIA}} = \mathcal{O} \left(O \cdot i_{\text{DS}} \cdot \tilde{N}_{\text{DS}} (U + 1) \right) + \mathcal{O} \left(O \cdot i_{\text{US}} \cdot \tilde{N}_{\text{US}} (U + 1) \right), \quad (5.4)$$

where O denotes the number of iterations in the outer stage; U denotes the number of users; i_{DS} and i_{US} denote the number of iterations in the downstream and upstream inner stages, respectively; \tilde{N}_{DS} denotes the average number of subcarriers in downstream assigned over all downstream outer stage iterations; and \tilde{N}_{US} denotes the average number of subcarriers in the upstream assigned over all upstream outer stage iterations. The complexity of the OSBA for a particular transmission direction is [15]:

$$C_{\text{OSBA}} = \mathcal{O} \left(N_{\text{dir}} U (R^{n, \max} + 1)^U 33^U \right), \quad (5.5)$$

where N_{dir} denotes the number of subcarriers assigned in a particular transmission directions. For both transmission directions based on (5.5), the complexity of the OSBA is

$$C_{\text{OSBA}} = \mathcal{O} \left(N_{\text{DS}} U (R^{n, \max} + 1)^U 33^U \right) + \mathcal{O} \left(N_{\text{US}} U (R^{n, \max} + 1)^U 33^U \right). \quad (5.6)$$

First, we analyze the complexity of the NRIA and the OSBA for the two-user case ($U = 2$). For the NRIA the maximum number of outer iterations is $O_{\max} = 10$, as shown in Section 4.5, when $K = 8$ subbands and $N = 4096$ subcarriers. The expected number of downstream and upstream inner stage iterations for the two-user case to achieve the desired accuracy is smaller than 50; thus, $i_{\text{DS}} < 50$ and $i_{\text{US}} < 50$. This statement is also confirmed by the plots in Figures 4.13 and 4.14. Substituting $O = 10$ and $i_{\text{DS}} = i_{\text{US}} = 50$ into (5.4) yields:

$$C_{\text{NRIA}} = \mathcal{O} \left(1.5 \cdot 10^3 \tilde{N}_{\text{DS}} \right) + \mathcal{O} \left(1.5 \cdot 10^3 \tilde{N}_{\text{US}} \right). \quad (5.7)$$

Correspondingly for the OSBA after substituting $R_{\max} = 15$ in (5.6), we get

$$C_{\text{OSBA}} = \mathcal{O} \left(557.6 \cdot 10^3 N_{\text{DS}} \right) + \mathcal{O} \left(557.6 \cdot 10^3 N_{\text{US}} \right). \quad (5.8)$$

From (5.7) and (5.8) we can conclude that also for the two-user case the complexity of the OSBA is much higher than the complexity of the NRIA. When the number of users increases it is obvious from (5.4) and (5.6) that the computational complexity of the OSBA increases faster than of the NRIA. This is because the complexity of the NRIA increases linearly with the number of users, whereas the complexity of the OSBA increases exponentially with the number of users. When the number of users in the OSBA is larger than a few, it effectively fails to deliver any result in a reasonable time.

For the network scenario in Figure 5.4, the symmetric bitrates in Table 5.6 and asym-

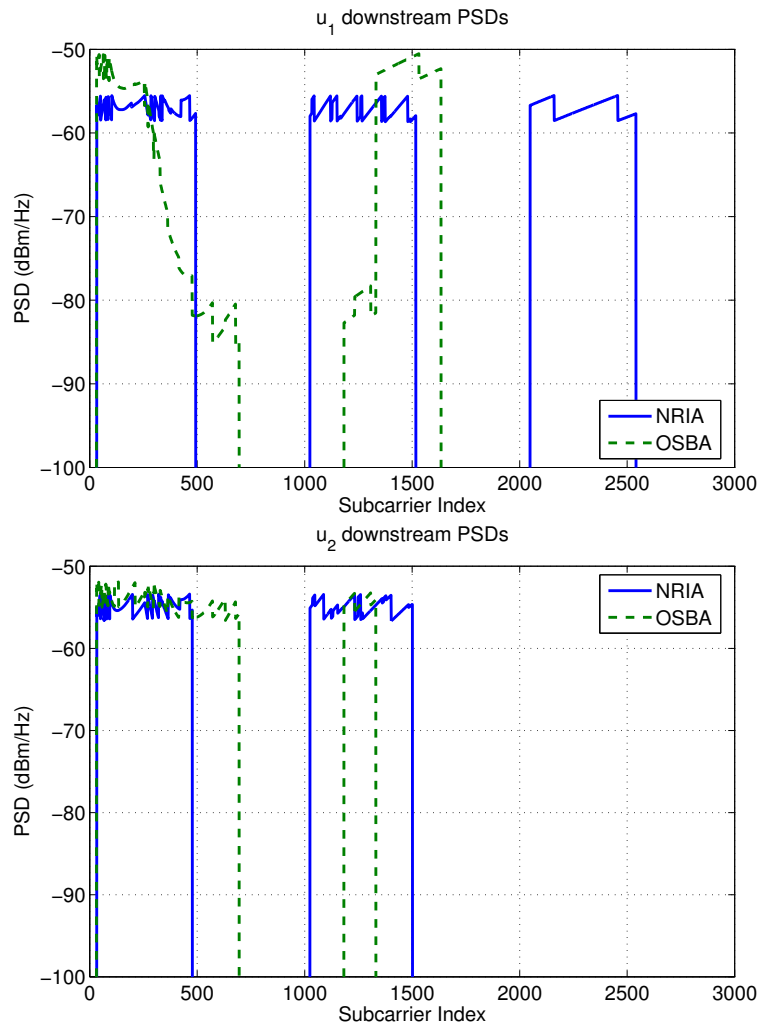


FIGURE 5.16: Downstream transmit PSDs of the NRIA and the OSBA for users' bitrates given in Table 5.7. With these transmit PSDs the NRIA suffers a loss of 4.9% in bitrates compared to the OSBA.

metric bitrates in Table 5.7 achieved by the OSBA are higher than those achieved by the NRIA. This is because the OSBA generates better optimized power allocations compared to the power allocations generated by the NRIA. We analyze this in detail for the asymmetric bitrates given in Table 5.7.

Figures 5.16 and 5.17 show the downstream and upstream transmit PSDs of the OSBA and the NRIA corresponding to asymmetry $a = 1.25$. The optimized downstream and upstream subcarrier allocations found by the NRIA for this two-user scenario are:

$$I_{DS} = \{32 \dots 493, 1025 \dots 1517, 2049 \dots 2541\}, \text{ and}$$

$$I_{US} = \{494 \dots 1024, 1518 \dots 2048, 2542 \dots 2782\}.$$

The downstream and upstream PSDs of the NRIA have similar shapes to those shown when comparing the NRIA for $a = 1.25$ with the IWFA. However, the downstream and upstream PSDs generated by OSBA have completely different shapes compared to those

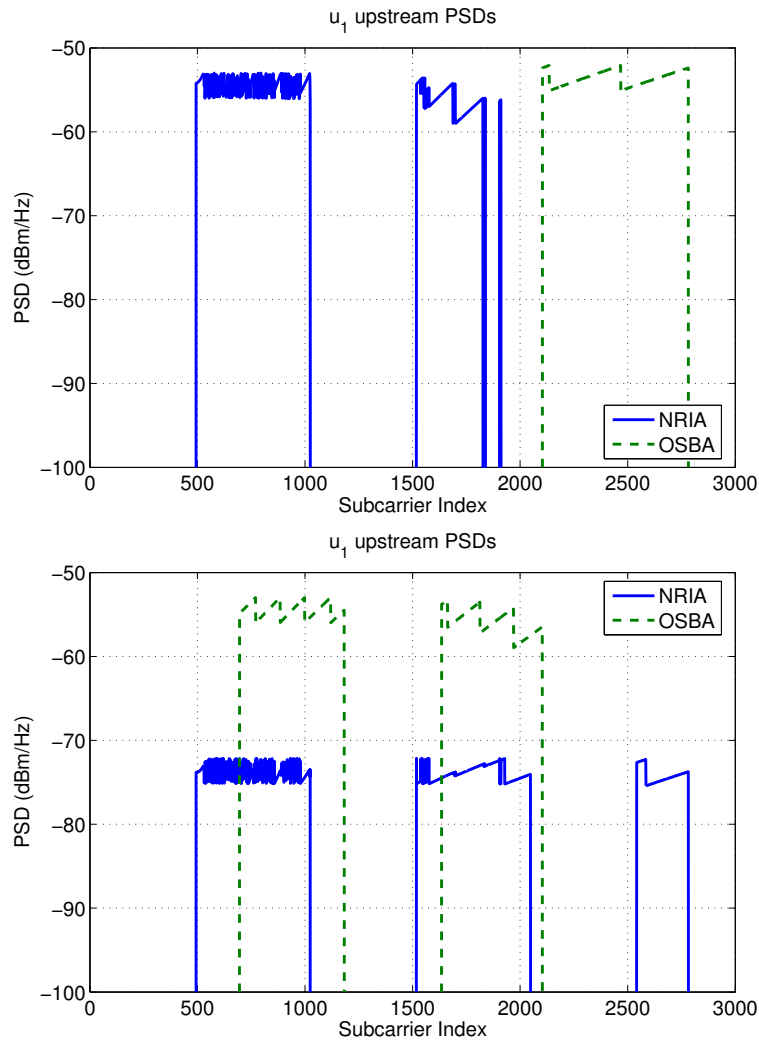


FIGURE 5.17: Upstream transmit PSDs of the NRIA and the OSBA for users' bitrates given in Table 5.7. With these transmit PSDs the NRIA suffers a loss of 4.5% in bitrates compared to the OSBA.

generated by the IWFA.

Figure 5.16 shows that the OSBA will partially reduce the transmit power for user u_1 in the downstream direction. The PSD at high frequencies of the first downstream subband and at low frequencies of the second downstream subband is reduced. Therefore, the users do not disturb each other significantly. In the upstream direction, as can be seen in Figure 5.17, the PSDs of both users for the OSBA do not overlap at all. They are flat, because the transmitters see more or less flat noise-to-channel-gain ratio (\mathcal{N}/\mathcal{H} , cf. Section 4.1) over all used subcarriers.

It is worth mentioning that the OSBA outperforms the NRIA in the same network scenarios and user bitrate combinations for which the OSBA outperforms the IWFA. As recognized by Cioffi *et al.* [28] the OSBA gains over the IWFA particularly when loop lengths differ greatly in the same binder. This was the case for the scenario used in these comparisons. Furthermore, from the rate regions of the OSBA in Figure 5.15 and the IWFA in Figure 5.7 (see also Figure 5.18) we conclude: the OSBA shows better

performance than the IWFA particularly when the bitrate (priority) value assigned to the shorter loop is moderately higher than the bitrate (priority) value assigned to the longer loop. When the bitrates assigned to both users are approximately equal it can be seen from the plots that the OSBA and the IWFA perform similarly. In all cases, where the IWFA and the OSBA show similar performance, the NRIA outperforms both because the band plan generated by the NRIA is adapted to better serve needs of all users.

5.5 Flexibility of the NRIA in the Bitrate Assignment

One of the major advantages of the NRIA over the IWFA and the OSBA is its flexibility to assign a broad range of the downstream and upstream bitrate combinations to users. On the other hand, the IWFA and the OSBA have little flexibility, because they assume a fixed band plan.

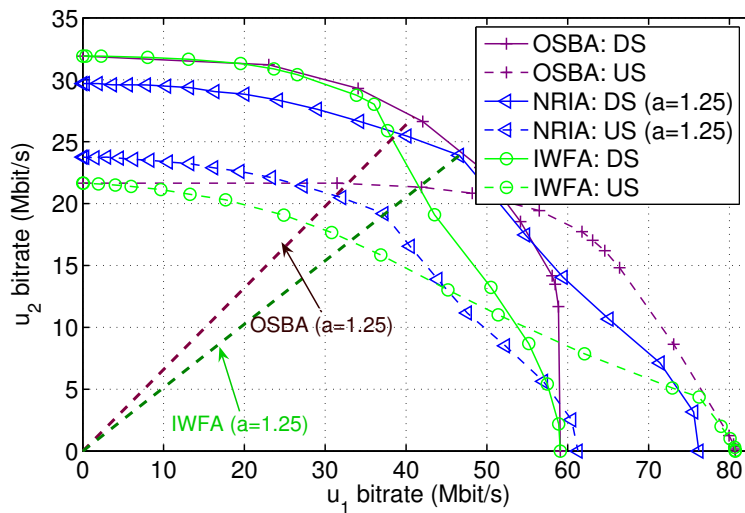


FIGURE 5.18: Downstream and upstream rate regions of the IWFA, the OSBA, and the NRIA for $a = 1.25$, $\alpha_{1,DS} = \alpha_{1,US}$, and $\alpha_{2,DS} = \alpha_{2,US}$.

For example, Figure 5.18 shows the rate regions of all three algorithms: the IWFA, the OSBA, and the NRIA with asymmetry $a = 1.25$ for the two-user case network scenario shown in Figure 5.4. Note that the plots in Figure 5.18 are not new plots, but combine the plots from Figures 5.7 and 5.15 in a single figure. The plots show, as also mentioned in Section 5.3.1, that the IWFA and the OSBA satisfy the desired bitrate relations defined in (5.3) only for two pairs of bitrate combinations, which are achieved at the intersection of the corresponding dashed line with the downstream and upstream rate regions of the IWFA and the OSBA, respectively. The dashed lines that fulfill the desired relations are shown in Figure 5.18 and they are different for the IWFA and the OSBA. The NRIA satisfies (5.3) for any two pairs of bitrate combinations that are at the intersection of any line that starts at the origin of the bitrate axes with the downstream and upstream rate region boundaries of the NRIA.

From the rate regions in Figure 5.18 we conclude that the NRIA supports many downstream and upstream user bitrate combinations that cannot be supported by the IWFA and

TABLE 5.8: Some bitrate combinations that can be supported by the NRA but not by the IWFA and the OSBA (corresponding to Figures 5.14 and 5.18).

Asymmetry	Direction	User u_1 (Mbit/s)	User u_2 (Mbit/s)
$a = 1.00$	DS/US	25.0	25.0
$a = 1.00$	DS/US	35.0	23.0
$a = 1.00$	DS/US	15.0	26.0
$a = 1.25$	DS	25.0	28.0
$a = 1.25$	US	20.0	22.5
$a = 1.25$	DS	13.3	29.3
$a = 1.25$	US	10.2	23.3

the OSBA. Table 5.8 summarizes some bitrate combinations that can be supported by the NRA but not by the IWFA or the OSBA. Note that these bitrate combinations are generated under the constraint of equal downstream and upstream user priorities and for the asymmetry parameter values $a = 1.00$ and $a = 1.25$.

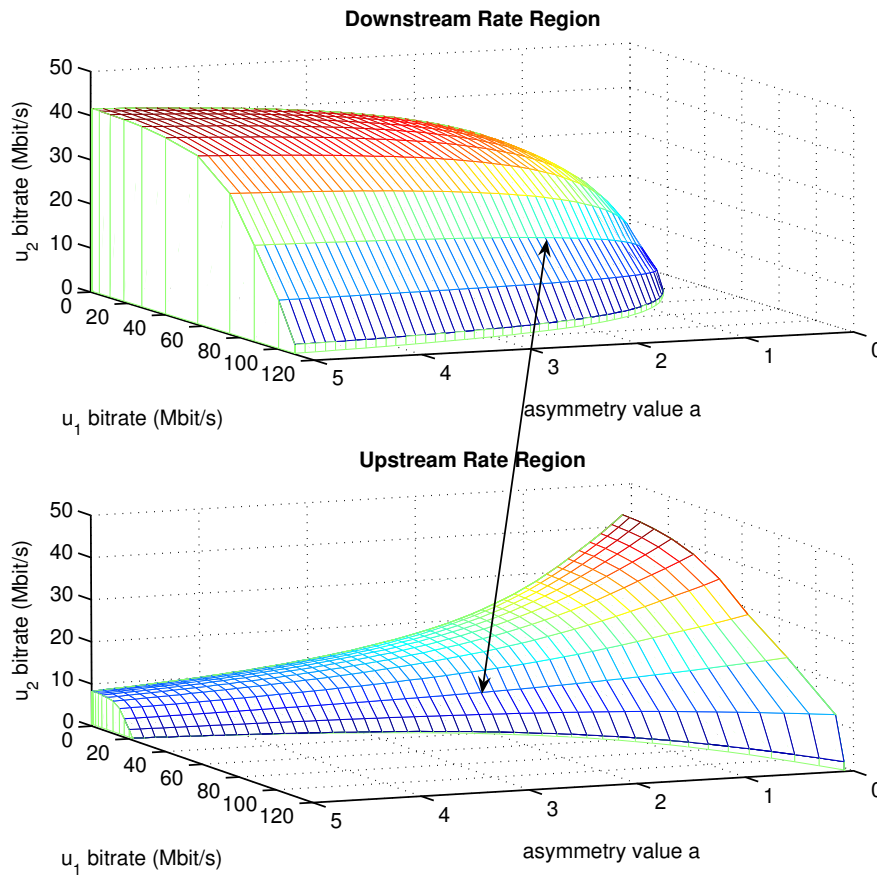


FIGURE 5.19: Downstream and upstream rate regions of the NRA for different asymmetry value a , $\alpha_{1,DS} = \alpha_{1,US}$, and $\alpha_{2,DS} = \alpha_{2,US}$.

As explained in Section 5.2, for the two-user case the downstream and upstream rate regions of the NRIA are five-dimensional and dependent. To better illustrate the space of bitrate combinations that can be supported by the NRIA, Figure 5.19 shows the downstream and upstream rate regions of the NRIA for the asymmetry values $a = [0.1, \dots, 5]$. All simulations were performed for the two-user case network scenario in Figure 5.4 and the simulation parameters as specified in Section 5.3. The plots were generated under the constraints: $\alpha_{1,DS} = \alpha_{1,US}$ and $\alpha_{2,DS} = \alpha_{2,US}$.

Figure 5.19 should be read as follows: For a given asymmetry parameter a we take one curve from downstream rate region and one curve from upstream rate region. For example for $a = 2$ the downstream and upstream curves are plotted again in Figure 5.20 for the sake of clarification. Figure 5.20 then should be read as Figure 5.2 in Section 5.2.

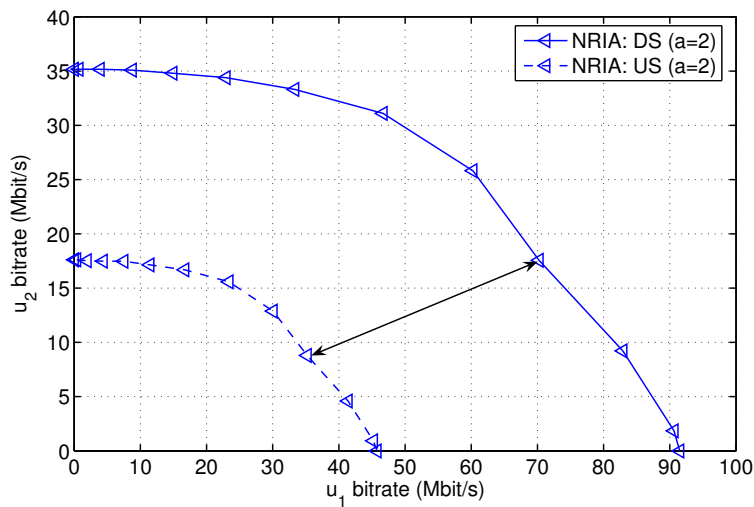


FIGURE 5.20: Downstream and upstream rate regions of the NRIA for different asymmetry value $a = 2$, $\alpha_{1,DS} = \alpha_{1,US}$, and $\alpha_{2,DS} = \alpha_{2,US}$.

From the explanation given above, the NRIA simultaneously supports only those pairs of downstream and upstream bitrate combinations from the rate regions in Figure 5.19 that are generated for $\alpha_{u,DS} = \alpha_{u,US}$ and the same value of a . Figures 5.19 and 5.20 show one example of such pairs of bitrates connected by an arrow.

In practice the NRIA supports a much larger space of bitrate combinations, but unfortunately this cannot easily be illustrated graphically. However, comparing Figures 5.18 and 5.19 gives a good insight about the space of bitrate combinations that can be supported by the NRIA compared to that supported by the IWFA and the OSBA.

5.6 Comparison of the NRIA with the bi-IWFA

The IWFA assumes a fixed band plan, as discussed in Section 5.3, so it performs worse than the NRIA, which searches for an optimized band plan. As a result, Cioffi [24] has suggested to compare the NRIA with the bi-directional IWFA (bi-IWFA). The bi-IWFA does not fix the band plan, but assumes an echo-cancelled transmission scheme and lets the IWFA decide for each loop which subcarriers should be used exclusively for down-

stream or the upstream and which should be used simultaneously for both transmission directions.

Before presenting simulation results comparing the performance of the NRIA with the bi-IWFA, we first analyze the convergence criteria for the IWFA. Based on these criteria we derive the convergence criteria for the bi-IWFA.

5.6.1 Convergence of the IWFA and the bi-IWFA

For two users, $U = 2$, Yu *et al.* in [122] have proved the following: At least one pure Nash equilibrium (see Section 3.2.1) exists if

$$\gamma_1(f)\gamma_2(f) < 1, \text{ for all } f, \quad (5.9)$$

where

$$\begin{aligned} \gamma_1(f) &= \Gamma \frac{\mathcal{H}_{21}(f)}{\mathcal{H}_{22}(f)}, \\ \gamma_2(f) &= \Gamma \frac{\mathcal{H}_{12}(f)}{\mathcal{H}_{11}(f)}, \end{aligned}$$

where Γ denotes the SNR gap; \mathcal{H}_{11} and \mathcal{H}_{22} are the parameters defined in (2.7) and denote the squared magnitude of the direct channel transfer functions of the first and the second users, respectively; likewise, \mathcal{H}_{21} and \mathcal{H}_{12} denote the squared magnitude of the FEXT coupling functions from the first user to the second user and from the second user to the first user, respectively. Furthermore, if any of the conditions $\epsilon_0 < 1$, $\epsilon_1 + \epsilon_2 < 1/2$, or $\epsilon_1 + \epsilon_3 < 1/2$ is satisfied, then the Nash equilibrium is unique and stable. The ϵ_0 , ϵ_1 , and ϵ_2 are defined as: $\epsilon_0 = \sup \{\gamma_1(f)\} \sup \{\gamma_2(f)\}$, $\epsilon_1 = \sup \{\gamma_1(f)\gamma_2(f)\}$, $\epsilon_2 = \sup \{\gamma_1(f)\} (1/F) \int_0^F \gamma_2(f) df$, and $\epsilon_3 = \sup \{\gamma_2(f)\} (1/F) \int_0^F \gamma_1(f) df$; where “sup” denotes the supremum operation; and bandwidth $F = 1/2T$, where T is the sampling rate.

If the conditions for existence and uniqueness of the Nash equilibrium are satisfied, then the IWFA for the two-user Gaussian interference channel converges, and it converges to a unique Nash equilibrium from any starting point [122]. It can be shown that the above criteria are satisfied for the scenario in Figure 5.4, whose transfer and coupling functions are shown in Figure 5.5. From (5.9) it can be concluded that the convergence criteria will not be fulfilled in network scenarios where the direct channel transfer functions have low values and the FEXT coupling functions have high values.

For more than two users, $U > 2$, in [23] (see also [121]) it has been shown that the IWFA converges and has a unique Nash equilibrium if

$$\max \left\{ \Gamma \frac{\mathcal{H}_{uv}(f)}{\mathcal{H}_{uu}(f)} \right\} < \frac{1}{U-1}, \quad \forall f, u, v; \quad u \neq v \text{ for } u, v = 1, \dots, U, \quad (5.10)$$

where $\mathcal{H}_{uu}(f)$ denotes the squared magnitude of the direct channel transfer function of user u and $\mathcal{H}_{uv}(f)$ denotes the squared magnitude of the FEXT coupling function from user v to user u .

In the bi-IWFA, many users may use the same subcarriers (frequencies) simultaneously

for transmitting either in the downstream or the upstream direction. Both criteria (5.9) and (5.10) appears in $\mathcal{H}_{uv}(f)$ and shows the FEXT couplings. However, to calculate the convergence criteria for the bi-IWFA we should also take into account the NEXT coupling functions in addition to the FEXT coupling functions. We can still use (5.10) to verify the convergence criteria of the bi-IWFA by using the model shown in Figure 5.21, where the NEXT coupling is transformed into a “virtual” FEXT coupling. Furthermore, the number of users (loops) is increased to the “virtual” number of users, which is twice the number of users in a network scenario. Thus, for U users the bi-IWFA converges if:

$$\max \left\{ \Gamma \frac{\mathcal{H}_{u\bar{v}}(f)}{\mathcal{H}_{uu}(f)} \right\} < \frac{1}{2U-1}, \quad \forall f, u, \bar{v}; \quad u \neq \bar{v} \quad \text{for} \quad \begin{cases} u = 1, \dots, U, \\ \bar{v} = 1, \dots, 2U, \end{cases} \quad (5.11)$$

where $\mathcal{H}_{u\bar{v}}(f)$ denotes either the squared magnitude of the FEXT or the squared magnitude of the virtual FEXT coupling from Loop \bar{v} to Loop u .

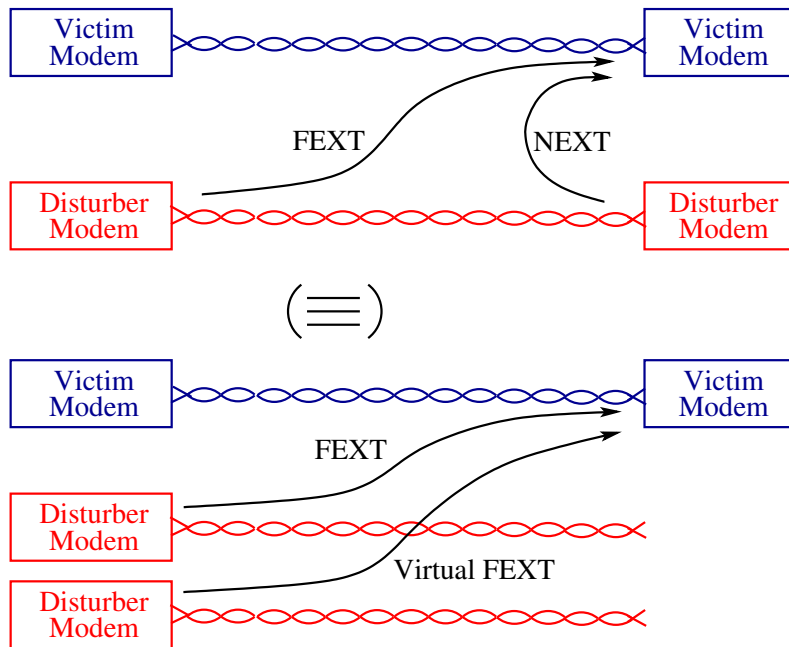


FIGURE 5.21: Virtual FEXT used to model the NEXT by the bi-IWFA.

The criteria (5.9) and (5.10) determine the convergence space of the IWFA, whereas the criterion (5.11) determines the convergence space of the bi-IWFA. However, they are not necessary; thus, if they are not fulfilled this does not imply that the IWFA and the bi-IWFA will not converge. We have found network scenarios that were built based on measured FEXT couplings from the cables of different manufactures where the convergence criterion in (5.9) is not fulfilled. However, the IWFA has always converged and in “most” network scenarios also to a unique solution. In our experience, both the IWFA and the bi-IWFA converge if (5.9), (5.10), and (5.11) are “moderately” violated. If the convergence criteria are “strongly” violated both the IWFA and the bi-IWFA still converge, but the convergence point is not unique. We will show an example in the next section for the bi-IWFA when the converge point is not unique. We have never encountered a network scenario where the IWFA and the bi-IWFA have not converged. To construct network

scenarios we have used not only the NEXT and FEXT models described in Section 2.4.2, but also the measured NEXT and FEXT couplings of different cables. Unfortunately, there are no theoretical results indicating the space where the IWFA and the bi-IWFA do not converge.

Yamashita and Luo in [121] have given a theoretical example, which by simulations show a case where the IWFA has not converged. The simulations in [121] are performed for $\Gamma \frac{\mathcal{H}_{uv}(f)}{\mathcal{H}_{uu}(f)}$ chosen from the interval $[0.99, \dots, 1]$. Such a network scenario can be encountered by the bi-IWFA when the NEXT (in our model in Figure 5.21 the virtual FEXT) couplings have high values and the direct channels have high attenuations. However, in the IWFA this is not realistic, because it uses the FDD transmission scheme and therefore only FEXT couplings are of interest. The FEXT couplings in practice are usually from 10^{-1} to 10^{-6} smaller than the direct channel couplings.

5.6.2 Simulations

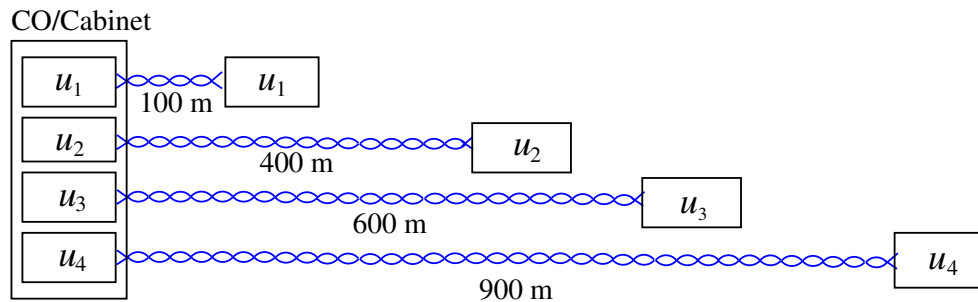


FIGURE 5.22: Network scenario used to compare the NRIA and the bi-IWFA.

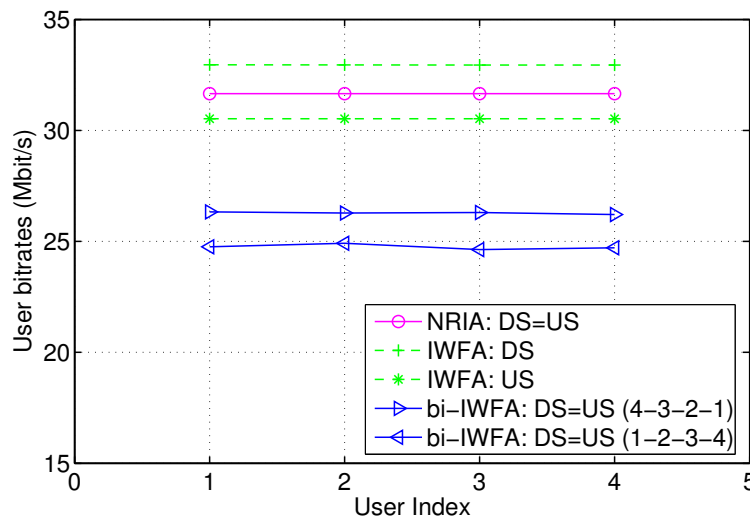


FIGURE 5.23: Users' downstream and upstream supported bitrates for the NRIA and the bi-IWFA for the network scenario shown in Figure 5.22.

The simulation scenario used to compare the performance of the NRIA with the bi-IWFA is shown in Figure 5.22. We have selected a network scenario with four users,

because in a two-user case an echo-cancellation (EC) transmission scheme will usually outperform any another algorithm that assumes FDD transmission. The reason for this is that the gain achieved with EC is higher than the loss from the self-NEXT noise of a single disturber.

For the network scenario in Figure 5.22 the criterion (5.11) is not fulfilled for all loops due to high NEXT couplings. Hence, the bi-IWFA might have not a unique Nash equilibrium. For this scenario, we have recognized that the performance of the bi-IWFA depends on the user ordering during the iterations. Therefore, we have performed simulations with the iteration orderings $u_1-u_2-u_3-u_4$ and $u_4-u_3-u_2-u_1$.

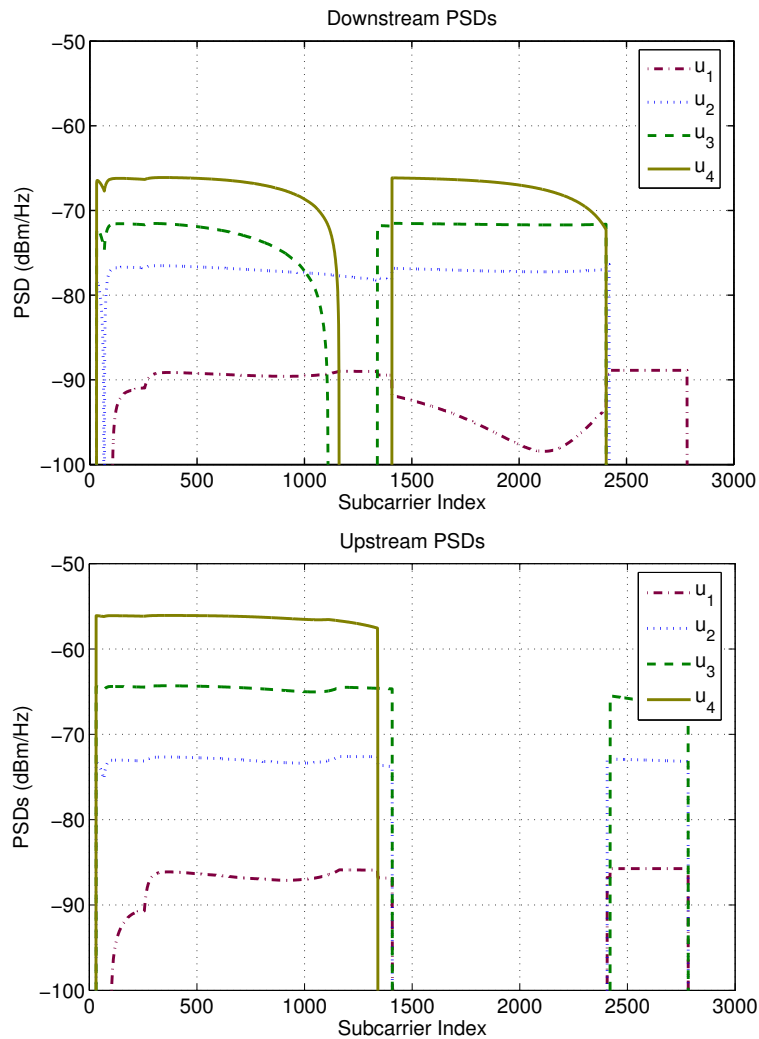


FIGURE 5.24: The downstream and upstream transmit PSDs of the bi-IWFA for users' bitrates shown in Figure 5.23 when the iteration order $u_4-u_3-u_2-u_1$ is selected.

For these simulations we have searched for symmetric and equal bitrates for all users. The simulation results are summarized in Figure 5.23. When the bi-IWFA is deployed bitrates of approximately 26.2 Mbit/s and 24.6 Mbit/s can be supported by each user for the iteration orders $u_4-u_3-u_2-u_1$ and $u_1-u_2-u_3-u_4$, respectively. With the NRIA, a bitrate of more than 31.6 Mbit/s can be achieved by each user in each transmission direction. Thus,

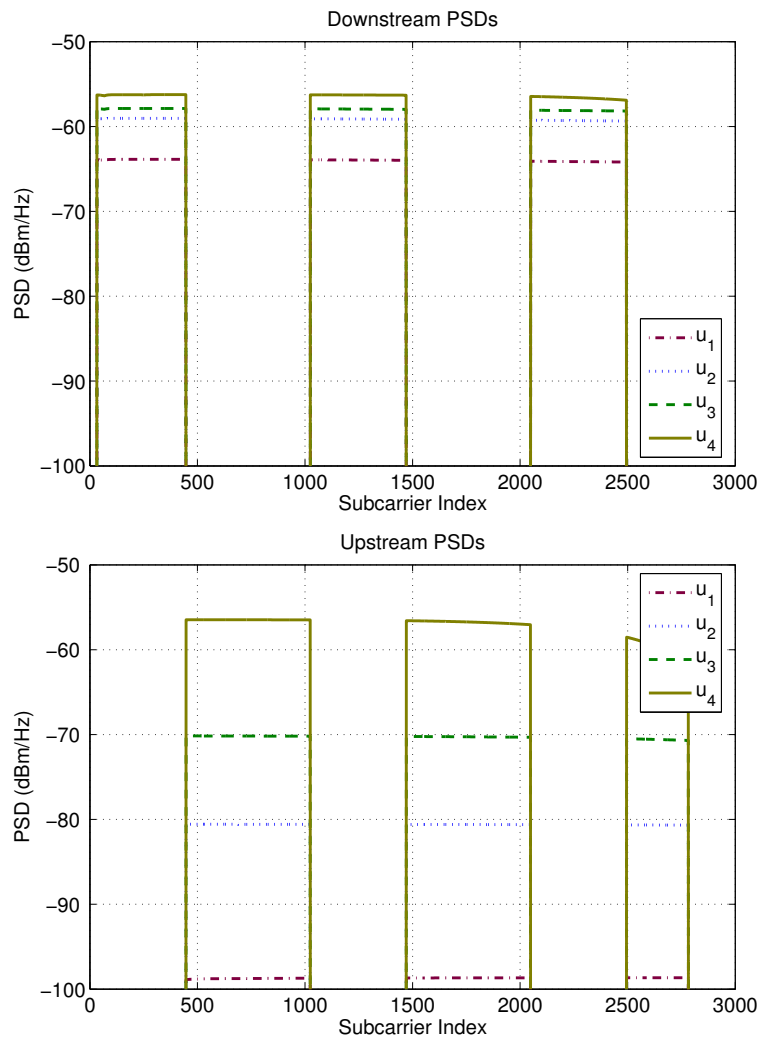


FIGURE 5.25: The downstream and upstream transmit PSDs of the NRIA for users' bitrates values shown in Figure 5.23.

for this case a bitrate increase of more than 20% is achieved with the NRIA for each user compared to the bi-IWFA with the best iteration order $u_4-u_3-u_2-u_1$. This simulation is also performed with the IWFA using the band plan "997", as described in Section 5.3. Figure 5.23 shows that the IWFA performs better than the bi-IWFA for the given scenario. The reason for this can be explained as follows: due to the several NEXT couplings the crosstalk noise is high; however, the noise has not such a high level that the transmitters will decide for FDD transmission when the transmit PSDs of all transmitters are "moderately" low. As Chung and Cioffi [22] have recognized, in these environments the IWFA shows significantly worse performance than the PSDs have high levels.

The downstream and upstream transmit PSDs of the bi-IWFA for the iteration order $u_4-u_3-u_2-u_1$ are shown in Figure 5.24. The transmit PSDs for the iteration order $u_1-u_2-u_3-u_4$ are not included, but were found to have quite different shapes. Figure 5.24 shows that only user u_4 utilizes the maximum total power for the upstream direction. Therefore, u_4 determines the maximum bitrates of all other users. From the PSDs we can recognize three main regions: frequencies lower than approximately 6.2 MHz (subcarrier 1438) are

used simultaneously for both transmission directions; frequencies between 6.2 MHz and 10.4 MHz (subcarrier 2405) are used only for downstream transmission; and frequencies from 10.4 MHz to 12 MHz (subcarrier 2782) are used simultaneously for both transmission directions. Figure 5.25 shows that in contrast to the bi-IWFA, the NRIA allows user u_4 to utilize the maximum total power in both transmission directions.

5.7 Comparison of the NRIA with the UPBO in VDSL

As mentioned in Chapter 3, the power back-off (PBO) is the most sophisticated technique for static spectrum management (SSM) in DSL systems. Thus, in this section we compare the performance of the NRIA with the standardized upstream PBO (UPBO) in VDSL. Furthermore, to be more practical, we analyze the performance of the NRIA with the UPBO for the measured FEXT couplings of a 0.4 mm cable with 50 pairs.

5.7.1 Simulation Environment

Figure 5.26 shows a simulation scenario, in which all users are connected to a CO or to a cabinet. There are fifteen users and a distance of 50 m between two successive users.

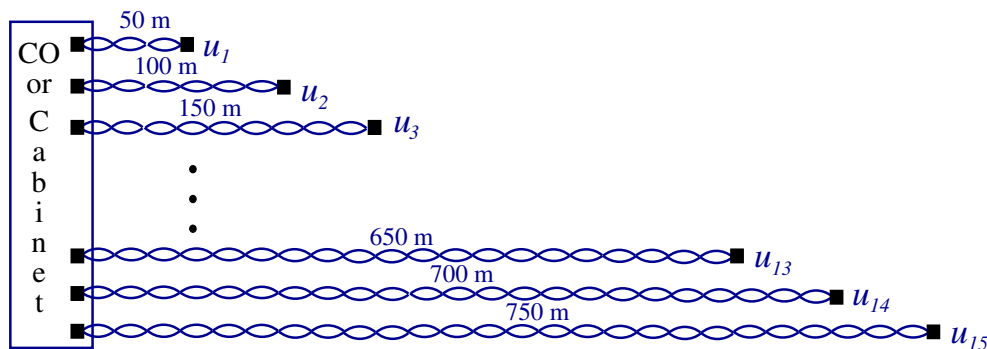


FIGURE 5.26: Simulation Scenario. The maximum loop length is 750 m (for user u_{15}).

The main simulation parameters are as follows. The NRIA does not need a PSD-mask constraint, because the total power constraint alone is sufficient to ensure the spectral compatibility among the users. However, for a fair comparison the maximum PSD-mask constraint is set to -60 dBm/Hz for all simulations. For the UPBO the simulations are performed for the ETSI 99% worst-case FEXT coupling model as specified in Section 2.4.2, which is shown again in Figure 5.27 with the diamond-marked line; and for the measured FEXT couplings of a 0.4 mm cable with 50 pairs (vendor identification: F02YHJA2Y 50x2x0.4). For the NRIA the simulations are performed only for the measured FEXT couplings. Figure 5.27 shows the equal level FEXT (EL-FEXT) couplings of all fifteen twisted pairs used, which are selected randomly from the 50 possible pairs. The definition of the EL-FEXT is given in Section 2.4.2.

The insertion losses per unit length in all twisted pairs in our cable are very similar, as can be seen in Figure 5.28. Therefore, for all simulations we assume that all twisted pairs have equal insertion loss per unit length and we use the model shown in Figure

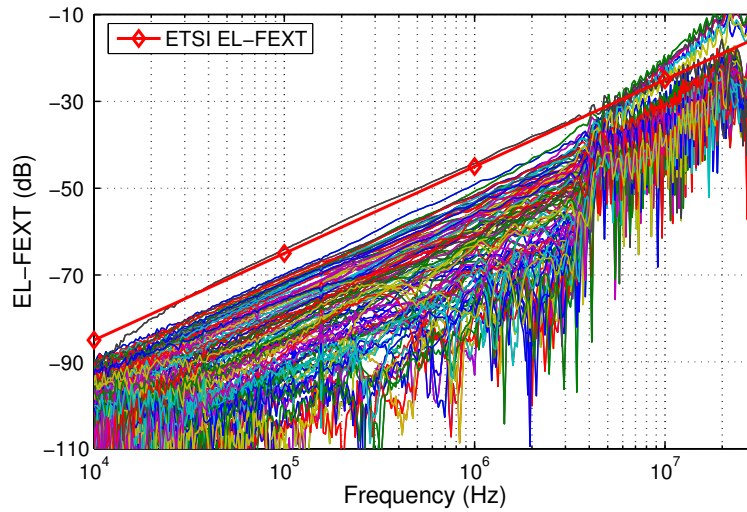


FIGURE 5.27: Measured EL-FEXT values between fifteen pairs in a 0.4 mm cable with 50 pairs.

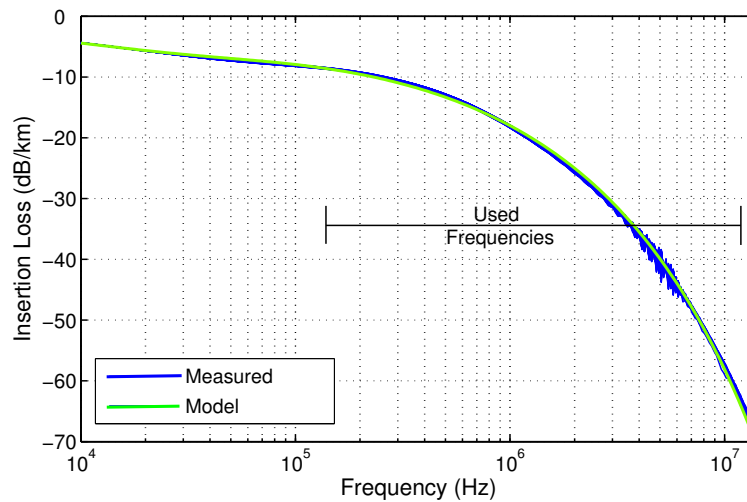


FIGURE 5.28: Measured insertion losses of all 50 pairs and the model used for simulation.

5.28. Furthermore, to take into account for the alien noise at both NT and LT sides, we have added the ETSI VDSL “Noise model A”, which PSDs are shown in Figure 5.3. The parameters for the standardized VDSL UPBO were selected as defined in [40] for this type of noise (see also Section 3.1.3). For UPBO all simulations were performed for the band plan “997” with the subcarrier allocations as specified in (5.1). All other parameters in the NRIA were set as in Section 5.6 when comparing the NRIA with the IWFA.

5.7.2 Simulation Results

Current DMT systems usually work in the margin adaptive mode, that is, they fix the transmit PSDs and allocate the bits over the subcarriers to adapt to the noise environment such that the noise margin is maximized. Another way is to assume a worst-case noise

environment as described in Section 3.1.3. In this case, there is no need to estimate the noise from the other DSL systems, but the supported bitrates will be very pessimistic.

We first show the bitrates supported by each user for the UPBO with the 99% worst-case and the measured FEXT couplings shown in Figure 5.27. Then, we compare the performance of the NRIA with the UPBO for the measured FEXT couplings.

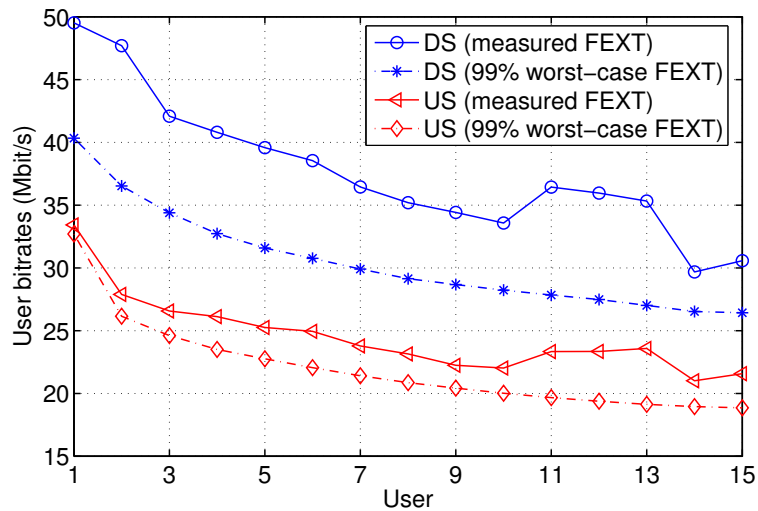


FIGURE 5.29: Supported bitrates for the ETSI UPBO with 99% worst-case and measured FEXT couplings. DS and US denote the downstream and upstream transmission direction, respectively.

Figure 5.29 shows the supported bitrates of all users with the UPBO for the 99% worst-case and measured FEXT couplings. To calculate the self-FEXT noise at the input of each modem for the 99% worst-case FEXT coupling, the FSAN noise calculation method was used, as described in Section 2.4.2. As the FEXT couplings between the different twisted pairs are different, we have not performed pair selection, but have deployed the DSL systems in the twisted pairs randomly. The plots in Figure 5.29 show substantial increase in the supported bitrates when the measured FEXT couplings are used to calculate the noise. The increase in the bitrates is higher in the downstream than in the upstream, because in the downstream direction all VDSL modems transmit with the maximum PSD mask. In the upstream direction the users disturb each other due to the near-far problem, but they transmit with some “optimized” PSDs as calculated by the UPBO algorithm.

There are some interesting points to note from the bitrates shown in Figure 5.29. The received PSDs at the CO or cabinet of all users are the same due to the definition of the standardized UPBO in VDSL as described in Section 3.1.3. Under the 99% worst-case FEXT assumption the users close to the cabinet achieve higher bitrates than those located far away. The reason for this can be explained as follows. For the cable attenuation shown in Figure 5.28 the FEXT noise increases with the loop length. As a result, the users close to the cabinet receive less noise than the users far away due to higher coupling lengths. Thus, the insertion loss alone is not sufficient to determine the level of the transmit PSD masks as is done in the current standardized VDSL UPBO. In the case of the measured FEXT couplings users u_{11} , u_{12} , and u_{13} support higher bitrates than users u_8 , u_9 , and u_{10}

in both transmission directions. This is a result of lower FEXT couplings between the loops on which users u_{11} , u_{12} , and u_{13} are deployed and the loops used by the others. The same also holds true for users u_{14} and u_{15} . This effect further strengthens our conclusion that the insertion loss alone is not sufficient to determine the optimal level of the transmit PSD masks.

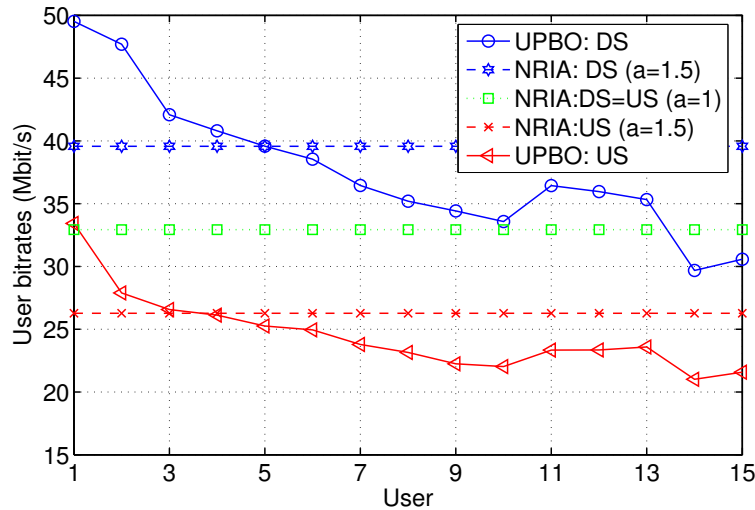


FIGURE 5.30: Comparison of the supported bitrates of the ETSI UPBO in VDSL with the NRIA for $a = 1$ and $a = 1.5$. For all simulations the measured FEXT couplings were used.

As described in Section 3.1.3, the main drawback of using the standardized UPBO is that the transmit PSDs of the users are optimized for the worst-case noise environment, and are not optimal when deployed in an actual network scenario. Furthermore, due to the fixed transmit PSDs, the maximum bitrates that can be offered to users are fixed no matter what their needs. For the scenario in Figure 5.26 only the bitrates shown in Figure 5.29 can be supported. Let us explain with two simple examples what bitrates can be offered to users in practice.

Example 1: Let us assume that we want to offer equal and symmetric bitrates to all users. The bitrates that can be delivered to all users are determined by the smallest supported bitrate, which is that of u_{15} in the upstream direction (approximately 19 Mbit/s when the 99% worst-case FEXT coupling is assumed) or that of u_{14} in the upstream (approximately 21.5 Mbit/s when the measured FEXT couplings are used).

Example 2: Figure 5.29 shows that for the measured FEXT couplings the downstream bitrate of each user is approximately 50% higher than the upstream bitrate. If we want again to offer equal bitrates to all users, but the downstream bitrate of each user should be 50% higher than the upstream bitrate, then approximately 30 Mbit/s and 20 Mbit/s can be offered to each user in the downstream and upstream directions, respectively.

Now, we analyze the performance improvement when the NRIA is deployed in the scenario in Figure 5.26. For all simulations we assume equal user priority values $\alpha_{u,dir}$, thus for a particular transmission direction all users support equal bitrates. The simulations are performed with the asymmetry parameter value $a = 1$ and $a = 1.5$ for a simple compar-

ison with the two examples discussed above. When $a = 1$, approximately 33 Mbit/s can be offered to all users as shown in Figure 5.30. If we compare this value with the bitrates in *Example 1* of 19 Mbit/s and 21.5 Mbit/s, the NRIA increases the supported bitrates by more than 73% and 53%, respectively. When $a = 1.5$ approximately 39 Mbit/s and 26 Mbit/s can be offered to all users in the downstream and upstream directions, respectively. In this case, the NRIA increases the supported bitrates by approximately 30% over the values obtained in *Example 2*.

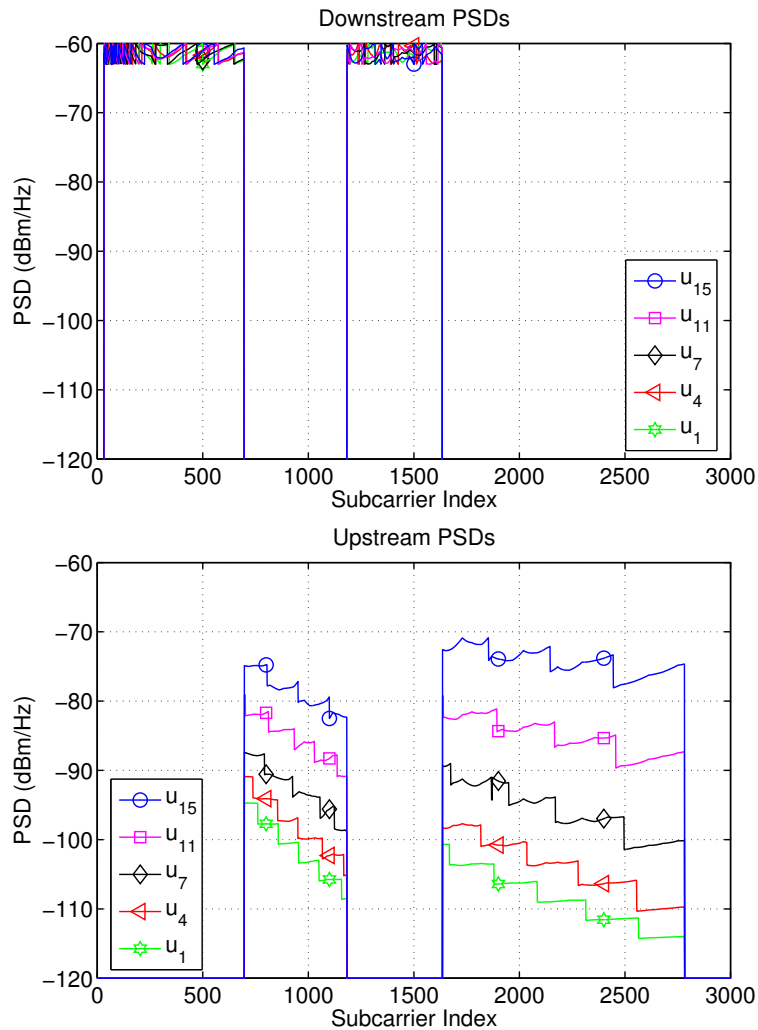


FIGURE 5.31: Downstream and upstream transmit PSD masks of users u_1 , u_4 , u_7 , u_{11} , and u_{15} for static spectra and UPBO.

The corresponding downstream and upstream transmit PSDs for the UPBO and the NRIA when $a = 1.5$ are shown in Figures 5.31 and 5.32. The PSDs are generated for the measured FEXT couplings.

From the PSDs with the UPBO it can be seen that in the downstream direction all users transmit with the maximum transmit PSDs. In the upstream direction, the users allocated close to the cabinet transmit with lower PSDs than the users allocated far away. However,

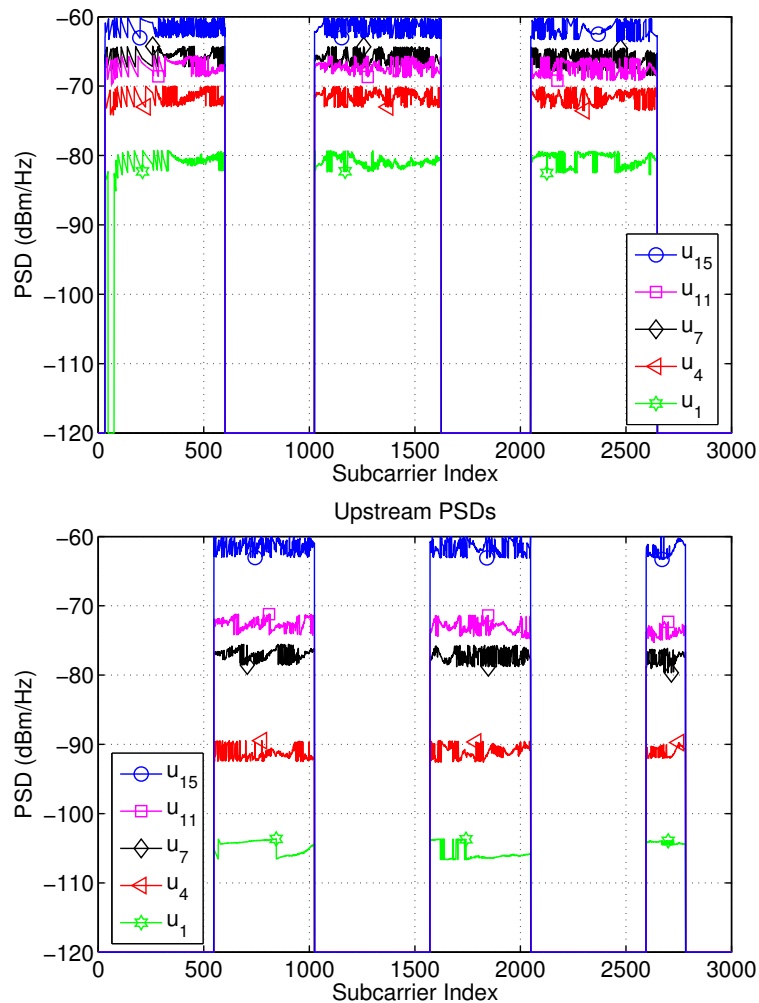


FIGURE 5.32: Downstream and upstream transmit PSD masks of users u_1 , u_4 , u_7 , u_{11} , and u_{15} for the NRIA.

none of the users uses the maximum total power, because the loop attenuation of u_{15} was not so high that the standardized UPBO would allow him to use the maximum transmit PSD.

With the NRIA we have searched in each transmission direction for equal user bitrates. From the NRIA's PSDs it can be seen that u_{15} transmits with the maximum transmit PSD in both transmission directions. In the upstream the users close to the cabinet reduce the transmit PSDs to avoid disturbing the users located far away. In the downstream, however, the regularity in the transmit PSDs does not hold. From the plots, we can see that u_7 transmits with higher PSD than u_{11} , although the loop attenuation of u_{11} is higher than that of u_7 . The reason for this is that u_7 receives more crosstalk noise from the other users than u_{11} . Therefore the high loop attenuation of user u_{11} is compensated by noise with low PSD.

From the simulations shown we conclude that the NRIA significantly improves the performance of all users in distributed networks compared to the standardized static spectra and UPBO.

5.8 Comparison of the NRIA with an Exhaustive Search

As mentioned before the NRIA is the only proposed algorithm that jointly optimizes the band plan (subcarrier allocation) and the power allocation for each user. We mentioned in Section 4.3 that there is no other algorithm that solves such an optimization problem. In this section we compare the performance of the NRIA with an exhaustive search for an “optimal” subcarrier allocation. We still use the inner stage of the NRIA to perform power allocation, because our aim is to show how close we are to the optimum by using our proposed *ad hoc* scheme to search for optimized subcarrier allocations as described in Section 4.4.

The simulation scenario showed in Figure 4.10 (Section 4.6) is used for all simulations, which is also used to analyze the initialization of the input parameters in the NRIA. To make the exhaustive search tractable a certain number of subcarriers are grouped into a subband. Simulations with the exhaustive search were performed for $K = 16$ subbands with an equal number of subcarriers per subband. Thus the inner stage of the NRIA was executed 65536 times. Simulations with the NRIA were performed for $K = 8$, $K = 16$, and 32 subbands.

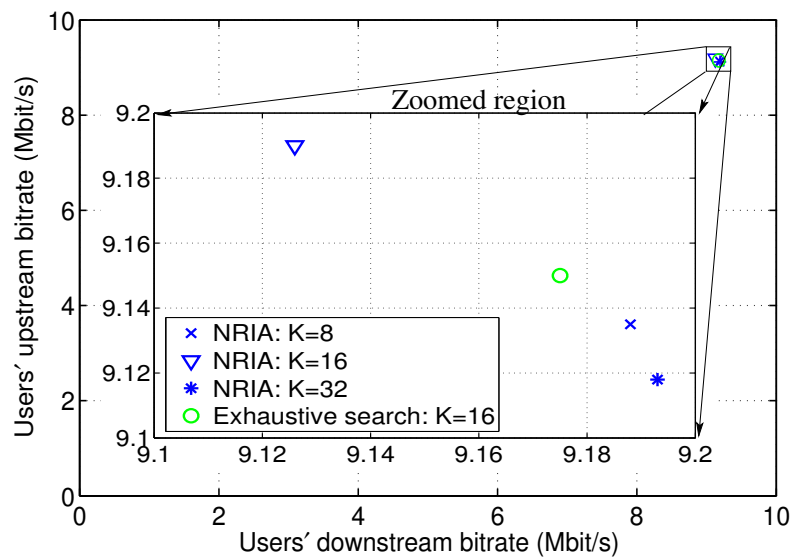


FIGURE 5.33: Comparison of the NRIA with exhaustive search for the optimal subband allocation. With the exhaustive search the simulations were performed with $K = 16$ subbands. With the NRIA the simulations were performed with $K = 8$, $K = 16$, and 32 subbands.

Figure 5.33 shows the supported bitrates of the exhaustive search and the NRIA. The results show that the bitrates supported by the NRIA and the exhaustive search are practically the same. Furthermore in the case of the exhaustive search, not shown here, for many subband allocations (out of 65536) the users achieve similar bitrates. From this we conclude that there are many downstream and upstream subcarrier allocations that show similar performance. This can also be concluded from the bitrates supported by the NRIA for different numbers of subbands in Figure 4.11.

Chapter 6

The Constrained Normalized-Rate Iterative Algorithm

The normalized-rate iterative algorithm (NRIA) presented in Chapter 4 finds, for the pre-defined asymmetry parameter a and the downstream and upstream user priorities $\alpha_{u,DS}$ and $\alpha_{u,US}$, an optimized band plan (common to all users) and a unique power allocation for each user and each transmission direction. We showed by simulation in Chapter 5 that the NRIA achieves better bitrate performance than the iterative water filling algorithm (IWFA) [122], the bi-directional IWFA (bi-IWFA) [24], and the standardized upstream power back-off (UPBO) in VDSL. Furthermore, we also showed by simulation that the NRIA can achieve almost as good performance as the optimal spectrum balancing algorithm (OSBA) [14], but with much lower complexity.

In this chapter we present the constrained normalized-rate iterative algorithm (C-NRIA). The C-NRIA extends the NRIA by ensuring fixed bitrates to some of the users while assigning variable bitrates to the remaining users on a best-effort basis. We call these users ‘fixed-rate users’ and ‘variable-rate users’. However, both types of users are incorporated in the DSM optimization process by the C-NRIA in order to find an efficient FDD band plan and a unique power allocation for each user and each transmission direction.

Network service providers that offer DSL often face a difficult dilemma: how to efficiently balance the cable resources among fixed-rate and variable-rate users in both transmission directions while preserving a number of desirable properties like certain priorities among the users and certain ratios between the downstream and upstream bitrates. Here, we address this high-dimensional non-convex optimization problem and describe how it is possible to solve it efficiently with the C-NRIA. The solution is based on a key observation, which describes in a simple way how the bitrates of all users are related. With this insight we show that it is sufficient to introduce only a *single* balancing parameter for the NRIA to split the capacity appropriately among the fixed-rate and the variable-rate users. The resulting C-NRIA searches for the appropriate value of this balancing parameter in order to find the desired operation point, which grants the fixed-rate users their target bitrates. The C-NRIA solves this optimization problem for sharing the cable resources among the fixed-rate and variable-rate users in a suboptimal way. The suboptimality of the C-NRIA only concerns the subcarrier allocation and power allocations found by the NRIA. The C-NRIA is optimal concerning the sharing of the cable capacity among the fixed-rate and variable-rate users.

This chapter is organized as follows. Section 6.1 derives the mathematical framework required to solve the optimization problem when the bitrates of some users are fixed. Section 6.2 formulates the optimization problem based on the mathematical framework in Section 6.1. Section 6.3 presents the constrained NRIA as a practical method to solve the optimization problem formulated in Section 6.2. Section 6.4 shows some simulation results concerning the constrained NRIA.

6.1 Mathematical Framework

Here, as with the NRIA, we are interested to jointly maximize the bitrates of all users. Now, however, we introduce other additional constraints, which fix the bitrates of some users to some specified values for both transmission directions.

In this section we develop a mathematical framework required to solve the optimization problem when the bitrates of some users are fixed. This framework is based on the problem formulation derived for the NRIA in Chapter 4. We will show that only one additional parameter is sufficient, which we call the balancing parameter and denote by s , to adjust the sharing of the cable resources among the fixed-rate and variable-rate users for both transmission directions. For the sake of simplicity we first develop the solution for a single transmission direction. Later we extend it to both the downstream and upstream transmission directions.

6.1.1 Single Transmission Direction

Assume that there are U^F fixed-rate users and U^V variable-rate users, where $U^F + U^V = U$. Let R_u^F , for $u = 1, \dots, U^F$, and R_u^V , for $u = 1, \dots, U^V$, denote the bitrates of the fixed-rate and variable-rate users, respectively. Furthermore, let T_u^F for $u = 1, \dots, U^F$ and T_u^V for $u = 1, \dots, U^V$, denote the corresponding target bitrates of the fixed-rate and variable-rate users, respectively. We assume that the selected target bitrates assigned to the fixed-rate users can always be supported, *i.e.*, $R_u^F \equiv T_u^F$. In Section 6.3 we show how their maximum values can be determined.

Based on (4.5) and (4.6) the priority values and the bitrates of the fixed-rate and variable-rate users are related (in the selected direction) by

$$\underbrace{\frac{R_1^F}{\alpha_1^F} = \frac{R_2^F}{\alpha_2^F} = \dots = \frac{R_{U^F}^F}{\alpha_{U^F}^F}}_{\text{fixed-rate users}} = \underbrace{\frac{R_1^V}{\alpha_1^V} = \frac{R_2^V}{\alpha_2^V} = \dots = \frac{R_{U^V}^V}{\alpha_{U^V}^V}}_{\text{variable-rate users}}, \quad (6.1)$$

and

$$\sum_{u=1}^{U^F} \alpha_u^F + \sum_{u=1}^{U^V} \alpha_u^V = 1, \quad (6.2)$$

where α_u^F and α_u^V denote the priority values of the fixed-rate and variable-rate users, respectively. Note that the α_u^F values required to achieve the fixed bitrates are unknown in advance. However, by substituting R_u^F with T_u^F in the left-hand side of (6.1) we can easily determine the relations among all of them.

For the right-hand side in (6.1), the variable-rate users, neither R_u^V nor α_u^V are known in advance. But once again we can determine the relations among the α_u^V parameters by using the target bitrates for the variable-rate users, T_u^V . However, note that when the algorithm converges the bitrates assigned to the variable-rate users, R_u^V , can be smaller or larger than those targeted. Nevertheless, the relations in (6.1) still hold. The α_u^F and α_u^V should be selected such that (6.1) and (6.2) are fulfilled.

Example 1: We illustrate the selection of initial values for α_u^F and α_u^V for a network scenario with four users: two fixed-rate and two variable-rate users, thus, $U^F = 2$ and $U^V = 2$. We select $T_1^F = 20$ Mbit/s and $T_2^F = 10$ Mbit/s for the fixed-rate users. Suppose that we aim to offer the bitrates $T_1^V = 5$ Mbit/s and $T_2^V = 10$ Mbit/s to the variable-rate users (which may not be obtained). From these values and (6.1) we have the following independent equations:

$$\frac{\alpha_1^F}{\alpha_2^F} = 2; \quad \frac{\alpha_1^F}{\alpha_1^V} = 4; \quad \text{and} \quad \frac{\alpha_1^F}{\alpha_2^V} = 2. \quad (6.3)$$

From (6.3) and (6.2): $\alpha_1^F = 4/9$, $\alpha_2^F = 2/9$, $\alpha_1^V = 1/9$, and $\alpha_2^V = 2/9$. \square

Jointly increasing (or decreasing) the bitrates of one user group requires jointly decreasing (increasing) the bitrates of the other user group. The same holds also for the user priority values. It is possible to search exhaustively for the priority values for which the fixed-rate users attain their target bitrates and which satisfy the relations defined in (6.1) under the constraint (6.2). However, this involves examining a large number of combinations and it is therefore infeasible in practice. The following theorem is useful for developing a simple method to search for the desired user priority values.

Theorem 1 *Given the bitrate relations (6.1) and constraint (6.2) one parameter is sufficient for properly balancing the bitrates of the fixed-rate and variable-rate users against each other.*

The proof of Theorem 1 is lengthy and is given in Appendix A.4.

The main results of Theorem 1 are as follows. The balance parameter s determines how the priority values among the fixed-rate and variable-rate users should be adjusted. The updated priority values for the fixed-rate users from (A.24) are

$$\check{\alpha}_u^F = \alpha_u^F + \frac{s \cdot \alpha_u^F}{\sum_{u=1}^{U^F} \alpha_u^F}, \quad \text{for } u = 1, \dots, U^F. \quad (6.4)$$

And similarly the updated priority values for the variable-rate users from (A.25) are

$$\check{\alpha}_u^V = \alpha_u^V - \frac{s \cdot \alpha_u^V}{\sum_{u=1}^{U^V} \alpha_u^V}, \quad \text{for } u = 1, \dots, U^V. \quad (6.5)$$

Furthermore, the search space for the balance parameter, s , must be kept within the interval $\left[-\sum_{u=1}^{U^F} \alpha_u^F, \sum_{u=1}^{U^V} \alpha_u^V\right]$. Thus, there exists an s within the given interval for which the fixed-rate users achieve their target bitrates. The two extreme cases are: 1)

$s = -\sum_{u=1}^{U^F} \alpha_u^F$, which assigns the total cable capacity to the variable-rate users and 2) $s = \sum_{u=1}^{U^V} \alpha_u^V$, which assigns the total cable capacity to the fixed-rate users.

The task at hand is therefore to find the appropriate s that gives the desired $\check{\alpha}_u^F$ and $\check{\alpha}_u^V$, satisfies (6.2), and grants the fixed-rate users their target bitrates. One efficient method to obtain this goal goes like this: by using the initial values of α_u^F and α_u^V ($\check{\alpha}_u = \alpha_u$ for $s = 0$) we calculate the supported bitrates of all users, which by definition satisfy (6.1). Thus, we need to check if these resulting supported bitrates of the fixed-rate users are larger, smaller, or equal to the corresponding target bitrates. Note that for the given user priority values the bitrates of all users satisfy (6.1). Therefore, we need only to check for the supported bitrate of a particular fixed-rate user u . One of these three cases occurs:

1. $R_u^F > T_u^F$; search among the negative values of s .
2. $R_u^F < T_u^F$; search among the positive values of s .
3. $R_u^F = T_u^F$; the initial user priority values are the correct ones, which results in $s = 0$.

These cases are illustrated in Figure 6.1.

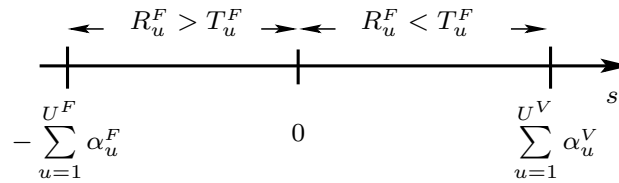


FIGURE 6.1: Illustration of the search space for the balancing parameter s .

Increasing the priority values of the fixed-rate users increases also their bitrates. Equation (6.4) shows that the user priority values of the fixed-rate users are increased by increasing the value of the balancing parameter s . Therefore the bi-section algorithm can be used to search for s when case 1 or case 2 arises. Actually, the bi-section could have been used from the start to search for s . We will take this approach, because we find out after calculating the supported bitrates for the initial user priority values whether the achieved bitrates for the variable-rate users will be higher or lower than the bitrates we aim to offer them. Furthermore, due to the use of the bi-section search there will be at most one more iteration to find the appropriate value of s compared to the case when bi-section had been used from the start.

6.1.2 Downstream and Upstream Transmission Directions

DSL systems offer bi-directional transmission, so the target bitrates of all users must be selected for both transmission directions. Specifically, based on (4.7) for the initialized user priority values and a defined asymmetry parameter a , the downstream and upstream bitrates of the fixed-rate users are related by:

$$R_{u,DS}^F = a \cdot \frac{\alpha_{u,DS}^F}{\alpha_{u,US}^F} \cdot R_{u,US}^F, \quad \text{for } u = 1, 2, \dots, U^F. \quad (6.6)$$

Similarly for the variable fixed-rate users:

$$R_{u,DS}^V = a \cdot \frac{\alpha_{u,DS}^V}{\alpha_{u,US}^V} \cdot R_{u,US}^V, \quad \text{for } u = 1, 2, \dots, U^F. \quad (6.7)$$

That is, the downstream and upstream priority values for each user are related and cannot be selected arbitrarily. For given target bitrates of fixed-rate and variable-rate users based on (6.6) and (6.7) we can define these relations:

$$a \cdot \frac{\alpha_{u,DS}^F}{\alpha_{u,US}^F} = c_u^F \left(= \frac{T_{u,DS}^F}{T_{u,US}^F} \right) \quad \text{for } u = 1, 2, \dots, U^F, \quad (6.8)$$

$$a \cdot \frac{\alpha_{u,DS}^V}{\alpha_{u,US}^V} = c_u^V \left(= \frac{T_{u,DS}^V}{T_{u,US}^V} \right) \quad \text{for } u = 1, 2, \dots, U^V, \quad (6.9)$$

where c_u^F and c_u^V are constants. In addition, (6.2) must be satisfied for both transmission directions.

To achieve the target bitrates for the fixed-rate users, which is the main goal, the relations in (6.1) must hold while searching for the priority values of the fixed-rate and variable-rate users. Note that these relations must hold for both transmission directions. However, in the general case we cannot select new downstream and upstream priority values for the fixed-rate and variable-rate users that simultaneously satisfy the relations defined in (6.1) for both transmission directions as well as the relations in (6.8) and (6.9) for both user groups. There are two possible solutions:

- s1. Keep the NRIA design asymmetry parameter a fixed and search for new user priority values that achieve the target bitrates of the fixed-rate users. In this case, (6.1) is satisfied for both transmission directions and (6.8) for the fixed-rate users, but not (6.9) for the variable-rate users.
- s2. Search for a new asymmetry parameter \check{a} and new user priority values that achieve the target bitrates of the fixed-rate users. In this case, (6.1) is satisfied for both transmission directions, and (6.8) and (6.9) for both fixed-rate and variable-rate users.

We will select the second strategy, s2, calculating a new asymmetry value \check{a} , which preserves the bitrate relations (6.8) and (6.9). Thus, the new constraints are:

$$\check{a} \cdot \frac{\check{\alpha}_{u,DS}^F}{\check{\alpha}_{u,US}^F} = c_u^F \quad \text{for } u = 1, 2, \dots, U^F, \quad (6.10)$$

$$\check{a} \cdot \frac{\check{\alpha}_{u,DS}^V}{\check{\alpha}_{u,US}^V} = c_u^V \quad \text{for } u = 1, 2, \dots, U^V, \quad (6.11)$$

where c_u^F and c_u^V are the constants calculated from (6.8) and (6.9).

Let us assume that we have calculated the new $\check{\alpha}_{u,DS}^F$ and $\check{\alpha}_{u,DS}^V$ as in (6.4) and (6.5).

The new $\check{\alpha}_{u,US}^F$ and $\check{\alpha}_{u,US}^V$ from (6.10) and (6.11) are calculated by

$$\check{\alpha}_{u,US}^F = \check{a} \cdot \frac{\check{\alpha}_{u,DS}^F}{c_u^F} \quad \text{for } u = 1, 2, \dots, U^F, \quad (6.12)$$

$$\check{\alpha}_{u,US}^V = \check{a} \cdot \frac{\check{\alpha}_{u,DS}^V}{c_u^V} \quad \text{for } u = 1, 2, \dots, U^V, \quad (6.13)$$

where \check{a} is unknown.

The parameter \check{a} is calculated as follows. For the upstream transmission direction, based on (6.2) the new upstream priority values must satisfy

$$\sum_{u=1}^{U^F} \check{\alpha}_{u,DS}^F + \sum_{u=1}^{U^V} \check{\alpha}_{u,DS}^V = 1. \quad (6.14)$$

Substituting the upstream priority values of the fixed-rate and variable-rate users in (6.14) and solving for \check{a} results in:

$$\check{a} = \frac{1}{\sum_{u=1}^{U^F} \frac{\check{\alpha}_{u,DS}^F}{c_u^F} + \sum_{u=1}^{U^V} \frac{\check{\alpha}_{u,DS}^V}{c_u^V}}. \quad (6.15)$$

In a similar way we can derive the new asymmetry value \check{a} based on the upstream priority values of the fixed-rate and variable-rate users as in the following. We calculate the new $\check{\alpha}_{u,US}^F$ and $\check{\alpha}_{u,US}^V$ as in (6.4) and (6.5). The new $\check{\alpha}_{u,DS}^F$ and $\check{\alpha}_{u,DS}^V$ from (6.10) and (6.11) are calculated by

$$\check{\alpha}_{u,DS}^F = c_u^F \cdot \frac{\check{\alpha}_{u,US}^F}{\check{a}} \quad \text{for } u = 1, 2, \dots, U^F,$$

$$\check{\alpha}_{u,DS}^V = c_u^V \cdot \frac{\check{\alpha}_{u,US}^V}{\check{a}} \quad \text{for } u = 1, 2, \dots, U^V,$$

Based on (6.2) the new downstream priority values must satisfy

$$\sum_{u=1}^{U^F} \check{\alpha}_{u,US}^F + \sum_{u=1}^{U^V} \check{\alpha}_{u,US}^V = 1. \quad (6.16)$$

Substituting the downstream priority values of the fixed-rate and variable-rate users in (6.16) and solving for \check{a} results in:

$$\check{a} = \sum_{u=1}^{U^F} c_u^F \check{\alpha}_{u,US}^F + \sum_{u=1}^{U^V} c_u^V \check{\alpha}_{u,US}^V.$$

Hereafter, we assume that \check{a} is always calculated based on the downstream priority values as in (6.15).

6.2 Problem Formulation

In this section we formulate the optimization problem for sharing cable resources among fixed-rate and variable-rate users. Without loss of generality we assume that the selected target bitrates of the fixed-rate users can be achieved. We show later in Section 6.3 how we can calculate the maximum bitrates that can be offered to the fixed-rate users. Before we proceed further we derive the formulas for calculation of the bitrates for the fixed-rate and variable-rate users based on the developments in Chapter 4.

The number of bits in a DMT symbol for fixed-rate user u in the upstream transmission direction, based on (4.1) and (4.9), is given by

$$R_{u,US}^F = \sum_{n \in I_{US}} R_u^{F,n} = \sum_{n=0}^{N-1} \beta_{US}^n R_u^{F,n},$$

where $R_u^{F,n}$ denotes the number of bits of fixed-rate user u on subcarrier n ; I_{US} represents the set of upstream subcarrier indices that are used for the upstream transmission direction; and β_{US}^n denotes the subcarrier indicators as defined in (4.8). The number of downstream bits, $R_{u,DS}^F$, is derived correspondingly.

Based on (4.2), the number of bits loaded on subcarrier n by user u , for two-dimensional symbols, is calculated by

$$R_u^{F,n} = \log_2 \left(1 + \frac{\mathcal{H}_{uu}^{F,n} \mathcal{P}_u^{F,n}}{\Gamma \mathcal{N}_u^{F,n}} \right),$$

where Γ is the SNR gap; $\mathcal{H}_{uu}^{F,n}$ is the squared magnitude of the channel transfer function of fixed-rate user u on subcarrier n ; thus,

$$\mathcal{H}_{uu}^{F,n} = |H_{uu}^{F,n}|^2, \quad (6.17)$$

and $\mathcal{N}_u^{F,n}$ is the noise of fixed-rate user u on subcarrier n , which based on (4.3) is calculated by

$$\mathcal{N}_u^{F,n} = \sum_{\substack{v=1 \\ v \neq u}}^{U^F} \mathcal{H}_{uv}^{F,n} \mathcal{P}_v^{F,n} + \sum_{v=1}^{U^V} \mathcal{H}_{uv}^{FV,n} \mathcal{P}_v^{V,n} + \mathcal{P}_V^n,$$

where $\mathcal{P}_v^{F,n}$ and $\mathcal{P}_v^{V,n}$ denote the power spectral densities (PSDs) of the v -th fixed-rate and variable-rate users on subcarrier n , respectively; \mathcal{P}_V^n denotes the PSD of the background noise on subcarrier n ; $\mathcal{H}_{uv}^{F,n}$ denotes the squared magnitude of the channel transfer function from fixed-rate user v to fixed-rate user u on subcarrier n ; and $\mathcal{H}_{uv}^{FV,n}$ denotes the squared magnitude of the channel transfer function from variable-rate user v to fixed-rate user u on subcarrier n . Accordingly the expressions for the variable-rate users are derived.

Assuming the developments in the last section and Section 4.3 the optimization problem for optimally sharing cable resources among all users, when the bitrates of the fixed-rate users are predefined, is given as:

$$\text{maximize } \sum_{u=1}^{U^F} (R_{u,DS}^F + R_{u,US}^F) + \sum_{u=1}^{U^V} (R_{u,DS}^V + R_{u,US}^V), \quad (6.18a)$$

subject to:

$$\sum_{u=1}^{U^F} R_{u,DS}^F + \sum_{u=1}^{U^V} R_{u,DS}^V = \check{\alpha} \left(\sum_{u=1}^{U^F} R_{u,US}^F + \sum_{u=1}^{U^V} R_{u,US}^V \right), \quad (6.18b)$$

$$\frac{R_{1,DS}^F}{\check{\alpha}_{1,DS}^F} = \frac{R_{2,DS}^F}{\check{\alpha}_{2,DS}^F} = \dots = \frac{R_{U^F,DS}^F}{\check{\alpha}_{U^F,DS}^F} = \frac{R_{1,DS}^V}{\check{\alpha}_{1,DS}^V} = \frac{R_{2,DS}^V}{\check{\alpha}_{2,DS}^V} = \dots = \frac{R_{U^V,DS}^V}{\check{\alpha}_{U^V,DS}^V}, \quad (6.18c)$$

$$\frac{R_{1,US}^F}{\check{\alpha}_{1,US}^F} = \frac{R_{2,US}^F}{\check{\alpha}_{2,US}^F} = \dots = \frac{R_{U^F,US}^F}{\check{\alpha}_{U^F,US}^F} = \frac{R_{1,US}^V}{\check{\alpha}_{1,US}^V} = \frac{R_{2,US}^V}{\check{\alpha}_{2,US}^V} = \dots = \frac{R_{U^V,US}^V}{\check{\alpha}_{U^V,US}^V}, \quad (6.18d)$$

$$R_{u,DS}^F = T_{u,DS}^F, \quad u = 1, 2, \dots, U^F, \quad (6.18e)$$

$$R_{u,US}^F = T_{u,US}^F, \quad u = 1, 2, \dots, U^F, \quad (6.18f)$$

$$\sum_{n=0}^{N-1} \beta_{DS}^n \mathcal{P}_{u,DS}^{F,n} \leq \mathcal{P}_{u,DS}^{\max}, \quad u = 1, 2, \dots, U^F, \quad (6.18g)$$

$$\sum_{n=0}^{N-1} \beta_{DS}^n \mathcal{P}_{u,US}^{F,n} \leq \mathcal{P}_{u,US}^{\max}, \quad u = 1, 2, \dots, U^F, \quad (6.18h)$$

$$\sum_{n=0}^{N-1} \beta_{DS}^n \mathcal{P}_{u,DS}^{V,n} \leq \mathcal{P}_{u,DS}^{\max}, \quad u = 1, 2, \dots, U^V, \quad (6.18i)$$

$$\sum_{n=0}^{N-1} \beta_{DS}^n \mathcal{P}_{u,US}^{V,n} \leq \mathcal{P}_{u,US}^{\max}, \quad u = 1, 2, \dots, U^V, \quad (6.18j)$$

$$\beta_{DS}^n = 1 - \beta_{US}^n, \quad n = 0, 1, \dots, N-1, \quad (6.18k)$$

$$\sum_{u=1}^{U^F} \check{\alpha}_{u,US}^F + \sum_{u=1}^{U^V} \check{\alpha}_{u,US}^V = 1, \quad (6.18l)$$

$$\check{\alpha} = \frac{1}{\sum_{u=1}^{U^F} \frac{\check{\alpha}_{u,DS}^F}{c_u^F} + \sum_{u=1}^{U^V} \frac{\check{\alpha}_{u,DS}^V}{c_u^V}}, \quad (6.18m)$$

$$\check{\alpha}_{u,US}^F = \check{\alpha} \cdot \frac{\check{\alpha}_{u,DS}^F}{c_u^F} \quad \text{for } u = 1, 2, \dots, U^F, \quad (6.18n)$$

$$\check{\alpha}_{u,US}^V = \check{\alpha} \cdot \frac{\check{\alpha}_{u,DS}^V}{c_u^V} \quad \text{for } u = 1, 2, \dots, U^V, \quad (6.18o)$$

$$\beta_{DS}^n, \beta_{US}^n \in \{0, 1\}, \quad (6.18p)$$

$$\mathcal{P}_{u,DS}^n, \mathcal{P}_{u,US}^n \in [0, \mathbb{R}^+], \quad (6.18q)$$

$$0 \leq \check{\alpha}_{u,DS}^F \leq 1, \quad u = 1, 2, \dots, U^F, \quad (6.18r)$$

$$0 \leq \check{\alpha}_{u,DS}^V \leq 1, \quad u = 1, 2, \dots, U^V. \quad (6.18s)$$

In (6.18), c_u^F , c_u^V , $T_{u,DS}^F$, $T_{u,DS}^V$, $T_{u,US}^F$, and $T_{u,US}^V$ are constants and the designer's choice. Note that we have assumed that the selected target bitrates of the fixed-rate users can be supported. Here, as in Section 4.3, without loss of generality we do not consider the silent (unused) subcarriers.

To solve the optimization problem (6.18) we need to find:

- Two vectors for each user (fixed-rate and variable-rate), specifying the power allocation for downstream and upstream transmission directions: $\mathcal{P}_{u,DS} = [\mathcal{P}_{u,DS}^0, \mathcal{P}_{u,DS}^1, \dots, \mathcal{P}_{u,DS}^{N-1}]$, and $\mathcal{P}_{u,US} = [\mathcal{P}_{u,US}^0, \mathcal{P}_{u,US}^1, \dots, \mathcal{P}_{u,US}^{N-1}]$, respectively.
- One vector $\beta_{US} = [\beta_{US}^0, \beta_{US}^1, \dots, \beta_{US}^{N-1}]$, specifying the subcarrier allocation for the upstream direction. The subcarrier allocation for the downstream is calculated from (6.18k).
- The downstream priority values $\check{\alpha}_{1,DS}^F, \check{\alpha}_{2,DS}^F, \dots, \check{\alpha}_{U^F,DS}^F$ of the fixed-rate users for which the fixed-rate users achieve the desired target bitrates. The downstream priority values of the variable-rate users are selected such that (6.18l) and the right side of (6.1) are satisfied. The desired upstream priority values of the fixed-rate and variable-rate users are calculated by (6.18n) and (6.18o), respectively. The desired asymmetry parameter \check{a} is calculated by (6.18m).

The optimization problem (6.18) is not solvable with existing algorithms for the same reasons mentioned for the optimization problem (4.10) in Section 4.3. Everything we have concluded about the optimization problem (4.10) is also valid here and will not be repeated. In the next section we propose an algorithm to solve the optimization problem (6.18).

6.3 The Constrained Normalized-Rate Iterative Algorithm

The constrained normalized-rate iterative algorithm (C-NRIA) is based on the NRIA and is suboptimal. The suboptimality of the C-NRIA only concerns the power allocations and band plan (subcarrier allocation) found by the NRIA. The constrained NRIA is optimal concerning the sharing of the cable capacity among the fixed-rate and variable-rate users.

Based on the framework in the previous section the C-NRIA can now be introduced in a straightforward manner. First, before running the C-NRIA, it is necessary to find out if the selected downstream and upstream bitrates can be offered to the fixed-rate users. This can be checked by running the basic NRIA with only the fixed-rate users included in the optimization process with the asymmetry parameter and user priority values calculated according to *Example 2* given below. In this way, we can determine the maximum bitrates that can be offered to the fixed-rate users. Thus, if the desired bitrates for the fixed-rate users are smaller than the maximum bitrates found, the remaining cable resources will be utilized by the variable-rate users.

The pseudo-code of the C-NRIA is listed as Algorithm 2. The algorithm operates as follows. For the selected target bitrates of all users (fixed-rate and variable-rate), the C-NRIA calculates the corresponding asymmetry parameter as well as all the downstream and upstream priority values of both fixed-rate and variable-rate users, by using (6.18b) and (6.1). *Example 2* below demonstrates this calculation.

Algorithm 2: The constrained NRIA**Initialize:** T_{DS}^F, T_{US}^F {Mandated bitrates for the fixed-rate users} T_{DS}^V, T_{US}^V {Desired bitrates for the variable-rate users}From: T_{DS}^F, T_{US}^F and T_{DS}^V, T_{US}^V calculate: $\alpha_{DS}^F, \alpha_{DS}^V, \alpha_{US}^F, \alpha_{US}^V$; using (6.1) and (6.2)

$$s_{\min} = - \sum_{u=1}^{U^F} \alpha_u^F; \quad s_{\max} = \sum_{u=1}^{U^V} \alpha_u^V$$

 $s = 0$ **repeat**For s calculate: $\check{a}, \check{\alpha}_{DS}^F, \check{\alpha}_{DS}^V, \check{\alpha}_{US}^F, \check{\alpha}_{US}^V$; using (6.4), (6.5), (6.10), (6.11), and (6.15)

$$[R_{DS}^F, R_{US}^F, R_{DS}^V, R_{US}^V] = \mathbf{NRIA}(\check{a}, \check{\alpha}_{DS}^F, \check{\alpha}_{DS}^V, \check{\alpha}_{US}^F, \check{\alpha}_{US}^V)$$

if $R_{1,DS}^F > T_{1,DS}^F$ **then**

$$s_{\max} = s$$

else

$$s_{\min} = s$$

end if

$$s = \frac{s_{\min} + s_{\max}}{2}$$

until R_{DS}^F, R_{US}^F approach T_{DS}^F, T_{US}^F with some desired accuracy.

With these initial priority and asymmetry values, the basic NRIA is then executed. In Algorithm 2 this corresponds to the first loop for which $s = 0$, cf. (6.4) and (6.5). Depending on the bitrates supported for the fixed-rate users, one of the three cases occurs as described in Section 6.1.1 (see also Fig. 6.1). Then, we use the bi-section method to search for the appropriate value of s , until the target bitrates of the fixed-rate users are achieved with some predefined accuracy.

Example 2: To illustrate how to calculate the maximum bitrates that can be offered to the fixed-rate users we first show how to calculate \check{a} , $\check{\alpha}_u^F$, and $\check{\alpha}_u^V$ which satisfy the relations in (6.6) for both user groups.

In this example four users are assumed—two fixed-rate users and two variable-rate users. Furthermore, we select the following target bitrates for the fixed-rate users $T_{1,DS}^F = 33$ Mbit/s, $T_{2,DS}^F = 40$ Mbit/s, $T_{1,US}^F = 38$ Mbit/s, and $T_{2,US}^F = 47$ Mbit/s. We also aim to offer the variable-rate users the following bitrates: $T_{1,DS}^V = 15$ Mbit/s, $T_{2,DS}^V = 12$ Mbit/s, $T_{1,US}^V = 10$ Mbit/s, and $T_{2,US}^V = 5$ Mbit/s. The target bitrates assigned to the variable-rate users will not be guaranteed. However, the initial relations on the left-hand side of (6.6) for the selected target bitrates will always be satisfied.

The asymmetry parameter is calculated as in (4.4); thus, $a = 1$. The downstream and upstream priority values of the fixed-rate and the variable-rate users are calculated as in *Example 1* in Section 6.1.1. Table 6.1 summarizes the corresponding downstream and upstream priority values for the selected bitrates.

As explained in Section 6.1.1, we select $s = \alpha_{1,DS}^V + \alpha_{2,DS}^V = 0.27$ when we assign the

TABLE 6.1: The calculated downstream and upstream priority values for the selected target bitrates in *Example 1*.

User u	Fixed-rate user bitrates (Mbit/s)		Variable-rate user bitrates (Mbit/s)		Fixed-rate user priorities		Variable-rate user priorities	
	$T_{u,DS}^F$	$T_{u,US}^F$	$T_{u,DS}^V$	$T_{u,US}^V$	$\alpha_{u,DS}^F$	$\alpha_{u,US}^F$	$\alpha_{u,DS}^V$	$\alpha_{u,US}^V$
1	33	38	15	10	0.33	0.38	0.15	0.10
2	40	47	12	05	0.40	0.47	0.12	0.05
Σ	73	85	27	15	0.73	0.85	0.27	0.15

total cable resources to the fixed-rate users (*i.e.*, one of the extreme cases). Substituting $s = 0.27$ into (6.4) and (6.5) we get: $\check{\alpha}_{1,DS}^F = 0.45$, $\check{\alpha}_{2,DS}^F = 0.55$, $\check{\alpha}_{1,DS}^V = 0$, and $\check{\alpha}_{2,DS}^V = 0$.

For $a = 1$ and the α_u^F and α_u^V values according to Table 6.1, we get the constants c_u^F and c_u^V by using (6.8) and (6.9); thus, $c_1^F = 0.87$, $c_2^F = 0.85$, $c_1^V = 1.50$, and $c_2^V = 2.40$. Substituting these parameters c_u^F and c_u^V as well as $\check{\alpha}_{u,DS}^F$ and $\check{\alpha}_{u,DS}^V$ into (6.15) gives $\check{a} = 0.86$. Using (6.12) and (6.13) we get: $\check{\alpha}_{1,US}^F = 0.44$, $\check{\alpha}_{2,US}^F = 0.56$, $\check{\alpha}_{1,US}^V = 0$, and $\check{\alpha}_{2,US}^V = 0$. For these calculated values of \check{a} , $\check{\alpha}_{DS}^F$, and $\check{\alpha}_{US}^F$ we run the NRIA and find the maximum bitrates that can be supported in downstream and upstream for the fixed-rate users. \square

The complexity of the constrained NRIA can be reduced by fixing the band plan within the NRIA in different ways: fixing it to the band plan found when we calculate the maximum bitrates that can be offered to the fixed-rate users; fixing it after the first loop in Algorithm 2 is finished; or fixing it after the target bitrates of the fixed-rate users are satisfied with some predefined accuracy. Note that when the band plan is fixed we no longer need the asymmetry parameter \check{a} , which is used by the NRIA to determine how to share the band plan between the downstream and upstream transmission directions. This implies that the bitrates that are supportable for the variable-rate users satisfy (6.18c) and (6.18d) independently for both transmission directions, but not the defined downstream and upstream bitrate relations in (6.9). All these modifications in the constrained NRIA can be implemented in a straightforward way, so they will not be discussed further.

6.4 Simulation Results

In this section we give some simulation results concerning the C-NRIA. For all simulations we use the network scenario shown in Figure 6.2, with two fixed-rate users and two variables-rate users. The fixed-rate users are placed at 300 m and 900 m from the central office (CO) or cabinet. The variable-rate users are placed at 600 m and 1200 m apparat from the CO or cabinet.

The main simulation parameters are the same as those used in Section 4.6 where the initialization of the input parameters in the NRIA are analyzed. Thus, the maximum total power for each user and each transmission direction is set to 11.5 dBm. The center frequency separation between two successive subcarriers is 4.3125 kHz and the DMT symbol rate is 4 kHz, as specified in the VDSL DMT standards [4, 40, 41]. Furthermore, we assume a DMT system with $N = 2048$ subcarriers and we perform all simulations

with $K = 8$ subbands. To achieve a bit error rate of 10^{-7} we have assumed an SNR gap of $\Gamma = 12.3$ dB. The cable model used is the so-called “BT_dwug” [114], which has 0.5 mm conductors. The FEXT model used is the same as specified in Section 2.4.2 with $K_{\text{FEXT}} = -45$ dB at 1 MHz. The background noise is set to a flat level of -140 dBm/Hz.

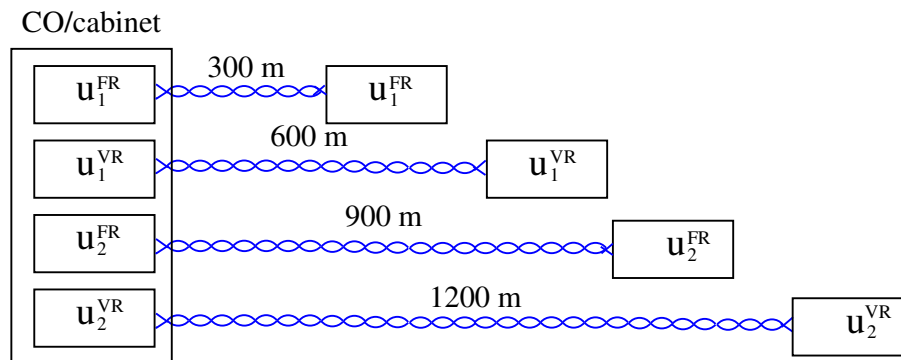


FIGURE 6.2: A network scenario with four users: two fixed-rate users and two variable-rate users.

Example 3: Assume that we have selected the bitrates given in Table 6.1 as the target bitrates for the fixed-rate users and as the desired bitrates for the variable-rate users. Thus, the same priority values given in Table 6.1 are assigned to all users and the asymmetry parameter is $a = 1$.

First, we should verify that the selected target bitrates for the fixed-rate users can be offered at all. As explained in Section 6.3, we verify this by running the basic NRIA with only the fixed-rate users included in the optimization process. Because we have used the bitrates and priority values in Table 6.1 we run the NRIA with the following values: $\check{a} = 0.86$, $\check{\alpha}_{1,\text{DS}}^{\text{F}} = 0.45$, $\check{\alpha}_{2,\text{DS}}^{\text{F}} = 0.55$, $\check{\alpha}_{1,\text{US}}^{\text{F}} = 0.44$, $\check{\alpha}_{2,\text{US}}^{\text{F}} = 0.56$, which have been calculated in *Example 2*. The NRIA finds that the maximum bitrates that can be supported for the fixed-rate users are $R_{1,\text{DS}}^{\text{F,max}} = 36.49$ Mbit/s, $R_{2,\text{DS}}^{\text{F,max}} = 44.06$ Mbit/s, $R_{1,\text{US}}^{\text{F,max}} = 41.77$ Mbit/s, and $R_{2,\text{US}}^{\text{F,max}} = 51.47$ Mbit/s. Thus, the selected target bitrates can be offered to the fixed-rate users.

TABLE 6.2: The supported bitrates and the calculated priority values for all users for the scenario in Figure 6.2 for $T_{1,\text{DS}}^{\text{F}} = 33$ Mbit/s .

User u	Fixed-rate user bitrates (Mbit/s)		Variable-rate user bitrates (Mbit/s)		Fixed-rate user priorities		Variable-rate user priorities	
	$R_{u,\text{DS}}^{\text{F}}$	$R_{u,\text{US}}^{\text{F}}$	$R_{u,\text{DS}}^{\text{V}}$	$R_{u,\text{US}}^{\text{V}}$	$\check{\alpha}_{u,\text{DS}}^{\text{F}}$	$\check{\alpha}_{u,\text{US}}^{\text{F}}$	$\check{\alpha}_{u,\text{DS}}^{\text{V}}$	$\check{\alpha}_{u,\text{US}}^{\text{V}}$
1	32.99	38.06	26.52	17.71	0.27	0.34	0.22	0.16
2	39.98	47.07	21.22	8.85	0.33	0.42	0.18	0.08
Σ	72.97	85.13	44.23	30.07	0.60	0.76	0.40	0.24

We then run the C-NRIA with the target bitrates from *Example 2*. The supported bitrates and the calculated priority values for all users are summarized in Table 6.2. By comparing the results in Table 6.2 and Table 6.1 we conclude that we can guarantee the

fixed-rate users the selected target bitrates and increase the bitrates of the variable-rate users by approximately 77% compared to the bitrates we first aimed to offer them. \square

Example 4: We now change the downstream target bitrate of the first fixed-rate user to $T_{1,DS}^F = 36$ Mbit/s. For this example we initialize the priority values for all users again to the values shown in Table 6.1. Thus, the new target bitrates of the other fixed-rate users are $T_{2,DS}^F = 43.63$ Mbit/s, $T_{1,US}^F = 41.45$ Mbit/s, and $T_{2,US}^F = 51.27$ Mbit/s. The supported bitrates and the calculated priority values for all users are summarized in Table 6.3. We conclude that to guarantee the fixed-rate users the selected target bitrates we should reduce the bitrates of the variable-rate users by approximately 33% compared to the bitrates we had aimed to offer them. \square

TABLE 6.3: The supported bitrates and the calculated priority values for all users for the scenario in Figure 6.2 for $T_{1,DS}^F = 36$ Mbit/s.

User u	Fixed-rate user bitrates (Mbit/s)		Variable-rate user bitrates (Mbit/s)		Fixed-rate user priorities		Variable-rate user priorities	
	$R_{u,DS}^F$	$R_{u,US}^F$	$R_{u,DS}^V$	$R_{u,US}^V$	$\check{\alpha}_{u,DS}^F$	$\check{\alpha}_{u,US}^F$	$\check{\alpha}_{u,DS}^V$	$\check{\alpha}_{u,US}^V$
1	36.00	41.54	10.08	6.73	0.37	0.40	0.10	0.07
2	43.63	51.34	8.06	3.36	0.45	0.50	0.08	0.03
Σ	79.63	92.88	18.14	10.09	0.82	0.90	0.18	0.10

Example 5: For this example we assign equal initial priority values to all users for both transmission directions. Thus, $\alpha_{1,DS}^F = \alpha_{2,DS}^F = \alpha_{1,DS}^V = \alpha_{2,DS}^V = \alpha_{1,US}^F = \alpha_{2,US}^F = \alpha_{1,US}^V = \alpha_{2,US}^V = 0.25$. We also select for this example the asymmetry parameter $a = 1$. Due to such a specific assignment of user priority values and the asymmetry parameter we are searching for symmetric bitrates for all users. Thus, no matter what bitrates are supported for the fixed-rate and variable-rate users the asymmetry parameter will be always 1. Furthermore, the downstream priority values of the fixed-rate users will be equal to their upstream priority values and the downstream priority values of the variable-rate users will be equal to their upstream priority values. The same also holds for the bitrates of the fixed-rate and variable-rate users.

We performed simulations for values of the balancing parameter s from -0.5 to 0.5 with a step size 0.02 . The supported bitrates of the fixed-rate and variable-rate users are shown in Figure 6.3. Based on the explanation in Section 6.1.1, two extreme cases arise when either $s = -0.5$ or $s = 0.5$. As can be seen in Figure 6.3, for $s = -0.5$ the total cable capacity is assigned to the variable-rate users, whereas for $s = 0.5$ the total cable capacity is assigned to the fixed-rate users. For any value of the balancing parameter s between -0.5 and 0.5 the cable capacity is shared between both users groups depending on the value of s . It can be seen from the plots that the bitrates of the fixed-rate users can be increased from 0 to 25 Mbit/s and this degrades the performance of the variable-rate users only slightly; or similarly the bitrates of the variable-rate users can be increased from 0 to 20 Mbit/s with only slight performance degradation of the fixed-rate users. Such an analysis allows us to determine how to select the bitrates of the fixed-rate users in practice without significantly degrading the performance of the variable-rate users or vice versa.

We analyze now the optimal downstream and upstream subcarrier allocations for the

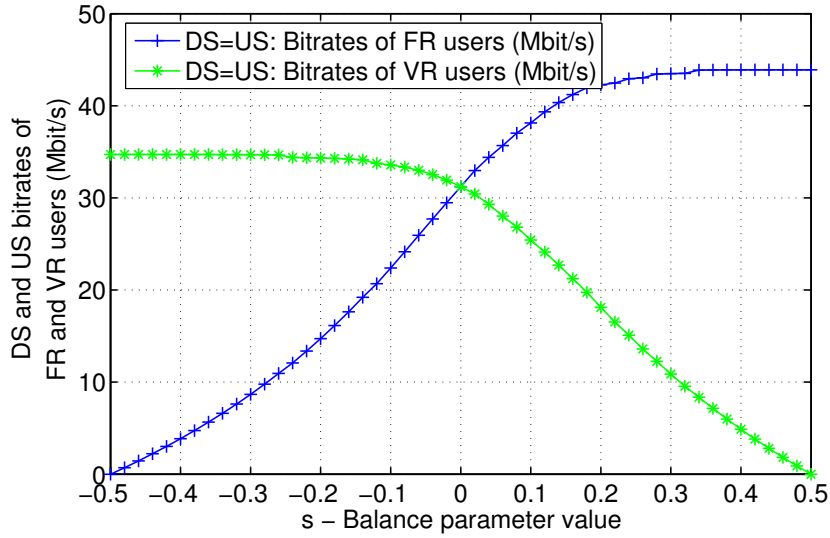


FIGURE 6.3: Downstream (DS) and upstream (US) bitrates of the fixed-rate (FR) and variable-rate (VR) users for different balancing parameter s values.

bitrates shown in Figure 6.3. As explained in the introduction to this section all simulations were performed for $K = 8$ subbands and $N = 2048$ subcarriers. For the reasons explained in Section 4.4.1.2 we started first with the downstream subband at the low frequency range. Furthermore, we have used for all simulations the binary search for the new subcarrier allocation shown in Figure 4.6. Thus, the downstream subcarrier allocation depends on the initialized subcarrier allocation and a value of the shifting parameter θ that determines how the initialized subband edges are shifted compared to the initial values:

$$I_{\text{DS}} = \{1, \dots, 255 - \theta, 512, \dots, 767 - \theta, \\ 1024, \dots, 1279 - \theta, 1536, \dots, 1791 - \theta\},$$

with $0 \leq \theta \leq 255$. The subcarriers not assigned to the downstream transmission direction are assigned to the upstream transmission direction, because we have not assume any silent subcarrier.

TABLE 6.4: The values of shifting parameter θ versus the balancing parameter s for the network scenario in Figure 6.2 and the bitrates shown in Figure 6.3.

s	-0.5	-0.4	-0.3	-0.2	-0.1	0	0.1	0.2	0.3	0.4	0.5
θ	37	37	37	39	41	41	37	29	25	23	21

For the bitrates shown in Figure 6.3 the values of shifting parameter θ and the corresponding values of balancing parameter s are shown in Table 6.4. Results in Table 6.4 show that in general for different balancing parameter values we have different optimal subcarrier allocations. \square

Chapter 7

Conclusions

This thesis has investigated techniques for assigning cable resources to multi-user DSL systems in an adaptive way. The art of assigning cable resources to mitigate the crosstalk noise among the users is known as dynamic spectrum management (DSM). The main goal of this thesis was to develop low-complexity DSM algorithms for multi-user DSL systems that use discrete multi-tone (DMT) modulation based and digital frequency division duplexing (D-FDD), also known as Zipper duplexing. The algorithms developed treat the crosstalk as noise to facilitate their deployment in current DMT systems.

Previously proposed DSM algorithms for FDD systems consider only user power allocations for a fixed frequency band plan. A fixed band plan in DMT systems results in a fixed subcarrier allocation assigned to the downstream and upstream transmission directions. Fixing the band plan also constrains the ratios between the downstream and upstream bitrates that can be offered to users. DSM should, however, use as many degrees of freedom as possible to better utilize the cable resources. A *dynamic spectrum* (dynamic band plan assignment) often helps to utilize the cable capacity more efficiently, because the cable capacity is assigned adaptively to the downstream and upstream directions based on the needs of users and the characteristics of the cable.

In general the optimization problems for finding the optimal band plan and optimal power allocations are very difficult. This is because such optimization problems are high-dimensional and involve both discrete and continuous variables. For a multi-user DSL system, when the aim is to mitigate the crosstalk, the optimal solution cannot be found with existing algorithms. This is due to the non-convexity of the optimization problem in its continuous variables.

We have developed a novel centralized DSM algorithm¹: the normalized-rate iterative algorithm (NRIA). The NRIA is the only algorithm that *jointly* optimizes the band plan (common to all users) for D-FDD systems and power allocations for all users. The NRIA finds an optimized band plan and *unique* power allocation for each user to jointly maximize the bitrates of all users.

The multi-user optimization problem solved by the NRIA is based on a novel problem formulation that has a strong practical advantage. It is based on two types of parameters which bridge the gap between the operators' DSL business models and DSM: the desired user priorities and the desired network asymmetry. The NRIA offers high performance in combination with low computational complexity, since it is designed to be practically implementable rather than obtaining the highest theoretical performance.

An inner iteration stage of the NRIA is based on the iterative water-filling algorithm

¹The centralized DSM algorithms are commonly referred to as DSM Level 2.

(IWFA) for finding efficient power allocations for all users. However, the NRIA extends the IWFA by automatically finding which user bitrates are achievable. This is accomplished by taking advantage of the centralized operation of the NRIA, which enables user cooperation. Furthermore, an outer iteration stage uses a simple but effective search strategy for finding an effective band plan. All these practical advantages combined make the NRIA attractive even for networks with many DSL users.

Simulations have shown that the NRIA achieves better bitrate performance than the IWFA, the bi-directional IWFA, and the standardized upstream power back-off (UPBO) method in VDSL. The NRIA can achieve almost as good performance as the optimal spectrum balancing algorithm (OSBA), but with significantly lower computational complexity. However, by utilizing the additional feature to search for an optimized band plan, the NRIA can offer bitrate combinations, and therefore DSL services, that cannot be offered by any other DSM algorithm.

We also introduced the constrained normalized-rate iterative algorithm (C-NRIA), an extension of the NRIA for solving the DSM optimization problem where the bitrates of some users need to be guaranteed and therefore fixed in advance. This reflects many important business scenarios where a number of customers in a network must be guaranteed a certain DSL service by the operator, while the remaining customers can be offered a best-effort service. We showed that a *single* balancing parameter is sufficient to split the cable resources among fixed-rate and variable-rate users in both transmission directions. Furthermore, we presented an efficient method to search for the desired value of the balancing parameter based on the bi-section algorithm. With simulation examples we showed how the C-NRIA can split the cable capacity between the two user groups in an efficient way.

This thesis presented two practical algorithms that *jointly* optimize the band plan and power allocations for multi-user DSL systems. The main difference between the NRIA and the C-NRIA is that they optimize the utilization of the cable capacity under different constraints. In the near future, the number of deployed DSL systems will increase and with it also the mixing of different services in the same access network. As a result, the benefits offered by the NRIA and the C-NRIA are obvious when deployed in DSL systems like VDSL, VDSL2, ADSL2, and ADSL2+.

Appendix A

Derivations of Some Proprieties of the NRIA and the C-NRIA

A.1 Relation Between the Downstream and Upstream Bitrates of Each User in the NRIA

In this appendix we show that

$$R_{u,DS} = a \cdot \frac{\alpha_{u,DS}}{\alpha_{u,US}} \cdot R_{u,US}, \text{ for } u = 1, 2, \dots, U.$$

holds.

As defined in Section 4.2 the ratio between the total desired downstream and upstream bitrates from (4.4) is given by

$$a = \frac{R_{1,DS} + R_{2,DS} + \dots + R_{U,DS}}{R_{1,US} + R_{2,US} + \dots + R_{U,US}}. \quad (\text{A.1})$$

For the downstream transmission direction the relation between the user priorities and the user bitrates from (4.5) is

$$\frac{R_{1,DS}}{\alpha_{1,DS}} = \frac{R_{2,DS}}{\alpha_{2,DS}} = \dots = \frac{R_{U,DS}}{\alpha_{U,DS}}, \quad (\text{A.2})$$

with

$$\alpha_{1,DS} + \alpha_{2,DS} + \dots + \alpha_{U,DS} = 1. \quad (\text{A.3})$$

Similarly for the upstream transmission direction

$$\frac{R_{1,US}}{\alpha_{1,US}} = \frac{R_{2,US}}{\alpha_{2,US}} = \dots = \frac{R_{U,US}}{\alpha_{U,US}}, \quad (\text{A.4})$$

with

$$\alpha_{1,US} + \alpha_{2,US} + \dots + \alpha_{U,US} = 1. \quad (\text{A.5})$$

Equation (A.1) can be rewritten as

$$R_{1,DS} + R_{2,DS} + \dots + R_{U,DS} = a(R_{1,US} + R_{2,US} + \dots + R_{3,US}). \quad (\text{A.6})$$

Based on (A.2), the downstream bitrates of all users can be represented depending on the downstream bitrate of the first user; thus,

$$R_{2,DS} = \frac{\alpha_{2,DS}}{\alpha_{1,DS}} R_{1,DS}; \dots; R_{U,DS} = \frac{\alpha_{U,DS}}{\alpha_{1,DS}} R_{1,DS}. \quad (\text{A.7})$$

Similarly for the upstream direction based on (A.4)

$$R_{2,US} = \frac{\alpha_{2,US}}{\alpha_{1,US}} R_{1,US}; \dots; R_{U,US} = \frac{\alpha_{U,US}}{\alpha_{1,US}} R_{1,US}. \quad (\text{A.8})$$

Substituting (A.7) and (A.8) into (A.6) yields:

$$R_{1,DS} \left(1 + \frac{\alpha_{2,DS}}{\alpha_{1,DS}} + \dots + \frac{\alpha_{U,DS}}{\alpha_{1,DS}} \right) = a R_{1,US} \left(1 + \frac{\alpha_{2,US}}{\alpha_{1,US}} + \dots + \frac{\alpha_{U,US}}{\alpha_{1,US}} \right).$$

or equivalently

$$R_{1,DS} \frac{\alpha_{1,DS} + \alpha_{2,DS} + \dots + \alpha_{U,DS}}{\alpha_{1,DS}} = a \frac{\alpha_{1,US} + \alpha_{2,US} + \dots + \alpha_{U,US}}{\alpha_{1,US}} R_{1,US}. \quad (\text{A.9})$$

Substituting (A.3) and (A.5) into (A.9) gives:

$$R_{1,DS} \frac{1}{\alpha_{1,DS}} = a \frac{1}{\alpha_{1,US}} R_{1,US},$$

or

$$R_{1,DS} = a \frac{\alpha_{1,DS}}{\alpha_{1,US}} R_{1,US}.$$

In the similar way this can be shown for each user u .

A.2 Discussion of Postulate 1, Section 4.4.1.5

In this appendix we will discuss the validity of Postulate 1 formulated in Section 4.4.1.5 and prove it for a special case.

Postulate 1 *Consider a multi-user D-FDD transmission system operating in an interference channel where each receiver considers the crosstalk signal as noise. For such a multi-user system the sum of the user bitrates increases if the power of each user increases.*

Using Theorem 2 below, we show that Postulate 1 is true for the case when all sub-carriers are utilized by all users under the assumption that the receivers operate with high signal-to-noise ratio (SNR). In our experience, Postulate 1 is also true when not all sub-carriers are used. Furthermore, in [32] it is shown that for a theoretical two-user Gaussian interference channel and different coupling values the sum of the bitrates is increased by

increasing the power of the two users.

Theorem 2 *Assume that receivers operate with high SNR. If all subcarriers are utilized by all users, the users consider the crosstalk signal as a Gaussian noise and none of the users utilize the maximum total power, the sum of the user bitrates always increases when the power of each user increases. That is,*

$$\sum_u \hat{R}_u > \sum_u R_u, \quad (\text{A.10})$$

where \hat{R}_u and R_u denote the bitrates of user u with and without power increase, respectively.

Proof: Without loss of generality we proof Theorem 2 for two users. The proof for the case with more than two users is a generalization of this case. First, (A.10) can be written as:

$$\hat{R}_1 + \hat{R}_2 > R_1 + R_2. \quad (\text{A.11})$$

The power allocations that corresponds to R_1 and R_2 are: $\mathcal{P}_1 = [\mathcal{P}_1^0, \mathcal{P}_1^1, \dots, \mathcal{P}_1^{N-1}]$ and $\mathcal{P}_2 = [\mathcal{P}_2^0, \mathcal{P}_2^1, \dots, \mathcal{P}_2^{N-1}]$, respectively. In the same way we will denote the increased power levels that corresponds to \hat{R}_1 and \hat{R}_2 with $\hat{\mathcal{P}}_1 = [\hat{\mathcal{P}}_1^0, \hat{\mathcal{P}}_1^1, \dots, \hat{\mathcal{P}}_1^{N-1}]$ and $\hat{\mathcal{P}}_2 = [\hat{\mathcal{P}}_2^0, \hat{\mathcal{P}}_2^1, \dots, \hat{\mathcal{P}}_2^{N-1}]$. We will now proceed to show that Theorem 2 follows as a consequence of the increase in $\hat{\mathcal{P}}_1$ and $\hat{\mathcal{P}}_2$.

First we note that increasing the bits in each subcarrier individually also increases their sum. That is, it is enough to study a particular subcarrier n in (A.11):

$$\hat{R}_1^n + \hat{R}_2^n > R_1^n + R_2^n, \quad (\text{A.12})$$

where all the bitrates are calculated based on (4.2).

The SNR at the receivers is much greater than one over all subcarriers due to our assumption that receivers operate with high SNR (this assumption is always true for the subcarriers that are utilized for data transmission). Under this assumption we can expand (A.12) using (4.2) and (4.3) to

$$\begin{aligned} & \log_2 \left(\frac{\mathcal{H}_{11}^n \hat{\mathcal{P}}_1^n}{\Gamma(\mathcal{H}_{12}^n \hat{\mathcal{P}}_2^n + \mathcal{P}_V^n)} \right) + \log_2 \left(\frac{\mathcal{H}_{22}^n \hat{\mathcal{P}}_2^n}{\Gamma(\mathcal{H}_{21}^n \hat{\mathcal{P}}_1^n + \mathcal{P}_V^n)} \right) > \\ & \log_2 \left(\frac{\mathcal{H}_{11}^n \mathcal{P}_1^n}{\Gamma(\mathcal{H}_{12}^n \mathcal{P}_2^n + \mathcal{P}_V^n)} \right) + \log_2 \left(\frac{\mathcal{H}_{22}^n \mathcal{P}_2^n}{\Gamma(\mathcal{H}_{21}^n \mathcal{P}_1^n + \mathcal{P}_V^n)} \right). \end{aligned}$$

Using the properties of the logarithm we can rewrite this as:

$$\frac{\hat{\mathcal{P}}_1^n \hat{\mathcal{P}}_2^n}{\left(\mathcal{H}_{12}^n \hat{\mathcal{P}}_2^n + \mathcal{P}_V^n \right) \left(\mathcal{H}_{21}^n \hat{\mathcal{P}}_1^n + \mathcal{P}_V^n \right)} > \frac{\mathcal{P}_1^n \mathcal{P}_2^n}{\left(\mathcal{H}_{12}^n \mathcal{P}_2^n + \mathcal{P}_V^n \right) \left(\mathcal{H}_{21}^n \mathcal{P}_1^n + \mathcal{P}_V^n \right)},$$

or equivalently,

$$\frac{\hat{\mathcal{P}}_1^n}{\mathcal{P}_1^n} \cdot \frac{\hat{\mathcal{P}}_2^n}{\mathcal{P}_2^n} > \frac{\mathcal{H}_{21}^n \hat{\mathcal{P}}_1^n + \mathcal{P}_V^n}{\mathcal{H}_{21}^n \mathcal{P}_1^n + \mathcal{P}_V^n} \cdot \frac{\mathcal{H}_{12}^n \hat{\mathcal{P}}_2^n + \mathcal{P}_V^n}{\mathcal{H}_{12}^n \mathcal{P}_2^n + \mathcal{P}_V^n}. \quad (\text{A.13})$$

In (A.13) we can identify the part that relates to the first user as:

$$\frac{\hat{\mathcal{P}}_1^n}{\mathcal{P}_1^n} > \frac{\mathcal{H}_{21}^n \hat{\mathcal{P}}_1^n + \mathcal{P}_V^n}{\mathcal{H}_{21}^n \mathcal{P}_1^n + \mathcal{P}_V^n}. \quad (\text{A.14})$$

From (A.14) we can derive

$$\hat{\mathcal{P}}_1^n > \mathcal{P}_1^n.$$

A corresponding relation is found for the second user and, since this is true for both users, (A.13) is always true. Thus, the left-hand side of (A.11) is always larger than the right-hand side. ■

Note that when $\mathcal{H}_{21}^n \hat{\mathcal{P}}_1^n \gg \mathcal{P}_V^n$ and $\mathcal{H}_{21}^n \mathcal{P}_1^n \gg \mathcal{P}_V^n$ the left-hand side of (A.14) is only slightly larger than the right-hand side. This means that there is only a minor increase in the sum of users' bitrates when the power of the signal is increased. Furthermore, when $\mathcal{P}_V^n = 0$, both sides in (A.14) are equal. Thus, there is no increase in the sum of the user bitrates when the power of each user increases. However, this is not important for communication over copper wires, because \mathcal{P}_V^n is never zero due to the thermal noise on copper, external noise sources such as radio noise, and also alien noise from the other DSL systems not included in the optimization process.

A.3 Complexity of the Modified Fixed-Margin Water-Filling Algorithm

This appendix calculates the number of operations required in the modified fixed-margin water-filling (FM-WF) algorithm called "*ModifiedFM-WM*" function in Algorithm 1, Section 4.4. The calculations are made for the case when the continuous bit-loading is used to perform power/bit allocation.

The pseudo-code of the modified FM-WF algorithm is listed as Algorithm 3 (on the next page). We can recognize two main parts. The first part up to line 15 calculates the PSD mask, which supports the given target bitrate T_{dir} . This part is very similar to the margin adaptive water-filling algorithm [30, 100]. If the energy contained within the PSD mask is smaller than or equal to the maximum power allowed for a particular user $P_{u,dir}^{\max}$ then the algorithm stops. If that is not the case, the algorithm goes to the second part (lines 16 to 27). In this part the algorithm calculates the bitrate that can be supported by $P_{u,dir}^{\max}$ and the power allocation over used subcarriers. This part is the rate adaptive water-filling algorithm [30, 100]. A detailed description of the parameters within this algorithm is omitted, because a detailed description of both margin adaptive and rate adaptive water-filling algorithms can be found in [30, 100] and the references therein.

First we calculate the maximum number of operations in Algorithm 3. Then we draw conclusions about the average computational complexity of the FM-WF algorithm.

Algorithm 3 Modified fixed-margin water-filling algorithm for continuous bit-loading algorithm

$g_u^n = \frac{\mathcal{H}_{uu}^n}{N_u^n}$ for $n \in I_{dir}$
 Sort g_u^n in increasing order: $g_u^n \rightarrow \vec{g}_u^n$
 {Find the PSD mask, which supports T_{dir} }
 $C_T = 2^{\frac{1}{N_{dir}} \left[T_{dir} - \sum_{i=1}^{N_{dir}} \log_2 \frac{\vec{g}_u^n}{\Gamma} \right]}$ {Constant on margin adaptive loading algorithm}
 5: $\mathcal{E}_u^{N_{dir}} = C_T - \frac{\Gamma}{\vec{g}_u^{N_{dir}}}$ {Energy value on subcarrier N_{dir} }
if $\mathcal{E}_u^{N_{dir}} < 0$ **then**
 $N_T, C_T = \mathbf{FunctionT}(N_{dir}, T_{dir}, \vec{g}_u^n)$
else
 $N_T = N_{dir}$
 10: **end if**
 $\mathcal{E}_u^n = C_T - \frac{\Gamma}{g_u^n}$ for $n = 1, \dots, N_T$
if $\sum_{n=1}^{N_T} \mathcal{E}_u^n \leq \mathcal{P}_{u,dir}^{\max}$ { T_{dir} is supported for given $\mathcal{P}_{u,dir}^{\max}$ } **then**
 $R_{u,dir} = T_{dir}$
 Update the PSD mask $\mathcal{P}_{u,dir}$ from \mathcal{E}_u
 15: **else**
 { Calculate the bitrate $R_{u,dir}$, which can be supported for given $\mathcal{P}_{u,dir}^{\max}$ }
 $C_R = \frac{1}{N_{dir}} \left[\mathcal{P}_{u,dir}^{\max} + \Gamma \sum_{i=1}^{N_{dir}} \frac{1}{\vec{g}_u^n} \right]$ {Constant on rate adaptive loading algorithm}
 $\mathcal{E}_u^{N_{dir}} = C_R - \frac{\Gamma}{\vec{g}_u^{N_{dir}}}$
 if $\mathcal{E}_u^{N_{dir}} < 0$ **then**
 20: $N_R, C_T = \mathbf{FunctionR}(N_{dir}, \mathcal{P}_{u,dir}^{\max}, \vec{g}_u^n)$
 else
 $N_R = N_{dir}$
 end if
 $\mathcal{E}_u^n = C_R - \frac{\Gamma}{g_u^n}$ for $n = 1, \dots, N_R$
 25: $\mathcal{R}_u^n = \log_2 \left(\frac{C_R * \vec{g}_u^n}{\Gamma} \right)$ for $n = 1, \dots, N_R$
 $R_{u,dir} = \sum_{n=1}^{N_R} \mathcal{R}_u^n$
 Update PSD mask $\mathcal{P}_{u,dir}$ from \mathcal{E}_u
end if

To calculate the maximum number of operations in Algorithm 3 we follow the path as described below:

- Calculating of subcarrier gains g_u in the first line requires N_{dir} divisions, where N_{dir} denotes the number of subcarriers in the set I_{dir} .
- The maximum number of operation to sort the g_u in increasing order in the set I_{dir} requires a maximum of $N_{dir}^2/2$ comparisons [30].
- To calculate C_T in line 4, $N_{dir} + 1$ additions/subtractions, $N_{dir} + 1$ divisions, and $N_{dir} + 1$ logarithmic/exponential operations are required.
- One subtraction and one division are needed to calculate $\mathcal{E}_u^{N_{dir}}$ in line 5.

Algorithm 4 Pseudo code of *FunctionT* and *FunctionR*

$N_T, C_T = \mathbf{FunctionT}(N_{dir}, T_{dir}, \vec{g}_u)$
Initialize: $N_{min} = 1, N_{max} = N_{dir} - 1$
for $i = 1$ to $\log_2(N_{dir})$ **do**
 $N^* = \frac{N_{max} + N_{min}}{2}$
5: $C_s = 2^{\frac{1}{N^*}} \left[T_{dir} - \sum_{i=1}^{N^*} \log_2 \frac{\vec{g}_u^i}{\Gamma} \right]$
 $\mathcal{E}_u^{N^*} = C_s - \frac{\Gamma}{g_u^{N^*}}$
if $\mathcal{E}_u^{N^*} \leq 0$ **then**
 $N_{max} = N^* - 1$
else
10: $N_{min} = N^* + 1$
 $N_T = N^*$
 $C_T = C_s$
end if
end for

15: $N_T, C_T = \mathbf{FunctionR}(N_{dir}, \mathcal{P}_{u,dir}^{max}, \vec{g}_u)$
Initialize: $N_{min} = 1, N_{max} = N_{dir} - 1$
for $i = 1$ to $\log_2(N_{dir})$ **do**
 $N^* = \frac{N_{max} + N_{min}}{2}$
 $C_s = \frac{1}{N^*} \left[\mathcal{P}_{u,dir}^{max} + \Gamma \sum_{i=1}^{N^*} \frac{1}{g_u^i} \right]$
20: $\mathcal{E}_u^{N^*} = C_s - \frac{\Gamma}{g_u^{N^*}}$
if $\mathcal{E}_u^{N^*} \leq 0$ **then**
 $N_{max} = N^* - 1$
else
 $N_{min} = N^* + 1$
25: $N_R = N^*$
 $C_R = C_s$
end if
end for

- Line 6 requires one comparison.
- Based on the pseudo code in Algorithm 4, the function “*FunctionT*” requires the following operations:
 - To calculate N^* in total $\log_2 N_{dir}$ additions and $\log_2 N_{dir}$ divisions are needed. The number of operations is $\log_2 N_{dir}$ due to the **for** loop.
 - From the pseudo code in Algorithm 4, the maximum number of operations to calculate C_s is required when \mathcal{E}_u takes a positive value at $N_{dir} - 1$ and negative value at N_{dir} . Thus, N^* takes the following values: $N_{dir}/2, 3N_{dir}/4, 7N_{dir}/8, \dots, N_{dir} - 1 = N_{dir} \cdot \log_2(N_{dir}/2) + 1$. However due to the binary search, when we saved the calculated value of C_s and either add or remove from it the new sum of $\log_2 \frac{\vec{g}_u}{\Gamma}$ of the added or removed \vec{g}_u elements, we always need only N_{dir} additions. Therefore, the calculation of C_s requires

$N_{dir} \log_2 N_{dir} + \log_2 N_{dir}$ additions/subtractions, $N_{dir} \log_2 N_{dir} + \log_2 N_{dir}$ divisions, and $N_{dir} \log_2 N_{dir} + \log_2 N_{dir}$ logarithmic/exponential operations.

- To calculate $\mathcal{E}_u^{N^*}$ in total $\log_2 N_{dir}$ subtractions and $\log_2 N_{dir}$ divisions are needed.
- In line 7, $\log_2 N_{dir}$ comparisons are required.
- Either line 9 or line 10 are called, but never both consecutively; therefore, we need $\log_2 N_{dir}$ additions/subtractions.

Thus, “*FunctionT*” requires: $N_{dir} \log_2 N_{dir} + 4 \log_2 N_{dir}$ additions/subtractions, $N_{dir} \log_2 N_{dir} + 3 \log_2 N_{dir}$ multiplications/divisions, $\log_2 N_{dir}$ comparisons, and $N_{dir} \log_2 N_{dir} + \log_2 N_{dir}$ logarithmic/exponential operations.

- A maximum of N_{dir} subtractions and N_{dir} divisions are needed in line 11.
- Line 12 requires a maximum of N_{dir} additions and one comparison.
- To calculate C_R in line 17 requires $N_{dir} + 1$ additions and $N_{dir} + 2$ multiplications/divisions.
- One subtraction and one division are needed to calculate $\mathcal{E}_u^{N_{dir}}$ in line 18.
- One comparison is required in line nineteen.
- Function “*FunctionR*” requires $N_{dir} \log_2 N_{dir} + 4 \log_2 N_{dir}$ additions/subtractions, $N_{dir} \log_2 N_{dir} + 4 \log_2 N_{dir}$ multiplications/divisions, and $\log_2 N_{dir}$ comparisons. The number of operations is calculated in the same way as when calculating the number of operations in “*FunctionT*”.
- A maximum of N_{dir} subtractions and N_{dir} divisions are needed in line 24.
- In line 25 a maximum of $2N_{dir}$ multiplications/divisions, and N_{dir} logarithmic operations are required.
- Calculating R_u requires a maximum of N_{dir} additions.

The maximum number of operations required in the modified FM-WF algorithm is summarized in Table A.1.

TABLE A.1: The maximum number of operations required in the modified FM-WF algorithm, when continuous bit-loading algorithm is used to perform power allocations. N_{dir} denotes the number of used subcarriers.

Operations	Number of operations in modified FM-WF algorithm		
	General case	$N_{dir} = 2048$ (10^3)	$N_{dir} = 512$ (10^3)
Add./Sub.	$2N_{dir} \log_2 N_{dir} + 8 \log_2 N_{dir} + 6N_{dir} + 4$	57.43	12.36
Comparisons	$N_{dir}^2/2 + 2 \log_2 N_{dir} + 3$	2097.18	131.09
Multip./Divi.	$2N_{dir} \log_2 N_{dir} + 7 \log_2 N_{dir} + 7N_{dir} + 5$	59.47	12.87
Log./Exp.	$N_{dir} \log_2 N_{dir} + \log_2 N_{dir} + 2N_{dir} + 1$	26.66	5.64

The results in Table A.1 show that the largest number of operations is required to sort the g_u , which requires a maximum of $N_{dir}^2/2$ comparisons. However, on average to sort the g_u are required only $N_{dir} \log_2 N_{dir}$ comparisons [30]. Therefore, the modified FM-WF algorithm has an average computational complexity of order $\mathcal{O}(N_{dir} \log_2 N_{dir})$. This is the same complexity order as of any water-filling algorithm. This can also be concluded from the pseudo code of Algorithm 3, as we call some form of margin adaptive water-filling algorithm only once and optionally the rate adaptive water-filling algorithm once.

A.4 Proof of Theorem 1, Section 6.1.1

In this appendix we prove Theorem 1 formulated in Section 6.1.1.

Theorem 1 *Given the bitrate relations (6.1) and constraint (6.2) one parameter is sufficient for properly balancing the bitrates of the fixed-rate and variable-rate users against each other. Proof:* Let us assume that there are U^F fixed-rate users and U^V variable-rate users with $U^F + U^V = U$. As shown in (6.2) the user priority values of the fixed-rate and variable-rate users satisfy

$$\sum_{u=1}^{U^F} \alpha_u^F + \sum_{u=1}^{U^V} \alpha_u^V = 1, \quad (\text{A.15})$$

where α_u^F and α_u^V denote the priority values of the fixed-rate and variable-rate users respectively. The right side of (A.15) equals the left side if and only if the value by which $\sum_{u=1}^{U^F} \alpha_u^F$ is increased (or decreased) is equivalent to the value by which $\sum_{u=1}^{U^V} \alpha_u^V$ is decreased (or increased). We call this value the balance parameter and denote it by s . Thus, we can write (A.15) as:

$$\left(\sum_{u=1}^{U^F} \alpha_u^F + s \right) + \left(\sum_{u=1}^{U^V} \alpha_u^V - s \right) = 1. \quad (\text{A.16})$$

Note that we assume that the selected target bitrates can be achieved by the fixed-rate users. Therefore, there is an s within the interval $\left[-\sum_{u=1}^{U^F} \alpha_u^F, \sum_{u=1}^{U^V} \alpha_u^V \right]$ for which the fixed-rate users achieve their target bitrates. Two extreme cases are: 1) $s = -\sum_{u=1}^{U^F} \alpha_u^F$, which assigns the total cable capacity to the variable-rate users and 2) $s = \sum_{u=1}^{U^V} \alpha_u^V$, which assigns the total cable capacity to the fixed-rate users.

Let us denote by s_u^F , for $u = 1, \dots, U^F$, the values by which the priority values of the fixed-rate users are increased (or decreased). Similarly, s_u^V , for $u = 1, \dots, U^V$, denote the values by which the priority values of the variable-rate users are decreased (or increased). We denote by $\check{\alpha}_u^F$, for $u = 1, \dots, U^F$, and $\check{\alpha}_u^V$, for $u = 1, \dots, U^V$, the new priority values of the fixed-rate and variable-rate users respectively. Thus, the new priority values of the fixed-rate users $\check{\alpha}_u^F$ based on (A.16) are:

$$\check{\alpha}_u^F = \alpha_u^F + s_u^F, \quad \text{for } u = 1, \dots, U^F, \quad (\text{A.17})$$

with

$$s = s_1^F + s_2^F + \dots + s_{U^F}^F. \quad (\text{A.18})$$

Similarly, the new priority values of the variable-rate users are given by:

$$\check{\alpha}_u^V = \alpha_u^V - s_u^V, \quad \text{for } u = 1, \dots, U^V, \quad (\text{A.19})$$

with

$$s = s_1^V + s_2^V + \dots + s_{UV}^V.$$

Thus, we need to determine the appropriate values of s_u^F for $u = 1, \dots, U^F$ and s_u^V for $u = 1, \dots, U^V$ to find the new priority values of the fixed-rate and variable-rate users. We calculate s_u^F and s_u^V based on the initialized priority values of the fixed-rate and variable-rate users, because we know them in advance.

For given α_u^F , from the definition in (6.1), the bitrates of the fixed-rate users and their priority values are related by

$$\frac{R_1^F}{\alpha_1^F} = \frac{R_2^F}{\alpha_2^F} = \dots = \frac{R_{U^F}^F}{\alpha_{U^F}^F}. \quad (\text{A.20})$$

When the priority values of the fixed-rate users are increased (or decreased), to achieve the target bitrates for the fixed-rate users, the bitrate relations in (A.20) are preserved when:

$$\frac{\alpha_1^F}{\alpha_z^F} = \left(\frac{\check{\alpha}_1^F}{\check{\alpha}_z^F} \right) = \frac{\alpha_1^F + s_1^F}{\alpha_z^F + s_z^F}, \quad \text{for } z = 2, \dots, U^F. \quad (\text{A.21})$$

Note that from all possible equations in (A.20) we have selected in (A.21) only those that are independent. For instance when $\frac{R_1^F}{\alpha_1^F} = \frac{R_2^F}{\alpha_2^F}$ and $\frac{R_1^F}{\alpha_1^F} = \frac{R_3^F}{\alpha_3^F}$ this also implies that $\frac{R_2^F}{\alpha_2^F} = \frac{R_3^F}{\alpha_3^F}$. After solving (A.21) and (A.18) for s_u^F depending on s and α_u^F we get:

$$s_1^F = \frac{s \cdot \alpha_1^F}{\sum_{u=1}^{U^F} \alpha_u^F}, s_2^F = \frac{s \cdot \alpha_2^F}{\sum_{u=1}^{U^F} \alpha_u^F}, \dots, s_{U^F}^F = \frac{s \cdot \alpha_{U^F}^F}{\sum_{u=1}^{U^F} \alpha_u^F}. \quad (\text{A.22})$$

In the similar way for the variable-rate users:

$$s_1^V = \frac{s \cdot \alpha_1^V}{\sum_{u=1}^{U^V} \alpha_u^V}, s_2^V = \frac{s \cdot \alpha_2^V}{\sum_{u=1}^{U^V} \alpha_u^V}, \dots, s_{U^V}^V = \frac{s \cdot \alpha_{U^V}^V}{\sum_{u=1}^{U^V} \alpha_u^V}. \quad (\text{A.23})$$

Substituting (A.22) into (A.17) yields:

$$\check{\alpha}_u^F = \alpha_u^F + \frac{s \cdot \alpha_u^F}{\sum_{u=1}^{U^F} \alpha_u^F}, \quad \text{for } u = 1, \dots, U^F, \quad (\text{A.24})$$

Substituting (A.23) into (A.19) yields:

$$\check{\alpha}_u^V = \alpha_u^V - \frac{s \cdot \alpha_u^V}{\sum_{u=1}^{U^V} \alpha_u^V}, \quad \text{for } u = 1, \dots, U^V. \quad (\text{A.25})$$

Equations (A.24) and (A.25) show that the balancing parameter s and the initial values of α_u^F and α_u^V are sufficient to determine the increased (or decreased) priority values of the fixed-rate users and the decreased (or increased) priority values of the variable-rate users. Increasing (or decreasing) the bitrates of the fixed-rate users follows from increasing (or decreasing) their priority values. The same holds true also for the variable-rate users. Therefore searching for the appropriate value of s is sufficient for properly balancing the bitrates of the fixed-rate and variable-rate users against each other. ■

Appendix B

Abbreviations

2B1Q	2-binary 1-quaternary
A/D	Analog-to-digital
ADSL	Asymmetric digital subscriber line
ANSI	American National Standards Institute
AFE	Analog front-end
ATIS	Alliance for Telecommunications Industry Solutions
BER	Bit-error rate
bi-IWFA	Bi-directional iterative water-filling algorithm
BRI	Basic rate integrated services digital network
C-NRIA	Constrained normalized-rate iterative algorithm
CAP	Carrierless amplitude/phase
CLEC	Competitive local exchange carrier
CE	Cyclic extension
CM	Common mode
CO	Central office
CP	Cyclic prefix
CPE	Customer premise equipment
CS	Cyclic suffix
D-FDD	Digital frequency division duplexing
D/A	Digital-to-analog
DDS	Digital data services
DFE	Decision-feedback equalizer
DFT	Discrete Fourier transform
DM	Differential mode
DMT	Discrete multi-tone
DS	Downstream
DSL	Digital subscriber line
DSM	Dynamic spectrum management
DSLAM	Digital subscriber line access multiplexer
EC	Echo cancellation
ETSI	European Telecommunication Standards Institute
EM	Expectation maximization
EWL	Equivalent working length
FDD	Frequency division duplexing
FDI	Feeder distribution interface
FEQ	Frequency-domain equalizer

FEXT	Far-end crosstalk
FFT	Fast Fourier transform
FM-WM	Fixed-margin water-filling
HAM	Amateur radio
HDSL	High-bitrate digital subscriber line
ILEC	Incumbent local exchange carrier
ICI	Inter-channel-interference
IDFT	Inverse discrete Fourier transform
IFFT	Inverse fast Fourier transform
ISDN	Integrated services digital network
ISI	Inter-symbol-interference
ITU	International Telecommunication Union
IWFA	Iterative water-filling algorithm
LT	Line termination
MCM	Multi-carrier modulation
MDF	Main distribution frame
MIMO	Multiple-input multiple-output
MUD	Multi-user detection
NEXT	Near-end crosstalk
NRIA	Normalized-rate iterative algorithm
NT	Network termination
OFDM	Orthogonal frequency division multiplexing
OSBA	Optimal spectrum balancing algorithm
PAR	Peak-to-average ratio
PBO	Power-back off
PLL	Phase locked loop
POTS	Plain old telephone service
PSD	Power spectral density
PAM	Pulse amplitude modulation
QAM	Quadrature amplitude modulation
RADSL	Rate-adaptive ADSL
RF	Radio frequency
RFI	Radio frequency interference
SCM	Single-carrier modulation
SMC	Spectrum management center
SSM	Static spectrum management
SDSL	Symmetric DSL
SHDSL	Symmetric high-bitrate DSL
SNR	Signal-to-noise ratio
UPBO	Upstream power-back off
US	Upstream
VCXO	Voltage controlled crystal oscillator
VDSL	Very high speed DSL
ZF	Zero-forcing
ZP	Zero-padding

Appendix C

Notation

Mathematical notation

x, X	Scalar variables
\mathbf{x}, \mathbf{X}	Column vectors
\mathbf{X}	Matrices
X^*	Complex conjugate of X
\mathbf{x}^T	Transpose of \mathbf{x}
$y[k]$	Function of a discrete variable k
$y(t)$	Function of a continuous variable t
$*$	Convolution
\otimes	Circular Convolution
$x[n]$	Element n of \mathbf{x}
$\sup\{\cdot\}$	Supremum operation
$\mathcal{O}(\cdot)$	Complexity order
\mathbb{R}^+	Field of real positive numbers

List of symbols

a	Asymmetry parameter, shows the ratio between the total DS and US bitrates
\check{a}	Updated value of a
dir	A particular transmission direction $dir \in \{\text{DS,US}\}$
f	Frequency
$f[n]$	Carrier frequency of n -th subcarrier
L	Length of the impulse response of the equivalent discrete-time channel
L_p	Length of cyclic prefix
L_s	Length of cyclic suffix
L_e	Length of cyclic extension
$h[k]$	Impulse response of the equivalent discrete-time channel
H	Channel transfer function
\mathcal{H}	Squared magnitude of H
H_{uu}^n	Direct channel transfer function of user u on subcarrier n
\mathcal{H}_{uu}^n	Squared magnitude of H_{uu}^n
H_{uv}^n	Crosstalk channel transfer function from user v to u on subcarrier n
\mathcal{H}_{uv}^n	Squared magnitude of H_{uv}^n
i_{dir}	Number of iterations in the inner stage of the NR-IA in direction dir (DS,US)
I_{dir}	Set of subcarriers assigned in direction dir

N	Number of subcarriers
N_{dir}	Number of subcarriers assigned in direction dir
\tilde{N}_{dir}	Average number of subcarriers assigned in direction dir in O iteration
\mathcal{N}	PSD of the total noise
$\mathcal{N}[n]$	PSD of the total noise on subcarrier n
\mathcal{N}_u^n	PSD of the total noise of user u on subcarrier n
O	Number of iterations in the outer stage of the NRIA
\mathcal{P}	Transmit PSD of a signal
$\hat{\mathcal{P}}$	Increased value of \mathcal{P}
$\mathcal{P}[n]$	Transmit PSD of a DMT signal on subcarrier n
\mathcal{P}_u^n	Transmit PSD of user u on subcarrier n
R	Number of bits in a DMT symbol
\tilde{R}	Average number of bits over N subcarriers
$R[n]$	Number of bits in subcarrier n
R_u	Number of bits of user u in a DMT symbol
\hat{R}_u	Increased value of R_u
$\bar{R}_{u,dir}$	Normalized bitrate of user u in direction dir ($R_{u,dir}/\alpha_{u,dir}$)
R_u^n	Number of bits of user u on subcarrier n
\hat{R}_u^n	Increased value of R_u^n
$R_{u,dir}$	Number of bits of user u in direction dir in a DMT symbol
$R_{u,dir}^n$	Number of bits of user u on subcarrier n in direction dir
R_u^F	Number of bits of fixed-rate user u in a DMT symbol
R_u^V	Number of bits of variable-rate user u in a DMT symbol
$R_{u,dir}^F$	Number of bits of fixed-rate user u in a DMT symbol in direction dir
$R_{u,dir}^V$	Number of bits of variable-rate user u in a DMT symbol in direction dir
U	Number of users
U^F	Number of fixed-rate users (those with fixed bitrates)
U^V	Number of variable-rate users (those with variable bitrates)
t	Time
T	Sampling rate
$T_{u,dir}$	Target bitrate of user u in direction dir
$T_{u,dir}^F$	Target bitrate of fixed-rate user u in a DMT symbol in direction dir
$T_{u,dir}^V$	Target bitrate of variable-rate user u in a DMT symbol in direction dir
$x(t)$	Signal transmitted over the channel
$x[k]$	k -th time-domain coefficients in the output of the DMT modulator
$x_m[k]$	$x[k]$ at m -th DMT symbol
$x_m^{CP}[k]$	k -th time-domain coefficient at m -th transmitted DMT symbol
$X[n]$	Frequency-domain component on subcarrier n in transmitter
$X_m[n]$	$X[n]$ at m -th DMT symbol
$y(t)$	Signal in the input of the receiver
$y[k]$	k -th time-domain coefficient in the input of the DMT demodulator
$Y[n]$	Frequency-domain component on subcarrier n in receiver
$Y_m[n]$	$Y[n]$ at m -th DMT symbol
$\tilde{Y}[n]$	Frequency-domain component in the output of the FEQ
$\tilde{Y}_m[n]$	$\tilde{Y}[n]$ at m -th DMT symbol

$\alpha_{u,dir}$	Priority value of user u in direction dir
$\alpha_{u,dir}^F$	Priority value of fixed-rate user u in direction dir
$\alpha_{u,dir}^V$	Priority value of variable-rate user u in direction dir
$\check{\alpha}_{u,dir}^F$	Updated value of $\alpha_{u,dir}^F$
$\check{\alpha}_{u,dir}^V$	Updated value of $\alpha_{u,dir}^V$
β_{dir}^n	Usage indicator of subcarrier n in direction dir
γ_{Code}	Coding gain
γ_{Loss}	SNR loss due to imperfect receiver design
γ_{Mod}	Modulation gap
γ_{Noise}	Noise margin
Γ	SNR gap

Bibliography

- [1] C. H. Aldana, E. de Carvalho, and J. M. Cioffi, "Channel estimation for multicarrier multiple input single output systems using the EM algorithm," *IEEE Transactions on Signal Processing*, vol. 51, no. 12, pp. 3280–3292, Dec. 2003.
- [2] ANSI, "Spectrum management for loop transmission systems," ANSI, Draft Standard T1.417-2000, Dec. 2000.
- [3] —, "Very-high-bit-rate Digital Subscriber Line (VDSL) Metallic Interface Part 1: Functional Requirement and Common Specification," ANSI, Draft Standard T1.424/Trial-Use Part1, Feb. 2000.
- [4] —, "Very-high-bit-rate Digital Subscriber Lines (VDSL) Metallic Interface, Part 3: Technical Specification of a Multi-Carrier Modulation Transceiver," ANSI, Draft Standard T1.424/Trial-Use Part3, Nov. 2000.
- [5] —, "Spectrum management for loop transmission systems, Issue 2," ANSI, Draft Standard T1E1.4/2003-002R3, May 2003.
- [6] —, "Dynamic spectrum management report," ANSI, Draft Standard T1E1.4/2003-018R, Feb. 2004.
- [7] R. Baldemair, "Time-domain equalization and digital notching in multicarrier systems," Ph.D. dissertation, Vienna University of Technology, 2001.
- [8] A. G. Bell, "Telephone-circuit," U.S. Patents No. 244,426 (July 1881).
- [9] J. A. C. Bingham, "Multicarrier modulation for data transmission: An idea whose time has come," *IEEE Communications Magazine*, vol. 28, no. 5, pp. 5–14, May 1990.
- [10] —, *ADSL, VDSL, and Multicarrier Modulation*. John Wiley & Sons, Inc., 2000.
- [11] J. Campello, "Practical bit loading for DMT," in *Proc. of the IEEE International Conference on Communications, ICC*, Vancouver, Canada, Jun. 2001, pp. 801–805.
- [12] —, "Discrete bit loading for multicarrier modulation systems," Ph.D. dissertation, Stanford University, 1999.

- [13] A. B. Carleial, "Interference channels," *IEEE Transactions on Information Theory*, vol. 24, no. 1, pp. 60–70, Jan. 1978.
- [14] R. Cendrillon, M. Moonen, J. Verliden, T. Bostoen, and W. Yu, "Optimal multiuser spectrum management for digital subscriber lines," in *Proc. of the IEEE International Conference on Communications, ICC*, Paris, France, Jun. 2004, pp. 1–5.
- [15] R. Cendrillon, "Multi-user signal and spectra co-ordination for digital subscriber lines," Ph.D. dissertation, Katholieke Universiteit Leuven, 2004.
- [16] R. W. Chang and R. A. Gibby, "A theoretical study of performance of an orthogonal multiplexing data transmission scheme," *IEEE Transactions on Communications*, vol. 16, no. 4, pp. 529–540, Aug. 1968.
- [17] W. Y. Chen, *DSL: Simulation Techniques & Standards Development for Digital Subscriber Lines*. Macmillan Technical Publishing, 1998.
- [18] W. Y. Chen, G. H. Im, and J. J. Werner, "Design of digital AM/PM transceivers," *ANSI TIE1.4 contribution 1992-149*, Aug. 1992.
- [19] G. Cherubini, "Optimum upstream power back-off and multiuser detection for VDSL," in *Proc. of the IEEE Global Telecommunications Conference, GLOBECOM*, San Antonio, TX, USA, Nov. 2001, pp. 375–380.
- [20] K. W. Choeng, W. J. Choi, and J. M. Cioffi, "Multiuser soft interference canceler via iterative decoding for DSL applications," *IEEE Journal on Selected Areas in Communications*, vol. 20, no. 2, pp. 363–371, Feb. 2002.
- [21] P. S. Chow, C. J. M., and J. A. C. Bigham, "A practical discrete multitone transceiver loading algorithm for data transmission over spectrally shaped channels," *IEEE Transactions on Information Theory*, vol. 43, pp. 773–775, Feb/Mar/Apr 1995.
- [22] S. T. Chung and J. M. Cioffi, "Rate and power control in a two-user multicarrier channel with no coordination: the optimal scheme vs. a suboptimal method," *IEEE Transactions on Communications*, vol. 51, no. 11, pp. 1768–2003, Nov 2003.
- [23] S. T. Chung, S. J. Kim, J. Lee, and J. M. Cioffi, "A game-theoretic approach to power allocation in frequency selective Gaussian interference channels," in *Proc. of the IEEE International Symposium on Information Theory, ISIT*, Yokohama, Japan, Jun.-Jul. 2003, p. 316.
- [24] J. M. Cioffi, "Use of bi-directional iterative water-filling," Vienna, Sep 2004, personal communication.
- [25] J. M. Cioffi, G. D. Dudevoir, M. V. Eyuboglu, and G. D. Forney, Jr., "MMSE decision feedback equalizers and coding: Parts I and II," *IEEE Transactions on Communications*, vol. 43, no. 10, pp. 2582–2604, Oct. 1995.

- [26] J. M. Cioffi and J. G. D. Forney, "Generalized decision-feedback equalization for packet transmission with ISI and Gaussian noise," in *Communication, Computation, Control and Signal Processing: A Tribute to Thomas Kailath*, A. Paulraj, V. Roychowdhury, and C. Schaper, Eds. Kluwer Academic, 1997, ch. 4, pp. 79–127.
- [27] J. M. Cioffi, J. Lee, and W. Yu, "Autonomous DSM mixture of symmetric and asymmetric service: Bi-directional iterative waterfilling (at Level 0 or at Level 1)," *ANSI T1E1.4 contribution 2002-058R1*, Feb. 2002.
- [28] J. M. Cioffi, W. Rhee, M. Mohseni, and M. H. Brady, "Band preference in dynamic spectrum management," in *Proc. of the European Signal Processing Conference, EUSIPCO*, Vienna, Austria, Sep. 2004, pp. 1205–1208.
- [29] J. M. Cioffi, W. Yu, G. Ginis, S. Zeng, M. Isaksson, F. Sjöberg, and R. Nilsson, "Digital duplexing: VDSL performance improvement by aversion of frequency guard bands," *ETSI/STC TM6 contribution 993t13a0*, Nov. 1999.
- [30] J. M. Cioffi, *Lecture Notes on Advanced Digital Communications*. Stanford University, 2002.
- [31] J. Cook, "Wideband impulsive noise survey of the access network," *BT Technical Journal*, vol. 11, no. 3, p. 155.
- [32] M. H. M. Costa, "On the Gaussian interference channel," *IEEE Transactions on Information Theory*, vol. 31, no. 5, pp. 607–615, Sep. 1985.
- [33] T. M. Cover and J. A. Thomas, *Elements of Information Theory*. John Wiley & Sons, Inc., 1991.
- [34] D. Daecke, "RFI ingress tests for SDSL," *ETSI/STC TM6 contribution 003t35*, Sep. 2000.
- [35] H. Dai and H. V. Poor, "Crosstalk mitigation in DMT VDSL with impulse noise," *IEEE Transactions on circuits and systems I: Fundamental Theory and Applications*, vol. 48, no. 10, pp. 1205–1213, 2001.
- [36] DSL Forum website. [Online]. Available: <http://www.dslforum.org>
- [37] I. Duma and B. Bolocan, "Optimal strategy on a twisted-pair channel using mixed-integer nonlinear programming," in *International Conference on Telecommunications, ICT*, 2002.
- [38] ETSI, "Transmission and Multiplexing (TM); Access networks; Spectral Management on metallic access networks; Part 1: Definitions and signal library," ETSI, Tech. Rep. TR 101 830-1, Version 1.3.1, Dec. 2002.
- [39] —, "Transmission and multiplexing (TM); Access transmission systems on metallic access cables; Asymmetric Digital Subscriber Line (ADSL) - European specific requirements [ITU-T Recommendation G.992.1 modified]," ETSI, Standard TS 101 388, Version 1.3.1, May 2002.

- [40] —, “Transmission and Multiplexing (TM); Access transmission systems on metallic access cables; Very high speed Digital Subscriber Line (VDSL); Part 1: Functional requirements,” ETSI, Standard TS 101 270-1, Version 1.3.1, Jul. 2003.
- [41] —, “Transmission and Multiplexing (TM); Access transmission systems on metallic access cables; Very high speed Digital Subscriber Line (VDSL); Part 2: Transceiver specification,” ETSI, Standard TS 101 270-2, Version 1.2.1, Jul. 2003.
- [42] —, “Transmission and Multiplexing (TM); Access networks; Spectral Management on metallic access networks; Part 2: Technical methods,” ETSI, Tech. Rep. TR 101 830-2, Version m01p20a8-Draft3, Jun. 2004.
- [43] —, “Transmission and Multiplexing (TM); Access networks; Spectral Management on metallic access networks; Part 3: Construction methods for spectral management rules,” ETSI, Tech. Rep. TR 101 830-3, Version m01p23a10, Sep. 2004.
- [44] B. Farhang-Boroujeny and M. Ding, “Design methods for time-domain equalizers in DMT transceivers,” *IEEE Transactions on Communications*, vol. 49, no. 3, pp. 554–562, Mar. 2001.
- [45] F. H. F. Fischer and J. B. Huber, “A new loading algorithm for discrete multitone transmission,” in *Proc. of the IEEE Global Telecommunications Conference, GLOBECOM*, London, UK, Nov. 1996, pp. 724–728.
- [46] C. A. Floudas, *Nonlinear and Mixed-Integer Optimization Fundamentals and Applications*. Princeton University Press, 1995.
- [47] FSAN VDSL working group, “A new analytical method for NEXT and FEXT noise calculation,” *ANSI T1E1.4 contribution 1998-189*, Jun. 1998.
- [48] G. Ginis and J. M. Cioffi, “Vectored transmission for digital subscriber line systems,” *IEEE Journal on Selected Areas in Communications*, vol. 20, no. 5, pp. 1085–1104, Jun. 2002.
- [49] G. Ginis, “Multi-line coordinated communication for broadband access networks,” Ph.D. dissertation, Stanford University, 2002.
- [50] I. E. Grossmann, “Review of nonlinear mixed-integer and disjunctive programming techniques,” *Optimization and Engineering*, vol. 3, pp. 227–252, 2002.
- [51] W. Henkel, T. Nordström, and W. Lenger, “Verbesserung der xDSL-performance durch das kabeldesign,” ITG-Fachtagung Kommunikationskabelnetze, Köln, Germany, Dec. 2001.
- [52] W. Henkel and V. Zrno, “PAR reduction revisited: An extension to Tellado’s method,” in *Proc. of the 6th International OFDM Workshop*, Hamburg, Germany, Sep. 2001, pp. 31.1–31.6.
- [53] M. L. A. Honig, P. Crespo, and K. Steiglitz, “Suppression of near- and far-end crosstalk by linear pre- and post-filtering,” *IEEE Journal on Selected Areas in Communications*, vol. 10, no. 3, pp. 614–629, Apr. 1992.

- [54] M. L. A. Honig, K. Steiglitz, and B. Gopinath, "Multichannel signal processing for data communications in the presence of crosstalk," *IEEE Transactions on Communications*, vol. 38, no. 4, pp. 551–558, Apr. 1990.
- [55] D. Hughes-Hartogs, "Ensemble modem structure for imperfect transmission media," U.S. Patents Nos. 4,679,227 (July 1987), 4,731,816 (March 1988) and 4,833,706 (May 1989).
- [56] M. Isaksson, T. Nordström, L. Olsson, and P. Ödling, "A DMT transmission system for high-speed communication on copper wire pairs," in *International Conference on Signal Processing Applications & Technology, ICSPAT*, Boston, MA, USA, Oct. 1995.
- [57] ITU-T, "High-speed Digital Subscriber Line (HDSL) transceivers," ITU, Standard G.991.1, Oct. 1998.
- [58] —, "Asymmetric Digital Subscriber Line ADSL Transceivers," ITU, Standard G.992.1, Jul. 1999.
- [59] —, "Asymmetric Digital Subscriber Line ADSL Transceivers 2 (ADSL2)," ITU, Standard G.992.3, Jul. 2002.
- [60] —, "Asymmetric Digital Subscriber Line ADSL Transceivers - extended bandwidth ADSL2 (ADSL2plus)," ITU, Standard G.992.5, May 2003.
- [61] —, "Single-pair High-speed Digital Subscriber Line (SHDSL) transceivers," ITU, Standard G.991.2, Dec. 2003.
- [62] —, "Very high speed digital subscriber," ITU, Standard G.993.1, Jun. 2004.
- [63] K. Jacobson, "Methods of upstream power backoff in very high-speed digital subscriber lines," *IEEE Communications Magazine*, vol. 39, no. 3, pp. 210–216, Mar. 2001.
- [64] K. Kerpez, "DSL spectrum management standard," *IEEE Communications Magazine*, vol. 40, no. 11, pp. 116–123, 2002.
- [65] K. Kerpez, D. Waring, S. Galli, J. Dixon, and P. Madon, "Advanced DSL management," *IEEE Communications Magazine*, vol. 41, no. 9, pp. 116–123, Sep. 2003.
- [66] H. W. Kuhn and S. Nasar, *The essential John Nash*. Princeton University Press, 2002.
- [67] J. C. Lagarias, J. A. Reeds, M. H. Wright, and P. E. Wright, "Convergence properties of the Nelder-Mead simplex method in low dimensions," *SIAM Journal on optimization*, vol. 9, no. 1, pp. 112–147, Aug. 1998.
- [68] Y.-P. Lin and S.-M. Phoong, "Perfect discrete multitone modulation with optimal transceivers," *IEEE Transactions on Signal Processing*, vol. 48, no. 6, pp. 1702–1711, Jun. 2000.

- [69] I. Mann, S. McLaughlin, W. Henkel, K. R., and T. Kessler, "Impulse generation with appropriate amplitude, length, inter-arrival, and spectral characteristics," *IEEE Journal on Selected Areas in Communications*, vol. 20, no. 5, pp. 901–912, Jun. 2002.
- [70] B. Muquet, Z. Wang, G. B. Giannakis, M. de Courville, and P. Duhamel, "Cyclic prefix or zero padding for wireless multicarrier transmissions?" *IEEE Transactions on Communications*, vol. 50, no. 12, pp. 2136–2148, 2002.
- [71] J. F. Nash, "Non-cooperative games," Ph.D. dissertation, Faculty of Princeton, University in Candidacy, 1950.
- [72] J. A. Nelder and R. Mead, "A simplex method for function minimization," *Computer Journal*, vol. 7, pp. 308–313, Jul. 1965.
- [73] R. Nilsson, T. Magesacher, S. Trautmann, and T. Nordström, "Radio frequency interference suppression in DSL," in *Fundamentals of DSL Technology*, ser. CRC, P. Golden, H. Dedieu, and K. Jacobsen, Eds. CRC Press, To be published 2005, ch. 13.
- [74] R. Nilsson, F. Sjöberg, M. Isaksson, J. M. Cioffi, and S. K. Wilson, "Autonomous synchronization of a DMT-VDSL system in unbundled networks," *IEEE Journal on Selected Areas in Communications*, vol. 20, no. 5, pp. 1055–1063, Jun. 2002.
- [75] T. Nordström and D. Bengtsson, "The FTW xDSL simulator, version 3.0b1." [Online]. Available: <http://xdsl.ftw.at/xdslsimu>
- [76] T. Nordström, D. Bengtsson, and D. Statovci, "Simulating xDSL," To appear 2005.
- [77] P. Ödling, B. Mayr, and S. Palm, "Technical impact of the unbundling process and regulatory action," *IEEE Communications Magazine*, vol. 38, no. 5, pp. 74–80, May 2000.
- [78] V. Oksman, "Optimization of the PSD_REF for upstream power back-off in VDSL," *ANSI T1E1.4 contribution 2001-102R1*, Feb. 2001.
- [79] V. Oksman and J. M. Cioffi, "Noise models for VDSL performance verification," *ANSI T1E1.4 contribution 1999-438R2*, Dec. 1999.
- [80] A. V. Oppenheim, R. W. Schfer, with, and J. R. Buck, *Discrete-Time Signal Processing*. Prentice Hall, 1989.
- [81] A. Peled and A. Ruiz, "Frequency domain data transmission using reduce computational complexity algorithms," in *Proc. of the International Conference on Acoustics, Speech and Signal Processing, ICASSP*, Apr. 1980, pp. 964–967.
- [82] T. Pollet and M. Peeters, "Synchronization with DMT modulation," *IEEE Communications Magazine*, vol. 37, no. 4, pp. 80–86, Apr. 1999.

- [83] ———, “A new digital timing correction scheme for DMT systems combining temporal and frequential signal properties,” in *Proc. of the IEEE International Conference on Communications, ICC*, New Orleans, LA, USA, Jun. 2000, pp. 1805–1808.
- [84] T. Pollet, P. Spruyt, and M. Moeneclaey, “The BER performance of OFDM systems using non-synchronized sampling,” in *Proc. of the IEEE Global Telecommunications Conference, GLOBECOM*, San Francisco, CA, USA, pp. 253–257.
- [85] J. G. Proakis, *Digital Communications*. McGraw-Hill, 2001.
- [86] Prof. Cioffi DSM website. [Online]. Available: <http://isl.stanford.edu/~cioffi/dsm>
- [87] W. D. Reeve, *Subscriber Loop Signaling and Transmission Handbook: Analog*. IEEE Press, New York, 1992.
- [88] ———, *Subscriber Loop Signaling and Transmission Handbook: Digital*. IEEE Press, New York, 1995.
- [89] T. R. Rowbotham, “Local loop developments in the U.K.” *IEEE Communications Magazine*, vol. 29, no. 3, pp. 50–59, Mar. 1990.
- [90] M. Russell, “Proposed text clarifying use of templates and masks,” *ANSI T1E1.4 contribution 1999-220*, Apr. 1999.
- [91] B. R. Saltzberg, “Performance of an efficient parallel data transmission systems,” *IEEE Transactions on Communications*, vol. 15, no. 6, pp. 805–811, Sep. 1967.
- [92] R. B. Salzberg, “Comparison of single-carrier and multitone digital modulation for ADSL applications,” *IEEE Communications Magazine*, vol. 36, no. 11, pp. 114–120, Nov. 1998.
- [93] N. P. Sands and S. K. Jacobsen, “Pilotless timing recovery for baseband multi-carrier modulation,” *IEEE Journal on Selected Areas in Communications*, vol. 20, no. 5, pp. 1047–1054, June 2002.
- [94] A. Scaglione, G. B. Giannakis, and S. Barbarossa, “Redundant filterbank precoders and equalizers part I: Unification and optimal designs,” *IEEE Transactions on Signal Processing*, vol. 47, no. 7, pp. 1988–2006, Jul. 1999.
- [95] S. Schelstraete, “UPBO & the transmit PSD mask,” *ANSI T1E1.4 contribution 2001-076*, Feb. 2001.
- [96] ———, “Defining upstream power backoff for VDSL,” *IEEE Journal on Selected Areas in Communications*, vol. 20, no. 5, pp. 1064–1074, May 2002.
- [97] A. Sendonaris, V. V. Veeravalli, and B. Aazhang, “Joint signaling strategies for approaching the capacity of twisted-pair channels,” *IEEE Transactions on Communications*, vol. 46, no. 5, pp. 673–685, May 1998.

- [98] F. Sjöberg, M. Isaksson, R. Nilsson, P. Ödling, S. K. Wilson, and P. O. Börjesson, "Zipper: A duplex method for VDSL based on DMT," *IEEE Transactions on Communications*, vol. 47, no. 8, pp. 1245–1252, Aug. 1999.
- [99] F. Sjöberg, R. Nilsson, M. Isaksson, P. Ödling, and P. O. Börjesson, "Asynchronous Zipper," in *Proc. of the IEEE International Conference on Communications, ICC*, Vancouver, Canada, Jun. 1999, pp. 231–235.
- [100] T. Starr, J. M. Cioffi, and P. Silverman, *Understanding Digital Subscriber Line Technology*. Prentice Hall, 1999.
- [101] T. Starr, M. Sorbara, J. M. Cioffi, and P. Silverman, *DSL Advanced*. Prentice Hall, 2003.
- [102] D. Statovci, R. Nilsson, and T. Nordström, "Generic detection model for DMT based modems," *ETSI/STC TM6 contribution 034t23r2*, Nov. 2003.
- [103] D. Statovci and T. Nordström, "Adaptive resource allocation in multiuser FDD-DMT systems," in *Proc. of the European Signal Processing Conference, EUSIPCO*, Vienna, Austria, Sep. 2004, pp. 1213–1216.
- [104] —, "Adaptive subcarrier allocation, power control, and power allocation for multiuser FDD-DMT systems," in *Proc. of the IEEE International Conference on Communications, ICC*, Paris, France, Jun. 2004, pp. 11–15.
- [105] D. Statovci, T. Nordström, and R. Nilsson, "The normalized-rate iterative algorithm: A practical dynamic spectrum management method for DSL," *Accepted for publication in EURASIP Applied Signal Processing Advanced Signal Processing Techniques for Digital Subscriber Lines*, 2005.
- [106] —, "The constrained normalized-rate iterative algorithm," *submitted to the IEEE Global Telecommunications Conference, GLOBECOM*, 2005.
- [107] D. Statovci *et al.*, "Revised upstream power back-off for VDSL," To appear 2005.
- [108] R. Suci, E. van den Bogaert, J. Varlinden, and T. Bostoen, "Insuring spectral compatibility of iterative water-filling," in *Proc. of the European Signal Processing Conference, EUSIPCO*, Vienna, Austria, Sep. 2004, pp. 1209–1212.
- [109] G. Taubök and W. Henkel, "MIMO systems in the subscriber-line network," in *Proc. of the 5th International OFDM Workshop*, Hamburg, Germany, Sep. 2000, pp. 18.1–18.3.
- [110] Texas Instruments, "A band plan framework for VDSL2," *ANSI T1E1.4 contribution 2003-503*, Feb. 2002.
- [111] C. Valenti, "NEXT and FEXT models for twisted-pair North American loop plant," *IEEE Journal on Selected Areas in Communications*, vol. 20, no. 5, pp. 893–900, Jun. 2002.

- [112] J. K. van de Beek, M. Sandell, and P. O. Börjesson, "ML estimation of time and frequency offset in OFDM systems," *IEEE Transactions on Signal Processing*, vol. 45, no. 7, pp. 1800–1805, Jul. 1997.
- [113] J. K. van de Beek, M. Sandell, M. Isaksson, and P. O. Börjesson, "Low-complex frame synchronization in OFDM systems," in *Proc. of the International Conference on Universal Personal Communication, ICUCP*, Tokyo, Japan, Nov. 1995, pp. 982–986.
- [114] R. F. M. van den Brink, "Cable reference models for simulating metallic access networks," *ETSI/STC TM6 contribution 970p02r3*, Permanent Document, Jun. 1998.
- [115] B. van den Heuvel and R. Perisco, "PSD masks for VDSL, and corresponding templates," *ETSI/STC TM6 contribution 024t03r1*, Nov. 2002.
- [116] J. Varlinden, "The target PSD obtained with iterative waterfilling is almost flat," *ANSI T1E1.4 contribution 2003-295*, Dec. 2003.
- [117] S. Verdu, *Multiuser Detection*. Cambridge University press, 1998.
- [118] P. Viswanath, D. N. C. Tse, and V. Anantharam, "Asymptotically optimal waterfilling in vector multiple-access channels," *IEEE Transactions on Information Theory*, vol. 47, no. 1, pp. 241–267, Jan. 2001.
- [119] S. B. Weinstein and P. M. Ebert, "Data transmission by frequency-division multiplex using the discrete Fourier transform," *IEEE Transactions on Communications*, vol. 19, no. 5, pp. 628–634, Oct. 1971.
- [120] J. J. Werner, "The HDSL environment," *IEEE Journal on Selected Areas in Communications*, vol. 9, no. 6, pp. 785–800, Aug. 1991.
- [121] N. Yamashita and Z.-Q. Luo, "A nonlinear complementarity approach to multiuser power control for digital subscriber lines," *Optimization Methods and Software*, vol. 19, no. 5, pp. 633–652, Oct. 2004.
- [122] W. Yu, W. Rhee, S. Boyd, and J. M. Cioffi, "Distributed multiuser power control for digital subscriber lines," *IEEE Journal on Selected Areas in Communications*, vol. 20, no. 5, pp. 1105–1115, Jun. 2002.
- [123] C. Zeng, C. Aldana, A. A. Salvekar, and J. M. Cioffi, "Crosstalk identification in xDSL systems," *IEEE Journal on Selected Areas in Communications*, vol. 19, no. 8, pp. 1488–1495, Aug. 2001.
- [124] C. Zeng and J. M. Cioffi, "Crosstalk cancellation in xDSL systems," *ANSI T1E1.4 contribution 2001-142*, May 2001.

Curriculum Vitae

Driton Statovci, citizen of Kosova,
born on January 23th, 1972, in Batllavë, Kosova.

Married to Valbona Statovci, née Murati, since January 28th, 1998.

Two sons: Ardit Statovci, born on December 27th, 2001, and

Art Statovci, born on January 5th, 2004.

Education

1999-2005 *Vienna University of Technology, Austria.*

PhD studies in electrical engineering.

1997-1998 *Viennese University Preparation Programme, Austria.*

Intensive German courses.

28.02.1996 *University of Prishtina, Faculty of Electrical Engineering, Kosova.*

Received the academic degree 'Inxhinier i diplomuar' (equivalent to a master's degree or Dipl.-Ing in Austria).

1990-1995 *University of Prishtina, Faculty of Electrical Engineering, Kosova.*

Studies in electrical engineering.

1988-1990 *Gymnasium "Sami Frasheri" in Prishtinë, Kosova.*

1986-1988 *Gymnasium "8 Nëntori" in Podujevë, Kosova.*

1978-1986 *Primary School "Luigj Gurakuqi" in Batllavë, Kosova.*

Employment

since Feb. 2002 *Forschungszentrum Telekommunikation Wien (ftw.), Vienna, Austria.*

Research in digital subscriber line technologies and dynamic spectrum management.

Aug. 2000 - Feb. 2002 *Ahead Communication Systems, Vienna, Austria.*

Working in system design for transmitting data and voice over DSL access networks. At the same time I was delegated by Ahead Communications Systems as a researcher at the Telecommunications Research Center Vienna (ftw.).

Sep. 1996 - Sep. 1997 *Electrical Engineering Secondary School "Gjin Gazulli" in Prishtina, Kosova.*

Teaching in field of telecommunications and computer networks.